“2-Steps in 1-pot: enzyme cascades for the synthesis of chiral vicinal amino alcohols“

Inaugural-Dissertation

zur Erlangung des Doktorgrades
der Mathematisch-Naturwissenschaftlichen Fakultät
der Heinrich-Heine-Universität Düsseldorf

vorgelegt von

Torsten Sehl
aus Tönisvorst

Jülich, November 2013

aus dem Institut für Bio- und Geowissenschaften 1
(IBG-1: Biotechnologie)

Forschungszentrums Jülich GmbH

Gedruckt mit der Genehmigung der
Mathematisch-Naturwissenschaftlichen Fakultät der
Heinrich-Heine-Universität Düsseldorf

Referent: Frau Prof. Martina Pohl
Korreferent: Herr Prof. Jörg Pietruszka

Tag der mündlichen Prüfung: 28.01.2014

Selbstständigkeitserklärung

Hiermit versichere ich an Eides Statt, dass die vorgelegte Dissertation von mir selbstständig und ohne unzulässige fremde Hilfe unter Beachtung der „Grundsätze zur Sicherung guter wissenschaftlicher Praxis an der Heinrich-Heine-Universität“ erstellt worden ist.

Bisher habe ich keine erfolgslosen Promotionsversuche unternommen und diese Dissertation nicht an einer anderen Fakultät vorgelegt.

_____	_____
Ort, Datum	Torsten Sehl

“The fortunate idea came to me to orient my crystals with reference to a plane perpendicular to the observer and then I noticed that the confused mass of crystals of paratartrate could be divided into two groups according to the orientation of their facets of symmetry. In one group, the facet of symmetry nearer my body was inclined to my right with reference to the plane of orientation which I just mentioned, whereas the facet of asymmetry was inclined to my left in the other. The paratartrate appeared as a mixture of two kinds of crystals, some asymmetric to the right, some asymmetric to the left.” [1, 2]

(Louis Pasteur, 1982-1895)

In dedication to my dear grandfather Otto Drese…

List of publications, awards, invention disclosures, conference talks

Publications in journals

T. Sehl, R. C. Simon, H. C. Hailes, J. M. Ward, U. Schell, M. Pohl, D. Rother
TTC-based screening assay for ω-transaminases: a rapid method to detect reduction of 2-hydroxy ketones. Journal of Biotechnology (2012), 159(3):188-94. doi: 10.1016/j.jbiotec.2011.12.023. Epub 2012 Jan 2.

T. Sehl, H. C. Hailes, J. M. Ward, R. Wardenga, E. v. Lieres, H. Offermann, R. Westphal, M. Pohl, D. Rother
Two Steps in One Pot: Enzyme Cascade for the Synthesis of Nor(pseudo)ephedrine from Inexpensive Starting Materials. Angewandte Chemie International Edition (2013), 52(26):6772-5. doi: 10.1002/anie.201300718. Epub 2013 May 9.

T. Sehl, H. C. Hailes, J. M. Ward, R. Wardenga, E. v. Lieres, H. Offermann, R. Westphal, M. Pohl, D. Rother
Zwei Schritte in einem Reaktionsgefäß: Enzymkaskaden zur selektiven Synthese von Nor(pseudo)ephedrin aus kostengünstigen Ausgangsmaterialien (German edition). Angewandte Chemie (2013), 125(26):6904-6908. doi: 10.1002/ange.201300718. Epub 2013 May 9.

T. Sehl, H. C. Hailes, J. M. Ward, U. Menyes, M. Pohl, D. Rother
Efficient two-step biocatalytic strategies for the synthesis of all nor(pseudo)ephedrine isomers. Green Chemistry (2014), doi:10.1039/C4GC00100A.

Publications in books

T. Sehl, J. Kulig, R. Westphal, D. Rother
Synthetic enzyme cascades for valuable diols and amino alcohols – smart composition and optimisation strategies. Book chapter for `Industrial Biocatalysis´, editor: Prof. P. Grunwald, in press.

Patent applications

D. Rother, M. Pohl, T. Sehl, Á. Gómez Baraibar (2013)
2-Schritt Synthese zur Herstellung von (1*S*,2*S*)-Norpseudoephedrin (Cathine) durch Kopplung einer (*S*)-selektiven Lyase und einer (*S*)-selektiven Transaminase.
Deutsche Patentanmeldung: 10 2013 009 631.6

D. Rother, M. Pohl, T. Sehl (2013)
2-Schritt Synthese zur Herstellung von (1*S*,2*S*)-Norpseudoephedrin (Cathine) durch Kopplung einer (*S*)-selektiven Transaminase und einer (*S*)-selektiven Alkoholdehydrogenase.
Deutsche Patentanmeldung: 10 2013 009 145.4

Conference talks

(presenting author underlined)

T. Sehl, D. Rother, J. Pietruszka, W. Wiechert, M. Pohl (2010)
Two-step biocatalytic approach for the synthesis of chiral amino alcohols
1st CLIB-GC Symposium, Düsseldorf, Germany

D. Rother, J. Kulig, T. Sehl, W. Kroutil, M. Ward, H.C. Hailes, W. Wiechert, M. Pohl (2012)
Modular synthetic enzyme cascades for the production of valuable chiral precursors
Multistep-Enzyme-Catalysis-Processes 2012, Graz, Austria

T. Sehl, H.C. Hailes, J.M. Ward, W. Wiechert, M. Pohl, D. Rother (2012)
Recycling Cascade combining ThDP-dependent Lyases and ω-Transaminases for the Synthesis of Chiral Amino Alcohols
DECHEMA-Jahrestagung der Biotechnologen und ProcessNet-Jahrestagung, Karlsruhe, Germany

D. Rother, T. Sehl, J. M. Ward, H.C. Hailes, R. Wardenga (2013)
Novel recycling enzyme cascades for the stereoselective production of norephedrine and norpseudoephedrine
1st International Symposium on Transaminase Biocatalysis, Stockholm, Sweden

D. Rother, J. Kulig, T. Sehl, W. Kroutil, M. Ward, H.C. Hailes, R. Wardenga, W. Wiechert, M. Pohl (2013)
Smart composition of synthetic enzyme cascades for the production of valuable vicinal diols and amino alcohols
BioTrans 2013, Manchester, England

Poster presentations

(presenting author underlined)

T. Sehl, H.C. Hailes, J.M. Ward, W. Wiechert, M. Pohl, D. Rother (2010)
Identification and characterisation of enzymes for the synthesis of chiral amino alcohols
Biocat 2010 - 5th International Congress on Biocatalysis, Hamburg, Germany

T. Sehl, H.C. Hailes, J.M. Ward, W. Wiechert, M. Pohl, D. Rother (2010)
Identification and characterisation of enzymes for the synthesis of chiral amino alcohols
DECHEMA-Jahrestagung der Biotechnologen und ProcessNet-Jahrestagung, Aachen, Germany

T. Sehl, R. Westphal, H.C. Hailes, J.M. Ward, W. Wiechert, M. Pohl, D. Rother (2012)
From aldehydes / keto acids via 2-hydroxy ketones to amino alcohols: ThDP-dependent enzymes and ω-transaminases in a novel 2-step 1-pot cascade reaction
Multistep-Enzyme-Catalysis-Processes 2012, Graz, Austria

T. Sehl, R. Westphal H.C. Hailes, J.M. Ward, W. Wiechert, M. Pohl, D. Rother (2012)
Novel and Sustainable Recycling Cascade combining ThDP-dependent Lyases and ω-Transaminases for the Synthese of Chirale Amino Alcohols
DECHEMA-Jahrestagung der Biotechnologen und ProcessNet-Jahrestagung, Karlsruhe, Germany

T. Sehl, R. Westphal H.C. Hailes, J.M. Ward, E. v. Lieres, W. Wiechert, M. Pohl, D. Rother (2013)
Novel Recycling Enzyme Cascades for the Stereoselective Production of Norephedrine and Norpseudoephedrine
1st International Symposium on Transaminase Biocatalysis, Stockholm, Sweden

T. Sehl, R. Westphal H.C. Hailes, J.M. Ward, E. v. Lieres, W. Wiechert, M. Pohl, D. Rother (2013)
Enzymatic recycling cascades: In two steps to optically pure nor(pseudo)ephedrines
BioTrans 2013, Manchester, England

Poster award: BioTrans 2013, Manchester, England

T. Sehl, R. Westphal H.C. Hailes, J.M. Ward, E. v. Lieres, W. Wiechert, M. Pohl, D. Rother (2012)
Enzymatic recycling cascades: In two steps to optically pure nor(pseudo)ephedrines

Abstract

Amino alcohols, and especially nor(pseudo)ephedrines, are compounds with various applications in organic synthesis and in the pharmaceutical industry. The strategies to these chiral molecules by classical chemical or chemo-enzymatical syntheses are challenging and therewith draw interest for industrial research efforts. In this thesis, the potential of enzyme cascades for the synthesis of chiral primary vicinal amino alcohols was demonstrated. In detail, the 2-step cascades combining thiamine diphosphate (ThDP)-dependent enzymes and ω-transaminases were investigated for the synthesis of nor(pseudo)ephedrines. This approach represents a completely new strategy for getting access to chiral amino alcohols. These valuable chemicals are now accessible in a highly atom- and step-efficient enzymatic process in only two reaction steps from inexpensive, achiral starting materials.

Development of a novel screening assay for ω-transaminases

In the developed synthetic enzyme cascade, amino alcohols are accessible via a carboligation of aldehydes and α-keto acids, followed by a subsequent reductive amination of the α-hydroxy ketone intermediate catalysed by ω-transaminases. For a fast and reliable screening of ω-transaminase activity in these reductive amination reactions, a novel screening assay was developed. This assay is meanwhile used by other working groups and companies to screen enzymatic reductive amination reactions. Using this assay, we identified valuable biocatalysts for the reductive amination of acetoin, 2-hydroxyacetophenone and phenylacetylcarbinol (PAC). The reductive amination of PAC was of special importance, since is the reaction intermediate in the 2-step cascade for the synthesis of nor(pseudo)ephedrines.

1-Pot 2-step cascade combining ThDP-dependent enzymes and ω-transaminases

The 2-step synthesis of (1*R*,2*S*)-norephedrine was investigated for the combination of the (*R*)-selective ThDP-dependent acetohydroxyacid synthase-I (AHAS-I) from *Eschericia coli* and the (*S*)-selective ω-transaminase from *Chromobacterium violaceum*. A major challenge was the low thermodynamic equilibrium constant for the reductive amination reaction. The equilibrium constant for the reductive amination of PAC with alanine as an amine donor was determined: $K_{eq} = 8.81 \cdot 10^{-4}$. As a direct consequence, even with a 5-fold excess of alanine the conversion did not exceed 5 %. This challenge in the second reaction step was overcome by removal of the co-product (pyruvate) with the enzyme of the first reaction step (AHAS-I). This enzyme catalyses the carboligation of two pyruvate molecules to acetolactate. In process mode optimisations, best results were obtained for the 1-pot sequential cascade mode. Under optimised reaction conditions 78 % of the benzaldehyde (10 mM) was converted to (1*R*,2*S*)-norephedrine (*ee* >99 %, *de* >98 %). This is the first example where a reaction equilibrium shift was performed in cascade reactions without the addition for further enzymes, reactants or co-solvents. If this cascade is performed for

the combination of AHAS-I and the (*R*)-selective ω-transaminases from *Aspergillus terreus* (*At*-(*R*)TA) in the 1-pot 2-step sequential mode, product concentrations up to 90 mM (= 90 % conversion) could be reached. The gained product (1*R*,2*R*)-norpseudoephedrine again exhibits excellent stereoselectivity (*ee* >99 %, *de* >98 %).
Moreover, not only a simple co-product removal was tested, but even a recycling of the pyruvate in the first cascade step was possible. In case of the 2-step recycling cascade with AHAS-I and *At*-(*R*)TA, 86 % (= 17.2 mM) of the benzaldehyde (20 mM) was converted to (1*R*,2*R*)-norpseudoephedrine (*ee* >99 %, *de* >98 %) while only 10 mM pyruvate was initially present in the reaction setup. This novel 'recycling cascade' concept increases atom economy of reactions and can theoretically be applied in any cascade reactions where co-products from a later step can be recycled for a previous step.

1-Pot 2-step cascade combining ω-transaminases and alcohol dehydrogenases

For the synthesis of the pharmaceutical (1*S*,2*S*)-norpseudoephedrine, a highly (*S*)-selective lyase is required in the first reaction step. However, such a lyase is currently not available. Therefore, an alternative strategy was investigated. Starting from 1-phenylpropane-1,2-dione, the combination of (*S*)-selective transaminase from *Chromobacterium violaceum* with the alcohol dehydrogenase from *Lactobacillus brevis* resulted in the formation of (1*S*,2*S*)-norpseudoephedrine with excellent stereoselectivity (*ee* >98 %, *de* >99 %). This novel biocatalytic reaction cascade can be seen as a valuable alternative synthesis strategy to complement the amino alcohol platform.

Zusammenfassung

Aminoalkohole, und insbesondere Nor(pseudo)ephedrine, sind Verbindungen mit vielseitigen Anwendungen in organischen Synthesen und in der pharmazeutischen Industrie. Die Herstellung dieser chiralen Moleküle ist durch klassische chemische Synthesewege häufig schwierig und daher Gegenstand aktueller Forschung. In dieser Arbeit wurde das Potential von Enzymkaskaden zur Synthese von chiralen primären vicinalen Aminoalkoholen demonstriert. Eine zweistufige Kaskade, bestehend aus Thiamindiphosphat (ThDP)-abhängigen Enzymen und ω-Transaminasen, wurden für die Synthese von Nor(pseudo)ephedrinen erforscht. Dieser Ansatz stellt eine neue Strategie zur Synthese von chiralen Aminoalkoholen dar. Die wertvollen Produkte können in einem Reaktionsgefäß mit zwei Reaktionsschritten ausgehend von preiswerten, achiralen Ausgangsmaterialien hergestellt werden.

Entwicklung eines neuartigen *Screening*-Tests für ω-Transaminasen

In der neu entwickelten synthetischen Enzymkaskade, sind Aminoalkohole über eine Carboligation von Aldehyden und α-Ketosäuren zugänglich. Anschließend erfolgt eine reduktive Aminierung des Zwischenprodukts (2-Hydroxyketon) durch ω-Transaminasen. Für ein schnelles und zuverlässiges Screening von ω-Transaminase-Aktivität wurde ein neuartiger *Screening*-Test entwickelt. Dieser wird mittlerweile von anderen Wissenschaftlern genutzt, um enzymatische reduktive Aminierungsreaktionen zu untersuchen. In unseren Arbeiten konnten Biokatalysatoren für den Umsatz von Acetoin, 2-Hydroxyacetophenon und Phenylacetylcarbinol (PAC) identifiziert werden. Die reduktive Aminierung von PAC war dabei von besonderer Bedeutung, da PAC das Syntheseintermediat in der 2-Schritt-Kaskade zur Gewinnung von Nor(pseudo)ephedrinen ist.

2-Schritt-Kaskade: ThDP-abhängige Enzyme kombiniert mit ω-Transaminasen

Die zweistufige Synthese von (1*R*,2*S*)-Norephedrin erfolgte durch Kombination des (*R*)-selektiven ThDP-abhängigen Enzyms Acetohydroxysäuresynthase-I (AHAS-I) aus *Escherichia coli* mit der (*S*)-selektiven ω-Transaminase aus *Chromobacterium violaceum*. Eine Herausforderung war die geringe thermodynamische Gleichgewichtskonstante der reduktiven Aminierung im zweiten Reaktionsschritt. Für die Reaktion von PAC mit Alanin als Amindonor ($K_{eq} = 8{,}81 \cdot 10^{-4}$) ist selbst bei einem 5-fachen Überschuss von Alanin nur ein maximaler Umsatz von 5 % erreichbar. Dieses Problem konnte durch Entfernung des Co-Produkts (Pyruvat) mit dem Enzym des ersten Reaktionsschrittes (AHAS-I) gelöst werden. Dabei wird Pyruvat zu Acetolactat umgesetzt.
Nach Optimierung verschiedener Reaktions- und Prozessparameter konnte (1*R*,2*S*)-Norephedrin mit einem Umsatz von 78 % in der zweistufige Synthese generiert werden. Das Produkt hatte eine hohe optische Reinheit (*ee* >99 % und *de* >98 %). Diese Enzymkaskade ist das erste Beispiel, bei dem die Verschiebung eines

Reaktionsgleichgewichts ohne Zugabe weiterer Enzyme, Reaktanten oder Lösungsmittel durchgeführt werden konnte. Bei einer analogen Kaskade zur stereoselektiven Synthese von (1*R*,2*R*)-Norpseudoephedrin konnte durch Kombination der AHAS-I mit der (*R*)-selektiven ω-Transaminasen *At*-(*R*)TA aus *Aspergillus terreus* eine Produktkonzentration von 90 mM (*ee* >99 %, *de* >98 %) erreicht werden.

Pyruvat, das Co-Produkt der ω-Transaminase-Reaktion, ist gleichzeitig auch ein Substrat, das von der AHAS-I bei der Synthese von PAC im ersten Kaskadenschritt benötigt wird. Führt man die Synthese in einem Reaktionsgefäß aus, kann so das Co-Produkt in den ersten Kaskadenschritt zurückgeführt werden. Bei dieser sogenannten Rezyklierungskaskade konnte in der Kombination aus AHAS-I und *At*-(*R*)TA 17,2 mM (1*R*,2*R*)-Norpseudoephedrin aus nur 10 mM Pyruvat erzeugt werden. Dieses Kaskadenkonzept stellt eine neue Art der Prozessführung dar und kann zur Erhöhung der Atomökonomie von Reaktionen beitragen. Theoretisch wäre es in allen Kaskadenreaktionen einsetzbar, bei der Nebenprodukte aus einem späteren Schritt als Substrate für vorherige Reaktionsschritte genutzt werden können.

2-Schritt-Kaskade: ω-Transaminasen kombiniert mit Alkoholdehydrogenasen

Für die Synthese des pharmazeutisch-aktiven Wirkstoffs (1*S*,2*S*)-Norpseudoephedrin wäre in der oben genannten Kaskade ein hoch (*S*)-selektives Enzym im ersten Reaktionsschritt erforderlich. Da ein solches Enzym derzeit nicht bekannt ist, wurde eine alternative Strategie erforscht. Ausgehend von 1-Phenyl-1,2-diketon, kann (1*S*,2*S*)-Norpseudoephedrin durch Kombination der (*S*)-selektiven ω-Transaminase mit einer (*S*)-selektiven Alkoholdehydrogenase in hohen optischen Reinheiten (*ee* >98 %, *de* >99 %) erzeugt werden. Diese biokatalytische Reaktionskaskade ergänzt als wertvolle alternative Synthesestrategie die Plattform an zugänglichen Aminoalkoholen.

Table of contents

List of scheme, figures and tables

Schemes:

Figures:

Tables:

List of abbreviations

AADH	amino acid dehydrogenase
AAO	amino acid oxidase
ACS	American Chemical Society
ADH	alcohol dehydrogenase
AHAS	acetohydroxyacid synthase
ALS	acetolactate synthase
APPO	1-amino-1-phenylpropane-2-one
ATA	amine transaminases
BAL	benzaldehyde lyase
BFD	benzoylformate decarboxylase
CCE	crude cell extract
CPHPE	1-cyclopropyl-2-hydroxy-2-phenylethanone
de	diastereomeric excess
dr	diastereomeric ratio
EC	enzyme class
E .coli	*Escherichia coli*
ee	enantiomeric excess
LWC	lyophilised whole cells
FAD	flavin adenine dinucleotide
FDA	US Food and Drug Administration
FDH	formate dehydrogenase
GC	gas chromatography
GCI	Green Chemistry Institute
GDH	glucose dehydrogenase
GlDH	glutamate dehydrogenase
2-HAP	2-hydroxy-1-phenylethanone
HEPES	4-(2-hydroxyethyl)-1-piperazineethanesulfonic acid
HPLC	high performance liquid chromatography
HPP	1-hydroxy-1-phenylpropan-1-one
HMBP	1-hydroxy-3-methyl-1-phenylbutan-2-one
IPTG	Isopropyl-ß-D-thio-galactopyranoside
K_{eq}	reaction equilibrium constant

KG	keto glutarate
LDH	lactate dehydrogenase
MBA	methylbenzylamine
MDH	malate dehydrogenase
NAD	nicotinamide adenine dinucleotide, oxidised
NADH	nicotinamide adenine dinucleotide, reduced
NEA	1-(naphthalen-1-yl)-ethanamine
NE	norephedrine
NPE	norpseudoephedrine
N(P)E	nor(pseudo)ephedrine; norephedrine and/or norpseudoephedrine
PAC	phenylacetylcarbinol
PDC	pyruvate decarboxylase
PLP	pyridoxal-5-phosphate
PMP	pyridoxamine-5-phosphate
PPA	phenylpropanolamine
PPC	phenylpropionylcarbinol
PPDO	1-phenylpropane-1,2-dione
TA	transaminase
THNA	tetrahydronaphthalen-1-amine
ThDP	thiamine diphosphate
TTC	2,3,4-triphenyltetrazolium chloride
U	units [µmol substrate (or product) per min]
USD	United States Dollar

1 Introduction

1.1 The impact of chirality in organic compounds

Chiral organic compounds have found application way before chirality itself was discovered. The history of herbal remedies with chiral active drugs goes back approximately five millennia.[3] Among a large list, examples like februgine (reported 2735 B.C. for the treatment of fever), quinine (used since the 16th century as an antimalarial agent) and cathinone or cathine (sympathomimetic action known since centuries[4, 5]) were reported.[3]

As previously reviewed,[3, 6, 7] the basis for the discovery of chirality was the invention of circularly polarised light by Malus 1809. Only a few years later Arago and Biot observed left (levorotatory) or right (dextrorotatory) rotation of polarised light in different crystals and liquids. In 1848 Pasteur demonstrated that two different non-superimposable mirror images of sodium ammonium tartrate crystals exist, which rotate polarised light differently after separation (see figure 1-1). Based on these studies, van't Hoff and Le Bel presented independently the concepts of the asymmetric carbon atom in 1884. Only a few years later, first examples were reported demonstrating that one isolated isomer has a different physiological action in human body than its mirror image – as it is well known from cocaine (1894), atropine (1903) or epinephrine (1908).[3, 6, 7]

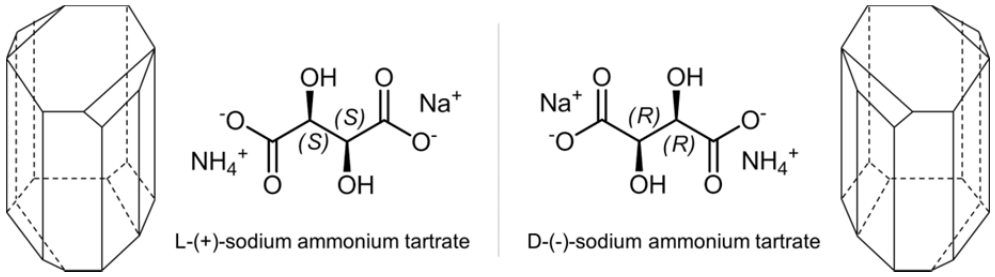

Figure 1-1: Structure and hemihedral crystals of (+) and (−) sodium ammonium tartrate
(figure adapted with permission from reference [8])

Although these examples for biological impact of chirality in drugs were recognised early, an industrial guidance was released by the "US Food and Drug Administration" (FDA)[9] and the "European Committee for Proprietary Medicinal Products" only recently in 1992. Since that date, racemates were rated as a composition of single

isomers, associated with a determination of physiological agent profiles for each isomer.[6, 10, 11] Today, a large number of examples are known, where a discrepancy in effects of stereoisomers can be observed: (*S*)-bupivaccaine for instance has a vasoconstrictor effect, which is not observed for its enantiomer.[12] Dextromethorphan is widely used as a cough suppressant, while levomethorphan has opioid effects.[13] Racemic D,L-carnitine was described to cause symptoms like myasthenia or cardiac arrhythmias. However, the optically pure L-isomer prevents these negative effects and is used for multifunctional applications.[14]

Plenty more examples for the relevance of chirality also in fields beyond the pharmaceutical industry (like in biochemicals, flavour or aroma chemicals, dyes, polymers, chemical catalysts…) are known, demonstrating the immense commercial potential of optically pure products.[10]

1.2 Production of optically pure compounds

In general, there are three ways to access to single optical isomers: chiral pool, resolution and asymmetric synthesis.[15-17]

Chiral pool methods are based on available chiral resources in nature. Compounds generated by the complexity of biological metabolism can be extracted from their native source (plants, microorganisms or animals) and used directly as natural products or as chiral building blocks in organic synthesis. This strategy provides advantages for instance when a target with challenging synthetic strategies is available from inexpensive natural sources. However, the limited number of natural products on the one hand and the availability of natural resources on the other hand restricts the applicability of chiral pool methods for industrial processes.[15]

Racemic mixtures are often much easier accessible than the pure enantiomers. Separation of single enantiomers from enantiomer mixtures is called resolution. Various techniques like preferential crystallisation, chromatographic methods or kinetic resolution have been developed to produce optically pure compounds.[10, 18-20] In all of these cases the yield is limited to 50 %, since often only one of both enantiomers is of interest. A smart solution, if applicable, is the dynamic kinetic resolution, where the undesired enantiomer is racemised in an additional reaction step, thus enabling 100 % conversion to the desired enantiomer.

Limitations of chiral pool methods and the lack of sustainability (caused by the low atom economy) of resolution techniques[21] can often be overcome by asymmetric synthesis.[17] Here, achiral substrates are converted via an asymmetric reaction to a chiral, non-racemic product. Many examples in all fields of organic synthesis indicate the relevance of asymmetric synthesis for industrial applications.[17]

The efficiency of an asymmetric synthesis approach is depending on several criteria like high stereoselectivity, conversion rates, availability and separability of chiral catalysts or auxiliaries.[17] Here, biocatalysis offers an immense potential within this field of organic synthesis as summarised in chapter 1.3.

1.3 Potential of industrial biotechnology

The chemical industry is one of the main economic sectors in the world. Within this field, industrial biotechnology, synonymously named white biotechnology (in Europe), has become a valuable and continuously growing market in the last decades.[22-27] Although absolute numbers for global economy benefits differ a lot, general trends are obvious. In a recent statistic (figure 1-2 a), the market for chemical goods has been summed up to a volume of $ 1.2 trillion (USD) in 2001 with a growth of 25 % to $ 1.5 trillion (USD) in 2010. The value of biotechnological processes decupled in the same time period from $ 30 billion to $ 310 billion (USD). In 2010, this already corresponded to one-fifth of the total market for chemicals. Moreover, it is estimated that the impact of biobased chemicals in contrast to the petrochemical industry will continuously grow the next decades (figure 1-2 b).[25, 27]

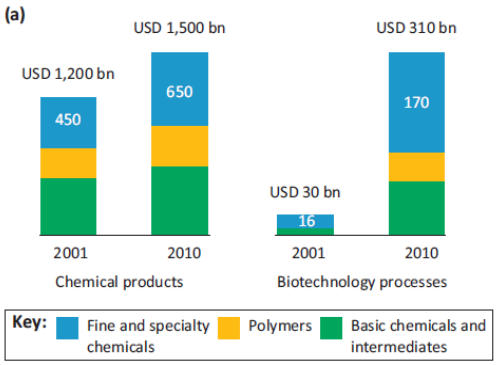

(b)

	2005		2010		2025	
Sector	Total	Biobased	Total	Biobased	Total	Biobased
Commodity	475	0.9	550	5-11	857	50-86
Specialty	375	5	435	87-110	679	300-340
Fine	100	15	125	25-32	195	88-98
Polymer	250	0.3	290	15-30	452	45-90
Total	1,200	21.2	1,400	132-183	2,183	483-614

Figure 1-2: Trends in production of biobased chemicals in relation to petrochemicals
(a) Global growth of biobased chemicals and polymers between 2001 and 2010. (b) US predictions for growth of the biobased industry until 2025. (adapted with permission from reference [27])

1.3.1 Enzymes in asymmetric synthesis

Biocatalysis, as part of the biotechnology platform, is nowadays used as a powerful tool for the synthesis of chemical compounds also in industrial scale applications.[28, 29] Applications of biocatalysts in the field of organic synthesis are known for all enzyme classes (EC)[30]: oxidoreductases (EC 1), transferases (EC 2), hydrolases (EC 3), lyases (EC 4), isomerases (EC 5) and ligases (EC 6). However, only ligases are still of low relevance in technical-scale syntheses.[23, 29, 31]

Advantages of enzymatic catalysis, especially in terms of asymmetric synthesis, are well known and pointed out in many reviews.[29, 31-33] Commonly, high regio-, chemo- and stereoselectivities are mentioned. This often enables a selective synthesis of target molecules, which are otherwise only accessible in multistep chemical reactions with several protection and deprotection steps. Furthermore, enzymes are often active under mild reaction conditions, such as ambient temperature, atmospheric pressure, water as reaction media or physiological pH. These points and the fact that the catalyst itself is biodegradable are often referred to an environmentally friendly, "green" chemical process. In addition to that, enzymatic reaction rates can be 10^8-10^{10} or in some cases even 10^{17} fold faster than the non-catalysed reaction, which is typically order of magnitudes better than known rates for chemical catalysts.[34] In theory, almost each organic reactions can be carried out by enzymes[22, 32] and the nowadays >4,000 identified different enzymes[31] enable already almost all of these reaction types.[32]

Although there is a large list of reasons for application of enzymes in organic syntheses, examples of biocatalytic or chemo-enzymatic processes in industry are still below expectation.[23] A major drawback is that the amount of '*Candida antarctica* lipase B type enzymes' that is available for the hydrolases, is still limited within other enzyme classes. Ideally, enzymes and the processes they are used in need to fulfil the following requisites for industry (adapted from [29]):

- atom economy and sustainability of the process
- availability and costs of the required substrates
- optical purity of the isolated product (*ee*, *de* >99 %)
- availability and characterisation data for the catalyst
- activity (>1 U mg^{-1}), stability and recyclability of the catalyst
- conversions (>95 %) and substrate concentrations (>100 g L^{-1})

According to a recently published review which summarises the "use of enzymes in organic synthesis and life sciences",[23] manufacturing processes with lipases, proteases and alcohol dehydrogenases are generally feasible for large scale applications. Although, the number of processes with amidases, nitrilases, hydroxynitrilases and transaminases has increased in the last years, there is still a great potential also for oxygenase and C-C bond forming enzymes (decarboxylases, aldolases, enoate/ene reductases). Here, an agreement between chemists and biologists as well as between industry and academia is suggested by the authors to fulfil the achievements for a broader range of biocatalytic large scale applications. Challenging tasks and requirements are (adapted from reference [23]):

- identification of novel robust biocatalysts especially for large scale applications
- screening kits of ready to use and stable enzymes for all EC classes have to be set up and/or need to be enlarged
- increase of functional characterisation data like optimal reaction conditions and substrate scope
- (*R*)- and (*S*)-selective catalysts are required to ensure the enantio-complementarity of synthesis route
- increase of catalytic activity is required for many enzymes

1.4 'Green' reductive amination – an "aspirational reaction" [35]

The vast majority of medical drugs and drug candidates contain amine groups or functional groups derived from amines.[35, 36] These groups often introduce chirality into a molecule, indicating the increasing interest for the development respective synthesis strategies. A large number of physiologically active compounds with a chiral amine motif can be synthesised from primary amines.[37] Selected examples for drugs with diverse applications derived from different building blocks are highlighted in scheme 1-1.

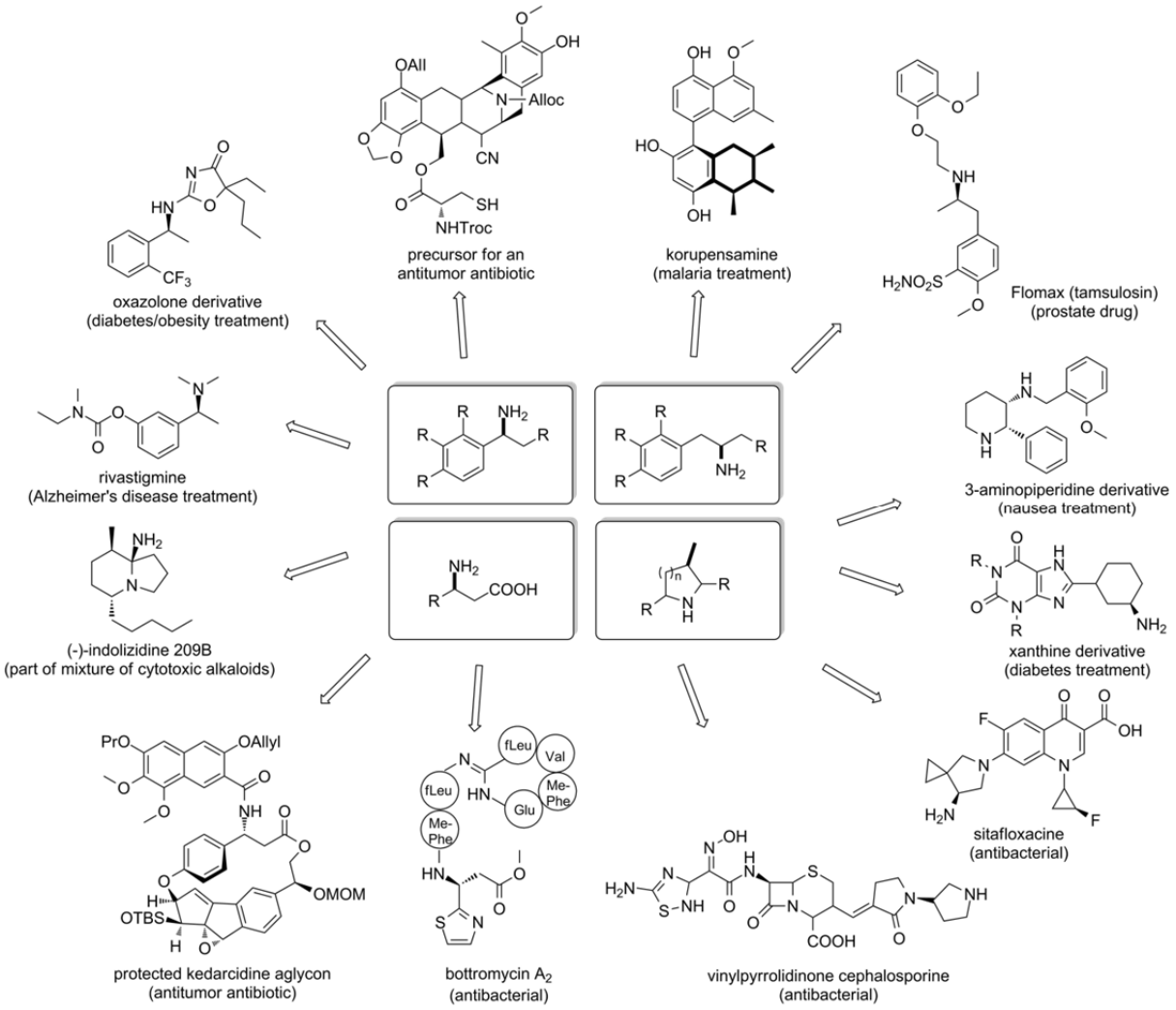

Scheme 1-1: Selected examples of the large platform of chiral amines used as synthons for the synthesis of physiological active compounds
(adapted with permission from reference [37])

1.4.1 Chemical synthesis of chiral amines

Various methods for the chemical synthesis of chiral amines are described in literature and were recently reviewed:[36]

Nucleophilic addition of carbanions to imines - radical addition to imines - Brønsted acid catalysed - reduction of imines by chiral Lewis bases - vinylogous Mannich reactions - metal-mediated hydrogenation - asymmetric reductive amination - hydrogenation of enamines - enamide reduction - reduction of nitrogen-based heteroaromatic compounds - asymmetric hydroamination - C-H amination - asymmetric Aza-Morita–Baylis–Hillman reaction.

For the synthesis of α-chiral primary amines, asymmetric addition of carbanions and asymmetric hydrogenation are frequently considered methods (scheme 1-2).[37] Starting from commercially available ketones or aldehydes, the substitution of the oxygen atom by a nitrogen atom results either in an aldimine or a ketimine. An additional reduction followed by a deprotection gives access to the desired amine. In both synthesis strategies, enantioselectivity is introduced either by using chiral auxiliaries[38-40] or by chiral ligands coordinated to metal complexes.[41, 42]

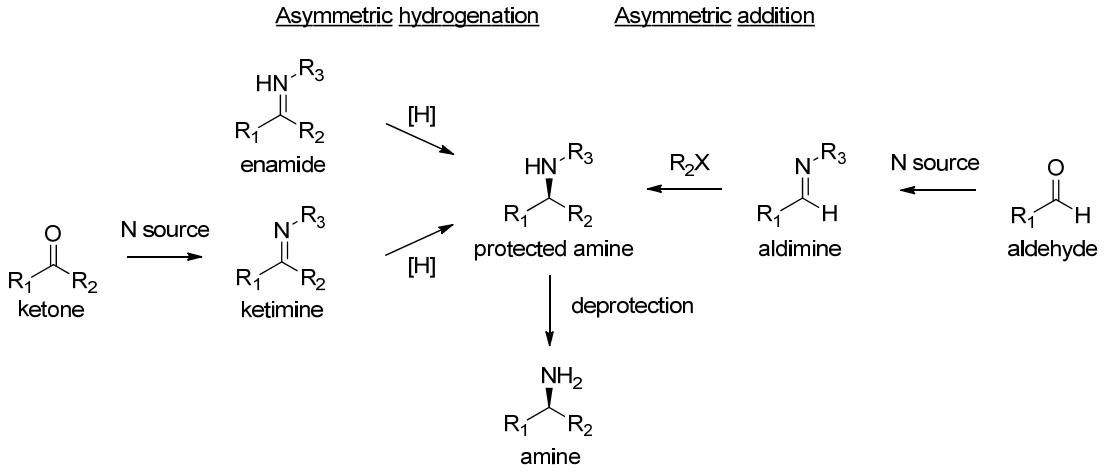

Scheme 1-2: Two frequently used chemical synthesis strategies for α-chiral amines are asymmetric hydrogenation and asymmetric addition.
(adapted with permission from reference [37])

Although a large number of methods exists, examples with high stereoselectivities (*ee*, *de* >99 %) are still rare. In addition, often expensive starting materials and/or multi-step reactions are required, so that further innovations in the field of amine synthesis will be necessary in future to solve future challenges.[36]

In 2005, the American Chemical Society (ACS), the Green Chemistry Institute (GCI) and various global pharmaceutical companies founded the "ACS GCI Pharmaceutical Roundtable". The overall aim was to bring "*key medicines to the patients with a minimal impact on the environment*".[35] This should be achieved by integration of more sustainable, 'greener' chemistry in pharmaceutical production processes.[35] The 2nd highest vote number by the Roundtable on "future priority research areas" got the chiral amines synthesis were especially the green reductive amination was highlighted as an "*aspirational reaction*" for future research activities.[35] Here, biocatalytic approaches offer a great potential to meet the above mentioned challenges.[37]

1.4.2 Biocatalytic synthesis of chiral amines

As an alternative to chemical synthesis strategies, several biocatalytic routes based on hydrolases, oxidoreductases, lyases and transferases have been developed to overcome the remaining challenges in chiral amine production (scheme 1-3).[37, 43]

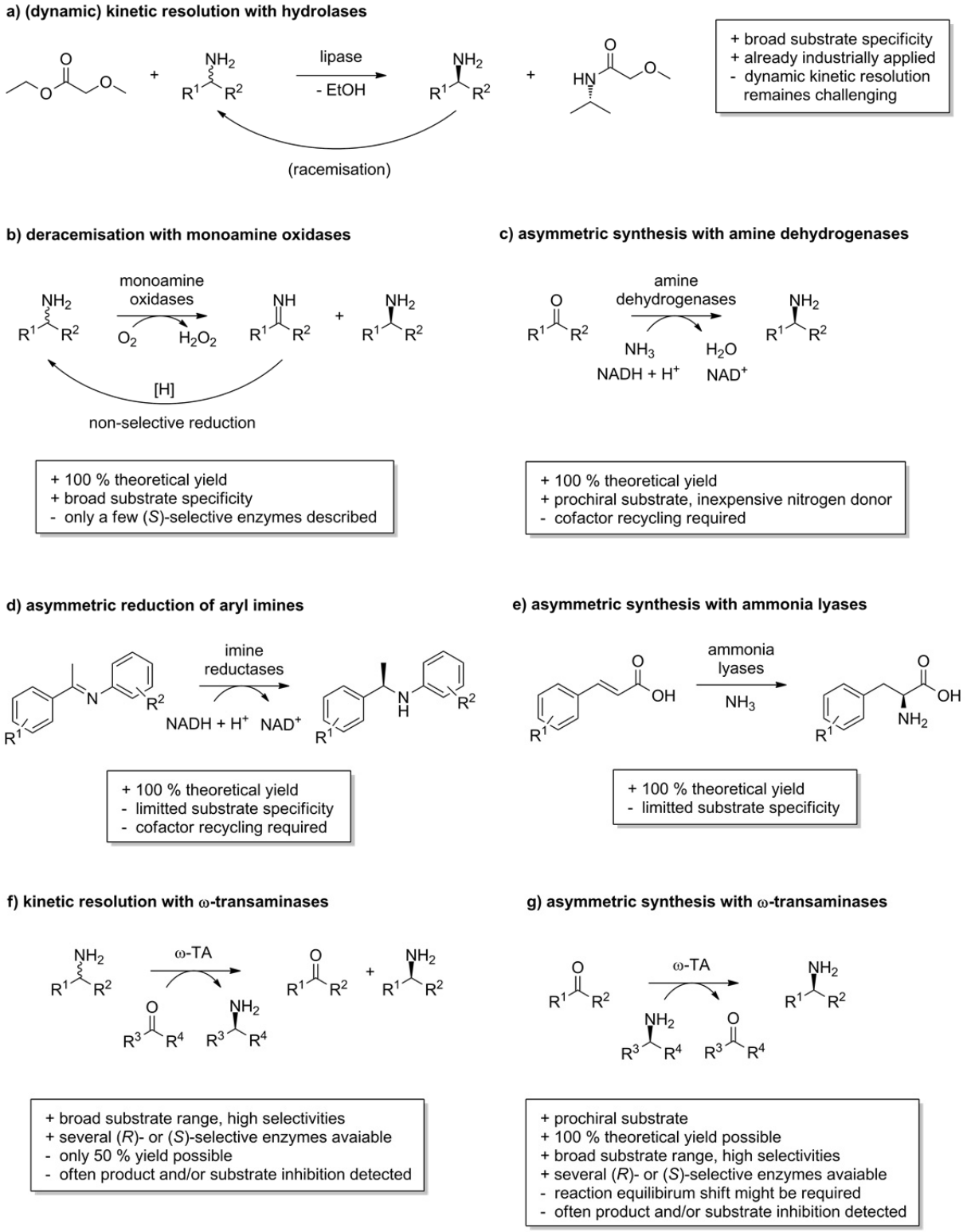

Scheme 1-3: Biocatalytic routes to optically active α-chiral primary amines
(adapted with permission from reference [37])

Each route provides advantages and drawbacks for specific parameters like substrate range, stereoselectivity, starting material, cofactor recycling and theoretical reaction yield (see scheme 1-3).[37]

Both, kinetic resolution with lipases or other hydrolases[44-48] and deracemisation with monoamine oxidases[49-52] offer valuable opportunities for the synthesis of optically pure amines. Especially the application of hydrolases is a frequently used technique in industry.[47, 53] However, only 50 % theoretical yield can be achieved, if a dynamic kinetic resolution cannot be applied. Moreover, achievement of high optical purity (>98 %) is challenging and often requires additional purification effort.[47, 53] Amine dehydrogenases are valuable catalysts, since an inexpensive amine donor can be used and enzymes with broad substrate ranges are known. Here, the most important requirement is the improvement of enantioselectivity for future applications. [54-56] Moreover, as for the imine reductases[57-60], an additional cofactor recycling is obligatory which increases reaction costs. Imine reductases and ammonia lyases[61-63] expand the biocatalytic platform but have limited substrate range and are thereby restricted to special applications.

ω-Transaminases can be used for kinetic resolution as well as for the asymmetric synthesis of chiral amines. The latter is often preferred, since on the one hand the theoretical yield is 2-fold higher[64] and on the other hand achiral precursors are usually less expensive than racemic mixtures.[65] Although challenges like low reaction equilibria and substrate/product inhibition need to be overcome, the broad substrate ranges, high enantioselectivities, fast reaction rates and the independency of cofactor recycling steps demonstrate the high potential of ω-transaminases.[64, 66-68] The application of these enzymes for the asymmetric synthesis of optically pure amines is discussed in the following chapter.

1.4.3 ω-Transaminases for the asymmetric synthesis of chiral amines

Transaminases, also known as aminotransferases, are pyridoxal-5'-phosphate (PLP)-dependent enzymes and catalyse the transfer of amino groups. These enzymes are ubiquitous in nature and crucial enzymes in the nitrogen metabolism within all kind of cells.[69]

1.4.3.1 Taxonomy of transaminases

According to the Enzyme Commission (EC) classification transaminases belong to the main class of transferases (EC 2).[30] Enzymes transferring an amine group are summarised in group EC 2.6.1, which is currently further divided in 101 subgroups[70] (EC 2.6.1.X) regarding their substrate specificities (like EC 2.6.1.1: aspartate transaminases, EC 2.6.1.2: alanine transaminases…). For a detailed classification, transaminases are sorted concerning fold types, sequence similarities, regio- and stereospecificities in different groups and classes.[71-73]

Transaminases require the cofactor pyridoxal-5'-phosphate (PLP). In general, PLP-dependent enzymes are grouped by their three-dimensional structure similarities in seven folding types (I–VII). However, transaminases can only be found in fold type I ("aspartate transaminase fold") and fold type IV ("D-alanine transaminase fold").[74, 75]

Table 1-1: Selected examples for classification of transaminases (TA) and their main amine donor/acceptor pairs[71-73]

fold type: classification based on three-dimensional structure
TA class: sorted by structure similarities

fold type	TA class	region specificity	enzyme EC name	main donor	main acceptor
I	I/II	α	aspartate TA	L-aspartate	oxaloacetic acid
		α	alanine TA	L-alanine	pyruvate
		α	aromatic TA	L-aromatic amino acids	α-keto glutarate
I	III	α	ornithine TA	ornithine	α-keto glutarate
		β	β-aminocarboxylic acid TA	β-aminocarboxylic acid	pyruvate
		γ	γ-aminobutyrate TA	γ-aminobutyrate	α-keto glutarate
		ω	(*S*)-selective ω-TA or amine TA	(*S*)-α-methyl-benzylamine	pyruvate
IV	IV	α	D-amino acid transaminases	D-amino acid	α-keto glutarate
		α	branched-chain amino acid TA	L-valine, L-(iso)leucine	α-keto glutarate
		ω	(*R*)-selective ω-TA or amine TA	(*S*)-α-methyl-benzylamine	pyruvate
I	V	α	(phospho)serine TA	L-(phospho)serine	pyruvate
I	VI		sugar amino TA	amino sugars	α-keto glutarate

Beside the three-dimensional structure, transaminases are divided by primary structure similarities into six classes (I-VI).[71] Often, sequence similarities correlate well with substrate specificities. Enzymes in classes I, II and V catalyse the transfer of an amino acid to a keto acid and are to a great extend involved in the amino acid metabolic pathway. In class III, transaminases are listed which accept substrates

with no acid group in α-position to the respective keto- or amino function. To this class belong non-α-amino acid transaminases such as the ornithine- or the γ-aminobutyrate transaminase and ω-transaminases (also called amine transferases). Class IV contains enzymes which accept substrates in different configurations. While branched-chain amino acid transaminases only accept L-amino acids like L-leucine, D-amino acid transaminases (such as D-alanine transaminase) and (*R*)-selective amine transferases (like the (*R*)-amine pyruvate transaminase from *Arthrobacter* sp.[76]) have also been described. Enzymes transferring amino groups from amino sugars are summarised in class VI.[71, 73]

A more general way for the classification of transaminases is the division in α-, β-, γ- and ω-transaminases concerning their regiospecificity.[72, 73, 77] α-Transaminases only accept substrates with an amino group in α-position to a carbonyl group, whereas β- and γ-transaminases prefer substrates with amines in β- or γ-position, respectively. In contrast, ω-transaminases catalyse the transfer of amine groups to aldehydes and ketones. However, often only α- and ω-transaminases are distinguished and other enzymes than α- are referred to as ω-transaminases.[66, 71, 72]

Moreover, transaminases can be distinguished regarding their stereoselectivity in D- or L-selective amino acid transaminases and (*S*)- or (*R*)-selective ω-transaminases, respectively.[66, 71, 72]

1.4.3.2 Reaction mechanism and stereoselectivity

The reaction mechanism of all PLP-dependent enzymes can be divided in two half reactions. In general PLP-dependent oxidoreductases, transferases, hydrolases, lyases and isomerases share a common initial deprotonation step, followed by different subsequent reaction steps.[69]

For transaminases, the first half reaction comprises three major steps (see scheme 1-4). First, an internal Schiff base (internal aldimine) between the PLP and the ε-amino group of a lysine is replaced by the reaction of an amine donor and the PLP (external aldimine). In the second step, the α-proton is abstracted from the aldimine by the lysine to form a quinoide intermediate, which is then reprotonated to a ketimine. In the final step of the first half reaction hydrolysis of the ketimine releases the keto co-product and the aminated pyridoxamine-5'-phosphate (PMP).

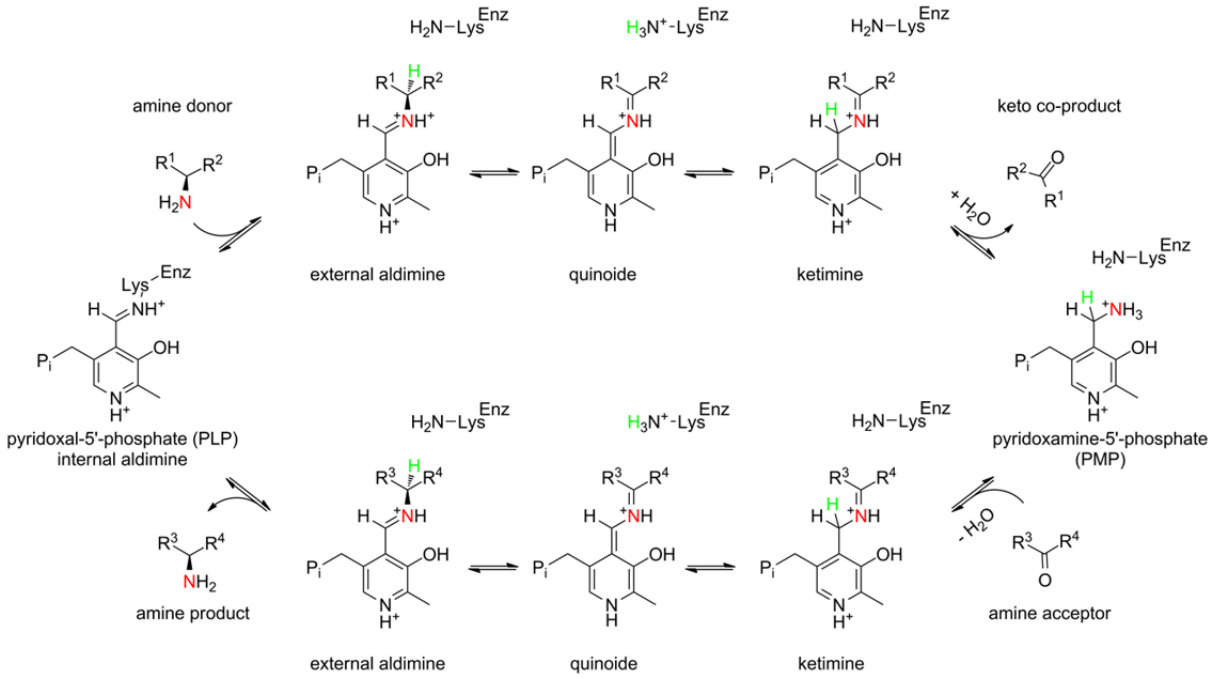

Scheme 1-4: Reaction mechanism of transaminases[71, 78-80]

The steps of the second half reaction take place in reverse order relative to the first half reaction. The amine group of PMP is transferred to an amine acceptor, which finally results in the release of the corresponding amino product and regenerated PLP in its internal aldimine form. The mechanistic model of transaminases is called ping-pong bi-bi mechanism.[71, 78-80]

ω-transaminases are only active as homodimers or higher-ordered oligomers since the active site is located at the interface of two monomers.[66] The stereoselectivity of transaminases is determined by the relative orientation of the residues attached to the external aldimine (see R^1 and R^2 in scheme 1-4). This orientation is a consequence of the active site structure, which determines the transition states' stabilities. Most of the known crystal structures of transaminases show two binding pockets with different capacities ("large" L and "small" S binding pocket) for the stabilisation of these residues in the active site (see scheme 1-5). In (*R*)- and (*S*)-selective ω-transaminases, the orientation of these binding sides are inverted. Therewith, the resulting amine is either formed in the (*R*)- or (*S*)-configuration, respectively (see scheme 1-5).[69, 71, 72, 81]

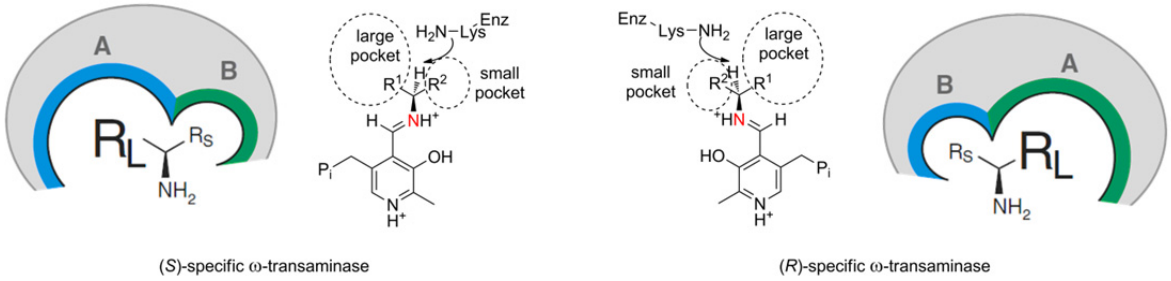

Scheme 1-5: Stereoselectivity of (*S*)- and (*R*)-selective ω-transaminases

1.4.3.3 Screening for ω-transaminase activity

When ω-transaminases became a hot-topic in industrial and academic research, the development of screening assays for a fast identification and characterisation of enzymes with novel properties was required. Meanwhile, various screening assays, each specific for different applications, are available.[66, 82]

Screening assays specific for α-transaminases, like the glutamate-/malate dehydrogenase assay (scheme 1-6-a)[83], are often based on the conversion of one amino acid or keto acid, respectively. If ω-transaminases accept these substrates, a screening with ketones/amines as co-substrates is feasible. Most of the known assays are based on this principle. The first screening assay for ω-transaminase was developed by Kim and co-workers. When a α-keto acid (such as pyruvate) is used as an amine acceptor, the resulting amino acid can be quantified by a coloured copper/amino acid complex (scheme 1-6-b).[84] Bornscheuer and co-workers published a conductivity screening assay based on the production of amino acids from α-keto acids (scheme 1-6-c).[85] In another assay, the accumulated amino acid is oxidised to the corresponding imine by an amino acid oxidase (scheme 1-6-d). The co-product, H_2O_2, can be detected colourimetrically when pyrogallol and horseradish peroxidase are added.[86] Moreover, the production of alanine from pyruvate can be used as a growth selection assay when alanine is used as a single nitrogen source (scheme 1-6-e).[87] This assay was used for a high-throughput screening of 85.000 PCR derived variants of the ω-transaminase from *Vibrio fluvialis*.[87]

a) glutamate-/ malate dehydrogenase assay

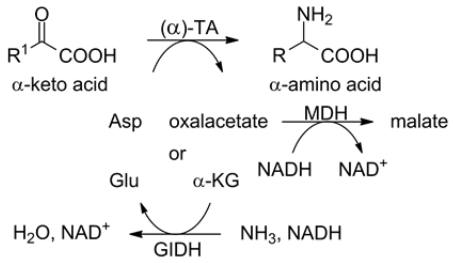

amine acceptors:	any keto acid
amine donors:	aspartate (Asp) and glutamate (Glu)

b) $CuSO_4$ / MeOH based assay

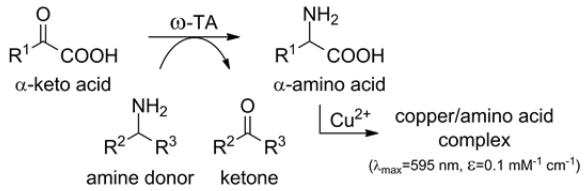

amine acceptors:	any keto acid
amine donors:	any primary amine and β-amino acids

c) conductivity assay

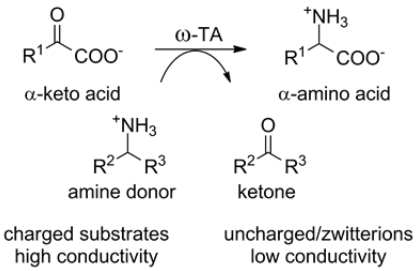

amine acceptors:	any keto acid
amine donors:	any primary amine

d) amino acid oxidase / horse radish peroxidase assay

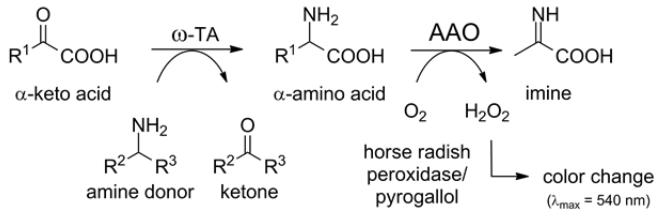

amine acceptors:	different keto acids
amine donors:	any primary amine

e) growth selection assay

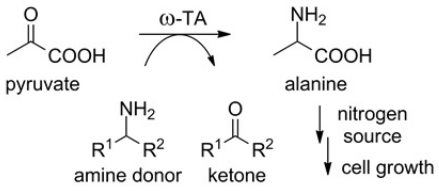

amine acceptors:	pyruvate
amine donors:	any non-toxic primary amine

f) pH indicator assay

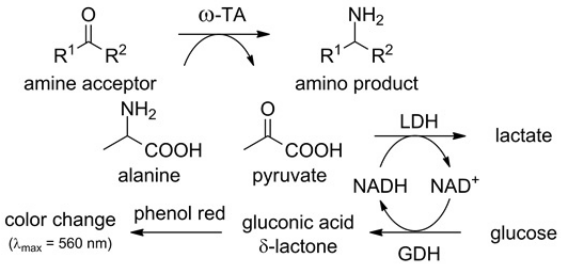

amine acceptors:	any ketone
amine donors:	alanine

g) methylbenzylamine / acetophenone assay

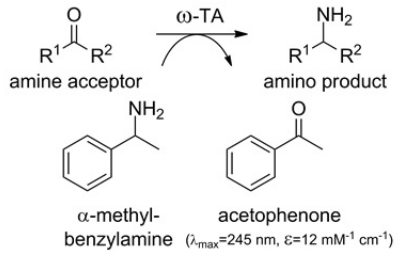

amine acceptors:	any ketone
amine donors:	α-methylbenzylamine

h) aminotetraline / tetralone assay

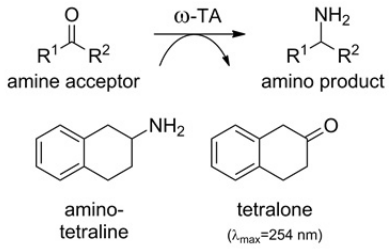

amine acceptors:	any ketone
amine donors:	aminotetraline

Scheme 1-6: Screening assays for ω-transaminases known from literature

α-KG: α-keto glutarate, Asp: aspartic acid, Glu: glutamic acid, MDH: malate dehydrogenase, GIDH: glutamate dehydrogenase, AAO: amino acid oxidase, TA: transaminase, GDH glucose dehydrogenase, LDH: lactate dehydrogenase

Vice versa, when alanine is used as an amine donor, the corresponding pyruvate is measured in a coupled enzymatic reaction combining a lactate dehydrogenase and a glucose dehydrogenase (scheme 1-6-f). Gluconic acid, produced in the cofactor regeneration step, causes a pH shift in the reaction medium which can be detected by a pH indicator.[88] In addition to these amino acid and keto acid based screening assays, Bornscheuer and co-workers developed an assay based on activities towards α-methylbenzylamine (scheme 1-6-g). The corresponding co-product, acetophenone, is detected photometrically at 245 nm.[89] Moreover, a screening assay based on degradation of amino tetralone (scheme 1-6-h) was used for the identification of more active and thermostable variants of the ω-transaminase from *Arthrobacter citreus*.[90]

By development of these screening assays the identification and partial characterisation of different wild type ω-transaminases was supported. Thus, high throughput screening of variant libraries for new enzyme properties was enabled. However, it is obvious that all assays are limited to specific applications. Besides their specific advantageous and drawbacks, they are based either on a specific set of amine donors or amine acceptors. Moreover, only two of the α-methylbenzylamine based assays and the amino tetralone assay do not presuppose enzymatic activity towards keto acids or amino acids, respectively. The development of novel screening assays with properties like high reliability, screening for enantioselectivity, independent substrate sets and high throughput compatibility is mandatory for future investigations and improvements of ω-transaminases.[82]

1.4.3.4 History, availability and substrate range of ω-transaminases

The very first application of ω-transaminases in chiral amines synthesis was published 1990 by the American company Celgene.[91] This example prompted research in academia to focus on the potential of these biocatalysts. Pioneering work was done by Shin and Kim in the late 1990s.[64, 92-94] They discovered ω-transaminases activity in microorganisms from soil samples, such as *Bacillus thuringiensis* and *Klebsiella pneumonia*.[93] In 1999, asymmetric synthesis with the (*S*)-selective ω-transaminase from *Vibrio fluvialis* was demonstrated.[64] This enzyme was purified and characterised in 2003 and crystallised in 2010.[95, 96] Meanwhile the potential for biotechnological applications has been broadly demonstrated[87, 97-100]

and pilot-plant scale applications in a packed-bed reactor[101] and a membrane reactor[102] were shown. Ward and co-worker performed a BLAST-based sequence homology search based on the protein sequence of the *V. fluvialis* ω-transaminase. Among a number of different novel wild type enzymes, the (*S*)-selective ω-transaminase CV2025 (or *Cv*-(*S*)TA) from *Chromobacterium violaceum* enlarged the application platform of ω-transaminase enormously due to its broad substrate range.[103]

More than 30 (*S*)-selective ω-transaminase are nowadays described in literature,[67] whereas the number of non-public available enzymes (especially in industry) is possibly much higher.[68] The gap of missing (*R*)-selective enzymes was initially closed by the identification of the ω-transaminase from *Arthrobacter* sp. KNK168.[76] This very potent wild type enzyme was engineered by Saville *et al.* for the asymmetric synthesis of the bulky-bulky substrate sitagliptin.[104] Moreover, 17 novel (*R*)-selective ω-transaminase have been identified by Höhne and Bornscheuer in 2010 via sequence alignment.[81] This discovery represents a significant contribution to the (*R*)-selective catalyst toolbox.

Nowadays, a broad substrate spectrum is covered by commercially available and literature-known ω-transaminases. Selected examples from a large list of compounds (recently published in several reviews[66, 68, 71]) are presented in scheme 1-7.

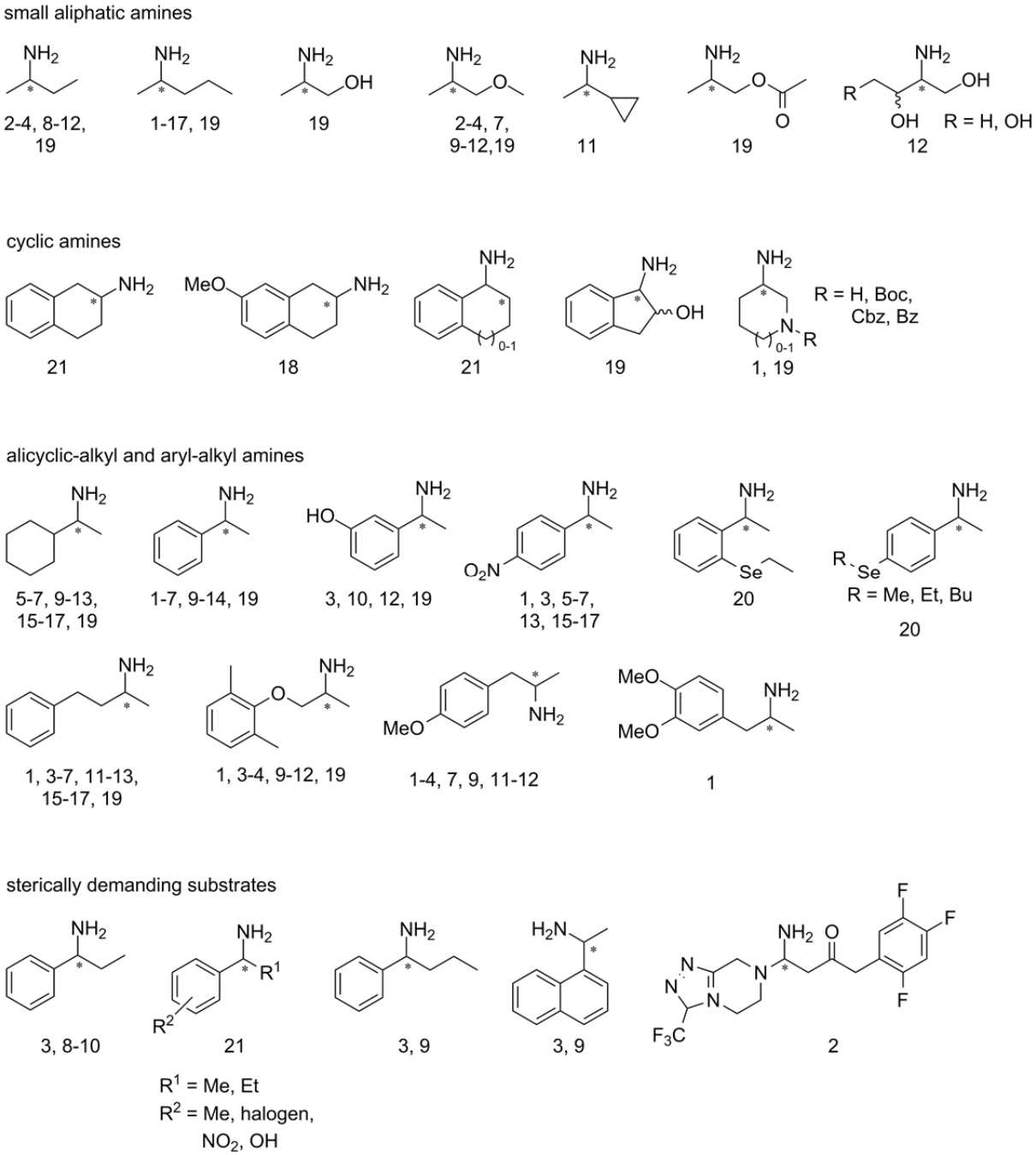

Scheme 1-7: Selected examples for the large substrate platform of chiral amines accepted by ω-transaminases (adapted with permission from reference [66, 68, 71])

Numbers 1-21 belong to selected ω-transaminases - (*R*) or (*S*) represents the stereoselectivities:

1: *Alcaligens denitrificans* (*S*); 2: *Ar*Rmut11* (*R*); 3: *Arthrobacter* sp. (*R*); 4: *Arthrobacter citreus* (*S*); 5: *Aspergillus fumigatus* (*R*); 6: *Aspergillus oryzae* (*R*); 7: *Aspergillus terreus* (*R*); 8: ATA-103** (*S*); 9: ATA-113** (*S*); 10: ATA-114** (*S*); 11: *Bacillus megaterium* (*S*); 12: *Chromobacterium violaceum* (*S*); 13: *Gibrella zeae* (*R*); 14: *Hyphomonas neptunium* (*R*); 15: *Mycobacterium vanbaalenii* (*R*); 16: *Neosartoya fischeri* (*R*); 17: *Penicilium crysogenum* (*R*); 18: *Pseudomonas fluorescens* (*S*); 19: *Vibrio fluvialis* (*S*); 20: other Celene, Codexis ATAs (see ref [66]); 21: ATA-117** (*R*)

* *Ar*Rmut11: 11-fold mutant of the Codexis transaminase ATA-117* (see ref. [104])

** ATA-XX: ω-transaminase nomenclature by Codexis (ATA: amine transaminases)

1.4.3.5 Reaction equilibrium – a challenge for ω-transaminases reactions

As mentioned above, transaminase catalysed reactions follow a ping-pong bi-bi mechanism consisting of two half reactions.[71, 78-80] Both half reactions have independent half reaction equilibrium constants (K_1 and K_2). The reaction equilibrium constant of the overall reductive amination step (K_{eq}) is given by the product of both half reaction constants (equation 1-1).

$$K_1 = \frac{[\text{keto co-product}]}{[\text{amine donor}]} \quad and \quad K_2 = \frac{[\text{amine product}]}{[\text{amine acceptor}]}$$

$$\Rightarrow K_{eq} = K_1 \cdot K_2 = \frac{[\text{keto co-product}] \cdot [\text{amine product}]}{[\text{amine donor}] \cdot [\text{amine acceptor}]}$$

Equation 1-1: Two independent reaction equilibrium constants of the first and the second half reaction (K_1 and K_2) contribute to the overall thermodynamic reaction equilibrium of the transaminase reaction (K_{eq})

A well-known problem for the application of ω-transaminases in processes is the low equilibrium constant of the overall reaction.[66, 68, 105] As a first example, Shin and Kim calculated the reaction thermodynamics for the syntheses of α-methylbenzylamine and pyruvate from acetophenone and alanine (scheme 1-8). The reaction equilibrium constant lies towards the substrate side (K_{eq} = 8.81·10^{-4}).[94] An easy and reliable experimental method to determine the equilibrium constant of ω-transaminase catalysed reactions was published by Woodley and co-workers in 2012.[105] As was known before, their studies demonstrate that the choice of the amine donor significantly influences the theoretical maximal conversion of the overall reaction due to the independent half reaction thermodynamics. E.g. for the same amine acceptor, a much higher conversion is achieved if α-methylbenzylamine is used instead of alanine. To shift the reaction equilibrium, an excess of the amine donor can be used if no substrate inhibition occurs and if the amine donor is inexpensive. This concept is often applied when isopropylamine can be used.[67]

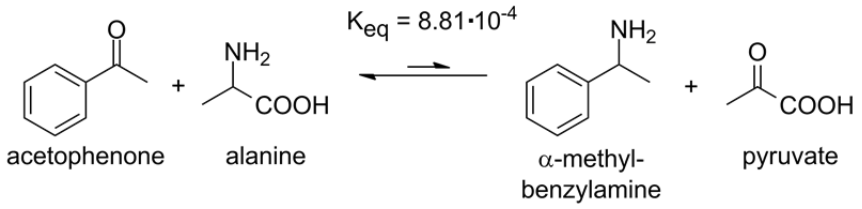

Scheme 1-8: Example of an equilibrium limitation in chiral amine synthesis.[94]

Moreover, the reaction can be shifted to completion when the product (either the amine or the keto co-product) is removed. Since this is a general issue, different chemical, enzymatic and reaction engineering approaches have been developed. These techniques have been summarised in several reviews.[66, 68, 105, 106]

The amine product can be removed e.g. by addition of an ion exchange resin to the reaction solution, which removed the amine reversibly from the reaction by binding it to the resin (scheme 1-9).[107] Moreover, a spontaneous follow-up reaction of the amine product (e.g. like an intra-molecular cyclisation[107, 108]) or another simultaneous chemical/enzymatical reaction can shift the reaction, if these additional reactions are feasible and/or desired.

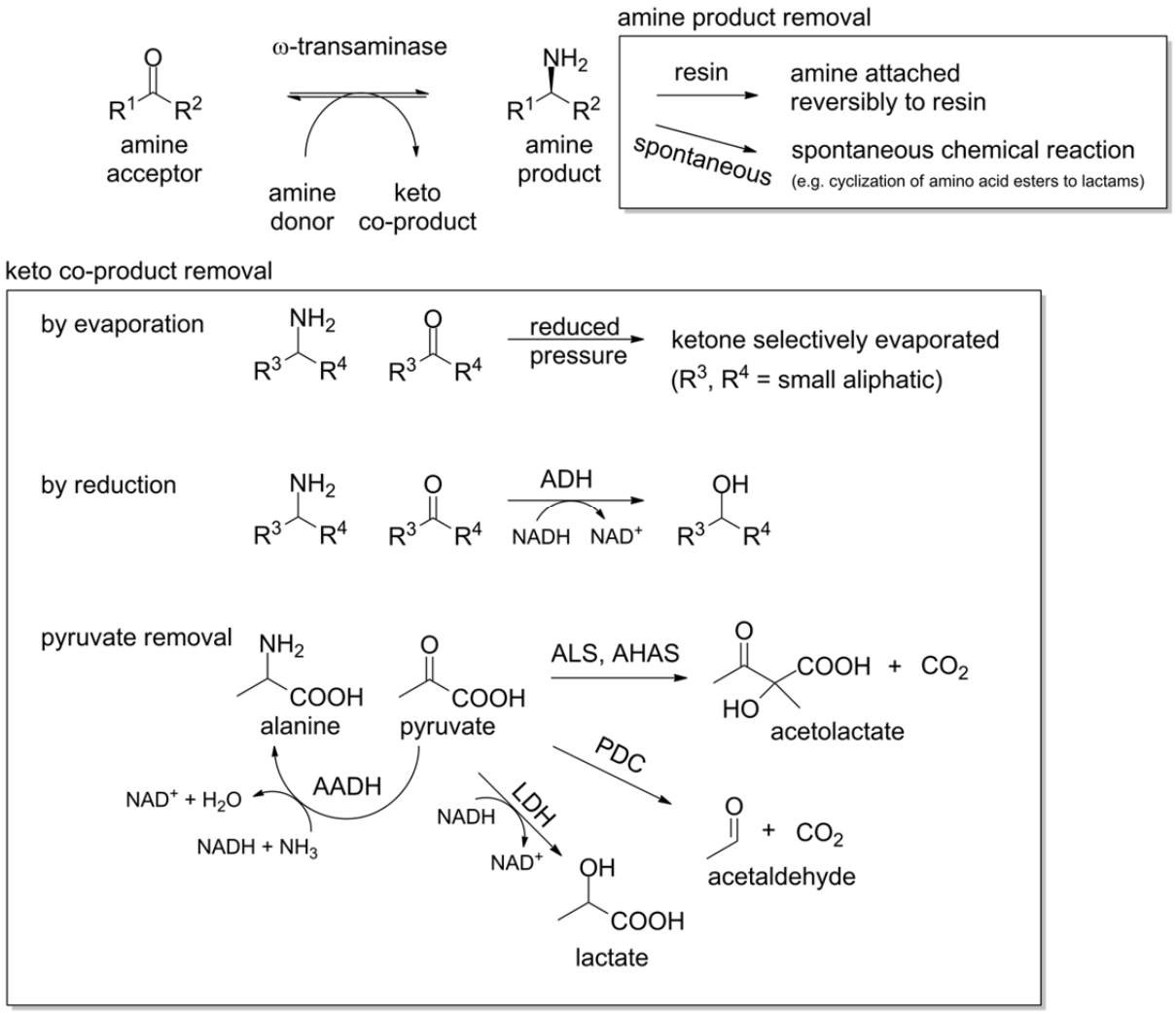

Scheme 1-9: Possibilities to shift the reaction equilibrium for ω-transaminase catalysed reductive amination reactions – (adapted with permission from reference [66]).

ADH: alcohol dehydrogenase, ALS: acetolactate synthase, AHAS: acetohydroxyacid synthases, PDC: pyruvate decarboxylase, LDH: lactate dehydrogenase, AADH: amino acid dehydrogenase

Often more generally applicable is a removal of the keto co-product. If small aliphatic amine donors (like isopropylamine[109] or butylamine[110]) can be used, it is possible to remove the corresponding ketones by evaporation under reduced pressure.[66, 109, 110] Moreover, reduction of the co-product acetophenone by alcohol dehydrogenases (ADH) shifts the reaction equilibrium e.g. when α-methylbenzylamine is used.[111] However, in this setup additional cofactor regeneration is required. A very well characterised and frequently applied method is enzyme-catalysed pyruvate removal using alanine as amine donor (see scheme 1-9).[66, 82] The equilibrium can be shifted by the addition of lactate dehydrogenases (LDH), pyruvate decarboxylases (PDC), acetolactate synthases (ALS) or acetohydroxyacid synthases (AHAS) and amino acid dehydrogenases (AADH), respectively. In general, enzyme-catalysed co-product removal is a suitable alternative to prevent high co-substrate concentrations. However, in all the described enzyme-based equilibrium shift reactions the addition of at least one further enzyme (or two, if additional cofactor regeneration is required) increases system complexity and reaction costs.

1.5 Chiral vicinal amino alcohols – valuable products from inexpensive starting materials

1.5.1 Synthetic strategies for valuable vicinal alcohols

The motif of vicinal (often also referred to as 1,2-) amino alcohols can be found in a variety of natural products, biologically active compounds and ligands and auxiliaries used in organic synthesis.[112-115] Since such compounds can contain two vicinal stereogenic centres, chirality plays an important role for amino alcohols used in asymmetric synthesis (such as Evans' chiral auxiliaries[115-117], oxaborolidines[118] or ephedrine derivatives[119-122]) as well as for those with pharmaceutical properties. Selected examples are highlighted in scheme 1-10.

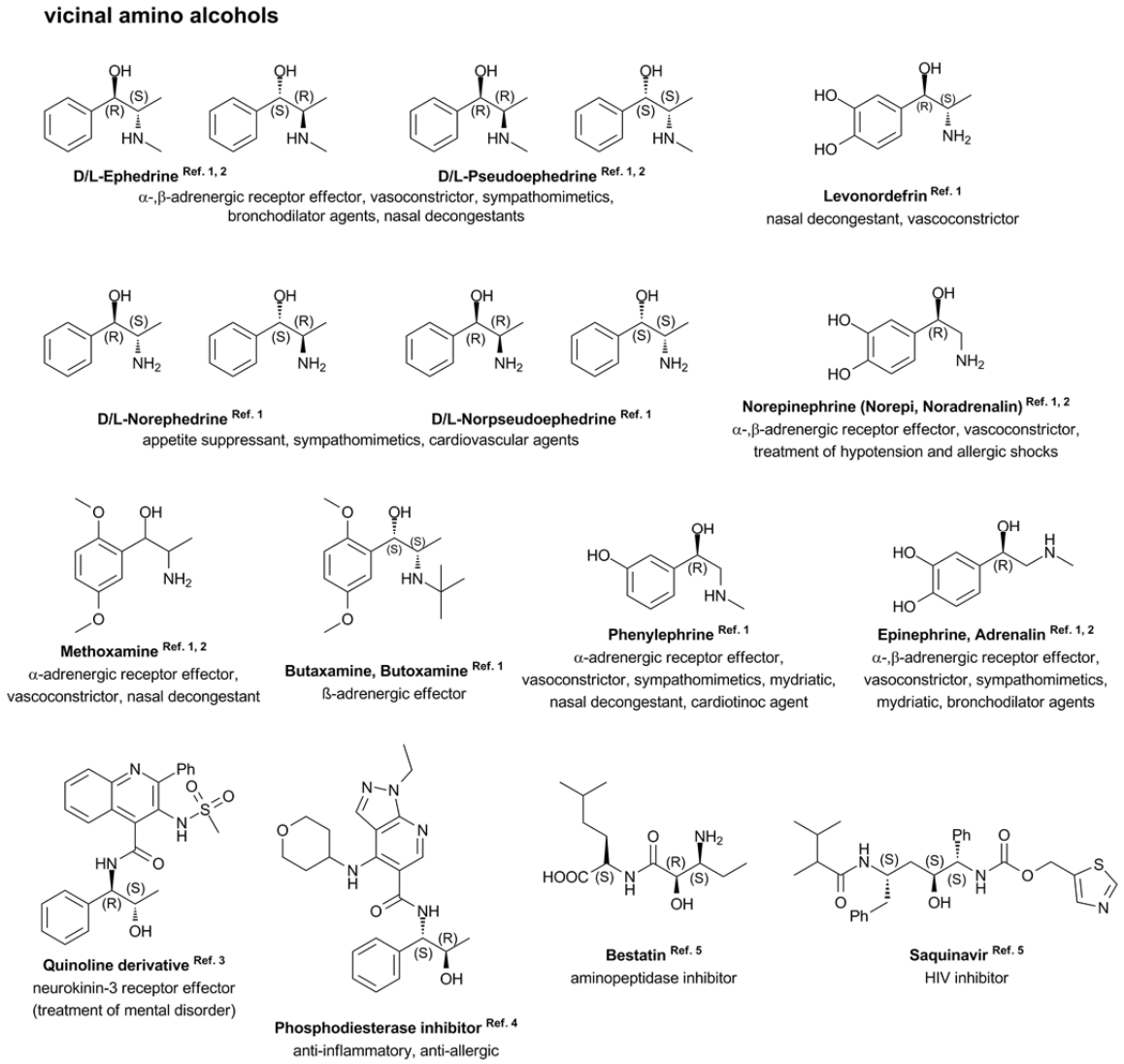

Scheme 1-10: Selected examples of pharmaceutically active compounds with vicinal amino alcohol motifs – (adapted with permission from reference [123])
References: Ref. 1: [124]; Ref. 2: [125]; Ref. 3: [126]; Ref. 4: [127]; Ref. 5:[113]

1.5.2 Synthetic routes towards chiral vicinal amino alcohols - chemical and enzymatic methods

Numerous chemical methods for the synthesis of chiral vicinal amino alcohols have been described in literature (see scheme 1-11).[112, 113, 128] Frequently used methods are based on functional group manipulation of molecules with two heteroatoms (such as addition of nucleophiles to α-hydroxy imines or α-amino aldehydes, reductive amination of α-hydroxy ketones and reduction of α-amino ketones). Moreover, oxygen/nitrogen heteroatom addition, Sharpless or Davies aminohydroxylation of olefins, ring opening of epoxides and acylaziridines or coupling reactions were

described.[113, 128] Especially in case of primary vicinal amino alcohols, the number of pure chemical syntheses reported with high yields, high optical purities and high regioselectivities is still rare or require multistep strategies.[112, 114]

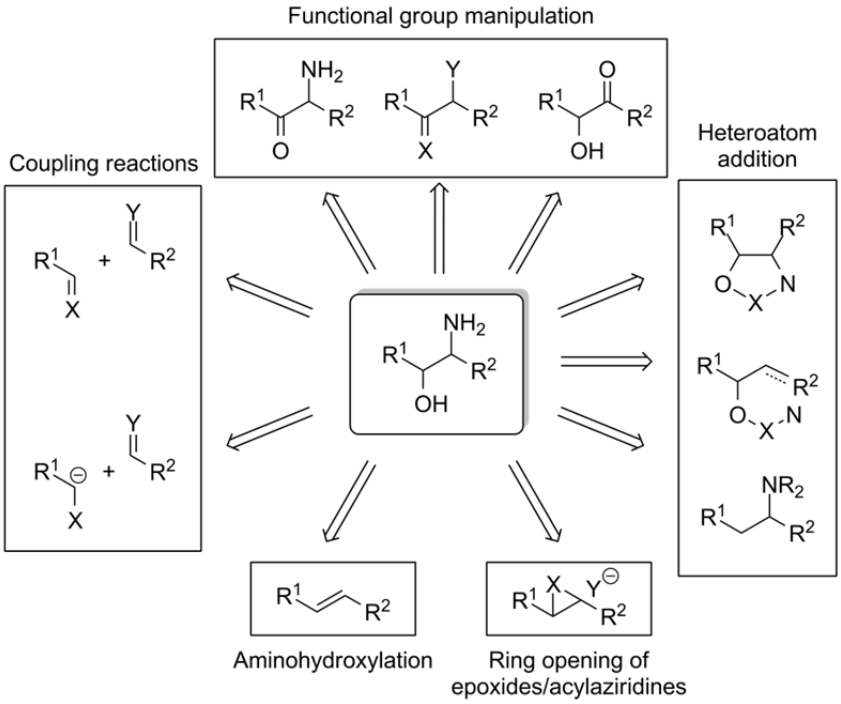

Scheme 1-11: Chemical synthesis of primary vicinal amino alcohols (adapted references [113, 128])

Various enzymatic or chemo-enzymatic synthesis routes have been published to access vicinal amino alcohols (scheme 1-12). A well-known example is the two-step synthesis of L-ephedrine patented by Hildebrandt and Hirsch from 1930,[129] which is still utilised to produce 120 t a^{-1}.[130] In the first step (*R*)-phenylacetylcarbinol is generated via fermentation with baker's yeast in the presence of benzaldehyde. Here, a pyruvate decarboxylase catalyses carboligation of pyruvate with benzaldehyde yielding (*R*)-phenylacetylcarbinol (scheme 1-12; strategy 1). Subsequently, L-ephedrine is formed by a chemical diastereoselective reductive amination with methylamine. Moreover, a chemo-enzymatic three-step synthesis of enantiomerically pure (1*R*,2*R*)-1-amino-2-indanol (*ee*, *de* >98 %) via chemical acetoxylation, lipase catalysed ester hydrolysis and reductive amination by ω-transaminases was published in 2006 (scheme 1-12 - strategy 2).[131] Another outstanding example is the combination of transketolases and ω-transaminases for the synthesis of 2-amino-1,3-diols (scheme 1-12 - strategy 3)[132, 133] such as (2*S*,3*S*)-2-aminopentane-1,3-diol[134] (26 % yield, *ee* >98 %, *de* 61 %) or (2*S*,3*S*)-2-amino-1,3,4-butanetriol[135] (26 % yield, single isomer).

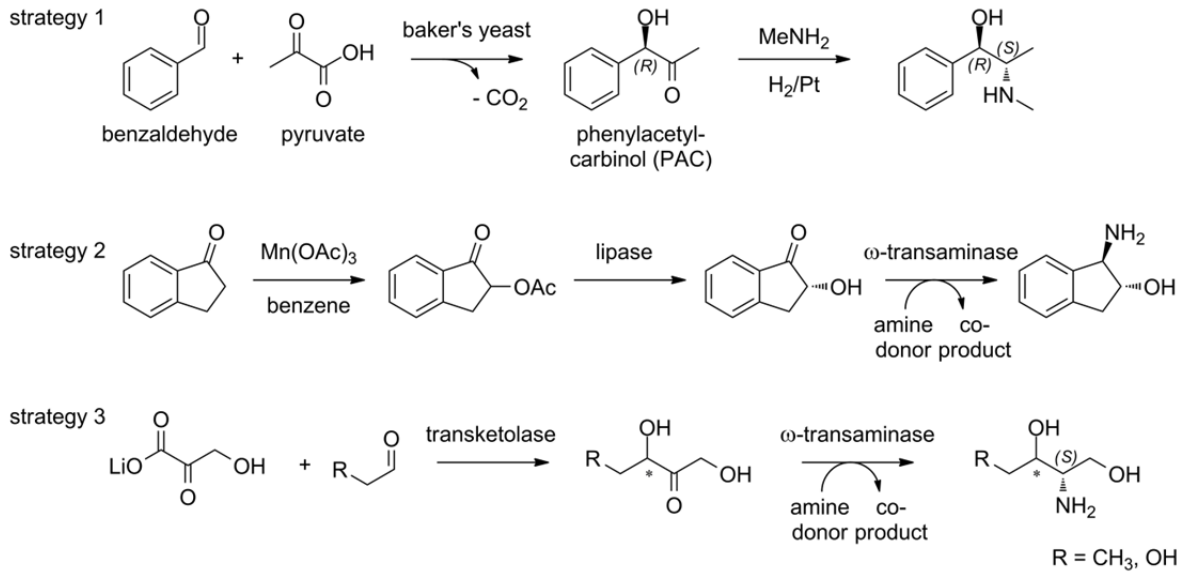

Scheme 1-12: Selected examples for the enzymatic and chemo-enzymatic synthesis of primary vicinal amino alcohols[129-135]

1.5.3 Nor(pseudo)ephedrines – interesting compounds with challenging synthetic strategies

Valuable chiral vicinal amino alcohols with challenging synthesis strategies are the four phenylpropanolamine (PPA) isomers: (1*S*,2*S*)-norpseudoephedrine, (1*R*,2*R*)-norpseudoephedrine (NPE), (1*S*,2*R*)-norephedrine and (1*R*,2*S*)-norephedrine (NE). These compounds belong to the amphetamine family of ephedra alkaloids and are found in plants like *khat* (*Catha edulis*)[136, 137] or in *Ephedra* species[138]. In the human body they are known to have sympathomimetic function[124] by acting as non-selective adrenergic receptor agonists[139] and norepinephrine re-uptake inhibitors[139]. As pharmaceuticals, PPA were used in the beginning of the 20th century for induction of mydriasis (dilation of pupils), to stabilise the blood pressure or as nasal decongestion.[140, 141] In early studies it turned out that PPA exhibits anorectic action therefore it was sold later on as an appetite suppressant[142]. Moreover it has been widely used in cold and flu medications.[143] However in 2000, the “Food and Drug Administration” (FDA) recommended that PPA should no longer be available for over-the-counter use[144], since permanent uptake increases the risk of haemorrhagic stroke[145-147]. Therefore, PPA was removed as an over-the-counter drug in most countries, but is still available on prescription.[148] On the German market, Cathine ((1*S*,2*S*)-norpseudoephedrine) is currently sold as the main drug in ALVALIN®

provided by the RIEMSER Pharma GmbH, which is sold as an appetite suppressant for short-term use.[149-151]

Beside the pharmacological interest, the four phenylpropanolamine stereoisomers are used as valuable synthons, ligands and chiral auxiliaries in various organic syntheses.[126, 127] A SciFinder® search (with unspecified stereochemistry in both stereogenic centres) resulted in 5071 different reactions where nor(pseudo)-ephedrines are used as reactants.[152] Selected examples from the large list of applications with optical pure N(P)E are the synthesis of a neurokinin-3 receptor antagonist (treatment of mental disorder)[125] and a phosphodiesterase inhibitor (anti-inflammatory, anti-allergic)[126] (scheme 1-10). Many more products derived from N(P)E can be found in literature.

As already specified in chapter 1.5.2, the enantiomerically and diastereomerically pure synthesis of primary vicinal amino alcohols is often challenging and the nor(pseudo)ephedrines do not represent an exception. Only optically pure (1*S*,2*S*)-NPE is currently sold as natural product isolated from *khat shrub* (Arabia, Ethiopia)[153]. For all four stereoisomers currently 355 different synthesis strategies with N(P)E as final products were described in SciFinder®.[152] However, only few of these strategies result in N(P)Es with good optical purities (*ee*, *de* >98 %). The number of routes decreases significantly when asymmetric synthesis is the method of choice. Some prominent methods have recently been reviewed[154] (scheme 1-13): (1*S*,2*S*)-NPE can be synthesised in eight steps from an chloramphenicol synthesis intermediate with excellent *ee* and *de* (>99 %)[155] in three steps with a *de* of 82 %[156]; (1*R*,2*R*)-NPE is accessible in five steps to with 82 % *ee*[157] or as a by-product in the Sharpless aminohydroxylation with an *ee* of 74 %[158, 159]; (1*S*,2*R*)-NE was synthesised in two chemical steps with an *ee* of 86 %[160], in a chemo-enzymatic reaction from benzaldehyde and nitroethane using a hydroxynitrile lyase (from *Hevea brasiliensis*) and H_2 reduction to give an *ee* ~95 % and a *dr* of 9:1[161] or by baker's yeast and $LiAlH_4$ reduction in *ee* ~95 % and a of *dr* of 9:1[162]; or (1*R*,2*S*)-NE in one step with a moderate *ee* of 76 %[163].

The methods reported for asymmetric syntheses of nor(pseudo)ephedrines, require either multi-step preparative routes, are based on relatively expensive reagents, or in particular lack high enantio- and diastereomeric puritiy.

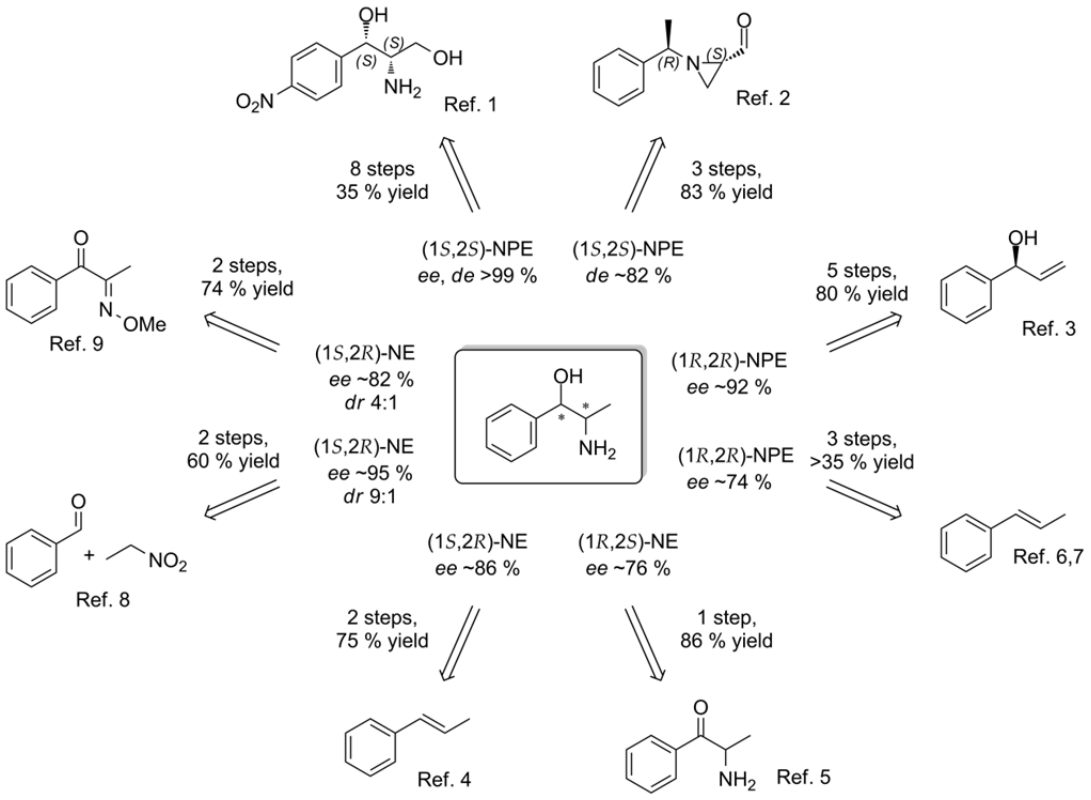

Scheme 1-13: Selected examples for the synthesis of nor(pseudo)ephedrines
Ref. 1 [155], Ref. 2 [156], Ref. 3 [157], Ref. 4 [160], Ref. 5 [163], Ref. 6 [154], Ref. 7 [155], Ref. 8 [161], Ref. 9 [162]

In 2012, a novel and highly stereoselective method was described for the synthesis of all four phenylpropanolamine isomers in high optical purities (*ee*, *de* >99 %).[154] Norephedrine isomers were accessible in four steps (40 % yield) and norpseudoephedrine in seven steps (35 % overall yield) starting from 2-phenyl-2-trimethylsilyloxyacetonitrile (scheme 1-14). However, a multi-step reaction protocol with several isolation and protection/deprotection steps is required.

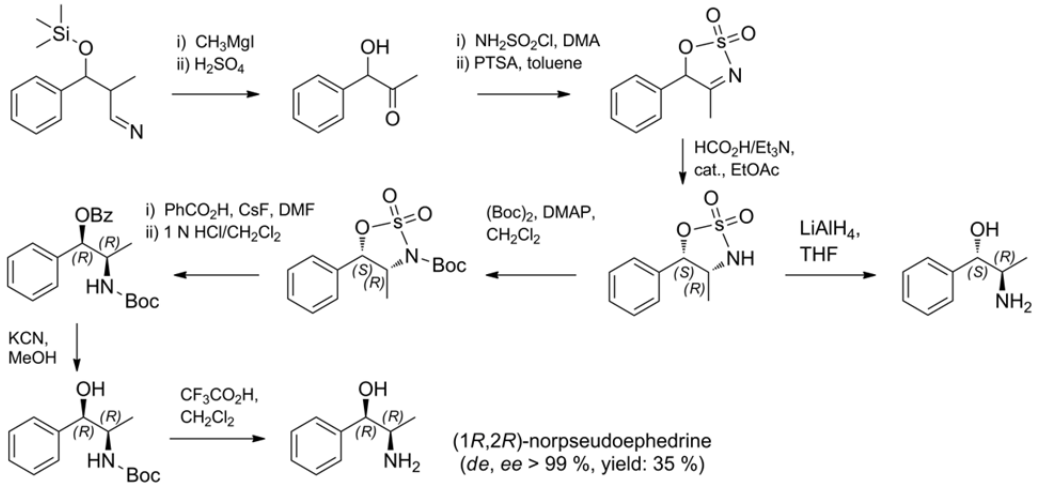

Scheme 1-14: Chemical synthesis strategy for all four nor(pseudo)ephedrine isomers in excellent optical purities of *ee*, *de* >99 % (here, (1*R*,2*R*)-NPE is shown)[154]

1.5.4 Nor(pseudo)ephedrine synthesis – what we can learn from nature

As mentioned in chapter 1.5.3, phenylpropanolamines can be found in plants. In 2011, the biochemical pathway (see scheme 1-15) of these and other phenylpropylamino alkaloids was published for *khat* (*Catha edulis*)[136] and in 2012 for some plants of *Ephedra* species[138].

In both types of plants, the suggested synthetic pathway contain benzaldehyde as an intermediate, which is derived from L-phenylalanine via non-oxidative deamination by a phenylalanine ammonia lyase and subsequent aldol cleavage by a benzaldehyde carboxyligase. In *khat*, a dehydrogenase catalyses the oxidation of benzaldehyde to benzoic acid and a thiamine diphosphate (ThDP)-dependent enzyme catalyses the carboligation with pyruvate to 1-phenylpropane-1,2-dione. In *Ephedra* species a reverse order of oxidation and carboligation was suggested. Here, hydroxypropiophenone and/or phenylacetylcarbinol (PAC) is synthesised from benzaldehyde first and a dehydrogenase catalyses the oxidation to 1-phenylpropane-1,2-dione. In both cases, this intermediate is transformed into (*S*)-cathinone by an (*S*)-selective ω-transaminase. In the last step of the (1*S*,2*S*)-norpseudoephedrine and (1*S*,2*R*)-norephedrine biosynthesis, either an (*S*)- or (*R*)-selective dehydrogenase reduces the keto group to an (*S*)- or (*R*)-configured alcohol (see scheme 1-15).

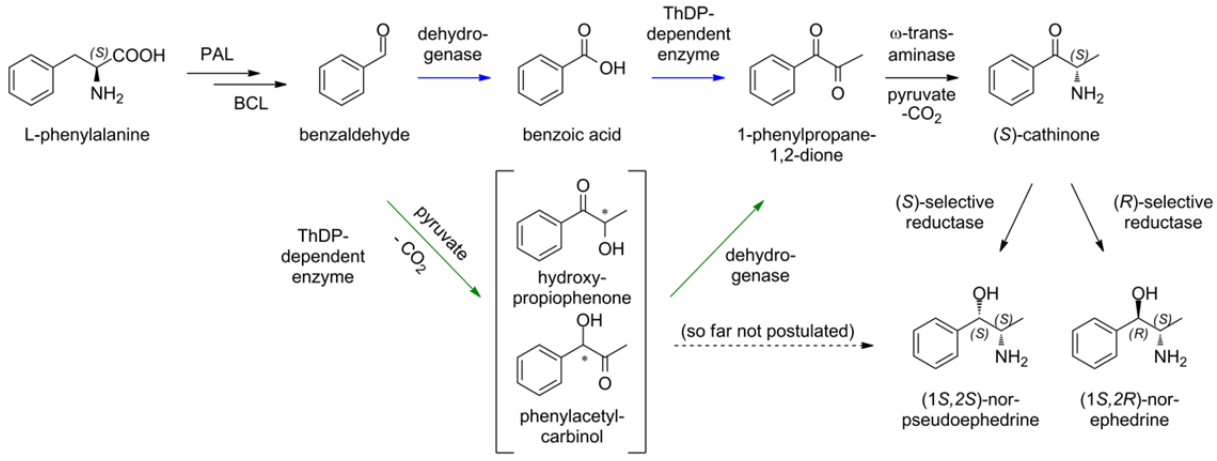

Scheme 1-15: Biochemical synthesis pathway of phenylpropanolamines.
Presented is the biosynthesis pathway of (1*S*,2*S*)-norpseudoephedrine and (1*S*,2*R*)-norephedrine in the plant *khat*[135] (synthesis via benzoic acid - blue arrows) and in *Ephedra* species[138] (synthesis via hydroxypropiophenone and phenylacetylcarbinol - green arrows). The synthesis of N(P)E from phenylacetylcarbinol in *Ephedra* species (dashed arrow) was so far not postulated.[138]

PAL: phenylalanine ammonia lyase, BCL: benzaldehyde carboxyligase, ThDP: thiamine diphosphate

The two biosynthetic intermediates 1-phenylpropane-1,2-dione (cheapest catalogue price: 0.73 € g^{-1})[164] and benzaldehyde (cheapest catalogue price: 0.006 € g^{-1})[165] are commercially available and moreover relatively inexpensive. Looking at the "trick" from nature, two independent asymmetric synthesis strategies for the production of phenylpropanolamines from these intermediates are conceivable (scheme 1-16).

The first strategy encompasses the reductive amination of 1-phenylpropane-1,2-dione by an ω-transaminase. The subsequent reduction of cathinone by a dehydrogenase gives access to nor(pseudo)ephedrine (scheme 1-16-A). Starting from benzaldehyde in the second strategy, a carboligation with (decarboxylated) pyruvate in the first reaction step generates phenylacetylcarbinol. As suggested by the biosynthetic pathway hypothesis, in the next step the already introduced stereochemistry might be removed by oxidation and two subsequent steps would be required to introduce stereochemistry again (see scheme 1-15). In contrast to this postulated biosynthetic pathway, a direct reductive amination of phenylacetylcarbinol could lead in only one step to the final products (scheme 1-16-B). As described in chapter 1.4.3, ω-transaminases are valuable catalysts for a 'green reductive amination' in this step. However, this has never been described in literature.

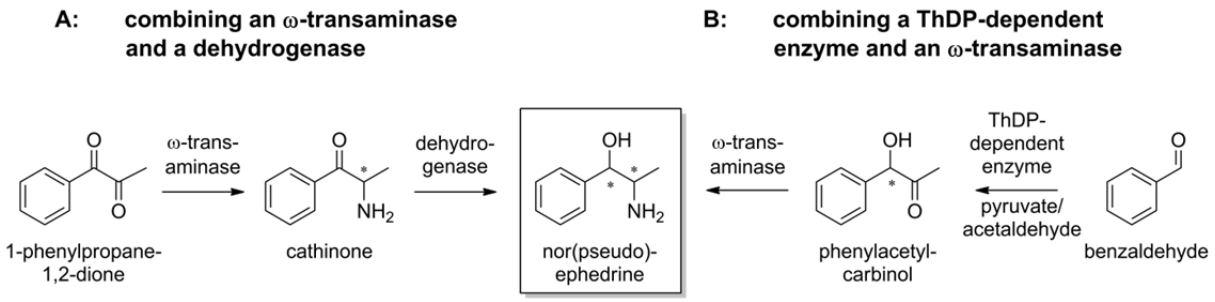

Scheme 1-16: Two novel strategies for the asymmetric synthesis of phenylpropanolamines

A: reductive amination by an ω-transaminase and subsequent reduction by a dehydrogenase opens access to nor(pseudo)ephedrines. **B:** the carboligation of benzaldehyde with (decarboxylated) pyruvate generates phenylacetylcarbinol and in contrast to the postulated biosynthetic pathway (scheme 1-15) an ω-transaminase could catalyse the reductive amination to the desired amino alcohol. With highly selective enzymes in all steps, theoretically all four nor(pseudo)ephedrine isomers should be accessible in high purities.

Both synthesis strategies could theoretically give access to all four nor(pseudo)-ephedrine isomers. If highly selective enzymes are used in all steps, high optical purities of all compounds might be achievable. However, these novel synthesis strategies are described within this thesis for the first time.

1.5.5 Availability of enzymes for biocatalytic synthesis of nor(pseudo)-ephedrines

As mentioned above (see chapter 1.5.4), the combination of three different biocatalysts (ω-transaminases, dehydrogenases and ThDP-dependent enzymes) can open up the biocatalytic access for the production of nor(pseudo)ephedrines through respective enzyme cascades.

1.5.5.1 ThDP-dependent enzymes

ThDP-dependent enzymes are involved in many biosynthetic pathways and catalyse the formation and/or breakdown of C–C, C–S, C–N, C–O and C–P bonds.[166] For the formation of nor(pseudo)ephedrine (scheme 1-16-B), enzymes catalysing the highly stereoselective C-C bond formation (also called carboligation) are required. One focus was the access of all possible stereo- and regioisomers products for the ligation of an aromatic and an aliphatic aldehyde (or the corresponding α-keto acids, respectively) with high selectivities (scheme 1-17).

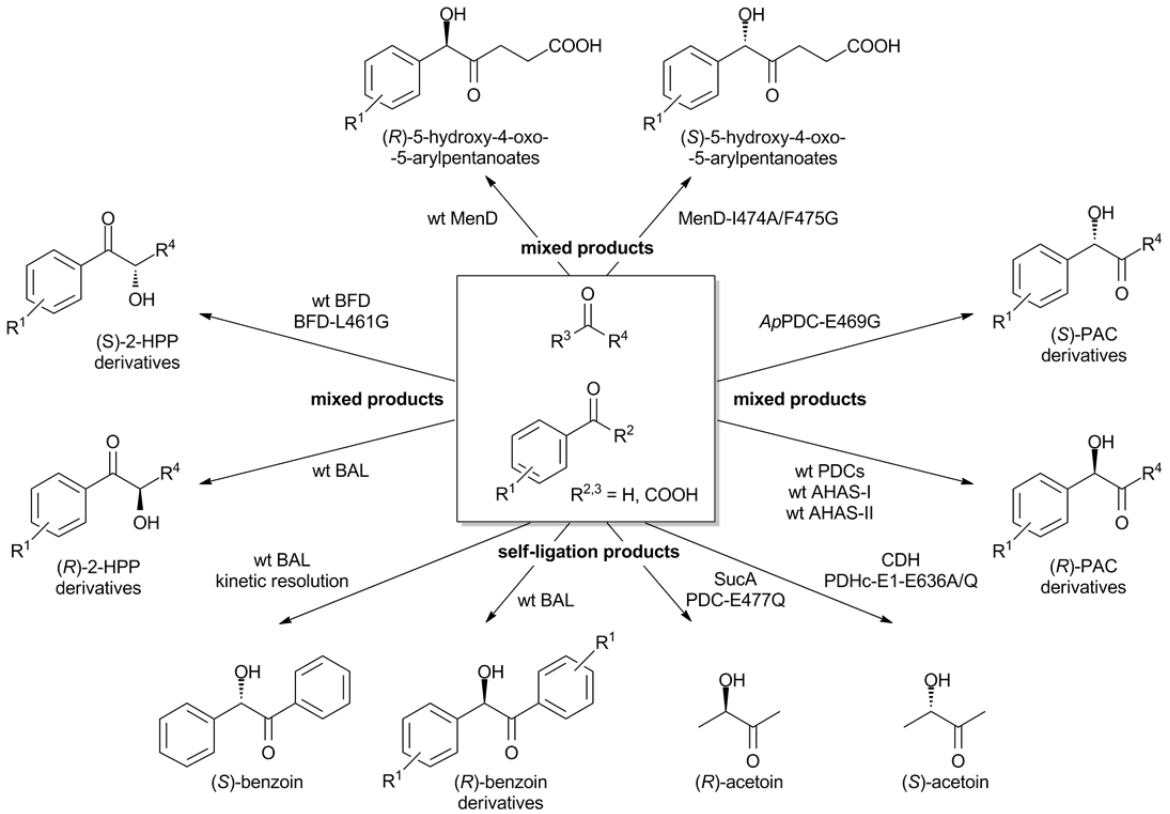

Scheme 1-17: **Examples of the ThDP-dependent enzyme toolbox for the asymmetric synthesis of α-hydroxy ketones.** More details can be found in reviews.[123, 167, 168]

BAL: benzaldehyde lyase (*Pseudomonas fluorescens*), PDC: pyruvate decarboxylase (*Acetobacter pasteurianus*: *Ap*PDC), BFD: benzoylformate decarboxylase (*Pseudomonas putida*), SucA (E1 subunit of the α-keto glutarate dehydrogenase complex in *Escherichia coli*), CDH: cyclohexane-1,2-dione hydrolase (*Azoarcus* sp.), AHAS: acetohydroxyacid synthases (*Escherichia coli*), MenD: 2-succinyl-5-enolpyruvyl-6-hydroxy-3-cyclohexene-1-carboxylate synthase (*Escherichia coli*).

This subclass of ThDP-dependent enzymes was intensively studied within the last decades. Due to this, various wild type enzymes and variants are available for the asymmetric synthesis of α-hydroxy ketones (scheme 1-17).[167-172] The toolbox created in the working group "Biocatalysis and Biosensors" of Prof. Martina Pohl and Dr. Dörte Rother (IBG-1, Forschungszentrum Jülich GmbH, Germany) currently contains 20 wild type enzymes and more than 150 active variants. Three of those ThDP-dependent enzymes have been used in this thesis.

*Ap*PDC-E469G (pyruvate decarboxylase variant from *Acetobacter pasteurianus*)

As its natural function, the wild type *Ap*PDC (EC 4.1.1.1) catalyses the cleavage of pyruvate to acetaldehyde and CO_2 in the oxidative metabolism of *Acetobacter pasteurianus*.[173] In organic syntheses, the enzyme has been used for various carboligation reactions.[168, 169, 174] The carboligation can be performed with aldehydes as well as α-keto acids as donors and benzaldehyde derivatives as acceptors. Since the enzyme is highly (*R*)-selective, an (*S*)-selective variant was generated by a point mutation in the active site of wild type *Ap*PDC, where a glutamate in position 469 was replaced by glycine. This mutation opened up a region in the active site, the so called (*S*)-pocket, allowing for the synthesis of (*S*)-phenylacetylcarbinol (PAC) and derivatives thereof.[174] Compared to the wild type enzyme ($ee_{(R)\text{-PAC}}$ = 97 %), the variant *Ap*PDC-E469G catalyses the synthesis of (*S*)-PAC with an *ee* of 61 % in buffer in the presence of 20 % (v/v) DMSO[174] and with an *ee* of 89 % in the absence of organic solvents[175].

AHAS-I (acetohydroxyacid synthases from *Escherichia coli*)

Acetohydroxyacid synthases (AHAS, EC 2.2.1.6) are found in plants, bacteria, algae and fungi, where they are involved in the biosynthesis of branched-chain amino acids (valine, leucine, isoleucine) and other biosynthetic precursors (like pantothenate and coenzyme A).[176, 177] Besides, the acetohydroxyacid synthase I from *Escherichia coli* (AHAS-I) is known to catalyse also the carboligation of benzaldehyde and (decarboxylated) pyruvate to (*R*)-PAC with high enantioselectivity (*ee* >98 %).[178, 179] Mechanistic studies revealed that first pyruvate is bound to the ThDP cofactor in the active site. After decarboxylation, CO_2 is released from the active site while the hydroxyl-ethyl group remains covalently attached to the C2-atom of the thiazolium-ring in ThDP (hydroxyl-ethyl-ThDP).[179] This acyl group can be ligated with a second

pyruvate molecule acting as acyl-acceptor yielding acetolactate. In contrast to this, (*R*)-PAC is formed if the hydroxyl-ethyl group is transferred to benzaldehyde. The reaction rates for the carboligation towards acetolactate and PAC, respectively, in presence of pyruvate and benzaldehyde (at equal concentrations) indicate that acetolactate is the kinetically favoured product (fast ligation of two pyruvate molecules), while PAC is the thermodynamically favoured product (concentration of acetolactate decreases over the time while PAC is the major product under steady-state conditions).[179] For the carboligation of benzaldehyde and pyruvate the optimal pH-range was found between pH 6.5-8.0.[180]

*Pf*BAL (benzaldehyde lyase from *Pseudomonas fluorescens*)

Due to a benzaldehyde lyase (BAL, EC 4.1.2.38), the gram-negative bacteria *Pseudomonas fluorescens* is able to grow on carbon sources like anisoin or benzoin.[181] Until now, there is no other enzyme known that catalyses the cleavage of benzoins into the respective benzaldehyde derivatives. In terms of carboligation, BAL shows outstanding high activity, a broad substrate range and high (*R*)-selectivities for a broad range of products.[182] One example is the synthesis (*R*)-HPP with an *ee* >99 % and >300 U mg^{-1}.[182] These properties have been used for (*S*)-benzoin production in kinetic resolution mode from racemic benzoin.[183] The concept was further investigated within the PhD thesis of Álvaro Gómez Baraibar, who developed the so called “chiral polishing” of (*S*)-PAC. Starting from moderate optical purity ($ee_{(S)\text{-PAC}}$ ~70 %), (*S*)-PAC is enriched to >97 % *ee* by a *Pf*BAL catalysed kinetic resolution (scheme 1-18).[184]

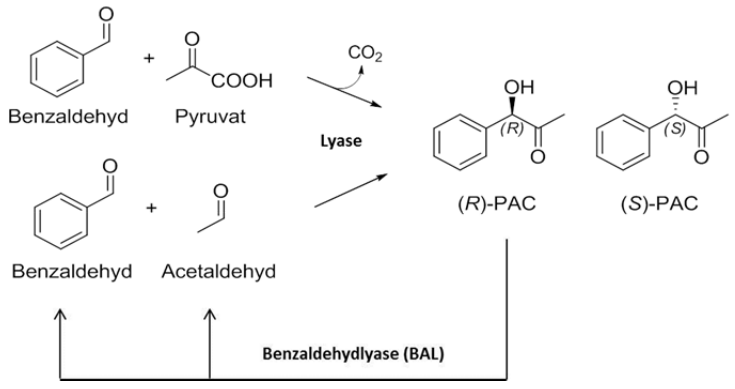

Scheme 1-18: “Chiral polishing” of (*S*)-PAC.
(*S*)-PAC with a low optical purity generated by catalysis of a lyase (e.g. by *Ap*PDC-E469G) is converted to highly pure (*S*)-PAC with an *ee* >97 % by *Pf*BAL (highly (*R*)-selective) catalysed kinetic resolution.

1.5.5.2 Alcohol dehydrogenases

For a substrate similar to cathinone, Kihumbu *et al.* showed that the synthesis of 1-phenylpropane-1,2-diol by enzymatic reduction of 1-hydroxy-1-phenylpropan-1-one (HPP) is feasible.[185] This concept was further investigated in the PhD thesis of Justyna Kulig.[186] Beside others, the properties of different wild type alcohol dehydrogenases and a carbonyl reductase were compared concerning the reduction of HPP. Highest activity and excellent (*S*)-stereoselectivity for the reduction of bulky substrates like PAC was found for the alcohol dehydrogenase from *Ralstonia* sp. (*R*ADH). An (*R*)-selective enzyme with valuable properties is the *Lb*ADH from *Lactobacillus brevis*.[186, 187]

*Lb*ADH (alcohol dehydrogenase from *Lactobacillus brevis*)

The *Lactobacillus brevis* alcohol dehydrogenase (*Lb*ADH, EC 1.1.1.2) is a versatile catalyst with a broad substrate scope, including linear and branched aliphatic as well as aromatic and aromatic-aliphatic aldehydes ketones and diketones.[187, 188] The enzyme has a pH-optimum for the reduction at pH 6.5-8.5 and for oxidation at pH 7-10.[189] The (*R*)-selective enzyme was used as well in industrial processes such as for the production of (*R*)-ethyl-3-hydroxybutanoate.[28, 190] Moreover, the production of (1*S*,2*S*)- and (1*S*,2*R*)-1-phenylpropane-1,2-diol from (*R*)- or (*S*)-HPP was already shown to be feasible in gram-scale with excellent stereoselectivity (*ee* >99 %, *de* >98 %) and good reaction yields (>85 %).[185] In this example, the cofactor NADPH was recycled by a commercially available formate dehydrogenase (FDH, EC 1.2.1.2) in presence of sodium formate in excess.[185]

*R*ADH (alcohol dehydrogenase from *Ralstonia* sp.)

The alcohol dehydrogenase from *Ralstonia* sp. (*R*ADH) is a useful enzyme for the reduction of bulky-bulky and bulky-small ketones.[186, 187, 191] *R*ADH has a broad pH-optimum at pH 6–9.5 for the reduction reaction and a sharp optimum at pH 10–11.5 for the oxidation reactions. Highest stability was found between pH 5.5–8 at 8–15 °C only in the presence of $CaCl_2$. For the reduction of HPP to 1-phenylpropane-1,2-diol, the enzyme is highly (*S*)-selective (*ee* >99 %) with activities of 362 U mg^{-1} and 17 U mg^{-1} for the reduction of (*R*)-HPP and (*S*)-HPP, respectively.[186]

1.5.5.3 Toolboxes of (*R*)- and (*S*)-selective ω-transaminases

As summarised in chapter 1.4.3.4, nowadays various (*S*)- and (*R*)-selective ω-transaminases are available for reductive amination of ketones and aldehydes to the respective amines. One toolbox of (*S*)-selective ω-transaminases was developed by Ward, Hailes and co-workers.[103] In the last years, the missing gap of (*R*)-selective enzymes was filled by the work of Bornscheuer, Höhne and co-workers.[81] These (*R*)-selective ω-transaminases are now sold by the company Enzymicals AG. In a cooperation with the working groups of Prof. John M. Ward and Prof. Helen C. Hailes from the University College London and later on as well with the Enzymicals AG, we got access to 20 (*S*)-selective and seven (*R*)-selective wild type ω-transaminases.

(*S*)-selective ω-transaminases toolbox

In order to identify enzymes with new properties, Ward and co-worker performed a BLAST-based sequence homology search using the ω-transaminase (TA) from *Vibrio fluvialis* as a template. As a result, further (*S*)-selective ω-TA from different organisms were identified (see appendix II):

Saccharopolyspora erythraea (*Se*TA), *Streptomyces avermilitis* (*Sa*TA), *Streptomyces coelicolor* (*Sc*TA), *Thermobifida fusca* (*Tf*TA), *Pseudomonas putida* (*Pp*TA), *Pseudomonas aeruginosa* (*Pa*TA), *Chromobacterium violaceum* (*Cv*TA, also referred to as CV2025), *Klebsiella pneumoniae* (*Kp*TA), *Escherichia coli* (*Ec*TA).

Only two of these ω-TA have been described in literature. The enzyme from *Pseudomonas aeruginosa* was used in a 2-step synthesis together with a transketolase to produce a single isomer of 2-amino-1,3,4-butanetriol with overall yields of 21 %.[135] The best characterised and widely applied enzyme is the CV2025 (EC 2.6.1.18). Its broad substrate range (chapter 1.4.3.4) and the application for 1,3-amino alcohol syntheses (chapter 1.5.2) have been discussed previously. The enzyme has a pH optimum at pH 8-10 and shows a ~10-fold higher activity in HEPES buffer compared to phosphate buffer at the same pH.[103] For a wide range of substrates (especially for bulky-aliphatic ketones/amines), this ω-transaminase is highly (*S*)-selective (e.g. synthesis of (*S*)-α-methylbenzylamine with an *ee* >99 %).[103] Since 2012, crystal structures of the enzyme (two of the apo form, one of the holo

form, one in an intermediate state (without substrate/inhibitor) and one with an inhibitor) are available.[192, 193] Using this structural knowledge, active site variants like CV2025-F88A/A231F with inverted small and large pockets sizes were generated (see chapter 1.4.3.2). This variant shows in general decreased (*S*)-selectivity for most substrates compared to the wild type enzyme and is moreover (*R*)-selective for a limited range of cyclic amines.[194]

(*R*)-selective ω-transaminases toolbox

In 2010, 17 novel (*R*)-selective ω-transaminases from different origins were discovered by an *in silico* approach. Based on structural information and protein sequences of (*S*)-selective ω-transaminase, protein databases were screened for enzymes with complementary enantiopreference.[81, 195] Nowadays, seven of these (*R*)-selective ω-transaminases are commercially available by Enzymicals AG[196] and were provided within a cooperation with this company as lyophilised crude cell extracts:

Aspergillus fumigatus (*Af*TA), *Gibberella zeae* (*Gz*TA), *Neosartorya fischeri* (*Nf*TA), *Aspergillus oryzae* (*Ao*TA), *Aspergillus terreus* (*At*TA), *Penicillium chrysogenum,* (*Pc*TA), *Mycobacterium vanbaalenii* (*Mv*TA)

All enzymes are known to catalyse the reductive amination reactions of bulky-aliphatic substrates with excellent stereoselectivities (e.g. synthesis of (*R*)-α-methyl-benzylamine from acetophenone with an *ee* >99 %).[81] Moreover, these enzymes have been broadly used for various applications (see chapter 1.4.3.4).

1.6 Enzymatic cascade reactions – advantages and challenges

As described in chapter 1.5 for the specific example of amino alcohols, the synthesis of compounds with more than one chiral centre usually requires more than one catalytic step. The combination of two or more catalysed reactions is defined as a reaction cascade.[197-204] In general, these multi-step reactions can be subdivided in two types of cascades:

A) “domino” reaction cascade:
An unstable product of a reaction step undergoes a spontaneous reaction to form a stable product. Examples for spontaneous (chemical) reactions are Diels-Alder reactions, rearrangement, fragmentation and cyclisation.[199]

B) “tandem” reaction cascade:
The combination of several catalysed reactions which could in principle be performed separately (one after another) is called “tandem” cascade. Here, the reaction intermediates need to be stable.[197, 201]

In addition to this, cascades are defined as biocatalytic cascades when at least one biocatalytic step is involved. This includes multi-enzymatic, chemo-enzymatic and enzyme-initiated spontaneous (domino) reactions.[197] For the synthesis of amino alcohols, such as nor(pseudo)ephedrines two different 2-step enzymatic (tandem) cascades were investigated in this thesis (see chapters 1.5.4 and 1.5.5).

1.6.1 Enzyme (tandem) cascades: cascade designs and reaction modes

Four different general designs of enzymatic cascade reactions were known (scheme 1-19 A-D).[197] The most simple cascade is the ‘linear cascade’, where a product is synthesised via one (or more) intermediates (scheme 1-19 A). ‘Orthogonal cascades’ are more complex. Here, the product formation is coupled to a cofactor/co-substrate regeneration step or co-product removal reactions (scheme 1-19 B). In ‘cyclic cascades’ one substrate of the reaction mixture is enriched by removal of the other, which is then subsequently converted back into the starting material (scheme 1-19 C). A typical example is the dynamic kinetic resolution of racemic compounds. Similar to orthogonal cascades, in ‘parallel cascades’ product formation is coupled to the synthesis of a co-product (scheme 1-19 D). Here, the co-product is not removed and is optimally a valuable second product.

In addition to different reaction designs, a cascade can be performed in different reaction modes: The classical reaction mode is a multi-step reaction performed in several reaction vessels (pots). Here, isolation of reaction intermediates after each reaction step is required: “X-step X-pot reaction”. Moreover, cascades can be performed in 1-pot without isolation of the reaction intermediates. If these reactions are performed one after another, such systems are referred to as “1-pot X-step sequential cascade” In a “1-pot X-step simultaneous cascade” all catalysts are added

in one reaction vessel at the same time. For a “1-pot 2-steps linear cascades” these different reaction modes are itemised in scheme 1-19 (A-1 to A-3).

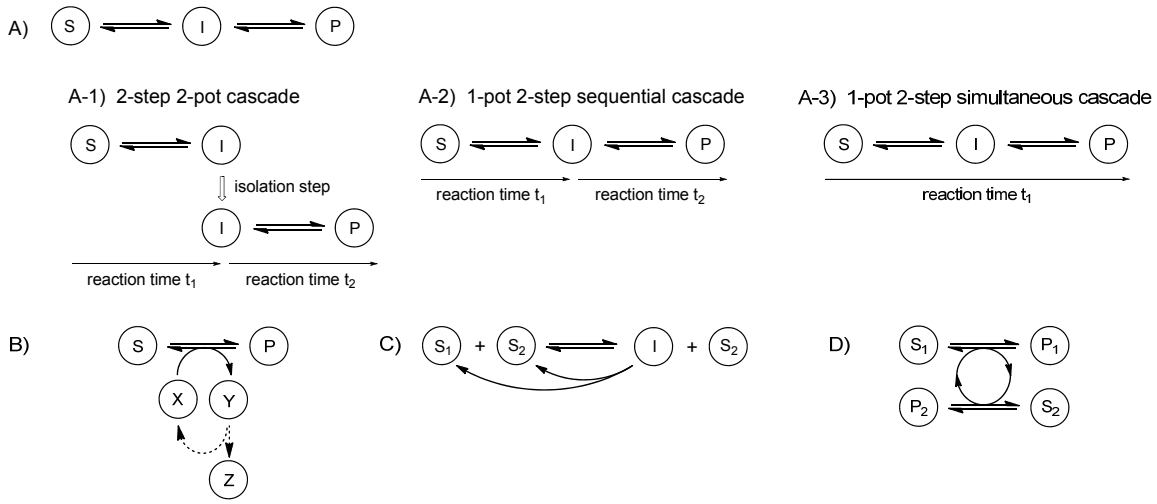

Scheme 1-19: Different cascade designs and reaction modes for a 2-step enzymatic cascade (modified from references: [197, 203])

Enzymatic cascade designs: A) linear cascade, B) orthogonal cascade, C) cyclic cascade, D) parallel cascade[197] and different reactions modes of a 2-step linear cascade[203]: A-1) 2-steps 2-pots, A-2) 1-pot 2-step sequential cascade (the 2nd step is performed after the 1st reaction), A-3) 1-pot 2-step simultaneous cascade (both reactions are performed simultaneously).

A cascade where all reactions can be performed in one pot, reduces not only the number of intermediate isolation steps, it thereby decreases amount of chemicals (reagents, solvents and/or absorbents), lowers energy consumption and reduces waste production. Each point does not only contribute to a more efficient process in terms of production costs, but simultaneously to a more environmentally friendly reaction process.[201-203, 205-208] In general, the most time-efficient way to perform such a cascade is the simultaneous mode, where all catalysts act at the same time. Moreover, the complexity of the reaction procedure is reduced when all components of a multi-step reaction can be added at once. In contrast to this, the complexity of the system is significantly increased. If side reactions occur (e.g. caused by substrate competition with an enzyme of another reaction step), the benefit of an easier simultaneous mode needs to be compared with lower purification effort and most likely higher reaction yield in a sequential mode.[197, 200, 201, 208] Especially in simultaneous cascades, an optimal interplay of all catalysts is required. Optimal cascade parameters (such as pH, temperature, substrate concentrations and the

relative ratio of enzymes) have to be found. Since reaction engineering of multi-parameter systems can be rather challenging, implementation of mathematical modelling (see chapter 1.6.2) can help to increase reaction yields by finding optimal operation windows.[197, 200]

1.6.2 Easy and efficient multi-parameter optimisation

Multi-parameter optimisation, often required for classical reaction engineering, is time consuming and due to the number of experiments as well cost intensive. One main challenge is the intersection between statistical relevance/significance of data and their interpolations on the one hand and the number of experiments on the other. Here, design of experiments (DOE) offers a mathematical way to minimise the number of necessary experiments by building a relationship between independent variable factors and the outcomes of an experiment.[209-211] This relationship can for example be visualised in a 3-D plot (see scheme 1-20) where two variables (x1 and x2 – e.g. pH, temperature, substrate concentrations and enzyme ratio) are plotted against one outcome factor (y, e.g. reaction yield or optical purity).

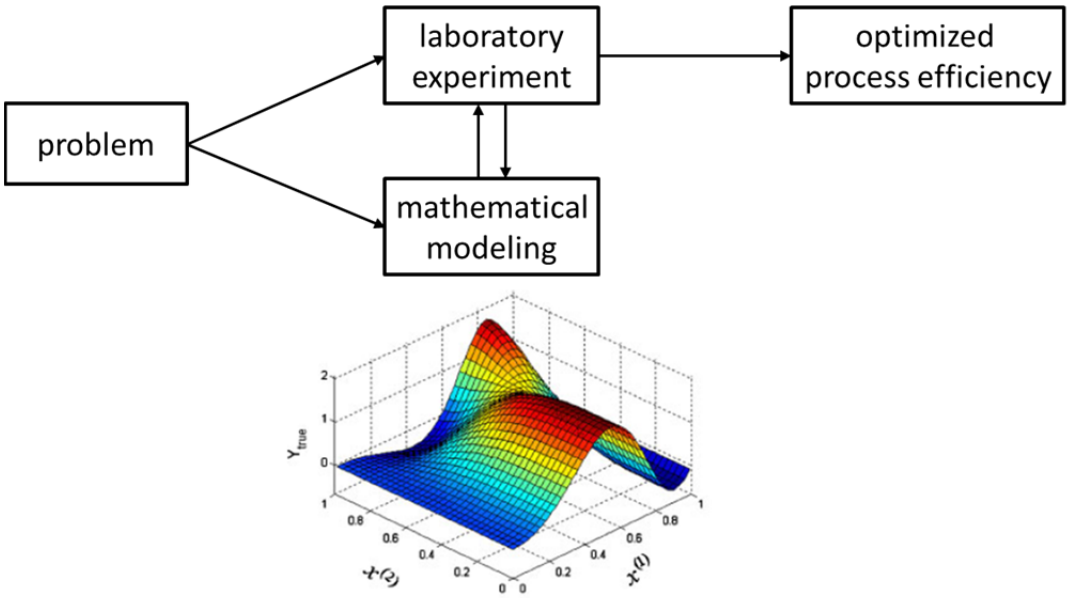

Scheme 1-20: Basis steps for reaction engineering supported by mathematical modelling[200] e.g. via the Kriging method and 3-D visualisation (see 3-D plot).

Various methods for mathematically supported reaction engineering are described in literature.[197, 200] One approach is the so called “Kriging method”. In this statistical method the values of an interpolating function are determined by a weighted sum of all measurement data. These weights are locally computed, such that the expectation value of the interpolating function matches the true value with minimised deviation but highest statistical significance. Thus, the Kriging method allows an optimal interpretation of experimental datasets. Further mathematical details on the Kriging method can be found in the literature.[212, 213]

2 Aim of the work

One focus of the working group “Biocatalysis and Biosensors” (IBG-1, Forschungszentrum Jülich GmbH, Germany), headed by Prof. Martina Pohl and Dr. Dörte Rother, is to offer biocatalytic solutions for challenging synthesis strategies. Amino alcohols are valuable compounds for the pharmaceutical as well as for the chemical industry. An example from this large list of valuable molecules are the four stereoisomers of nor(pseudo)ephedrine. To enable the biocatalytic access to these compounds was of special interest for this thesis. Known chemical synthesis routes and chemo-enzymatic reaction cascades towards these products often require multiple steps or lack high stereo- and regioselectivities.

As summarised in chapter 1.5.4, 2-hydroxy ketones are intermediates in natural biosynthetic pathways of amino alcohols. Synthetically, 2-hydroxy ketones can be synthesised from aldehydes or respective 2-keto acids by using ThDP-dependent enzymes. An enzyme toolbox consisting of 20 wild type enzymes and more than 150 active variants was developed in the working group of Prof. Pohl and Dr. Rother to generate a platform of various 2-hydroxy ketones with high selectivities. Among this platform, specifically (*R*)- and (*S*)-phenylacetylcarbinol (PAC) represented a perfect starting point to access all four nor(pseudo)ephedrines by reductive amination of the prochiral carbonyl group. A goal of this thesis was to identify appropriate biocatalysts for the reductive amination of these 2-hydroxy ketones. Respective catalytic activity was assumed for ω-transaminases (see chapter 1.5.4). A toolbox for the screening of 18 (*S*)- and eight (*R*)-selective ω-transaminases was available from cooperation partners (chapter 1.5.5.3).

Development of an efficient screening assay for ω-transaminases

To analyse the potential of these ω-transaminases for the reductive amination of 2-hydroxy ketones in general, and for PAC specifically, an efficient screening assay had to be developed. This assay should allow a rapid analysis of the substrate range independent of the amine donor (co-substrate) spectrum.

Strategies for the biocatalytic synthesis of nor(pseudo)ephedrine

ω-Transaminases with promising properties for the reductive amination of PAC should be tested in combination with ThDP-dependent enzymes for the 2-step synthesis of nor(pseudo)ephedrines (scheme 2-1).

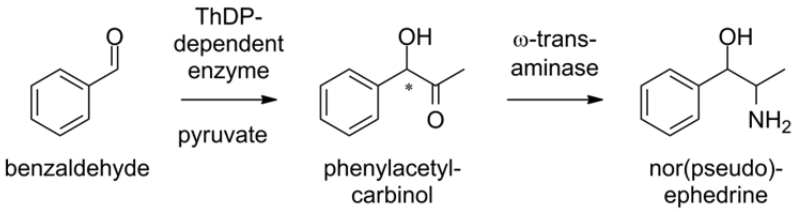

Scheme 2-1: Synthesis of nor(pseudo)ephedrines combining ThDP-dependent enzymes and ω-transaminases

As an alternative to this synthetic route, a second strategy for the synthesis of synthesis of nor(pseudo)ephedrines is deduced from the natural biosynthesis pathways (chapter 1.5.5.3). Starting from 1-phenylpropane-1,2-dione, the combination of an ω-transaminase in the first step with subsequent alcohol dehydrogenase catalysed reduction could be evaluated according to scheme 2-2.

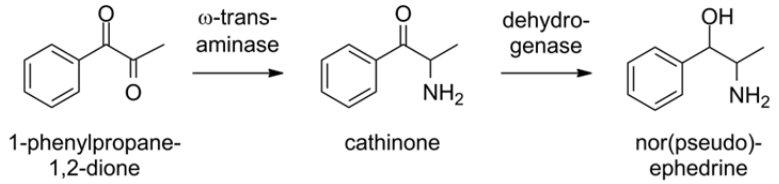

Scheme 2-2: Synthesis of nor(pseudo)ephedrines combining ω-transaminases and dehydrogenase

A special challenge of both approaches is to identify reaction conditions, under which both enzymes are active in a cascade reaction with optimal productivity and for that high stereoselectivity and low by-products are feasible.

3 Publications

3.1 TTC-based screening assay for ω-transaminases: a rapid method to detect reduction of 2-hydroxy ketones

Journal of Biotechnology (2012)
159(3):188-94. doi: 10.1016/j.jbiotec.2011.12.023. Epub 2012 Jan 2.

3.2 Two steps in one pot: Enzyme cascade for the synthesis of nor(pseudo)ephedrine from inexpensive starting materials

Angewandte Chemie International Edition (2013)
52(26):6772-5. doi: 10.1002/anie.201300718. Epub 2013 May 9.

3.3 Efficient 2-step biocatalytic strategies for the synthesis of all nor(pseudo)ephedrine isomers

Green Chemistry (2014), in press, doi:10.1039/C4GC00100A.

3.1 TTC-based screening assay for ω-transaminases: a rapid method to detect reduction of 2-hydroxy ketones

G Model
BIOTEC-5959; No. of Pages 7
ARTICLE IN PRESS
Journal of Biotechnology xxx (2012) xxx–xxx
Contents lists available at SciVerse ScienceDirect
Journal of Biotechnology
journal homepage: www.elsevier.com/locate/jbiotec

TTC-based screening assay for ω-transaminases: A rapid method to detect reduction of 2-hydroxy ketones

Torsten Sehl[a], Robert C. Simon[a,1], Helen C. Hailes[b], John M. Ward[c], Ursula Schell[c,2], Martina Pohl[a], Dörte Rother[a,*]

[a] Institute of Bio- and Geosciences, IBG-1: Biotechnology, Forschungszentrum Jülich GmbH, Leo-Brandt-Str. 1, 52425 Jülich, Germany
[b] Department of Chemistry, University College London, 20 Gordon Street, London WC1H 0AJ, UK
[c] Department of Biochemistry and Molecular Biology, University College London, Gower Street, London WC1H 6BT, UK

ARTICLE INFO

Article history:
Received 11 October 2011
Received in revised form
22 December 2011
Accepted 23 December 2011
Available online xxx

Keywords:
ω-Transaminase
Chiral amino alcohols
Asymmetric reductive amination
Colourimetric screening assay
TTC
2-Hydroxy ketones

ABSTRACT

A rapid TTC-based screening assay for ω-transaminases was developed to determine the conversion of substrates with a 2-hydroxy ketone motif. Oxidation of the compounds in the presence of 2,3,5-triphenyltetrazolium chloride (TTC) results in a reduction of the colourless TTC to a red-coloured 1,3,5-triphenylformazan. The enzymatic reductive amination of a wide range of various aliphatic, aliphatic–aromatic and aromatic–aromatic 2-hydroxy ketones can be determined by the decrease of the red colouration due to substrate consumption. The conversion can be quantified spectrophotometrically at 510 nm based on reactions, e.g. with crude cell extracts in 96-well plates. Since the assay is independent of the choice of diverse amine donors a panel of ω-transaminases was screened to detect conversion of 2-hydroxy ketones with three different amine donors: L-alanine, (*S*)-α-methylbenzylamine and benzylamine. The results could be validated using HPLC and GC analyses, showing a deviation of only 5–10%. Using this approach enzymes were identified demonstrating high conversions of acetoin and phenylacetylcarbinol to the corresponding amines. Among these enzymes three novel wild-type ω-transaminases have been identified.

1. Introduction

Chiral vicinal amino alcohols are versatile building blocks for organic synthesis, as ligands and chiral auxiliaries (Ager et al., 1996; Fehr and Galindo, 1996) or as synthons for pharmaceutically active compounds (Bergmeier, 2000), such as drugs like ephedrine and norephedrine, the sphingosine derivative sulfobacin B (Kamiyama et al., 1995), the HIV protease inhibitor saquinavir (Ohta and Shinkai, 1997) and the aminopeptidase inhibitor bestatin (Nakamura et al., 1976; Umezawa et al., 1976). Vicinal amino alcohols can be synthesised by a reductive amination of 2-hydroxy ketones. Numerous substituted 2-hydroxy ketones are accessible biocatalytically in highly enantiopure forms (Hoyos et al., 2009; Müller et al., 2009).

Recently, the biocatalytic reductive amination of prochiral ketones by ω-transaminases (ω-TAs) has gained considerable interest (Höhne and Bornscheuer, 2009; Hopwood et al., 2011; Savile et al., 2010; Ward and Wohlgemuth, 2010). Transaminases with high turnover numbers and excellent selectivities have been described (Koszelewski et al., 2010; Schätzle et al., 2011; Tufvesson et al., 2011). In addition, a few ω-TAs reactions have already been successfully implemented into industrial processes at a multi ton scales, e.g. at Cambrex (Scarlato, 2009) and DSM (DSM, 2011). Beside reaction engineering strategies, enzymes with improved affinities towards substrates, reduced substrate and/or product inhibition, as well as activities against novel compounds need to be identified for further applications (Hopwood et al., 2011; Koszelewski et al., 2010; Ward and Wohlgemuth, 2010). Therefore, efficient and rapid screening assays need to be developed in order to screen newly discovered enzymes and mutant libraries.

Previously, ω-TAs screening assays with various advantages and disadvantages depending on their respective application have been reported. Among these the quantification of the reaction from pyruvate to alanine by the formation of coloured Cu-alanine complexes has been described (Hwang and Kim, 2004). In other assays the accumulating pyruvate is detected by multienzyme cascades based on either a pH-shift (Truppo et al., 2009) or a colourimetric oxidase–peroxidase reaction (Hopwood et al., 2011). Further, a spectrophotometric assay based on the activity towards (*S*)-α-methylbenzylamine (MBA) has been published (Schätzle et al.,

* Corresponding author. Tel.: +49 2461616772; fax: +49 2461613870.
E-mail address: do.rother@fz-juelich.de (D. Rother).
[1] Present address: Department of Chemistry, Organic and Bioorganic Chemistry, University of Graz, 8010 Graz, Austria.
[2] Present address: Biopharm, Process Research, GlaxoSmithKline Plc., Gunnels Wood Road, Stevenage, Herts SG1 2NY, UK.

0168-1656/$ – see front matter © 2012 Elsevier B.V. All rights reserved.
doi:10.1016/j.jbiotec.2011.12.023

Please cite this article in press as: Sehl, T., et al., TTC-based screening assay for ω-transaminases: A rapid method to detect reduction of 2-hydroxy ketones. J. Biotechnol. (2012), doi:10.1016/j.jbiotec.2011.12.023

G Model
BIOTEC-5959; No. of Pages 7
ARTICLE IN PRESS
2 T. Sehl et al. / Journal of Biotechnology xxx (2012) xxx–xxx

2009). While these assays are useful and well suited for the screening of either the amine donors or the amine acceptors, in this work we have established a rapid screening assay for ω-TAs, which can be used to determine the conversion of various chiral and prochiral compounds with a 2-hydroxy ketone motif, independent of the choice of the amine donor. This assay can be used not only with purified enzymes but also with crude cell extracts and moreover the detection of time-dependent conversion rates is feasible.

2. Materials and methods

2.1. Construction of the expression vectors

Putative ω-transaminases had been identified by a BLASTP search for homologous of the ω-TA from *Vibrio fluvialis* JS17 as described previously (Kaulmann et al., 2007). The coding region of the transaminases PP5182 (gene bank accession no. NP_747283) was amplified from genomic DNA of *Pseudomonas putida* KT2440 using a 5′-CATATGAGCGTCAACAACCCGCAAA-3′ forward and a 5′-CTCGAGTTATTGAATCGCCTCAAGGGTCAG-3′ reverse primer. From the same organism PP2799 (gene bank accession no. NP_744943) was amplified with a forward primer 5′-CATATGAGCACCCACTCTTCAACCGTTCAG-3′ and a reverse primer 5′-CTCTAGTTACAGCAGGTGCTGTGAGCGCG-3′ under exchanging the native stop-codon from TGA to TAA. The gene coding for the enzyme PA0221 (gene bank accession no. NP_248912) was amplified from genomic DNA of *Pseudomonas aeruginosa* PAO2 using a 5′-CATATGACCGCTCAGCTCAACCCGCAGC-3′ forward and a 5′-CTCGAGTCAGAGCACGCCGATCTCGCGC-3′ reverse primer. Using these primers *Nde*I restriction sites at the N-terminus and *Xho*I sites at the C-terminus were included, respectively. Conditions for PCR and the cloning of the amplified genes into a pET29a vector (Novagen) were performed like described for the construction of the expression vector for the enzyme CV2025 from *Chromobacterium violaceum* previously (Kaulmann et al., 2007).

2.2. Expression and preparation of ω-TAs

E. coli BL21(DE3) was transformed with the ω-TAs coding plasmids and grown in lysogeny broth medium containing 50 mg/L kanamycin at 37 °C until an $OD_{600\,nm}$ of 0.6–0.8 was reached. Enzyme expression was induced by addition of 1 mM isopropyl-β-D-thiogalactopyranoside. During expression (4 h) temperature was lowered to 30 °C. Afterwards, cells were harvested and stored at −20 °C. For cell disruption the cells were suspended in 10× (v/w) lysis buffer containing 100 mM HEPES (pH 7.5), 200 μM pyridoxal-5′-phosphate (PLP), 0.1% (w/v) lysozyme and 0.5 mM phenylmethylsufonyl fluoride and incubated for 20 min at 4 °C. The cells were disrupted by ultra sonification. The crude cell extract was centrifuged at 4 °C with 16,000 × *g* for 40 min and subsequently filtered through a 0.2 μm filter, diluted in assay buffer to a protein concentration of 5 mg/mL and used directly or stored as 500 μL aliquots at −20 °C.

2.3. TTC-based screening—assay setup

A stock solution containing 12.5 mM amine donor and 12.5 mM 2-hydroxy ketone was prepared in assay buffer (100 mM HEPES pH 7.5, 200 μM PLP). 80 μL of this solution was pipetted into each well of a 96-well microtiter plate (Medisorp, NUNC). The reaction was started by the addition of 20 μL crude cell extract to give a final protein concentration of 1 mg/mL and a donor/acceptor concentration of 10 mM. The reactions were carried out 4-fold. Two controls were performed each containing crude cell extract of *E. coli* BL21(DE3) transformed with an empty pET-29a vector: one lacking the respective 2-hydroxy ketone ("background") and the other one containing 10 mM of the 2-hydroxy ketone ("negative control").

To allow a more precise quantification of the conversion, each 96-well plate contained an internal calibration with 0–10 mM of the respective 2-hydroxy ketone. Therefore, the stock solution mentioned above was diluted in assay buffer before adding the enzyme solution. The plate was closed tightly with sealing sheets (Roth GmbH) to avoid evaporation and incubated for 16 h at 27 °C on an Infors-HT Multitron shaker (100 rpm).

2.4. TTC-based screening—colouration

A TTC-solution of 1 mg/mL 2,3,5-triphenyltetrazolium chloride (TTC) in a mixture of 1 volume 75% (v/v) EtOH and 3 volumes 1 M NaOH was prepared. Rapid addition of 40 μL TTC-solution with an Eppendorf Multipette to each well immediately stopped the reaction and colour formation commenced due to the reaction with non-transformed 2-hydroxy ketone. Depending on the 2-hydroxy ketone used the plate was incubated for a certain time (see Table 1) before the absorption was measured at 510 nm using a Multiskan Spectrum Microplate photometer (Thermo Fischer Scientific Inc.). The conversion was calculated after subtracting the background relative to the calibration curve.

The 2-hydroxyacetophenone (2-HAP) **3** and PAC **5** were diluted with assay buffer 1:10 according to the detection limits (see Fig. 2) before adding the TTC-solution.

2.5. TTC-based screening—time-dependent conversion

The time-dependent conversion of 10 mM PAC **5** by ω-TAs with equimolar amount of (*S*)-α-MBA **A** was performed as described before (Sections 2.2 and 2.3). To reduce the amount of samples the reactions were set up three times for each endpoint determination and a two-point calibration with 0 mM and 10 mM PAC was used to quantify the conversion. At different time points the conversion was measured according to the procedure described before (Section 2.4).

2.6. Preparation of 2-hydroxy ketones

Acetoin **1**, propioin **2** and 2-HAP **3** were purchased from Sigma–Aldrich and used without any further purification. The aromatic 2-hydroxy ketones **7**–**9** were synthesised and supplied by a cooperation partner accordingly to the published procedure (O'Toole et al., 2010).

2.6.1. Synthesis of rac-HPP **4**

The synthesis of racemic 2-hydroxy-1-phenylpropan-1-one (HPP) **4** was performed as described in the literature (Chen et al., 2008). Deviating from it the crude product was purified by filter flash chromatography (silica gel 200–300 mesh, eluent: PE/EtOAc = 90:10) yielding the 2-hydroxy ketone as a yellowish oil in 31% yield (0.46 g, 3.07 mmol).

R_f (PE/EtOAc 90:10) = 0.27; HPLC (Chiralcel OD-H: 250 mm × 4.6 mm × 5 μm, *n*-hexane/2-propanol = 90:10, 0.7 mL/min, 25 °C): R_t [(*S*)-**4**] = 18.7 min, R_t [(*R*)-**4**] = 20.6 min; ^{1}H NMR (600 MHz; $CDCl_3$): δ = 1.46 (d, $^3J_{3,2}$ = 7.1 Hz, 3 H, 3-H), 3.80 (brs, 1 H, OH), 5.17 (q, $^3J_{2,3}$ = 7.1 Hz, 1 H, 2-H), 7.51 (m_c, 2 H, arom.-H), 7.62 (m_c, 1 H, arom.-H), 7.93 (m_c, 2 H, arom.-H) ppm; ^{13}C NMR (151 MHz; $CDCl_3$): 22.3 (C-3), 69.3 (C-2), 128.7 (arom.-CH), 128.9 (arom.-CH), 134.0 (arom.-C_{ipso}), 202.4 ppm (C-1); GC–MS (70 eV, EI): *m*/*z* (%): 150 (15) [M^+], 105 [M-$C_7H_5O^+$] (100), 77 [M-$C_6H_5^+$] (37).

Please cite this article in press as: Sehl, T., et al., TTC-based screening assay for ω-transaminases: A rapid method to detect reduction of 2-hydroxy ketones. J. Biotechnol. (2012), doi:10.1016/j.jbiotec.2011.12.023

G Model
BIOTEC-5959; No. of Pages 7
ARTICLE IN PRESS
T. Sehl et al. / Journal of Biotechnology xxx (2012) xxx–xxx

Table 1
Amine acceptors **1**–**9** and amine donors **A**–**C** for ω-transaminases activity screening. For the amine acceptors **1**–**9** the compound specific colouration rates in [mAU/mM per minute incubation] are given. All reactions were started with 10 mM of the respective 2-hydroxy ketone and 10 mM of the respective amine donor (**A**–**C**). Compounds with a strong colouration rate require dilution prior to assay read-out.

Amine acceptors					
	Structure	Name	Colouration rate [mAU/(mM min)]	Recommended steps	
				Dilution	Incubation
1		Acetoin	0.034	–	2 min
2		Propioin	0.004	–	10 min
3		2-HAP	1.096	1:10	1 min
4		HPP	0.022	–	4 min
5		PAC	0.329	1:10	2 min
6	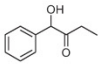	PPC	0.090	–	1 min
7	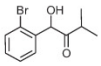		0.012	–	10 min
8	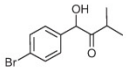		0.013	–	10 min
9	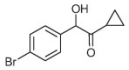		0.005	–	30 min
Amine donors					
	 (S)-α-MBA **A**	 benzylamine **B**	 L-alanine **C**		

*2.6.2. Preparation of (R)-PAC **5***

(*R*)-Phenylacetylcarbinol (PAC) **5** was provided by BASF AG. The yellow oil had a purity of >98% (NMR, GC). The sample did not contain any impurity of the regioisomer HPP **4**.

R_f (PE/EtOAc 90:10) = 0.27; HPLC (Chiralcel OD-H: 250 mm × 4.6 mm × 5 μm, *n*-hexane/2-propanol = 90:10, 0.7 mL/min, 25 °C): R_t [(*S*)-**5**] = 16.2 min, R_t [(*R*)-**5**] = 17.4 min, *ee* = 84%; ^{1}H NMR (600 MHz; $CDCl_3$): δ = 2.08 (s, 3 H, 3-H), 4.30 (brs, 1 H, OH), 5.09 (brs, 1 H, 1-H), 7.31–7.40 ppm (m, 5 H, arom.-H); ^{13}C NMR (151 MHz; $CDCl_3$): 25.3 (C-3), 80.2 (C-2), 127.4 (arom.-CH), 128.8 (arom.-CH), 129.1 (arom.-CH), 138.1 ppm (arom.-C_{ipso}), 207.2 (C-1); GC–MS (70 eV, EI): *m*/*z* (%): 150 [M^+] (15), 107 [M-$C_7H_7O^+$] (100), 75 [M-$C_6H_3^+$] (33).

*2.6.3. Synthesis of (R)-PPC **6***

Purification of the wild-type enzyme *Ap*PDC (pyruvate decarboxylases from *Acetobacter pasteurianus*) as well as synthesis of (*R*)-phenlypropionylcarbinol (PPC) was carried out as previously described (Rother et al., 2011). 18 mM benzaldehyde and 18 mM propanal were dissolved in 500 mL potassium phosphate buffer (50 mM, pH 7.0) containing 2.5 mM $MgSO_4$, 0.1 mM thiamine-diphosphate, and 20% (v/v) DMSO. After adding *Ap*PDC (0.3 U/mL) the reaction was run for 72 h at 30 °C under slow stirring. The reaction mixture was extracted with ethyl acetate (3 × 200 mL) and the combined organic layers were dried with $MgSO_4$ and evaporated. The crude product was purified by filter flash chromatography (eluent:PE/EtOAc = 90:10) to afford (*R*)–PPC **6** as a slightly yellow oil in 5% yield (74 mg, 0.45 mmol).

R_f (PE/EtOAc 90:10) = 0.33; HPLC (Chiralcel OD-H: 250 mm × 4.6 mm × 5 μm, *n*-hexane/2-propanol = 90:10, 0.7 mL/min, 25 °C): R_t [(*S*)-**6**] = 14.3 min, R_t [(*R*)-**6**] = 17.0 min, *ee* = 92%; ^{1}H NMR (600 MHz; $CDCl_3$): δ = 1.01 (t, $^3J_{4,3}$ = 7.3 Hz, 3 H, 3-H), 2.33 (dq, $^3J_{3a,4}$ = 7.3 Hz, $^2J_{3a,3b}$ = 17.8 Hz, 1 H, 3-H_a), 2.40 (dq, $^3J_{3b,4}$ = 7.3 Hz, $^2J_{3b,3a}$ = 17.8 Hz, 1 H, 3-H_b), 4.35 (d, $^3J_{OH,1}$ = 4.2 Hz, 1 H, OH), 5.1 (d, $^3J_{1,OH}$ = 4.2 Hz, 1 H, 1-H), 7.31–7.40 ppm (m, 5 H, arom.-H); ^{13}C NMR (151 MHz; $CDCl_3$): 7.6 (C-4), 31.2 (C-3), 79.5 (C-1), 127.3 (arom.-CH), 128.6 (arom.-CH), 128.9 (arom.-CH), 138.3 (arom.-C_{ipso}), 210.1 ppm (C-2); GC–MS (70 eV, EI): *m*/*z* (%): 164 [M^+] (2), 107 [M-$C_7H_7O^+$] (100), 75 [M-$C_6H_3^+$] (80).

Please cite this article in press as: Sehl, T., et al., TTC-based screening assay for ω-transaminases: A rapid method to detect reduction of 2-hydroxy ketones. J. Biotechnol. (2012), doi:10.1016/j.jbiotec.2011.12.023

G Model
BIOTEC-5959; No. of Pages 7
ARTICLE IN PRESS
4 T. Sehl et al. / Journal of Biotechnology xxx (2012) xxx–xxx

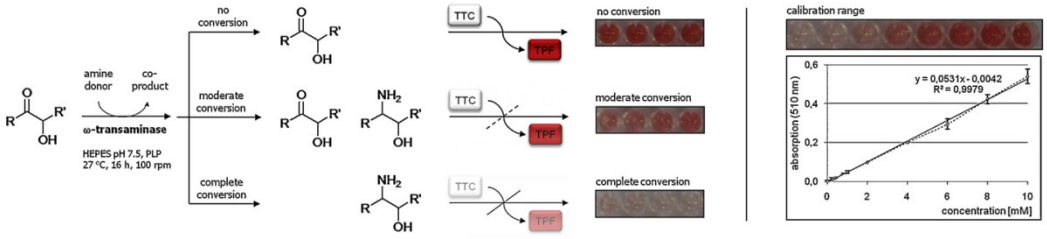

Fig. 1. TTC-based screening assay for ω-transaminases.

2.7. Instrumental analysis of 2-hydroxy ketone conversion

The reactions were set up analogously to the TTC-assay at a 500 μL scale. Instead of 96-well plates the reactions were incubated in Eppendorf tubes for 16 h at 27 °C and 100 rpm. The conversion was determined as a decrease of the substrates relative to a sample with crude cell extract of *E. coli* BL21(DE3) transformed with an empty vector. The data for each 2-hydroxy ketone in combination with the amine donors **A**, **B**, and **C** (see Table 1) were obtained from measurements of two independent samples.

Acetoin **1**, propioin **2** and 2-HAP **3** were quantified as a decrease of the substrate detected by gas chromatography. 200 μL reaction mixture was extracted with 200 μL EtOAc. For acetoin and propioin the chiral column FS-Cyclodex-β I/P (50 m × 320 μm × 25 μm) at a constant pressure of 0.25 bar and a temperature gradient of 15 °C/min from 120 to 190 °C was used. Typical retention times were: acetoin R_t [(*R*)-**1**] = 5.11 min, R_t [(*S*)-**1**] = 5.37 min, propioin R_t [(*R*)-**2**] = 8.81 min, R_t [(*S*)-**2**] = 9.08 min. 2-HAP (R_t = 12.95 min) was detected with a Chirasil-Dex CB column (20 m × 250 μm × 25 μm), a constant flow of 0.4 mL/min and a constant temperature of 140 °C.

The quantification of HPP **4**, PAC **5** and PPC **6** was performed by HPLC-analytics with the same LiChrospher RP-8 reverse phase column (250 mm × 4 mm, 5 μm). 20 μL of the reaction solution was added to 180 μL acetonitrile (ACN). A gradient was run from 25% (v/v) ACN to 100% (v/v) ACN with a re-equilibrium step for 5 min (oven temperature 27 °C, flow: 1 mL/min). Typically, the retention times and the UV detection wavelength were: HPP 10.16 min (250 nm), PAC 8.72 min (200 nm), PPC 12.39 min (200 nm).

3. Results and discussion

As outlined above, the aim of our work was to develop a rapid screening assay for ω-TAs indicating the conversion of amine acceptors with a 2-hydroxy ketone motif. 2,3,5-Triphenyltetrazolium chloride (TTC) can be used to detect a wide range of different aliphatic, aliphatic-aromatic and aromatic–aromatic 2-hydroxy ketones (Breuer et al., 2002). In the presence of the TTC-reagent these compounds are oxidised to the corresponding di-ketones by simultaneous reduction of TTC to 1,3,5-triphenylformazan (TFP). The intense red colouration of TFP can be detected and quantified photometrically at 510 nm. This principle was successfully applied for screening assays to detect activities of ThDP-dependent lyases (Breuer et al., 2002) as well as transketolase (Smith et al., 2006).

Fig. 1 shows the principle of the novel TTC-based screening assay for ω-transaminases. 2-Hydroxy ketones acting as amine acceptors in ω-TAs-catalysed reactions are converted to the respective 1,2-amino alcohols. By adding the TTC-reagent the amount of 2-hydroxy ketone, which was not converted to the 1,2-amino alcohol by the ω-TAs, is oxidised to the corresponding di-ketone and contributes to the red-colouration caused by the TFP. A positive screening hit is visible from de-colouration of the sample. An internal calibration with the respective 2-hydroxy ketone allows quantification of the conversion.

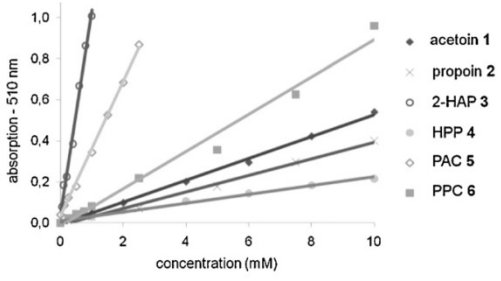

Fig. 2. Colouration (absorption at 510 nm) relative to the concentration of 2-hydroxy ketones **1**–**6** 1 min after addition of the TTC-reagent; propioin **2** is shown 10 min after TTC addition.

3.1. Determination of assay parameters

The colour intensity of 2-hydroxy ketones with the TTC-reagent is strongly dependent on the substrate concentration, the redox potential of the 2-hydroxy ketone and the incubation time before the photometrical readout is started. Therefore, the linear range of the colouration rate has to be determined for each 2-hydroxy ketone. 2-HAP **3** and PAC **5** show a rapid colouration within the minimal viable measuring time of 1 min after addition of the reagent (Fig. 2 and Table 1). To allow reliable measurements of such sensitively responding substrates dilution of the 2-hydroxy ketone solution prior to addition of the TTC-assay was required (Table 1). On the other hand, the incubation time needed to be extended for compounds with a slow colouration rate such as propioin **2**, or substrates **7**–**9** (Table 1). However, an incubation time of 30 min should not be exceeded due to precipitation of the formazane TFP.

The assay is not influenced by the amine donors **A**–**C**, the buffer, crude cell lysate, or the corresponding amino alcohols. Consequently, the colouration rates did not change significantly with different amine donors (data not shown).

3.2. Screening for 2-hydroxy ketone conversion by ω-TAs

The screening assay was developed for the use at a 100 μL scale in 96-well plates with crude cell lysate. To demonstrate its applicability, reactions with 10 mM of the amine acceptors **1**–**6** in combination with 10 mM of the amine donors (*S*)-α-methylbenzylamine **A**, benzylamine **B** and L-alanine **C** were screened for ω-transaminase conversion. Because of solubility

Please cite this article in press as: Sehl, T., et al., TTC-based screening assay for ω-transaminases: A rapid method to detect reduction of 2-hydroxy ketones. J. Biotechnol. (2012), doi:10.1016/j.jbiotec.2011.12.023

G Model
BIOTEC-5959; No. of Pages 7
ARTICLE IN PRESS
T. Sehl et al. / Journal of Biotechnology xxx (2012) xxx–xxx

problems, reactions with 2-hydroxy ketones **7**–**9** and (*S*)-α-methylbenzylamine were performed with 2 mM of amine donor and acceptor, respectively.

Putative ω-TAs from different organisms have been identified by a sequence-based search for homologous proteins of the (*S*)-selective ω-TA JS17 from *V. fluvialis* as described earlier (Kaulmann et al., 2007). Among these only the potential of the enzyme CV2025 from *Chromobacterium violaceum* to accept the amine donors **A**–**C** with the 2-hydroxy ketone acetoin **1** has already been described before (Kaulmann et al., 2007). Table 2 shows the results for all tested combinations of amine donors and amine acceptors of ω-TAs with positive screening hits. Beside CV2025 three novel transaminases could be identified which reduce 2-hydroxy ketones to the corresponding amino alcohols. PP5182 and PP2799, both from *P. putida*, show high conversion of PAC **5** and a slightly lower conversion of acetoin **1**. The enzyme PA0221 from *P. aeruginosa* is able to convert these substrates as well, but seems to be less active than the other enzymes. Further, PP2799 is, besides CV2025, the only enzyme in our screening showing significant conversion of 2-HAP **3**.

For all enzymes, except for the conversion of acetoin **1** by PA0221, the highest conversion rates were achieved with (*S*)-α-MBA **A**. This amine donor is known to be a substrate with a product favouring equilibrium constant. We could identify enzymes accepting L-alanine **C** as an amine donor, although the conversion rates were much lower, presumably due to the unfavoured equilibrium constant. Ways to overcome this problem have already been described (Koszelewski et al., 2010). A combination of our screening assay with in situ removal of the co-product pyruvate by decarboxylases (Höhne et al., 2008) is conceivable.

Although acetoin **1** and PAC **5** were converted by the enzymes described above, we remarkably did not get any significant positive screening result for propioin **2**, (*R*)-PPC **6** and the 2-hydroxy ketones **7**–**9**. From literature it is known, that the enzyme CV2025 is able to convert aliphatic substrates with the ketone vicinal to a methanol-group like 1,3-dihydroxypentan-2-one, L-erythrulose and D-xylulose (Kaulmann et al., 2007; Smith et al., 2009). Furthermore, the regioselectivity of this enzyme was described. While the aromatic-aliphatic compound 1,3-dihydroxy-1-phenylpropan-2-one, which is similar to PAC **5**, is converted, the regioisomer 2,3-dihydroxy-1-phenylpropan-1-one (similar to HPP **4**) is not (Smithies et al., 2009). Additionally to the previously published results, our investigations clearly underline that small structural changes of the substrates influence quite significantly the reactivities of this enzyme. For the ω-TA JS17 from *V. fluvialis* a two binding site model, consisting of a large and a small pocket for substrate binding, was proposed (Hirotsu et al., 2005; Shin and Kim, 2002). The small pocket was found to accommodate substituents not larger than ethyl groups. The steric hindrance could be a possible explanation also for the observation with other ω-TAs, if a similar fold is assumed (Hirotsu et al., 2005; Shin and Kim, 2002). Mutant libraries generated by either random or site-directed mutagenesis could be screened with our new assay in order to identify enzymes for the conversion of substrates with larger chains.

3.3. Validation of screening results

To evaluate the reliability of our screening results, colourimetric data were compared to GC and HPLC analyses (Table 2 and Fig. 3) for reactions run under identical conditions. In all cases the results of the TTC-screening assay fit well to the instrumental analyses showing a deviation of 5–10% in most cases, indicating that the TTC-assay is generally highly reliable. Furthermore, the chiral GC-analyses of *rac*-acetoin indicate, that there is no substrate selectivity regarding the (*S*)- or the (*R*)-enantiomer of the remaining substrate, since the *ee* of the substrate stays constant after enzymatic reduction.

Table 2
Screening results for the conversion of 2-hydroxy ketones by ω-TAs measured with the TTC-assay.

Enzyme ID	acetoin **1**			propioin **2**			2-HAP **3**			(*R*)-PAC **5**			(*R*)-PPC **6**		
	A[a]	B[a]	C[a]	A[a]	B[a]	C[a]	A[a]	B[a]	C[a]	A[a]	B[a]	C[a]	A[a]	B[a]	C[a]
Neg. control	–	–	–	–	–	–	–	–	–	–	–	–	–	–	–
CV2025	++++ (88%)	(+) (18%)	+ (26%)	–	–	–	+ (38%)	–	–	++++ (96%)	++ (23%)	+ (19%)	–	–	–
PP5182	+++ (60%)	(+) (16%)	(+) (15%)	–	–	–	–	–	–	++++ (94%)	++ (22%)	+ (22%)	–	–	–
PP2799	++ (49%)	–	+ (26%)	–	–	–	(+) (12%)	–	–	++++ (89%)	(+) (15%)	(+) (19%)	–	–	–
PA0221	–	–	+ (23%)	–	–	–	–	–	–	+ (33%)	–	–	–	–	–

Reaction conditions: 10 mM 2-hydroxy ketones and 10 mM amine donor **A**, **B**, or **C** in HEPES buffer (100 mM, pH 7.5), containing 200 μM PLP, 1 mg/mL crude cell extract, incubated in a 96-well plate at 27 °C, 100 rpm, 16 h.
"+" and (%): conversion of 2-hydroxy ketones measured as a decrease of absorbance at 510 nm after colouration with TTC-reagent. Conversion values (%) were determined relative to an internal calibration curve. "++++" ≥ 80%, "+++" ≥ 60%, "++" ≥ 40%, "+" ≥ 20%, "(+)" ≥ 10% conversion; cut-off: < 10% conversion.
Negative control: 1 mg/mL clarified crude cell extract of *E. coli* BL21(DE3) transformed with an empty plasmid (pET-29a).
Substrates **4**, **7**–**9**: no conversion was measured for the 2-hydroxy ketones **7**–**9** with (*S*)-α-methylbenzylamine (**A**); a combination with **B**, **C** was not determined. Results of the 2-hydroxy ketone **4**, see Section 3.3.
[a] Amine donor.

Please cite this article in press as: Sehl, T., et al., TTC-based screening assay for ω-transaminases: A rapid method to detect reduction of 2-hydroxy ketones. J. Biotechnol. (2012), doi:10.1016/j.jbiotec.2011.12.023

G Model
BIOTEC-5959; No. of Pages 7
ARTICLE IN PRESS
6 T. Sehl et al. / Journal of Biotechnology xxx (2012) xxx–xxx

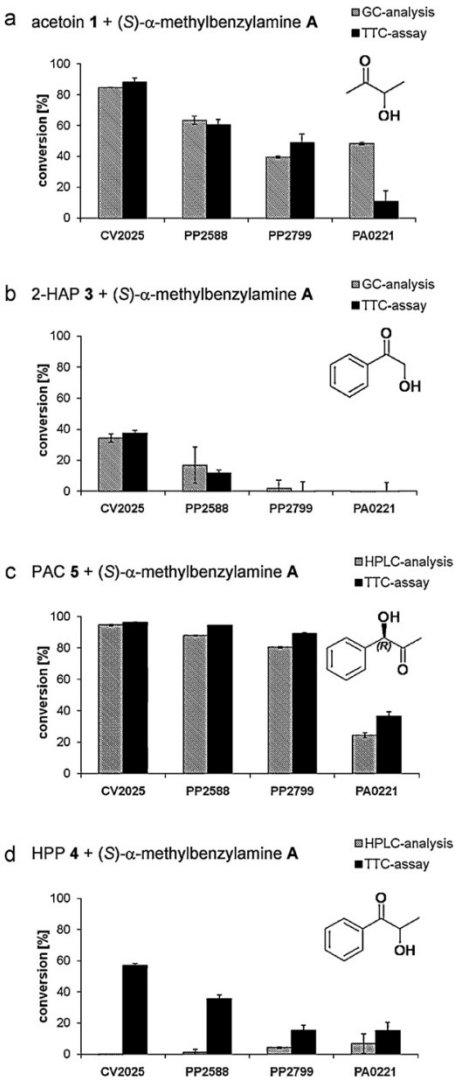

Fig. 3. Validation of the TTC-assay results (black) by GC and HPLC analysis (grey). Reactions with 10 mM acetoin **1** (a), 2-HAP **3** (b), PAC **5** (c), HPP **4** (d) and equal amounts of the amine donor (*S*)-α-MBA were performed in HEPES buffer (100 mM, pH 7.5) containing 200 μM PLP and 1 mg/mL crude cell extract. The reactions were incubated at 27 °C, 100 rpm for 16 h before the conversion was determined.

HPLC-analyses demonstrated that the conversion suggested for HPP **4** by the TTC-assay was misleading (Fig. 3d). In the presence of the crude cell extract the substrate HPP **4** is partially isomerised to PAC **5**. As was analysed by HPLC, around 5% of the regioisomer PAC **5** is formed, which is detectable in the empty-vector control, whereas no regioisomer was found in the presents of PAC-converting ω-TAs such as CV2025, PP5182 and PP2799. This suggests a direct consumption of the PAC **5** by those enzymes. Since PAC **5** has a 15-fold higher colouration rate in the TTC-assay compared to HPP **4**

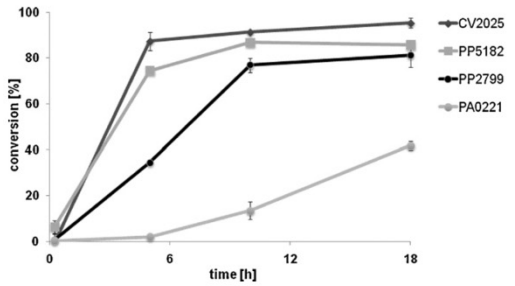

Fig. 4. Enzymatic conversion of PAC **5** (10 mM) with (*S*)-α-MBA **A** (10 mM) measured by the TTC-assay as an endpoint determination at different time points and plotted as a function of the reaction time.

(Fig. 2), these results can be explained. Interestingly, this problem does not occur with purified enzymes instead of crude cell lysate. Thus, one way to overcome this limitation could be working with purified enzyme.

3.4. Time-dependent conversion via TTC-assay

The TTC-assay is a rapid method to measure substrate conversion by an endpoint determination. By simply stopping the reaction after different time intervals we could demonstrate that it is also possible to analyse conversion rates of ω-TAs-catalysed reactions. Therefore reactions of 10 mM PAC **5** with equal amounts of (*S*)-α-MBA **A** were set up for each ω-TA as replicates in different wells of a 96-well plate. As the absorption behaviour of PAC **5** in the TTC-assay is known (Fig. 2 and Table 1), the internal calibration was reduced to only 2-points (0 mM and 10 mM PAC **5**), which slightly decreased the accuracy of the assay, but lowered the sample amount. Conversions were determined after 30 min, 4 h, 8 h and 18 h.

Using this experiment procedure we could demonstrate that the conversion of PAC **5** in presence of CV2025, PP5182, PP2799 is completed after 4–10 h (conversion 80–90%) while the reactions with PA0221 were considerably slower and only reached 40% conversion after 18 h (Fig. 4).

4. Conclusion

A rapid TTC-based screening assay for ω-transaminase reductive activity was developed, which allows measuring the conversion of various 2-hydroxy ketones. Since the assay is independent of the choice of the desired amine donor, we have screened a panel of different wild-type ω-TAs for the conversion of various 2-hydroxy ketones with three different amine donors. This allowed us to identify three novel ω-transaminases showing high conversion rates for acetoin **1**, 2-hydroxyacetophenone **3**, and phenylacetylcarbinol **5**.

The assay is with a deviation of 5–10% to HPLC/GC-analytics highly reliable in comparison, and sensitive enough to show background isomerisation which was catalysed by the crude cell extract in one case. Furthermore, we could demonstrate that the assay can also be used to determine time-dependent conversion rates. In addition, it is conceivable to use this assay with different amine donor–acceptor ratios or with additional enzymes and additives in order to shift the equilibrium constant for desired reactions.

Acknowledgements

This project was embedded in the CLIB-Graduate Cluster Industrial Biotechnology of the Heinrich-Heine-University Düsseldorf

Please cite this article in press as: Sehl, T., et al., TTC-based screening assay for ω-transaminases: A rapid method to detect reduction of 2-hydroxy ketones. J. Biotechnol. (2012), doi:10.1016/j.jbiotec.2011.12.023

G Model
BIOTEC-5959; No. of Pages 7
ARTICLE IN PRESS
T. Sehl et al. / Journal of Biotechnology xxx (2012) xxx–xxx 7

co-financed by the Ministry of Innovation, Science and Research of North Rhine-Westphalia. We are thankful to Dr. Kirsten Zeitler, University of Regensburg, for providing 2-hydroxy ketones **7–9**.

References

Ager, D.J., Prakash, I., Schaad, D.R., 1996. 1,2-Amino alcohols and their heterocyclic derivatives as chiral auxiliaries in asymmetric synthesis. Chem. Rev. 96, 835–876.
Bergmeier, S.C., 2000. The synthesis of vicinal amino alcohols. Tetrahedron 56, 2561–2576.
Breuer, M., Pohl, M., Hauer, B., Lingen, B., 2002. High-throughput assay of (*R*)-phenylacetylcarbinol synthesized by pyruvate decarboxylase. Anal. Bioanal. Chem. 374, 1069–1073.
Chen, C., Feng, X., Zhang, G., Zhao, Q., Huang, G., 2008. An efficient method for the synthesis of α-hydroxyalkyl aryl ketones. Synthesis, 3205–3208.
DSM, 2011. http://www.dsm.com/en_US/downloads/dpp/DSM_PDC_TechBiocatalysis.pdf. DSM Pharma Chemicals Code 0210.
Fehr, C., Galindo, J., 1996. Catalytic enantioselective protonation of enolates. Angew. Chem. Int. Ed. 33, 1888–1889.
Hirotsu, K., Goto, M., Okamoto, A., Miyahara, I., 2005. Dual substrate recognition of aminotransferases. Chem. Rec. 5, 160–172.
Höhne, M., Bornscheuer, U.T., 2009. Biocatalytic routes to optically active amines. ChemCatChem 1, 42–51.
Höhne, M., Kuhl, S., Robins, K., Bornscheuer, U.T., 2008. Efficient asymmetric synthesis of chiral amines by combining transaminase and pyruvate decarboxylase. ChemBioChem 9, 363–365.
Hopwood, J., Truppo, M.D., Turner, N.J., Lloyd, R.C., 2011. A fast and sensitive assay for measuring the activity and enantioselectivity of transaminases. Chem. Commun. 47, 773–775.
Hoyos, P., Sinisterra, J.-V., Molinari, F., Alcántara, A.s.R., Domínguez de María, P., 2009. Biocatalytic strategies for the asymmetric synthesis of α-hydroxy ketones. Acc. Chem. Res. 43, 288–299.
Hwang, B.-Y., Kim, B.-G., 2004. High-throughput screening method for the identification of active and enantioselective [omega]-transaminases. Enzyme Microb. Technol. 34, 429–436.
Kamiyama, T., Umino, T., Itezono, Y., Nakamura, Y., Satoh, T., Yokose, K., 1995. Sulfobacins A and B, novel von Willebrand factor receptor antagonists. II. Structural elucidation. J. Antibiot. 48, 929–936.
Kaulmann, U., Smithies, K., Smith, M.E.B., Hailes, H.C., Ward, J.M., 2007. Substrate spectrum of [omega]-transaminase from *Chromobacterium violaceum* DSM30191 and its potential for biocatalysis. Enzyme Microb. Technol. 41, 628–637.
Koszelewski, D., Tauber, K., Faber, K., Kroutil, W., 2010. Omega-transaminases for the synthesis of non-racemic alpha-chiral primary amines. Trends Biotechnol. 28, 324–332.
Müller, M., Gocke, D., Pohl, M., 2009. Thiamin diphosphate in biological chemistry: exploitation of diverse thiamin diphosphate-dependent enzymes for asymmetric chemoenzymatic synthesis. FEBS J. 276, 2894–2904.
Nakamura, H., Suda, H., Takita, T., 1976. X ray structure determination of (2*S*,3*R*) 3-amino-2-hydroxy-4-phenylbutanoic acid, a new amino acid component of bestatin. J. Antibiot. 29, 102–103.
O'Toole, S.E., Rose, C.A., Gundala, S., Zeitler, K., Connon, S.J., 2010. Highly chemoselective direct crossed aliphatic–aromatic acyloin condensations with triazolium-derived carbene catalysts. J. Org. Chem. 76, 347–357.
Ohta, Y., Shinkai, I., 1997. Saquinavir. Bioorg. Med. Chem. 5, 465–466.
Rother, D., Kolter, G., Gerhards, T., Berthold, C.L., Gauchenova, E., Knoll, M., Pleiss, J., Müller, M., Schneider, G., Pohl, M., 2011. S-selective mixed carboligation by structure-based design of the pyruvate decarboxylase from *Acetobacter pasteurianus*. ChemCatChem 2, 1587–1596.
Savile, C.K., Janey, J.M., Mundorff, E.C., Moore, J.C., Tam, S., Jarvis, W.R., Colbeck, J.C., Krebber, A., Fleitz, F.J., Brands, J., Devine, P.N., Huisman, G.W., Hughes, G.J., 2010. Biocatalytic asymmetric synthesis of chiral amines from ketones applied to sitagliptin manufacture. Science 329, 305–309.
Scarlato, G.R., 2009. Aminotransferases for commercial chiral amine manufacture. Special. Chem. Mag., 56–57.
Schätzle, S., Höhne, M., Redestad, E., Robins, K., Bornscheuer, U.T., 2009. Rapid and sensitive kinetic assay for characterization of omega-transaminases. Anal. Chem. 81, 8244–8248.
Schätzle, S., Steffen-Munsberg, F., Thontowi, A., Höhne, M., Robins, K., Bornscheuer, U.T., 2011. Enzymatic asymmetric synthesis of enantiomerically pure aliphatic, aromatic and arylaliphatic amines with (R)-selective amine transaminases. Adv. Synth. Catal. 353, 2439–2445.
Shin, J.S., Kim, B.G., 2002. Exploring the active site of amine:pyruvate aminotransferase on the basis of the substrate structure–reactivity relationship: how the enzyme controls substrate specificity and stereoselectivity. J. Org. Chem. 67, 2848–2853.
Smith, M.E., Kaulmann, U., Ward, J.M., Hailes, H.C., 2006. A colorimetric assay for screening transketolase activity. Bioorg. Med. Chem. 14, 7062–7065.
Smith, M.E.B., Chen, B.H., Hibbert, E.G., Kaulmann, U., Smithies, K., Galman, J.L., Baganz, F., Dalby, P.A., Hailes, H.C., Lye, G.J., Ward, J.M., Woodley, J.M., Micheletti, M., 2009. A multidisciplinary approach toward the rapid and preparative-scale biocatalytic synthesis of chiral amino alcohols: a concise transketolase-/ω-transaminase-mediated synthesis of (2*S*,3*S*)-2-aminopentane-1,3-diol. Org. Process Res. Dev. 14, 99–107.
Smithies, K., Smith, M.E.B., Kaulmann, U., Galman, J.L., Ward, J.M., Hailes, H.C., 2009. Stereoselectivity of an ω-transaminase-mediated amination of 1,3-dihydroxy-1-phenylpropane-2-one. Tetrahedron: Asymmetry 20, 570–574.
Truppo, M.D., Rozzell, J.D., Moore, J.C., Turner, N.J., 2009. Rapid screening and scale-up of transaminase catalysed reactions. Org. Biomol. Chem. 7, 395–398.
Tufvesson, P., Lima-Ramos, J., Jensen, J.S., Al-Haque, N., Neto, W., Woodley, J.M., 2011. Process considerations for the asymmetric synthesis of chiral amines using transaminases. Biotechnol. Bioeng. 108, 1479–1493.
Umezawa, H., Aoyagi, T., Suda, H., 1976. Bestatin, an inhibitor of aminopeptidase B produced by actinomycetes. J. Antibiot. 29, 97–99.
Ward, J., Wohlgemuth, R., 2010. High-yield biocatalytic amination reactions in organic synthesis. Curr. Org. Chem. 14, 1914–1927.

Please cite this article in press as: Sehl, T., et al., TTC-based screening assay for ω-transaminases: A rapid method to detect reduction of 2-hydroxy ketones. J. Biotechnol. (2012), doi:10.1016/j.jbiotec.2011.12.023

3.2 Two steps in one pot: Enzyme cascade for the synthesis of nor(pseudo)ephedrine from inexpensive starting materials

Angewandte Communications

Biocatalysis

DOI: 10.1002/anie.201300718

Two Steps in One Pot: Enzyme Cascade for the Synthesis of Nor(pseudo)ephedrine from Inexpensive Starting Materials**

*Torsten Sehl, Helen C. Hailes, John M. Ward, Rainer Wardenga, Eric von Lieres, Heike Offermann, Robert Westphal, Martina Pohl, and Dörte Rother**

A challenging task for chemical researchers in the next decade is the development of cleaner and more environmentally friendly reactions.[1] The traditional chemical syntheses of enantiomerically pure compounds often require multistep protocols with protection–deprotection steps as well as the isolation of potentially unstable intermediates, lowering the yields and sustainability of the overall process.[2]

Phenylpropanolamines, members of the amphetamine family of ephedra alkaloids, are compounds with multifunctional applications but challenging syntheses routes. The stereoisomers norpseudoephedrine (NPE) and norephedrine (NE) are used as building blocks for the preparation of ligands and chiral auxiliaries in organic syntheses[3] and also have direct applications as pharmaceutically active molecules.[4] Reported synthetic approaches to these compounds have disadvantages such as relatively expensive reagents, multistep preparative routes, and only moderate enantio- and diastereoselectivity.[5] Recently, a novel highly stereoselective method was described for the synthesis of all phenylpropanolamine isomers with *ee* and *de* values exceeding 99%.[6] Norephedrine isomers were accessible in four steps (40% yield) and norpseudoephedrine in seven steps (35% yield) starting from 2-phenyl-2-trimethylsilyloxyacetonitrile.

Synthetic enzyme cascades are valuable alternative routes for the stereoselective production of fine chemicals. Since the chemo- and stereoselectivities are typically high, the isolation of by-products and reaction intermediates can be circumvented[7] and thus the eco-efficiency increased.[8] Here we present an enzymatic one-pot two-step reaction for the synthesis of stereomerically pure (1*R*,2*S*)-NE and (1*R*,2*R*)-NPE from benzaldehyde and pyruvate (Scheme 1). A number of different ways to perform enzyme cascade reactions have already been described (for more details see Chapter 1 in the Supporting Information).[1b,2a,8a–c,9] Our one-pot two-step reaction combines many advantages of known synthesis strategies like high stereoselectivities, inexpensive starting materials, high step economy (only two steps), and an equilibrium shift without addition of further enzymes or cosubstrates.

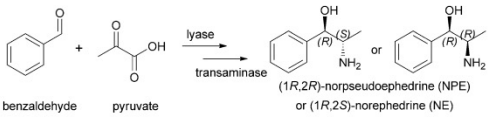

Scheme 1. One-pot two-step reaction for the synthesis of norpseudoephedrine (NPE) and norephedrine (NE).

In the first step pyruvate is decarboxylated and subsequently ligated to benzaldehyde yielding (*R*)-phenylacetylcarbinol ((*R*)-PAC). The reaction is catalyzed by the thiamine diphosphate (ThDP)-dependent acetohydroxyacid synthase I (AHAS-I) from *E. coli* which performs the decarboxylation of pyruvate and the subsequent carboligation without releasing the hydroxyethyl-ThDP (see Scheme 2).[10] (*R*)-PAC is obtained with high stereoselectivity ($ee > 98\%$) and can be converted directly to the desired (1*R*,2*S*)-NE and to (1*R*,2*R*)-NPE in the second step of the cascade (reductive amination) by selectively using (*S*)- and (*R*)-selective ω-transaminases (TAs), respectively. In our previous work a set of 18 different (*S*)-selective wild-type (*S*)TAs had been screened for the conversion of 2-hydroxy ketones.[11] For the reductive amination of (*R*)-PAC, the *Cv*-(*S*)TA from *Chromobacterium violaceum* gave the most promising results. To gain access to (1*R*,2*R*)-NPE, seven different (*R*)-selective (*R*)TAs from Enzymicals AG (see Chapter 2 in the Supporting Information) were tested.

The enzymatic reductive amination requires an amine donor as a cosubstrate. Through the clever combination of cosubstrates (here: alanine) and enzymes, the resulting by-product (here: pyruvate) of the second reaction step can serve as the substrate for the first step. This novel type of cascade design is referred to as a "recycling cascade" (Scheme 2 and Chapter 1 in the Supporting Information). We determined the

[*] M. Sc. T. Sehl, Dr. E. von Lieres, H. Offermann, Dipl.-Biotechnol. R. Westphal, Prof. Dr. M. Pohl, Dr. D. Rother
Institute of Bio- and Geosciences
IBG-1: Biotechnology, Forschungszentrum Jülich GmbH
Leo-Brandt-Strasse 1, 52425 Jülich, (Germany)
E-mail: do.rother@fz-juelich.de
Prof. H. C. Hailes
Department of Chemistry, University College London
20 Gordon Street, London WC1H OAJ (UK)
Prof. J. M. Ward
The Advanced Centre for Biochemical Engineering
Department of Biochemical Engineering, University College London
Torrington Place, London, WC1E 7JE (UK)
Dr. R. Wardenga
Enzymicals AG
Walther-Rathenau-Strasse 49a, 17489 Greifswald (Germany)

[**] This work was supported by the CLIB Graduate Cluster Industrial Biotechnology of the Heinrich-Heine-University Düsseldorf and financed by the DFG (German Research Foundation) in the frame of Research Group FOR 1296.

Supporting information for this article is available on the WWW under http://dx.doi.org/10.1002/anie.201300718.

Angewandte International Edition Chemie

product concentration (related to a total benzaldehyde concentration of 20 mM, Figure 3A).

In the case of *At*-(*R*)TA the cascade reaction is even more efficient (Figure 3B): (1*R*,2*R*)-NPE is accessible in the one-pot two-step sequential cascade with conversions greater than 96% and very high stereomeric purity ($de > 98\%$, $ee > 99\%$). After addition of another 10 mM benzaldehyde and fresh AHAS-I, the *At*-(*R*)TA was still active. Thus, without addition of further transaminase, 16.6 mM (1*R*,2*R*)-NPE (83% conversion) was obtained in 5 h by the complete one-pot two-step recycling cascade. Further addition of *At*-(*R*)TA did not considerably increase the final product concentration.

In summary, we have developed a strategy for the synthesis of (1*R*,2*S*)-NE and (1*R*,2*R*)-NPE. Both compounds are accessible in a biocatalytic one-pot two-step reaction in high stereoisomeric purity ($de > 98\%$, $ee > 99\%$) from inexpensive starting materials without isolation of the intermediate product. Additionally, these cascade reactions can be performed in a novel "recycling mode" in which the coproduct of the second step is removed without addition of further catalysts or cosubstrates and recycled as a substrate for the first cascade step.

By combining reaction and process optimization, the sequential cascade consisting of AHAS-I and *Cv*-(*S*)TA provided (1*R*,2*S*)-NE with a conversion of 80% (8.0 mM). For the production of (1*R*,2*R*)-NPE we could identify (*R*)-selective ω-TAs catalyzing the one-pot two-step cascade in a simultaneous mode with conversions up to 85% (8.5 mM). Moreover, in the sequential mode, formation of the side product (benzylamine) is reduced and (1*R*,2*R*)-NPE was obtained with a conversion exceeding 96% within 13 h. In the recycling step (addition of another 10 mM benzaldehyde, but no pyruvate) a total concentration of 16.6 mM (1*R*,2*R*)-NPE (83% conversion) was observed after further 5 h reaction time.

The recycling mode can be applied to any set of reactions for which a clever combination of cosubstrates and coproducts is possible, such that the coproducts of one reaction can be reused as substrates for the other. This approach optimizes the atom economy of the reaction by reducing the waste production.

Experimental Section

L-alanine (Merck), D-alanine (Sigma–Aldrich), and pyruvate (Sigma–Aldrich) were of >99% purity. Benzaldehyde (Sigma–Aldrich) was freshly distilled before use. The preparation of the catalysts *Cv*-(*S*)TA and AHAS-I is described in the supporting information. (*R*)-selective TAs are commercially available from Enzymicals AG (Germany) as lyophilized crude cell extracts. Descriptions of the reaction details, reaction analysis, cascade optimizations, and equilibrium determination can be found in the Supporting Information.

Received: January 27, 2013
Published online: May 9, 2013

Keywords: asymmetric synthesis · biocatalysis · enzyme cascades · phenylpropanolamine · ω-transaminase

[1] a) F. Cavani, *J. Chem. Technol. Biotechnol.* **2010**, *85*, 1175–1183; b) E. Ricca, B. Brucher, J. H. Schrittwieser, *Adv. Synth. Catal.* **2011**, *353*, 2239–2262.

[2] a) S. Shanmuganathan, D. Natalia, L. Greiner, P. Dominguez de Maria, *Green Chem.* **2012**, *14*, 94–97; b) M. J. Climent, A. Corma, S. Iborra, M. Mifsud, A. Velty, *Green Chem.* **2010**, *12*, 99–107.

[3] a) M. Sherman, *Spatial Statistics and Spatio-Temporal Data: Covariance Functions and Directional Properties*, Wiley, Hoboken, **2010**, ISBN: 9780470699584; b) G. Blay, I. Fernández, B. Monje, J. R. Pedro, *Tetrahedron Lett.* **2004**, *45*, 8039–8042; c) F. K. Cheung, A. M. Hayes, J. Hannedouche, A. S. Y. Yim, M. Wills, *J. Org. Chem.* **2005**, *70*, 3188–3197; d) D. A. Evans, M. D. Ennis, T. Le, N. Mandel, G. Mandel, *J. Am. Chem. Soc.* **1984**, *106*, 1154–1156; e) J. L. García Ruano, C. Alemparte, M. T. Aranda, M. M. Zarzuelo, *Org. Lett.* **2003**, *5*, 75–78; f) R. Guo, A. J. Lough, R. H. Morris, D. Song, *Organometallics* **2004**, *23*, 5524–5529; g) S. R. Hitchcock, D. M. Casper, J. F. Vaughn, J. M. Finefield, G. M. Ferrence, J. M. Esken, *J. Org. Chem.* **2004**, *69*, 714–718; h) C. Unaleroglu, A. E. Aydin, A. S. Demir, *Tetrahedron: Asymmetry* **2006**, *17*, 742–749.

[4] a) N. A. Flavahan, *J. Pharmacol. Exp. Ther.* **2005**, *313*, 432–439; b) R. B. Rothman, N. Vu, J. S. Partilla, B. L. Roth, S. J. Hufeisen, B. A. Compton-Toth, J. Birkes, R. Young, R. A. Glennon, *J. Pharmacol. Exp. Ther.* **2003**, *307*, 138–145; c) R. Krizevski, N. Dudai, E. Bar, E. Lewinsohn, *J. Ethnopharmacol.* **2007**, *114*, 432–438.

[5] J. A. Groeper, S. R. Hitchcock, G. M. Ferrence, *Tetrahedron: Asymmetry* **2006**, *17*, 2884–2889.

[6] H. K. Lee, S. Kang, E. B. Choi, *J Org Chem.* **2012**, *77*, 5454–5460.

[7] F. Lopez-Gallego, C. Schmidt-Dannert, *Curr. Opin. Chem. Biol.* **2010**, *14*, 174–183.

[8] a) A. Bruggink, R. Schoevaart, T. Kieboom, *Org. Process Res. Dev.* **2003**, *7*, 622–640; b) S. F. Mayer, W. Kroutil, K. Faber, *Chem. Soc. Rev.* **2001**, *30*, 332–339; c) J. H. Schrittwieser, J. Sattler, V. Resch, F. G. Mutti, W. Kroutil, *Curr. Opin. Chem. Biol.* **2011**, *15*, 249–256; d) R. A. Sheldon, *Green Chem.* **2007**, *9*, 1273–1283; e) R. A. Sheldon, *Chem. Commun.* **2008**, 3352–3365.

[9] C. V. Voss, C. C. Gruber, W. Kroutil, *Angew. Chem.* **2008**, *120*, 753–757; *Angew. Chem. Int. Ed.* **2008**, *47*, 741–745.

[10] S. Engel, M. Vyazmensky, S. Geresh, Z. Barak, D. M. Chipman, *Biotechnol. Bioeng.* **2003**, *83*, 833–840.

[11] T. Sehl, R. C. Simon, H. C. Hailes, J. M. Ward, U. Schell, M. Pohl, D. Rother, *J. Biotechnol.* **2012**, *159*, 188–194.

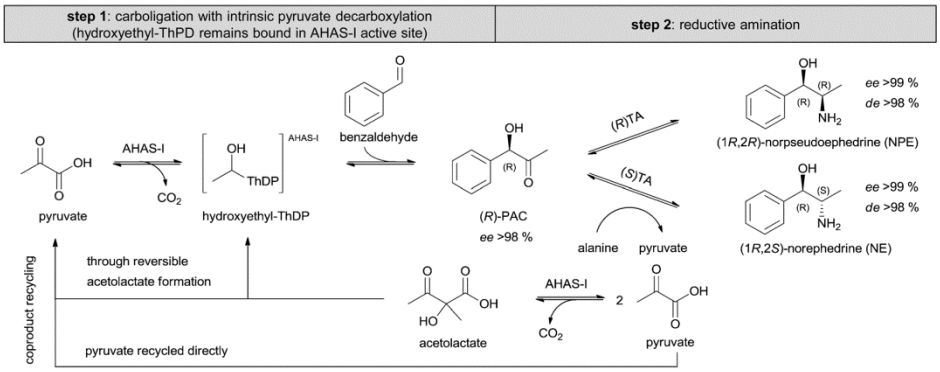

Scheme 2. One-pot two-step reaction for the synthesis of nor(pseudo)ephedrine performed as a recycling cascade combining acetohydroxyacid synthase I (AHAS-I) and a (*S*)- or (*R*)-selective ω-transaminases ((*R*)TA, (*S*)TA).

thermodynamic equilibrium constant for the reductive amination of PAC with alanine as the amine donor to be 2.31×10^{-3} (Chapter 4 in the Supporting Information). Consequently, when equimolar concentrations of alanine and PAC are used and the by-product pyruvate is not removed, a theoretical conversion of less than 5% is obtained (see Chapter 4.4 in the Supporting Information). In our reaction setup, pyruvate can be removed by two different carboligation reactions mediated by AHAS-I: 1) the carboligation with benzaldehyde yielding PAC or 2) a carboligation with another pyruvate molecule yielding acetolactate. The reversible reaction giving acetolactate is kinetically favored, whereas the reaction equilibrium lies on the side of PAC formation.[10] Thus, acetolacetate is a suitable substrate for the carboligation of (*R*)-PAC by the cleavage reaction to pyruvate and hydroxyethyl-ThDP.

A challenge in this one-pot two-step cascade is the fact that the starting material benzaldehyde might serve as a substrate for AHAS-I as well as for the ω-transaminases. As a consequence of the higher chemical reactivity of aldehydes relative to ketones and steric constraints in the active site of ω-TAs, it was not possible to find an enzyme among the 25 screened ω-TAs for which the reductive amination of PAC was kinetically favored over the reductive amination of benzaldehyde. The most promising (*S*)-selective transaminase *Cv*-(*S*)TA has a roughly 17-fold higher initial rate in the reaction with benzaldehyde than with PAC (Figure 1A). As a consequence, in a one-pot two-step cascade reaction where AHAS-I and *Cv*-(*S*)TA were added simultaneously, 98% of the benzaldehyde was converted to benzylamine (Figure 2A). However, in the case of the (*R*)-selective ω-TAs we could surprisingly identify enzymes for which the simultaneous one-pot two-step reaction provided (1*R*,2*R*)-NPE with conversions of up to 85% (Figure 2A). The initial rate activities of the ω-TA from *Aspergillus terreus* (*At*-(*R*)TA) for reactions with PAC and benzaldehyde were on the same order of magnitude (Figure 1B), but roughly ten times lower than the initial rates for the (*R*)-PAC formation

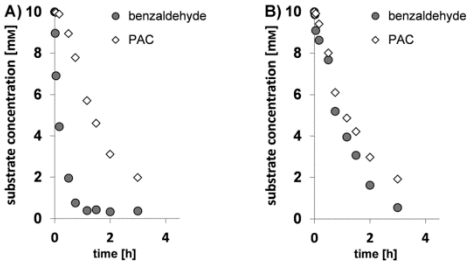

Figure 1. Conversion curves for the reductive amination of benzaldehyde (10 mM) and PAC (10 mM) by A) ω-TA *Cv*-(*S*)TA (1 mg mL^{-1}) and by B) *At*-(*R*)TA (1 mg mL^{-1}), respectively. The reaction was carried out in 100 mM HEPES (pH 7.5 with 200 μM pyridoxal-5′-phosphate (PLP), 50 μM flavine adenine dinucleotide (FAD), 100 μM ThDP, 5 mM $MgCl_2$) containing (*S*)- or (*R*)-α-methylbenzylamine (10 mM) as amine donor.

catalyzed by AHAS-I. These differences suffice to reduce the amount of formed by-product (benzylamine) to merely 10%.

In line with these experimental data, the NE/benzylamine ratio is low when the one-pot two-step reaction is performed as a simultaneous cascade including a recycling step. Here, both enzymes were added simultaneously to a mixture of 20 mM benzaldehyde, 10 mM pyruvate, and 50 mM alanine. Since no further pyruvate was added, product concentrations higher than 10 mM (NE or NPE) are only possible by the successful recycling of pyruvate that is generated by deamination of alanine. Remarkably, with *At*-(*R*)TA about 14 mM (1*R*,2*R*)-NPE and only 5.5 mM benzylamine were formed in this simultaneous recycling mode, while in case of the *Cv*-(*S*)TA the major product is benzylamine.

Although benzylamine can be separated from NPE and NE by column chromatography (mobile phase EtOAc/MeOH/NH_3 = 85:10:5), it is more advantageous to reduce

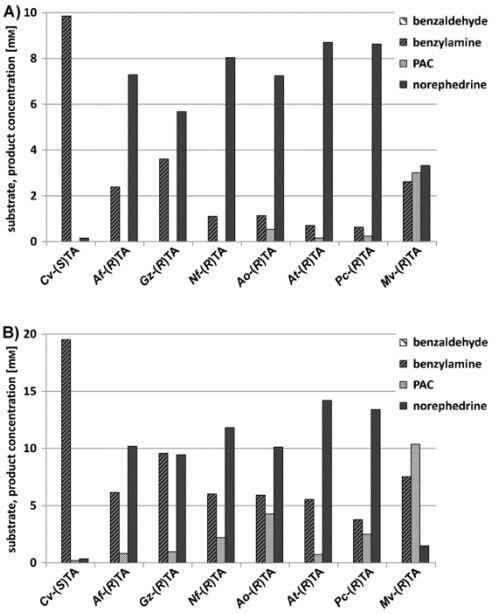

Figure 2. A) One-pot two-step simultaneous cascade and B) one-pot two-step simultaneously recycling cascade with *Cv*-(*S*)TA and seven (*R*)-selective TAs. For the one-pot two-step reaction 10 mM benzaldehyde, 10 mM pyruvate, and 50 mM D- or L-alanine were dissolved in 100 mM HEPES (pH 7.5 with 200 μM PLP, 50 μM FAD, 100 μM ThDP, 5 mM $MgCl_2$) and the two enzymes (AHAS-I and ω-TA) were added simultaneously. The recycling cascade reactions (B) were performed analogously with 20 mM benzaldehyde instead of 10 mM.

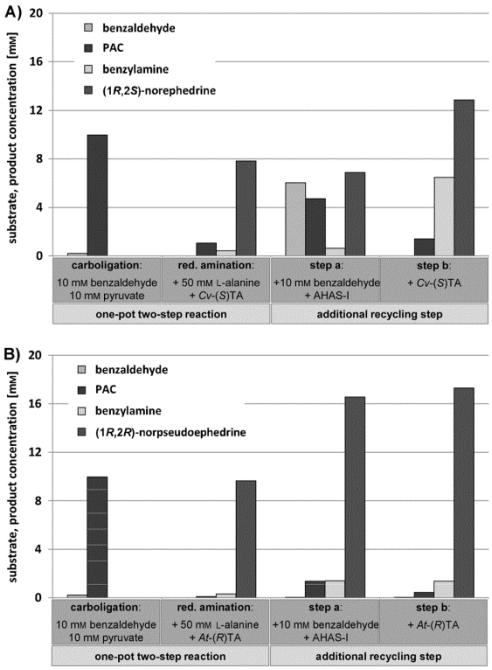

Figure 3. Synthesis of A) (1*R*,2*S*)-NE and B) (1*R*,2*R*)-NPE performed as a sequential one-pot two-step reaction with an additional recycling step (time-dependent reaction curve can be found in Chapter 6 in the Supporting Information). Reaction conditions: 100 mM HEPES (pH 7.5 with 200 μM PLP, 50 μM FAD, 100 μM ThDP, 5 mM $MgCl_2$), 25 °C, 100 rpm. One-pot two-step reaction: Carboligation (1 h): 10 mM benzaldehyde, 10 mM pyruvate, 0.5 mg mL^{-1} AHAS; reductive amination (12 h): +50 mM alanine, +1 mg mL^{-1} TA. Recycling step:step a: +10 mM benzaldehyde, +0.5 mg mL^{-1} AHAS-I (A: 1.5 h, B: 5 h); step b: +1 mg mL^{-1} TA (A: *Cv*-(*S*)TA, 12 h, B: *At*-(*R*)TA, 5 h).

the formation of byproducts by appropriate process engineering in order to increase process efficiency. There are two general ways to perform a cascade reaction: one is the already described simultaneous mode, the other one the so-called sequential mode, where the catalysts are added consecutively.[9] In our sequential synthetic enzyme cascade, the limiting step is the reductive amination. In order to circumvent this bottleneck, we optimized the reaction parameters of the reductive amination step regarding pH, temperature, the concentrations of transaminase and AHAS-I, and the amine donor/PAC ratio (see Chapter 5 in the Supporting Information). For the enzyme combination *Cv*-(*S*)TA/AHAS-I conversions exceeding 80% could be achieved under optimized cascade conditions (pH 7.5, 25 °C, 1 mg mL^{-1} *Cv*-(*S*)TA, 0.5 mg mL^{-1} AHAS-I, alanine/PAC = 5:1).

These optimized conditions were applied in the one-pot two-step sequential mode. Here, the transaminase was added after the benzaldehyde had been completely consumed in the AHAS-I-catalyzed carboligation step (after 1 h 100% conversion was achieved, Figure 3A). This increased the conversion of (1*R*,2*S*)-NE from 2% (Figure 2A: one-pot two-step simultaneous cascade) to 78% (7.8 mM, Figure 3A) with the combination AHAS-I/*Cv*-(*S*)TA. Under these conditions the undesired by-product benzylamine amounted to less than 0.5 mM (Figure 3A). Upon subsequent addition of further 10 mM of benzaldehyde and fresh AHAS-I, PAC was formed in a second carboligation step. Since no further pyruvate was added, this result demonstrates that the recycling of pyruvate, generated by deamination of alanine, was successful in this sequential enzyme recycling cascade mode. However, the reaction resulted in the formation of only 4.7 mM PAC (47% conversion), which is most likely due to the instability of acetolactate. If the latter is chemically decarboxylated to acetoin, it is no longer available for PAC formation. Moreover, acetoin (and probably also acetolactate) can act as substrates for *Cv*-(*S*)TA as described previously.[11] Further, neither the NE nor the benzylamine concentration increased significantly, which suggests almost complete inactivation of *Cv*-(*S*)TA (Figure 3A). Addition of fresh *Cv*-(*S*)TA started the reaction again yielding 12.9 mM (1*R*,2*S*)-NE (*de* > 98%, *ee* > 99%). This corresponds to roughly 65% of the possible

2-Steps in 1-pot: synthetic enzyme cascade for the synthesis of nor(pseudo)ephedrine from inexpensive starting material

--- Supplementary Information ---

Table of contents:

1.) Definition and explanation of different cascade reactions types

A number of different multi-enzyme cascade reactions have already been described.[1] In general, they can be subdivided into four types of cascade designs (Scheme 1, A-D).[1b] In the 'linear cascade' a single product is synthesized via one or more intermediates from a single substrate (Scheme 1A). In more complex enzyme cascades like the 'orthogonal cascade', product formation is coupled with a cofactor/co-substrate regeneration step or by-products removal reactions (Scheme 1B). Whereas in 'cyclic cascades' a mixture of substrates is transformed into an intermediate, which is subsequently converted back into starting material, so that one substrate is subsequently enriched (Scheme 1C). A typical example is the dynamic kinetic resolution of racemic compounds. In 'parallel cascade' reactions formation of two products by two biocatalytic reactions is coupled via their cofactors/co-substrates (Scheme 1D). Except for the linear cascade, all cascade modes require the introduction of further enzymes and/or co-substrates in order to allow cofactor regeneration or by-products removal to shift the reaction equilibrium. These additional components have to be separated from the desired products, which can lower the economy of the process.

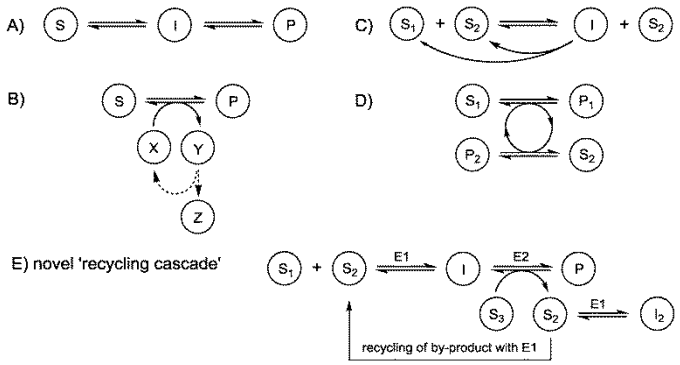

Scheme 1: Four previously described enzymatic cascade designs:[1b] A) linear cascade, B) orthogonal cascade, C) cyclic cascade, D) parallel cascade and E) the novel recycling cascade (adapted from ref. [1a])

Here, we present a novel type of cascade reaction, the 'recycling cascade' (Scheme 1E), which was developed for a two-step synthesis of chiral 2-amino alcohols. In this synthetic enzyme cascade acetaldehyde (upon decarboxylation of pyruvate) is ligated to an aromatic aldehyde by a thiamine diphosphate (ThDP)-dependent enzyme (E1) yielding a 2-hydroxy ketone which is subsequently reduced to a 2-amino alcohol by an ω-transaminase (E2). The enzymatic reductive amination requires an amine donor as co-substrate. By a smart combination of this co-substrate and enzyme E1 the reaction runs because E1 has two functions in this 1-pot cascade: beside formation of the 2-hydroxy ketone (scheme 1, intermediate I) it is further used to shift the equilibrium of the transaminase reaction, which is hampered by a low equilibrium constant. This equilibrium shift is possible because the co-product, formed upon deamination of the co-substrate, can be recycled as a substrate for the carboligation step. This removal shifts the equilibrium towards the desired product.

2.) Catalyst preparation

2.1) Cloning, expression and purification of ω-transaminase *Cv*-(*S*)TA

Preparation of ω-TA: Cloning[2], expression[3], and preparation of the cell-free extract[4] of the N-terminal His-tagged ω-TA *Cv*-(*S*)TA were performed as previously described. Protein purification (column material: Ni-NTA superflow, Qiagen, equipment: ÄKTApurifier, GE Healthcare) was performed in 100 mM HEPES buffer (pH 7.5) containing 200 µM pyridoxal-5'-phosphate (PLP). After one washing step (buffer + 25 mM imidazole) the ω-TA was eluted (buffer + 250 mM imidazole) and the buffer exchanged to 10 mM HEPES (pH 7.5) and 200 µM PLP using a Sephadex G-25 column (GE-Healthcare) before lyophilization. The transaminase was obtained in a purity >90 % as a lyophilized powder with a protein content of 70 % (w/w).

2.2) Cloning, expression and purification of acetohydroxyacid synthase I (AHAS-I)

Preparation of AHAS-I: The His-tagged AHAS-I was cloned[5] and expressed[6] as described in literature. Cell disruption was performed analogously to the process for the ω-TA (see 2.1), except the buffer ('AHAS-buffer'), which contained 100 mM potassium phosphate (KPi, pH 7.6), 500 mM KCl and 10 µM flavine adenine dinucleotide (FAD). Enzyme purification was also performed as described for ω-TA (see chapter 1.1), but with AHAS-buffer: after an equilibration step (AHAS-buffer + 20 mM imidazole) and one washing step (AHAS-buffer + 50 mM imidazole), the elution of AHAS was performed with AHAS-buffer + 250 mM imidazole. Before lyophilization the buffer was exchanged to 25 mM KPi (pH 7.5) and 10 µM FAD by using a Sephadex G-25 column (GE-Healthcare). The purity of AHAS-I lyophilized powder was >90 % and had a protein content of 15 % (w/w).

2.3) (*R*)-selective ω-transaminases

A commercially available toolbox of seven different (*R*)-selective ω-transaminases was provided by Enzymicals AG as lyophilized crude cell extract.[7]

Table 1: (*R*)-selective ω-transaminases provided by Enzymicals AG

(R)-selective TA	*Catalog no.*	*organism origin*
Af-(*R*)TA:	ECS-ATA01	*Aspergillus fumigatus*
Gz-(*R*)TA:	ECS-ATA02	*Gibberella zeae*
Nf-(*R*)TA:	ECS-ATA03	*Neosartorya fischeri*
Ao-(*R*)TA:	ECS-ATA04	*Aspergillus oryzae*
At-(*R*)TA:	ECS-ATA05	*Aspergillus terreus*
Pc-(*R*)TA:	ECS-ATA06	*Penicillium chrysogenum*
Mv-(*R*)TA:	ECS-ATA07	*Mycobacterium vanbaalenii*

3.) Reaction analytics

3.1) Quantification of benzaldehyde and phenylacetylcarbinol (PAC)

The extraction and quantification of PAC (R_t = 8.7 min) and benzaldehyde (R_t = 17.1 min) were performed by achiral HPLC-analysis as described before.[4] A typical chromatogram is presented in diagram 1.

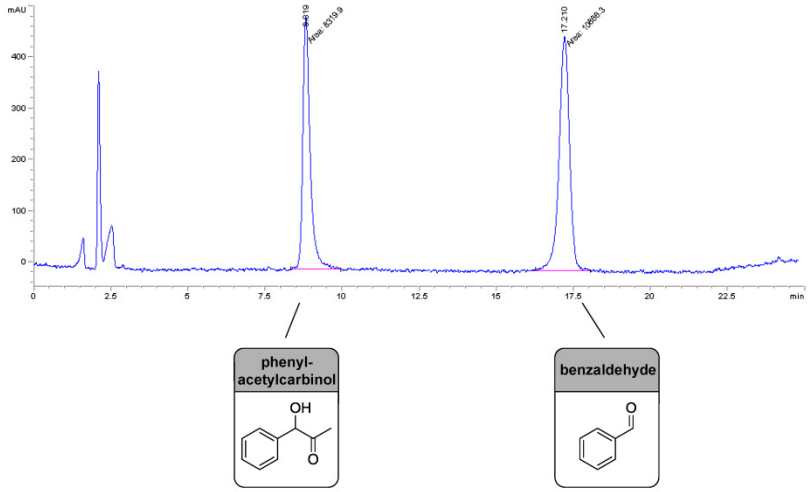

Diagram 1: Chromatogram of 10 mM benzaldehyde and 10 mM PAC on achiral HPLC analytics.[4]

3.2) Synthesis of reference compound: (1*S*,2*S*)-norpseudoephedrine

The enzymatic reductive amination of phenylacetylcarbinol (PAC) can theoretically result in four different stereoisomers of the product nor(pseudo)ephedrine: (1*S*,2*S*)-norpseudoephedrine, (1*R*,2*R*)-norpseudoephedrine, (1*S*,2*R*)-norephedrine, (1*R*,2*S*)-norephedrine. All isomers, except (1*S*,2*S*)-norpseudoephedrine were bought from Sigma Aldrich in a purity >99.5 %.

(1*S*,2*S*)-Norpseudoephedrine was synthesized starting from the (*S*)-PAC of a PAC mixture (with (*R*)-PAC having an *ee* = 84 %), which was provided by BASF AG as a yellow oil with a purity of >98 % (NMR, GC).[4] 10 mM (*R*)-PAC (141.1 mg, 0.939 mmol) and 10 mM (*S*)-α-methylbenzylamine were incubated with 1 mg/ml ω-TA (*Cv*-(*S*)TA) in 100 mM HEPES (pH 7.5), 200 µM PLP at room temperature under moderate stirring in 200 ml glass vials. After 16 h the conversion, based on the consumption of PAC, was >98 %. The solution was adjusted to pH 10 with triethylamine and extracted with ethyl acetate (5x100 ml). The combined organic layers were dried with $MgSO_4$ and evaporated. The crude product was purified by flash chromatography (eluent: $CHCl_3$/MeOH = 50:50) to afford a mixture of two nor(pseudo)ephedrine diastereomers (*de* = 84 %, according to ^{1}H-NMR and chiral GC) as a pale yellow oil in 85 % yield (121 mg, 0.801 mmol). The absolute configuration was determined by chiral GC comparison and co-injection of the available (1*R*,2*R*)-, (1*S*,2*R*)-, and (1*R*,2*S*)- isomers (see diagram 4 and 5).

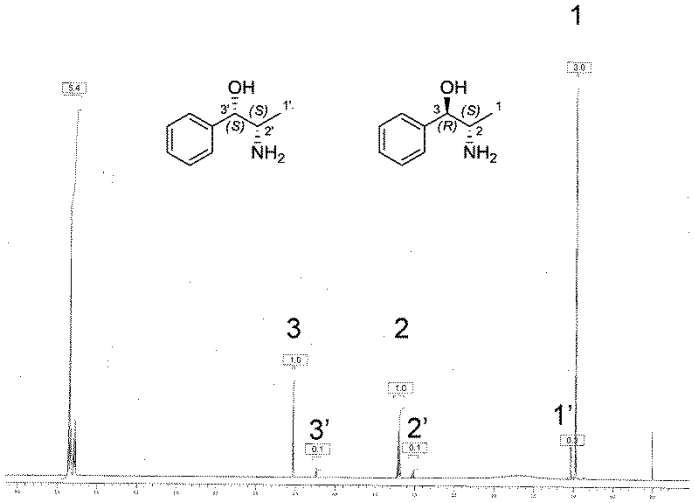

Diagram 2: ^{1}H-NMR (600 MHz; $CDCl_3$) of the diastereomer mixture obtained, (1*S*,2*S*)-norpseudoephedrine and (1*R*,2*S*)-norephedrine

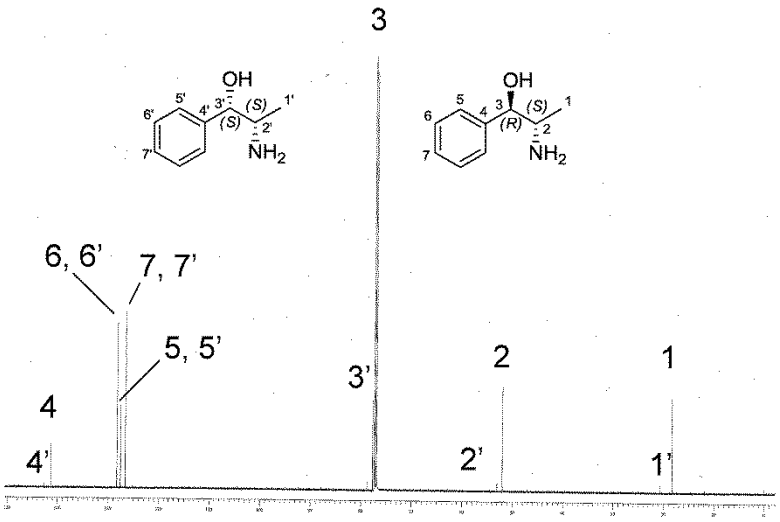

Diagram 3: ^{13}C-NMR (600 MHz; $CDCl_3$) of the diastereomer mixture obtained, (1*S*,2*S*)-norpseudoephedrine and (1*R*,2*S*)-norephedrine

(*R*)-phenylacetylcarbinol (starting material, provided by BASF[4])

R_f (PE/EtOAc 90:10) = 0.27; HPLC (Chiralcel OD-H: 250 mm × 4.6 mm × 5 µm, *n*-hexane/2-propanol = 90:10, 0.7 ml/min, 25 °C): R_t [(S)-5] = 16.2 min, R_t [(*R*)-5] = 17.4 min, *ee* = 84%; ^{1}H-NMR (600 MHz; $CDCl_3$): δ = 2.08 (s, 3 H, 3-H), 4.30 (brs, 1 H, OH), 5.09 (brs, 1 H, 1-H), 7.31–7.40 ppm (m, 5 H, arom.-H); ^{13}C-NMR (151 MHz; $CDCl_3$): 25.3 (C-1), 80.2 (C-2), 127.4 (arom.-CH), 128.8 (arom.-CH), 129.1 (arom.-CH), 138.1 ppm (arom.-C_{ipso}), 207.2 (C-3).

(1*S*,2*S*)- and (1*R*,2*S*)-nor(pseudo)ephedrine diastereomer mixture (obtained from the synthesis described above)

R_f ($CHCl_3$/MeOH = 50:50) = 0.25; chiral GC (Chirasil-DEX CB, 25 m x 0.25 mm x 0.25 µm; constant temperature of 150 °C): (1*S*,2*S*)-norpseudoephedrine = 25.4 min, (1*R*,2*S*)-norephedrine = 30.5 min; *de* = 84%; ^{1}H-NMR (1*R*,2*S*)-norephedrine (600 MHz; $CDCl_3$): δ = 0.97. (d, $J_{1\text{-}2}$=6.4, 3 H, 1-H), 1.7 (brs, 3 H, OH, NH_2), 3.20 (qd, $J_{2\text{-}1}$=6.4, $J_{2\text{-}3}$=4.9, 1 H, 2-H), 4.42 (d, $J_{3\text{-}2}$=4.9, 1 H, 3-H), 7.25–7.38 ppm (m, 5 H, arom.-H); ^{13}C-NMR (1*R*,2*S*)-norephedrine (600 MHz; $CDCl_3$): 18.2 (C-1), 51.9 (C-2), 77.0 (C-3), 126.5 (arom. C-5), 127.5 (arom. C-7), 128.2 (arom. C-6), 141.3 (arom. C-4) ppm. ^{1}H-NMR (1*S*,2*S*)-norpseudoephedrine (600 MHz; $CDCl_3$): δ = 1.03 (d, $J_{1\text{-}2}$=6.4, 3 H, 1'-H), 1.7 (brs, 3 H, OH, NH_2), 3.02 (m, 1 H, 2'-H), 4.24 (d, $J_{3\text{-}2}$=6.8, 1 H, 3'-H), 7.25–7.38 ppm (m, 5 H, arom.-H); ^{13}C-NMR (1*R*,2*S*)-norephedrine (600 MHz; $CDCl_3$): 20.6 (C-1'), 53.0 (C-2'), 78.7 (C-3'), 126.5 (arom. C-5'), 127.5 (arom. C-7'), 128.2 (arom. C-6'), 142.7 (arom. C-4') ppm.

3.3 Determination of absolute configuration of all norephedrine stereoisomers

The absolute configuration of all nor(pseudo)ephedrine isomers: (1*S*,2*S*)-norpseudpephedrine, (1*R*,2*R*)-norpseudoephedrine, (1*R*,2*S*)-norephedrine and (1*S*,2*R*)-norephedrine was determined with chiral GC analysis by comparison of the synthesized reference compound (see chapter 3.2 - diagram 4) and co-injection of the authentic compounds (diagram 5).

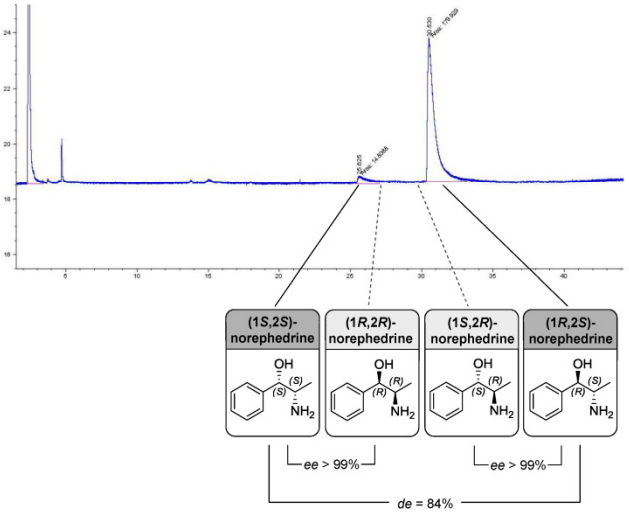

Diagram 4: Chromatogram of nor(pseudo)ephedrine isomers generated from reference compound synthesis (see chapter 3.2): (1*S*,2*S*)-norpseudoephedrine, (1*R*,2*S*)-norephedrine analyzed on a chiral GC Chirasil-DEX CB column (25 m x 0.25 mm x 0.25 µm) with a constant column temperature of 150 °C.

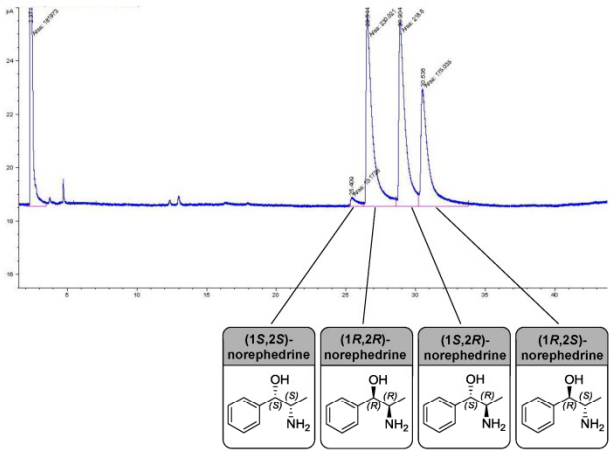

Diagram 5: Chromatogram of all nor(pseudo)ephedrine isomers: (1*R*,2*R*)-norpseudoephedrine and (1*S*,2*R*)-norephedrine as authentic samples (Sigma Aldrich) co-injected with (1*S*,2*S*)-norpseudoephedrine and (1*R*,2*S*)-norephedrine isomers synthesized reference compound (see chapter 3.2).

3.4) Quantification of benzylamine and nor(pseudo)ephedrine isomers

Nor(pseudo)ephedrine was extracted from reaction solutions upon addition of 100 µL NaOH (1 M) to a 200 µL sample obtained from the reaction. After centrifugation, 200 µL of the supernatant were extracted with 200 µL ethyl acetate containing an internal standard (0.1 µL/ml decane) for chiral gas chromatography analysis. For determination of the *ee* and *de* a Chirasil-DEX CB column (25 m x 0.25 mm x 0.25 µm) with a constant column temperature of 130 °C was used. Typical retention times of the four possible product isomers were: (1*S*,2*S*)-norpseudoephedrine = 25.4 min, (1*R*,2*R*)-norpseudoephedrine = 26.5 min, (1*S*,2*R*)-norephedrine = 28.9 min, (1*R*,2*S*)-norpseudoephedrine = 30.5 min (see diagram 5, chapter 3.3). For determination of conversion values a shorter method (linear gradient 100-150 °C with 20 °C/min, hold 150 °C for 6 min, then 180 °C for 3 min) on the same column was used. Typical retention times of the phenylpropanolamine signals were 6.9 min, benzylamine 2.4 min and the injection standard decane 1.8 min.

4.) Determination of the equilibrium constant for the reductive amination of PAC + alanine

The reaction equilibrium constant of the reaction with PAC and alanine to norephedrine and pyruvate (see scheme 2) was determined according to the method described by Tufvesson *et al.* 2012.[8]

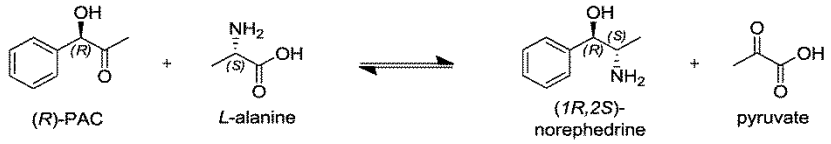

Scheme 2: Reaction equilibrium determined for the reaction of PAC+alanine to norephedrine and pyruvate

4.1) Reaction analytics

For determination of all reactant concentrations 20 µL reaction solution was added to 180 µL acetonitrile. From this sample 5 µL or 50 µL, respectively, were injected and analyzed on a LiChrospher RP-8 reverse phase column (250 mm × 4 mm, 5 µm) with a constant column temperature of 20 °C and mixture of H_2O (containing 0.3 % (v/v) H_3PO_4) and acetonitrile (2 min 100 % (v/v) H_2O (containing 0.3 % (v/v) H_3PO_4), followed by a linear gradient to 100 % (v/v) acetonitrile over 8 min and a regeneration step to 100 % (v/v) H_2O (containing 0.3 % (v/v) H_3PO_4). Typical retention times of the reactants were: alanine: 2.43 min, pyruvate 3.74 min, norephedrine = 7.89 min, PAC = 9.37 min. The injection volume and the corresponding linear concentration range at 200 nm for all compounds diluted as described above were: alanine (5 µL) 50-250 mM, pyruvate (5 µL) 1-50 mM, pyruvate (50 µL) 0.1-5 mM, norephedrine (5 µL) 0.1-5 mM, norephedrine (50 µL) 0.01-0.5 mM, PAC (5 µL) 0.1-10 mM.

4.2) Reaction procedure

All reactions were performed in 100 mM HEPES with 200 µM PLP and 0.5 mg/ml *Cv*-(*S*)TA purified enzyme (see chapter 1.1). In order to determine the equilibrium constant (K_{eq}), reactions with different substrates and product concentrations were set up in a way that the reaction quotient (Q) is initially higher, or respectively lower than the equilibrium constant. To estimate the equilibrium constant roughly a reaction with 10 mM PAC and 10 mM alanine was set up. After 12 h reaction time a product concentration of ~0.5 mM norephedrine was observed. Kq could be estimated to be ~ 0.0025 (see equation [#1]).

[#1] $$K_{eq} = \frac{[norephedrine]\cdot[pyruvate]}{[PAC]\cdot[alanine]} \approx \frac{[0.5\ mM]\cdot[0.5\ mM]}{[9.5\ mM]\cdot[9.5\ mM]} \approx 0.0025$$

4.3) Determination of the equilibrium constant

With the roughly estimated equilibrium constant in hand (see chapter 4.2), initial substrate and product concentration for 10 reactions with different reaction quotients were chosen (see table 2). After addition of 0.5 mg/ml transaminase *Cv*-(*S*)TA, the reactant concentrations and with it the reaction quotients were determined at different time points (diagram 6-A).

Table 2: Substrate and product concentration at the initial start point of the reaction and after 24 h

	reaction time: 0.033 h					reaction time: 24 h				
reaction	Q (0 h)	PAC [mM]	alanine [mM]	norephedrine [mM]	pyruvate [mM]	Q (24 h)	PAC [mM]	alanine [mM]	norephedrine [mM]	pyruvate [mM]
#1	0.94765	0.11	100.78	1.00	10.15	0.00230	1.14	100.93	0.03	9.41
#2	0.03946	1.78	89.57	0.90	6.98	0.00230	2.63	91.81	0.09	6.46
#3	0.01991	1.76	89.58	0.69	4.58	0.00227	2.37	92.47	0.11	4.35
#4	0.01056	1.78	88.82	0.46	3.64	0.00230	2.14	91.70	0.12	3.65
#5	0.00531	1.79	89.68	0.47	1.83	0.00224	2.04	91.09	0.22	1.93
#6	0.00329	1.80	90.02	0.29	1.82	0.00235	1.90	91.72	0.19	2.11
#7	0.00145	1.79	89.74	0.25	0.93	0.00231	1.75	91.23	0.28	1.32
#8	0.00049	2.75	133.63	0.19	0.93	0.00236	2.46	136.21	0.48	1.65
#9	0.00025	2.77	135.59	0.10	0.96	0.00237	2.38	135.74	0.45	1.71
#10	0.00005	2.76	177.98	0.05	0.52	0.00225	2.15	182.48	0.60	1.47

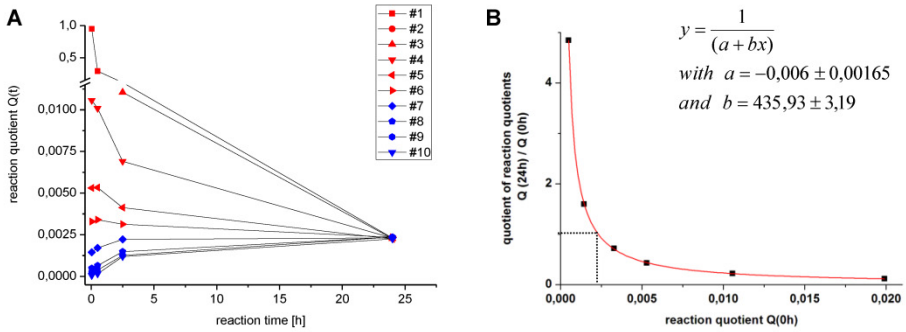

Diagram 6: Reaction quotients plotted against the reaction time (A) and quotient of the reaction quotients Q(0 h)/Q (24 h plotted against Q(0 h) (B)

After 24 h the reaction quotient converges in all reactions to the reaction equilibrium. Mathematically more precise the reaction equilibrium can be calculated from a plot where of the reaction quotients Q(0 h)/Q(24 h) were plotted against Q(0 h) (see Diagram 6-B). A reaction where no change in the reaction quotient over the time is observed, meaning Q(0 h)/Q(24 h)=1, the reaction was initially already in the thermodynamic equilibrium (Q(0 h) = K_{eq}). Thereby, the thermodynamic equilibrium constant can be calculated by solving the equation of the fit (diagram 6-B) with y = 1 (see equation [#2]). The thermodynamic equilibrium constant has a value of $2.31 \cdot 10^{-3}$.

[#2] $$K_{eq} = \frac{Q(24\,h)}{Q(0\,h)} = 1 \Rightarrow y = 1 = \frac{1}{(-0.006 + 435.93 \cdot x)}$$
$$\Leftrightarrow x = 2.31 \cdot 10^{-3} = K_{eq}$$

4.4) Calculation of the theoretical conversion from the reaction equilibrium constant

With the given reaction equilibrium constant (see chapter 4.3) the theoretical maximal conversion for reductive amination of PAC with different alanine concentrations (see scheme 2) can be calculated (see equation #3 and diagram 7).

[#3]

$$K_{eq} = \frac{[pyruvate]\cdot[norephedrine]}{[alanine]\cdot[PAC]} = \frac{[x]\cdot[x]}{[alanine-x]\cdot[PAC-x]}$$

$$\Leftrightarrow\ 0 = x^2 + \frac{[\text{alanine}]+[\text{PAC}]}{1/K_{eq}-1}x - \frac{[\text{alanine}][\text{PAC}]}{1/K_{eq}-1}$$

$$\Rightarrow\ x = -\frac{1}{2}\cdot\frac{[\text{alanine}]+[\text{PAC}]}{1/K_{eq}-1} + \sqrt{\left(\frac{1}{2}\cdot\frac{[\text{alanine}]+[\text{PAC}]}{1/K_{eq}-1}\right)^2 - \left(-\frac{[\text{alanine}][\text{PAC}]}{1/K_{eq}-1}\right)}$$

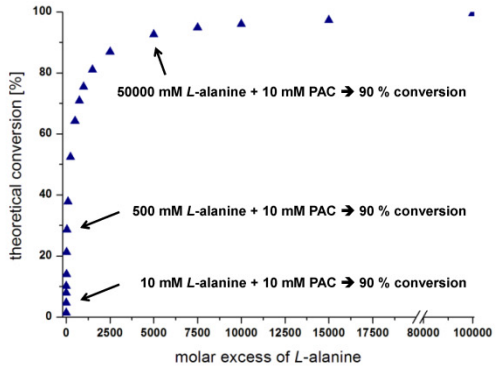

initial concentrations		concentration at reaction equilibrium					
alanine [mM]	PAC [mM]	alanine [mM]	PAC [mM]	pyruvate [mM]	NE [mM]	K_{eq}	conversion [%]
10	10	9,542	9,542	0,458	0,458	0,00231	4,58
30	10	29,21	9,212	0,788	0,788	0,00231	7,88
50	10	48,99	8,992	1,008	1,008	0,00231	10,08
100	10	98,60	8,602	1,398	1,398	0,00231	13,98
250	10	247,88	7,878	2,122	2,122	0,00231	21,22
500	10	497,14	7,139	2,861	2,861	0,00231	28,61
1000	10	996,22	6,220	3,780	3,780	0,00231	37,80
2500	10	2494,8	4,765	5,235	5,235	0,00231	52,35
5000	10	4993,6	3,580	6,420	6,420	0,00231	64,20
7500	10	7492,9	2,910	7,090	7,090	0,00231	70,90
10000	10	9992,5	2,464	7,536	7,536	0,00231	75,36
15000	10	14992	1,899	8,101	8,101	0,00231	81,01
25000	10	24991	1,310	8,690	8,690	0,00231	86,90
50000	10	49991	0,743	9,257	9,257	0,00231	92,57
75000	10	74991	0,520	9,480	9,480	0,00231	94,80
100000	10	99990	0,400	9,600	9,600	0,00231	96,00
150000	10	149990	0,274	9,726	9,726	0,00231	97,26
250000	10	249990	0,168	9,832	9,832	0,00231	98,32
500000	10	499990	0,085	9,915	9,915	0,00231	99,15
1000000	10	999990	0,043	9,957	9,957	0,00231	99,57

Diagram 7: Theoretical maximal conversion for the reaction of PAC with different alanine concentrations

5.) Optimization of the reductive aminiation of PAC with alanine and AHAS-I coupled equilibrium shift

Several parameters like pH, temperature, substrate and co-substrate concentrations as well as enzyme amount can offer potential for the optimization of an enzymatic reaction. These parameters were optimized for the reductive amination of PAC with alanine as an amine donor and AHAS coupled equilibrium shift (scheme 3). Furthermore, for an optimal process the minimal amount of enzymes (here ω-transaminase and AHAS-I) and co-substrates (here alanine) yielding the highest conversion values were identified.

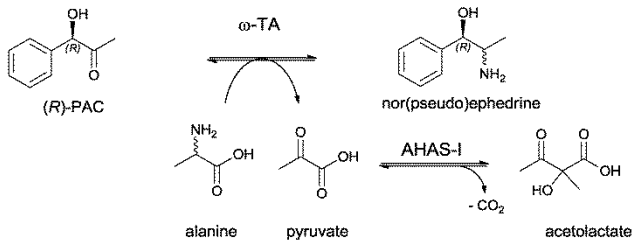

Scheme 3: Reductive aminiation of PAC with alanine and AHAS-I coupled equilibrium shift

5.1) Reaction procedure and analytics

All reactions for optimizing conversion of the reductive aminiation of PAC with alanine and AHAS-I coupled equilibrium shift were set up in 100 mM HEPES containing 200 µM PLP, 50 µM FAD, 100 µM ThDP and 5 mM $MgCl_2$ and incubated for 20 h in glass vials. The varied parameters pH, incubation temperature, enzyme concentration (*Cv*-(*S*)TA and AHAS-I) and L-alanine concentration were adjusted as declared for the corresponding experiment. The conversion is determined by the product concentration (see chapter 3.4).

5.2) Statistical data analysis and interpolation with the Kriging method

The conversion is studied as a function of various process parameters, and double measurements were performed at several parameter combinations. The Kriging method was used for estimating the true conversion at these double measurements and for interpolating between the measured parameter combinations. Kriging is a statistical method in which the values of the interpolating function are determined by a weighted sum of all measurements. In a rather complicated mathematical procedure, these weights are locally computed, such that the expectation value of the interpolating function matches the true conversion, and that the variance of the difference between the interpolating function and the true conversion is minimal. Also at the measured parameter combinations, the applied variant of the Kriging method approximates the true conversion by a weighted sum of all measurements, which is generally different from the mean of the two measurement values at that specific parameter combination. Moreover, the Kriging method allows improving the interpolation quality by incorporating trend functions that describe basic characteristics but cannot accurately describe all details of the conversion as a function of the process parameters. Further details on the Kriging method can be found in the literature.[9] The following trend function [#4] was chosen for the present study:

[#4] $$conversion = k_{max} \cdot \frac{x_1 + k_{11}}{x_1 + k_{12} + k_{13} \cdot x_2} \cdot \frac{x_2 + k_{21}}{x_2 + k_{22}}$$

The parameters k_{11} and k_{21} determine the height at the axes x_1=0 and x_2=0, respectively. The parameters k_{12} and k_{22} determine the initial slope in the direction of x_1 and x_2, respectively. The parameter k_{13} determines a decrease of the initial slope in the direction of x_1 when x_2 increases. The parameter k_{max} determines the height of the plateau. The axis x_1 denotes either alanine / PAC or *Cv*-(*S*)TA, whereas the axis x_2 always denotes AHAS-I. The parameter k_{max} is estimated in one procedure with the weights of the Kriging method. All other parameters of the trend function

are manually determined before the Kriging method is applied, such as to match the observed data as good as possible. The following parameters have been used in the presented figures:

	k_{11}	k_{12}	k_{13}	k_{12}	k_{22}
Figure 3	0	0.125	0	-0.100	0.150
Diagram 8a	0	0.050	0	0	0.100
Diagram 8b	0	0.125	0	0	0.250
Diagram 8c	0	0.125	0	0	0.250
Diagram 8d	0.125	1.375	0	0	0.150
Diagram 9	0	0.024	0.026	-0.040	2.360

Diagram 10 has been computed without using a trend function.

5.3) Parameter optimization: enzyme concentrations, alanine / PAC ratio, pH, reaction temperature

In independent reaction setups, the enzyme (*Cv*-(*S*)TA and AHAS-I) concentrations and the alanine/PAC ratio was varied while the pH (7.5) and the temperature (30 °C) of the reaction was constant (diagram 8 A-D). Reaction optima with a plateau shape were observed in all cases, where with an increase of the enzyme concentration no further increase of the product concentration was accessible (diagram 8 A-D). Here, optimal parameters in terms of reaction costs and efficiency are the minimal enzyme concentrations yielding the maximal conversion at the lowest amine donor/PAC ratio. In all cases the optimal *Cv*-(*S*)TA concentrations has a value of 1 mg/ml (diagram 8 A-D). In a plot of all values with different alanine/PAC ratio and AHAS-I concentrations at a constant *Cv*-(*S*)TA concentration of 1 mg/ml (diagram 9), the optimal parameter can be read out more easily: 0.5 mg/ml AHAS-I and a 5-fold excess of L-alanine/PAC. Moreover, with 250 mM L-alanine the significant lower conversion values indicate a putative substrate surplus inhibition.

For these optimized parameters the maximal conversion values in terms of pH and temperatures were determined to be at range pH of 7.5 - 8.0 and temperature of 25 - 30 °C (diagram 10). In a combination of all optimized parameters, the reductive aminiation of PAC to norephedrine with alanine and AHAS-I coupled equilibrium shift can be performed with a conversion of >80 %.

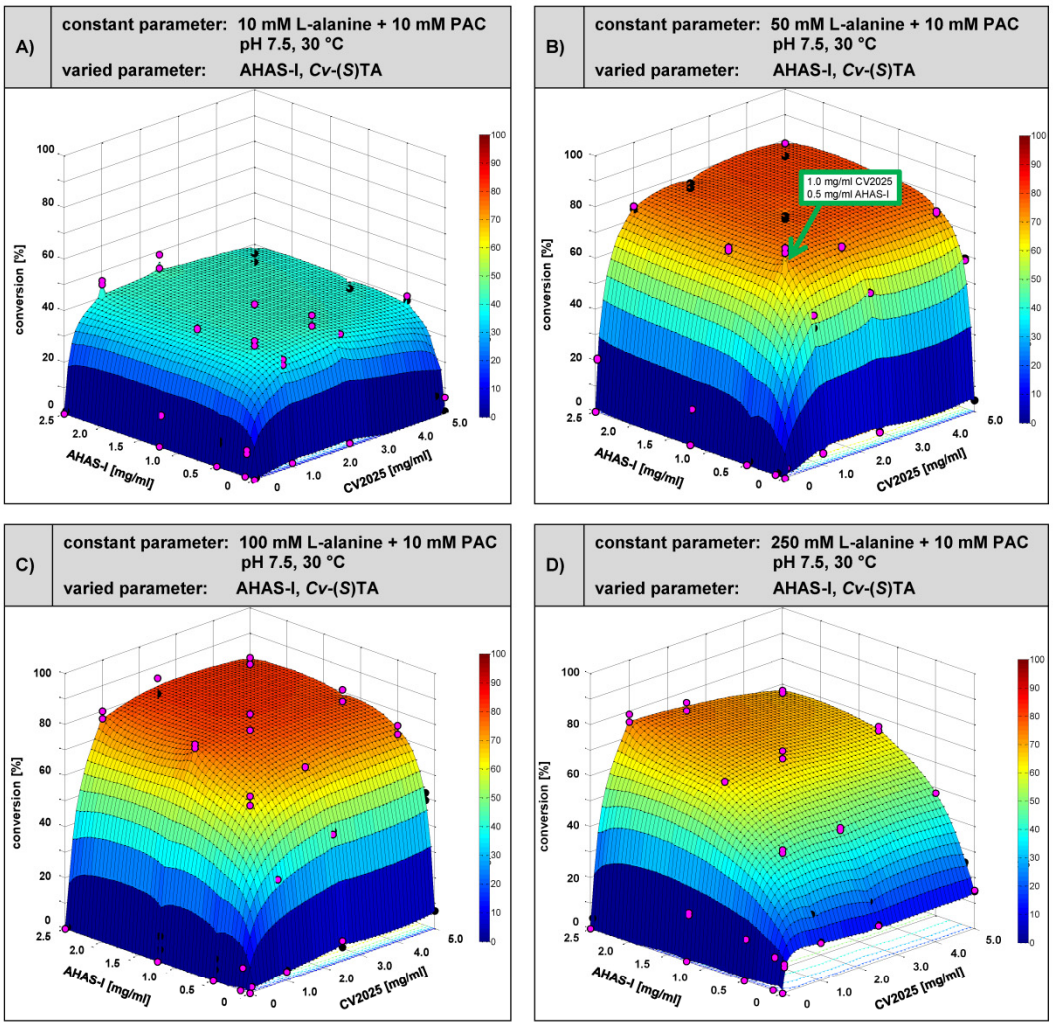

Diagram 8: Determination of optimal reaction parameters (here *Cv*-(*S*)TA, AHAS-I and L-alanine concentration) for the reductive amination of PAC with AHAS-I coupled equilibrium shift. The reactions were set up in 100 mM HEPES (pH 7.5) containing 200 µM PLP, 50 µM FAD, 100 µM ThDP and 5 mM $MgCl_2$ and incubated for 20 h at 30 °C in glass vials. For the statistical data analysis and for interpolating the data (pink dots) the 'kringing algorithm' (see chapter 5.2) was used.

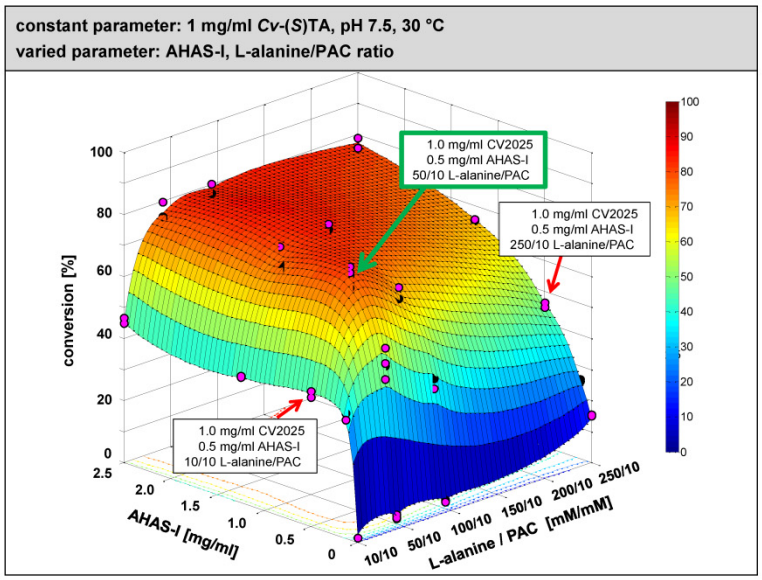

Diagram 9: Plot of all values with different L-alanine/PAC ratio and AHAS-I concentrations at constant transaminase concentrations of 1 mg/ml (see diagram 9).

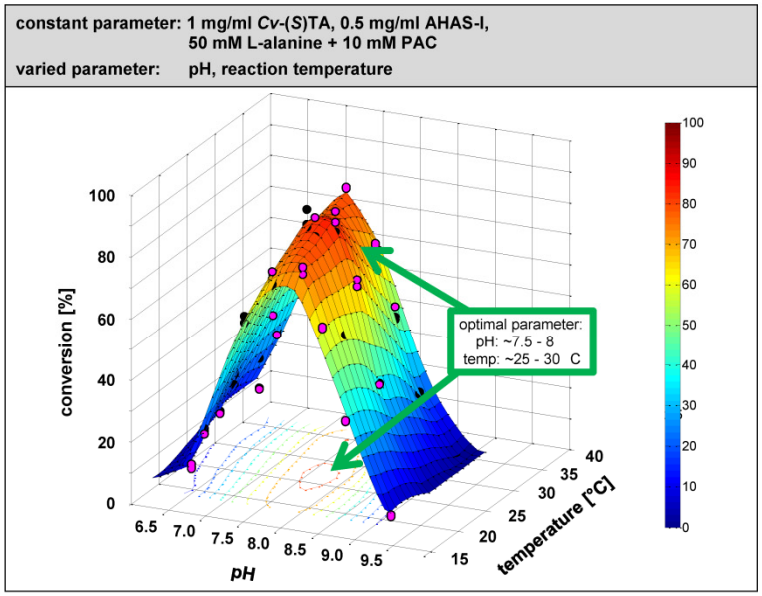

Diagram 10: Determination of optimal reaction parameters (here pH and reaction temperature) for the reductive amination of PAC with AHAS-I (0.5 mg/ml) coupled equilibrium shift and 1 mg/ml *Cv*-(*S*)TA. The reactions were set up in 100 mM HEPES containing 200 µM PLP, 50 µM FAD, 100 µM ThDP and 5 mM $MgCl_2$ and incubated for 20 h at different temperatures in glass vials. For the statistical data analysis and for interpolating the data (pink dots) the 'kringing algorithm' (see chapter 5.2) was used.

6.) 1-pot 2-step cascade reactions

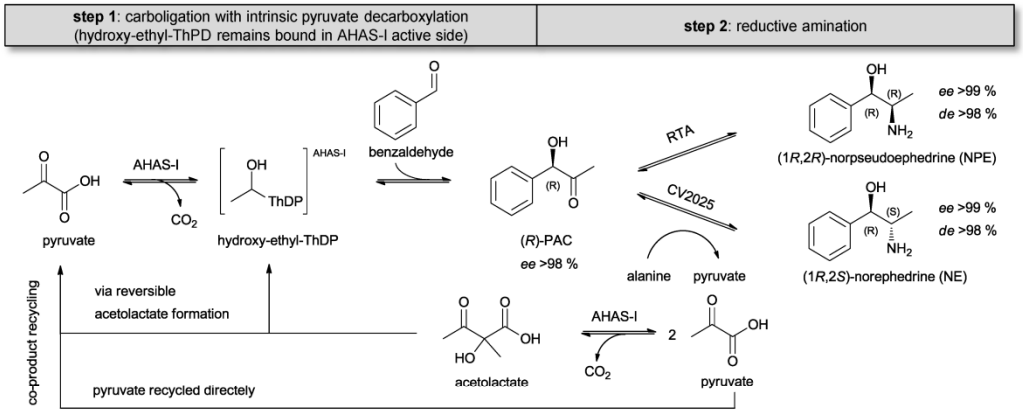

Scheme 4. 1-Pot 2-step cascade for the synthesis of nor(pseudo)ephedrine performed as a recycling cascade.

6.1) Reaction procedure and analytics

A general reaction procedure for the 1-pot 2-step sequential cascade reaction contained 10 mM benzaldehyde, 10 mM pyruvate and 50 mM alanine. D-alanine was used in case of (*R*)-selective TA, and respectively L-alanine for (*S*)-selective TA. The reaction with 1 mg/ml TA with 0.5 mg/ml AHAS-I was performed in 100 mM HEPES (pH 7.5), 200 µM pyridoxal-5'-phosphate (PLP), 50 µM flavin adenine dinucleotide (FAD), 100 µM thiamine diphosphate (ThDP), 5 mM $MgCl_2$ and incubated at 25 °C in glass vials with moderate shaking (100 rpm). For the additional recycling step 10 mM benzaldehyde, 0.5 mg/ml AHAS-I and if indicated 1 mg/ml TA was added. In case of the 1-pot 2-step simultaneous cascade 1 mg/ml TA and 0.5 mg/ml AHAS-I were added simultaneously to a solution containing 10 mM benzaldehyde (respectively 20 mM benzaldehyde in case of the recycling cascade), 10 mM pyruvate and 50 mM alanine. The time-dependent reductive amination of 10 mM benzaldehyde or 10 mM PAC was carried out with 1 mg/ml TA (*Cv*-(*S*)TA or *At*-(*R*)TA, respectively) in 100 mM HEPES (pH 7.5 with 200 µM PLP, 50 µM FAD, 100 µM ThDP, 5 mM $MgCl_2$) containing either (*S*)- or (*R*)-α-methylbenzylamine (10 mM) as amine donor. The concentrations of PAC and benzaldehyde were determined as described in chapter 3.1, for quantification of benzylamine and nor(pseudo)ephedrine see chapter 3.4. The enantiomeric excess of PAC and the *de* and *ee* of nor(pseudo)ephedrine were determined as described in chapter 3.2 and 3.3.

6.2) 1-pot 2-step syntheses of nor(pseudo)ephedrine performed as a sequential cascade with additional 'recycling step' (time-dependent reaction curves)

The 1-pot 2-step syntheses of nor(pseudo)ephedrine performed as a sequential recycling cascade was described in the main text (see description of table 1 – main text). Here, the time-dependent reaction curve for the syntheses of (1*R*,2*S*)-NE (diagram 11) and (1*R*,2R)-NPE (diagram 12) are shown.

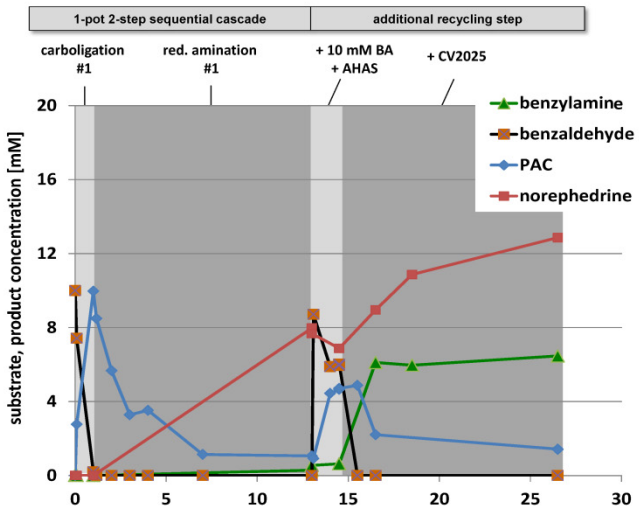

Diagram 11: Time-dependent reaction curve for the 1-pot 2-step syntheses of (1*R*,2*S*)-NE performed as a sequential cascade with additional 'recycling step' combining AHAS-I and *Cv*-(*S*)TA.
(interpolation between dots do not refer to actual concentrations)

Reaction conditions:	100 mM HEPES (pH 7.5 with 200 µM PLP, 50 µM FAD, 100 µM ThDP, 5 mM $MgCl_2$), 25 °C, 100 rpm
1-pot 2-step	carboligation #1: 10 mM benzaldehyde, 10 mM pyruvate, 0.5 mg/ml AHAS red. amination #1: + 50 mM L-alanine, + 1mg/ml ω-TA
recycling step	A: +10 mM benzaldehyde, + 0.5 mg/ml AHAS-I B: + 1 mg/ml *Cv*-(*S*)TA

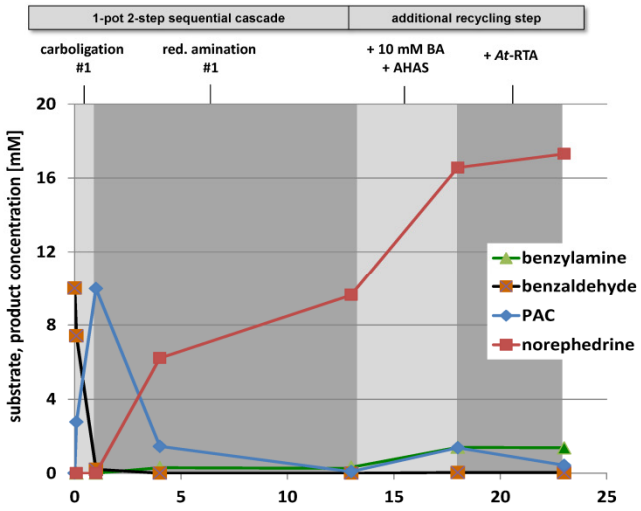

Diagram 11: Time dependent reaction curve for the 1-pot 2-step syntheses of (1*R*,2*R*)-NPE performed as a sequential cascade with additional 'recycling step' combining AHAS-I and *At*-(*R*)TA.
(interpolation between dots do not refer to actual concentrations)

Reaction conditions:	100 mM HEPES (pH 7.5 with 200 µM PLP, 50 µM FAD, 100 µM ThDP, 5 mM $MgCl_2$), 25 °C, 100 rpm
1-pot 2-step	carboligation #1: 10 mM benzaldehyde, 10 mM pyruvate, 0.5 mg/ml AHAS red. amination #1: + 50 mM D-alanine, + 1mg/ml ω-TA
recycling step	A: +10 mM benzaldehyde, + 0.5 mg/ml AHAS-I B: + 1 mg/ml *At*-(*R*)TA

7.) References

[1] a) J. H. Schrittwieser, J. Sattler, V. Resch, F. G. Mutti, W. Kroutil, *Curr. Opin. Chem. Biol.* **2011**, *15*, 249-256; b) E. Ricca, B. Brucher, J. H. Schrittwieser, *Adv. Synth. Catal.* **2011**, *353*, 2239-2262; c) S. F. Mayer, W. Kroutil, K. Faber, *Chem. Soc. Rev.* **2001**, *30*, 332-339; d) A. Bruggink, R. Schoevaart, T. Kieboom, *Org. Process Res. Dev.* **2003**, *7*, 622-640; e) S. Shanmuganathan, D. Natalia, L. Greiner, P. Dominguez de Maria, *Green Chem.* **2012**, *14*, 94-97; f) C. V. Voss, C. C. Gruber, W. Kroutil, *Angew. Chem. Int. Ed. Engl.* **2008**, *47*, 741-745.

[2] U. Schell, R. Wohlgemuth, J. M. Ward, *J. Mol. Cat. B: Enzym.* **2009**, *59*, 279-285.

[3] U. Kaulmann, K. Smithies, M. E. B. Smith, H. C. Hailes, J. M. Ward, *Enzyme Microb. Tech.* **2007**, *41*, 628-637.

[4] T. Sehl, R. C. Simon, H. C. Hailes, J. M. Ward, U. Schell, M. Pohl, D. Rother, *J. Biotechnol.* **2012**, *159*, 188-194.

[5] S. Engel, M. Vyazmensky, S. Geresh, Z. Barak, D. M. Chipman, *Biotechnol. Bioeng.* **2003**, *83*, 833-840.

[6] A. Bar-Ilan, V. Balan, K. Tittmann, R. Golbik, M. Vyazmensky, G. Hübner, Z. Barak, D. M. Chipman, *Biochem.* **2001**, *40*, 11946-11954.

[7] http://www.enzymicals.com/Enzymicals_Enzymes_v011.pdf.

[8] P. Tufvesson, J. S. Jensen, W. Kroutil, J. M. Woodley, *Biotechnol. Bioeng.* **2012**, *109*, 2159-2162.

[9] a) N. A. G. Cressie, *Statistics for Spatial Data, Revised Edition*, John Wiley & Sons, Ltd., ISBN: 9780471002550, **1993**; b) M. Sherman, *Spatial Statistics and Spatio-Temporal Data: Covariance Functions and Directional Properties*, John Wiley & Sons, Ltd., ISBN: 9780470699584, **2010**.

Angewandte Zuschriften

Biokatalyse

DOI: 10.1002/ange.201300718

Zwei Schritte in einem Reaktionsgefäß: Enzymkaskaden zur selektiven Synthese von Nor(pseudo)ephedrin aus kostengünstigen Ausgangsmaterialien**

*Torsten Sehl, Helen C. Hailes, John M. Ward, Rainer Wardenga, Eric von Lieres, Heike Offermann, Robert Westphal, Martina Pohl und Dörte Rother**

Die Entwicklung sauberer und umweltschonender Reaktionen wird eine anspruchsvolle Aufgabe für Chemiker in den nächsten zehn Jahren sein.[1] Klassische chemische Synthesen enantiomerenreiner Verbindungen erfordern oft mehrstufige Reaktionen, das Einführen und Entfernen von Schutzgruppen sowie gegebenenfalls die Isolierung instabiler Zwischenprodukte, was sowohl die Ausbeuten als auch die Nachhaltigkeit eines Prozesses reduzieren kann.[2]

Verbindungen mit vielseitigen Einsatzmöglichkeiten, aber anspruchsvollen Synthesestrategien, sind Phenylpropanolamine, die zur Amphetamin-Familie der Ephedra-Alkaloide gehören. Die Stereoisomere Norpseudoephedrin (NPE) und Norephedrin (NE) werden als Bausteine zur Herstellung von Liganden und chiralen Auxiliaren bei organischen Synthesen[3] oder direkt als pharmazeutisch aktive Moleküle[4] angewendet. Bekannte Methoden zur Herstellung dieser Stoffe haben allerdings Nachteile wie beispielsweise den Einsatz relativ teurer Reagentien, mehrstufige Synthesewege oder nur moderate Enantiomeren- und Diastereomerenreinheiten.[5] Vor Kurzem wurde eine neue, hoch selektive Methode zur Synthese aller Phenylpropanolamin-Isomere mit *ee*- und *de*-Werten >99% publiziert.[6] Ausgehend von 2-Phenyl-2-trimethylsilyloxyacetonitril sind die Norephedrin-Isomere in vier Stufen (40% Ausbeute) und die Norpseudoephedrin-Isomere in sieben Stufen (35% Ausbeute) zugänglich.

[*] M. Sc. T. Sehl, Dr. E. von Lieres, H. Offermann, Dipl.-Biotechnol. R. Westphal, Prof. Dr. M. Pohl, Dr. D. Rother
Institut für Bio- und Geowissenschaften, IBG-1: Biotechnologie
Forschungszentrum Jülich GmbH
Leo-Brandt-Straße 1, 52425 Jülich (Deutschland)
E-Mail: do.rother@fz-juelich.de
Prof. H. C. Hailes
Department of Chemistry, University College London
20 Gordon Street, London WC1H OAJ (Großbritannien)
Prof. J. M. Ward
The Advanced Centre for Biochemical Engineering, Department of Biochemical Engineering, University College London
Torrington Place, London, WC1E 7JE (Großbritannien)
Dr. R. Wardenga
Enzymicals AG
Walther-Rathenau-Straße 49a, 17489 Greifswald (Deutschland)

[**] Die Arbeiten wurden vom CLIB Graduierten-Cluster der Heinrich-Heine-Universität Düsseldorf und von der DFG im Rahmen der Forschergruppe FOR 1296 unterstützt.

Hintergrundinformationen zu diesem Beitrag sind im WWW unter http://dx.doi.org/10.1002/ange.201300718 zu finden.

Insbesondere für die stereoselektive Synthese von Feinchemikalien und Pharmazeutika sind synthetische Enzymkaskaden eine wertvolle Alternative. Aufgrund der meist hohen Chemo- und Stereoselektivitäten und der daraus resultierenden Vermeidung von Isolierungsschritten und Nebenprodukten[7] kann so besonders die Ökoeffizienz einer Reaktion gesteigert werden.[8] Wir präsentieren eine enzymatische Eintopf-Zweistufen-Reaktion zur Synthese von optisch reinem (1*R*,2*S*)-NE und (1*R*,2*R*)-NPE ausgehend von den kostengünstigen Ausgangsstoffen Benzaldehyd und Pyruvat (Schema 1). Verschiedene Möglichkeiten zur Durchführung von Enzymkaskaden wurden bereits beschrieben (Details in Kapitel 1 der Hintergrundinformationen).[1b,2a,8a–c,9]

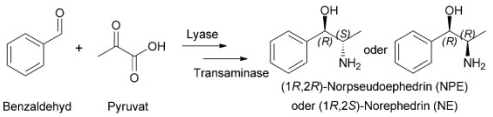

Schema 1. Eintopf-Zweistufen-Reaktion zur Synthese von Norpseudoephedrin und Norephedrin.

Unsere Eintopf-Zweistufen-Reaktion kombiniert Vorteile bekannter Synthesestrategien wie hohe Stereoselektivität, günstige Ausgangsmaterialien, hohe Schrittökonomie (nur zwei Stufen) und eine Gleichgewichtsverschiebung ohne Zusatz weiterer Enzyme oder Cosubstrate.

Im ersten Schritt wird Pyruvat decarboxyliert und anschließend mit Benzaldehyd zum Zwischenprodukt (*R*)-Phenylacetylcarbinol ((*R*)-PAC) ligiert. Die Reaktion wird durch die Thiamindiphosphat(ThDP)-abhängige Acetohydroxysäuresynthase I (AHAS-I) aus *E. coli* katalysiert. Dieses Enzym katalysiert die Decarboxylierung von Pyruvat und die anschließende Carboligation ohne das im aktiven Zentrum gebundene Hydroxyethyl-ThDP freizusetzen (Schema 2).[10] (*R*)-PAC wird mit hoher Enantiomerenreinheit (*ee* >98%) gebildet und kann ohne weitere Isolierung im zweiten Reaktionsschritt mit (*S*)- oder (*R*)-selektiven ω-Transaminasen ((*S*)- bzw. (*R*)TA) zum gewünschten (1*R*,2*S*)-NE bzw. (1*R*,2*R*)-NPE reduktiv aminiert werden. In unseren bisherigen Arbeiten wurden 18 (*S*)-selektive Wildtyp-Enzyme in Bezug auf die Umsetzung verschiedener 2-Hydroxyketone getestet.[11] Die vielversprechendsten Ergebnisse zur reduktiven Aminierung von (*R*)-PAC lieferte das Enzym

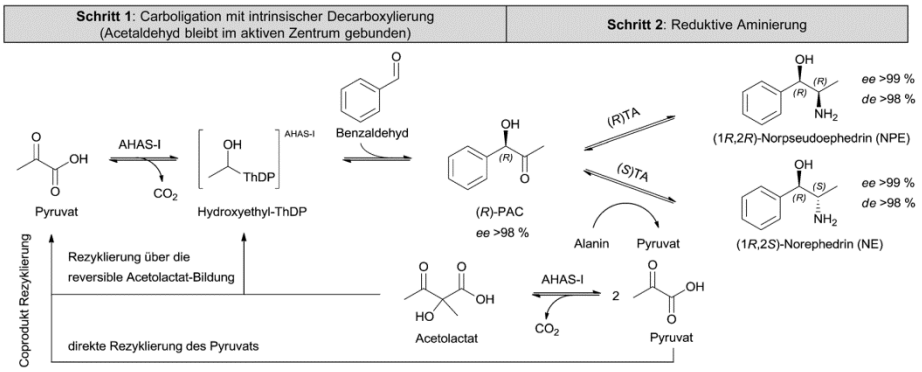

Schema 2. Eintopf-Zweistufen-Reaktion zur Synthese von Nor(pseudo)ephedrin als Rezyklierungskaskade durch Kombination der Acetohydroxysäuresynthase I (AHAS-I) und einer (*S*)- oder (*R*)-selektiven ω-Transaminase ((*S*)TA, (*R*)TA).

Cv-(*S*)TA aus dem Organismus *Chromobacterium violaceum*. Für den Zugang zu (1*R*,2*R*)-NPE wurden sieben weitere (*R*)-selektive Transaminasen der Firma Enzymicals AG (Kapitel 2 der Hintergrundinformationen) untersucht.

Für die enzymatische reduktive Aminierung wird ein Amindonor als Cosubstrat benötigt. Durch eine geschickte Kombination von Cosubstraten (hier: Alanin) und Enzymen kann das Nebenprodukt des zweiten Reaktionsschritts (hier: Pyruvat) als Substrat der ersten Reaktion fungieren. Diese neuartige Kaskadenreaktion wird als „Rezyklierungskaskade“ bezeichnet (Schema 2 und Kapitel 1 der Hintergrundinformationen). Die thermodynamische Gleichgewichtskonstante für die reduktive Aminierung von PAC mit Alanin als Amindonor wurde hier mit 2.31×10^{-3} bestimmt (Kapitel 4 der Hintergrundinformationen). Folglich liegt der maximale theoretische Umsatz ohne Gleichgewichtsverschiebung bei weniger als 5%, wenn äquimolare Konzentrationen von Alanin und PAC eingesetzt werden (Kapitel 4.4 der Hintergrundinformationen). In unserer Enzymkaskade kann Pyruvat ohne den Zusatz weiterer Enzyme über zwei verschiedene von der AHAS-I katalysierte Carboligationswege aus dem Gleichgewicht der Transaminasereaktion entfernt werden (Schema 2): 1) Carboligation mit Benzaldehyd zu (*R*)-PAC oder 2) Selbstligation zweier Pyruvat-Moleküle zu Acetolactat. Die reversible Reaktion zu Acetolactat ist zwar kinetisch bevorzugt, das thermodynamische Reaktionsgleichgewicht liegt aber auf Seiten der PAC-Bildung.[10] Somit ist auch intermediär gebildetes Acetolactat durch die reversible Spaltung zu Pyruvat und Hydroxyethyl-ThDP als Substrat für die Carboligation von (*R*)-PAC zugänglich.

Eine Herausforderung bei dieser Eintopf-Zweistufen-Kaskade ist die Tatsache, dass Benzaldehyd nicht nur als Substrat der Lyasereaktion fungieren, sondern auch in einer Nebenreaktion von Transaminasen reduktiv zu Benzylamin aminiert werden kann. Als Folge der höheren chemischen Reaktivität von Aldehyden gegenüber Ketonen und der sterischen Einschränkungen im aktiven Zentrum der TA war es nicht möglich, unter den 25 zur Verfügung stehenden TAs ein Enzym zu finden, bei dem die reduktive Aminierung von PAC im Vergleich zur Reaktion von Benzaldehyd kinetisch begünstigt ist. Die vielversprechendste (*S*)-selektive Transaminase *Cv*-(*S*)TA hat eine etwa 17-fach höhere Anfangsreaktionsgeschwindigkeit für Benzaldehyd als für PAC (Abbildung 1 A). Daher wurde in der simultanen Zweistufen-Kaskadenreaktion mit AHAS-I und *Cv*-(*S*)TA 98% des Benzaldehyds zu Benzylamin umgesetzt (Abbildung 2 A). Im Falle der (*R*)-selektiven TAs konnten hingegen Enzyme identifiziert werden, mit denen auch im simultanen Modus Umsätze von bis zu 85% (1*R*,2*R*)-NPE erzielt wurden (Abbildung 2 A). Hier liegen im Falle der *At*-(*R*)TA aus dem Organismus *Aspergillus terreus* die Anfangsreaktionsgeschwindigkeiten für PAC und Benzaldehyd etwa in der gleichen Größenordnung (Abbildung 1 B). Im Vergleich zur Anfangsreaktionsgeschwindigkeit der von AHAS-I katalysierten (*R*)-PAC-Bildung sind diese aber ca. 10-fach erniedrigt. Diese Unterschiede genügen, um die Benzylamin-Nebenproduktbildung auf etwa 10% zu reduzieren (Abbildung 2 A).

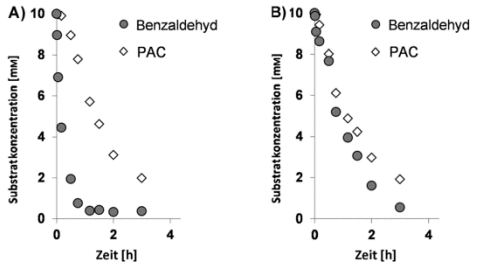

Abbildung 1. Umsatzkurven der reduktiven Aminierung von Benzaldehyd (10 mM) und PAC mit A) der ω-TA *Cv*-(*S*)TA (1 mg mL^{-1}) und B) *At*-(*R*)TA (1 mg mL^{-1}). Die Reaktion wurde in HEPES-Puffer (100 mM, pH 7.5 mit 200 μM Pyridoxal-5′-phosphat (PLP), 50 μM Flavinadenindinucleotid (FAD), 100 μM ThDP, 5 mM $MgCl_2$) und mit (*S*)- oder (*R*)-α-Methylbenzylamin (10 mM) als Amindonor durchgeführt.

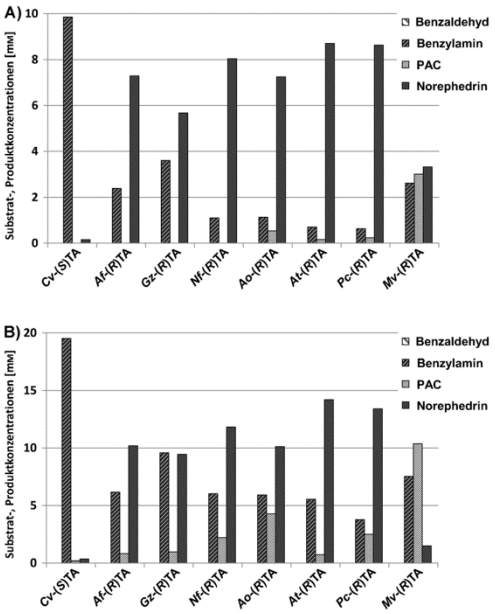

Abbildung 2. A) Simultane Eintopf-Zweistufen Kaskade und B) simultane Eintopf-Zweistufen Rezyklierungskaskade mit der *Cv*-(*S*)TA und sieben (*R*)-selektiven TAs. Für die Eintopf-Zweistufen-Reaktion wurden Benzaldehyd (10 mM), Pyruvat (10 mM) und D- oder L-Alanin (50 mM) in HEPES (100 mM, pH 7.5 mit 200 μM PLP, 50 μM FAD, 100 μM ThDP, 5 mM $MgCl_2$) gelöst und beide Enzyme (AHAS-I und ω-TA) simultan hinzugegeben. Die Rezyklierungskaskade (B) wurde analog mit 20 mM Benzaldehyd anstelle von 10 mM durchgeführt.

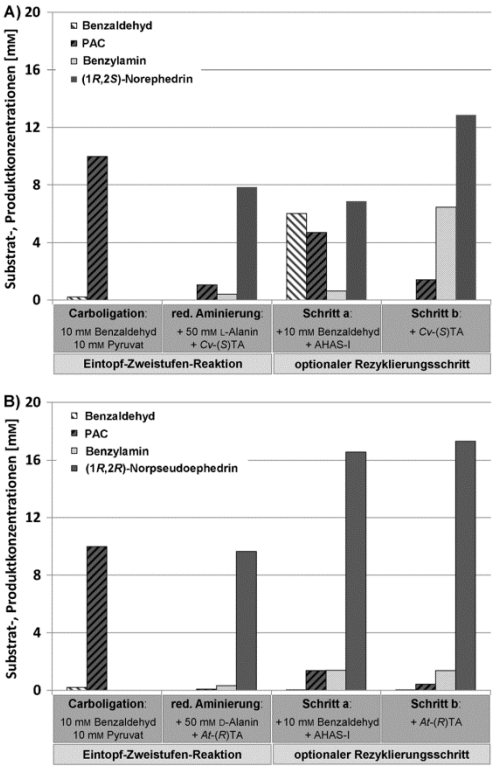

Abbildung 3. Synthese von A) (1*R*,2*S*)-NE und B) (1*R*,2*R*)-NPE als sequenzielle Eintopf-Zweistufen-Reaktion, durchführbar mit optionalem Rezyklierungsschritt (die zeitabhängigen Reaktionsverläufe sind in Kapitel 6 der Hintergrundinformationen zu finden). Reaktionsbedingungen: HEPES-Puffer (100 mM, pH 7.5 mit 200 μM PLP, 50 μM FAD, 100 μM ThDP, 5 mM $MgCl_2$), 25 °C, 100 rpm. Eintopf-Zweistufen-Reaktion: Carboligation (1 h): 10 mM Benzaldehyd, 10 mM Pyruvat, 0.5 mg mL^{-1} AHAS-I; reduktive Aminierung (12 h): +50 mM Alanin, +1 mg mL^{-1} TA. Rezyklierungsschritt: Schritt a: +10 mM Benzaldehyd, +0.5 mg mL^{-1} AHAS-I (A: 1.5 h, B: 5 h); Schritt b: +1 mg mL^{-1} TA (A: *Cv*-(*S*)TA, 12 h, B: *At*-(*R*)TA, 5 h).

Im Einklang mit diesen experimentellen Daten ist das Verhältnis NE/Benzylamin niedrig, wenn die Eintopf-Zweistufen-Reaktion als simultane Kaskade mit einem Rezyklierungsschritt durchgeführt wird. Hierbei wurden beide Enzyme gleichzeitig zu einem Reaktionsgemisch aus Benzaldehyd (20 mM), Pyruvat (10 mM) und Alanin (50 mM) gegeben. Da anfänglich nur 10 mM Pyruvat vorhanden waren, konnten Produktkonzentrationen von mehr als 10 mM (NE bzw. NPE) nur bei erfolgreicher Rezyklierung des aus Alanin gebildeten Pyruvats erreicht werden. In Falle der *At*-(*R*)TA wurden so 14 mM (1*R*,2*R*)-NPE und bemerkenswerterweise nur 5.5 mM Benzylamin gebildet (Abbildung 2B). Bei der analogen Reaktion mit der TA *Cv*-(*S*)TA ist hingegen Benzylamin mit mehr als 98% das Hauptprodukt (Abbildung 2B).

Benzylamin kann zwar von NPE bzw. NE durch Säulenchromatographie getrennt werden (mobile Phase EtOAc/MeOH/NH_3 = 85:10:5), um die Prozesseffizienz zu erhöhen, ist jedoch die Reduzierung der Nebenproduktbildung durch geeignete Verfahrenstechnik vorzuziehen. Im Allgemeinen gibt es zwei Wege, eine Kaskadenreaktion auszuführen. Der eine ist der bereits beschriebene simultane Reaktionsmodus, der andere der sequenzielle Modus, bei dem die Katalysatoren nacheinander zugegeben werden.[9] In der hier untersuchten sequenziellen Enzymkaskade ist der limitierende Schritt die reduktive Aminierung. Um diese Limitierung zu umgehen, wurden die Reaktionsparameter des reduktiven Aminierungsschritts bezüglich pH-Wert, Temperatur, Konzentrationen von Transaminasen und AHAS-I sowie Amindonor/PAC-Verhältnis optimiert (Kapitel 5 der Hintergrundinformationen). Für die Enzymkombination *Cv*-(*S*)TA/AHAS-I konnte der Umsatz unter optimierten Kaskadenbedingungen (pH 7.5, 25 °C, 1 mg mL^{-1} *Cv*-(*S*)TA, 0.5 mg mL^{-1} AHAS-I, Alanin/PAC = 5:1) auf über 80% gesteigert werden.

Diese optimierten Bedingungen wurden für die sequenzielle Eintopf-Zweistufen-Kaskade angewendet. Die Transa-

Angewandte 125 Chemie

minase wurde dabei erst im Anschluss an die zu 100% vollzogene AHAS-I-Reaktion hinzugegeben (Abbildung 3A). Dadurch konnte der Umsatz von (1*R*,2*S*)-NE bei der Kombination AHAS-I/*Cv*-(*S*)TA von ursprünglich 2% (Abbildung 2A: simultane Kaskade) auf 78% (7.8 mM) gesteigert werden (Abbildung 3A). Zusätzlich wurde die Bildung des Benzylamin-Nebenprodukts auf weniger als 0.5 mM reduziert (Abbildung 3A). Bei anschließender Zugabe von weiteren 10 mM Benzaldehyd und frischer AHAS-I wurde in einem zweiten Carboligationsschritt erneut PAC gebildet. Da kein weiteres Pyruvat zugesetzt wurde, zeigt dieses Ergebnis, dass die Rezyklierung von Pyruvat (durch Deaminierung von Alanin) auch in der sequenziellen Rezyklierungskaskade erfolgreich durchgeführt wird. Allerdings konnten hier anstelle der theoretisch möglichen 10 mM PAC nur 4.7 mM (47% Umsatz) zusätzlich durch die Rezyklierung generiert werden. Vermutlich ist dies auf die Instabilität des Acetolactats zurückzuführen, welches chemisch zu Acetoin decarboxylieren kann und somit für die PAC-Bildung nicht mehr zugänglich ist. Darüber hinaus kann Acetoin (und gegebenenfalls auch Acetolactat) als Substrat der *Cv*-(*S*)TA fungieren.[11] In diesem Schritt wurde keine deutliche Erhöhung der NE- oder Benzylamin-Konzentration beobachtet, was eine nahezu vollständige Inaktivierung von *Cv*-(*S*)TA impliziert (Abbildung 3A). Nach Zugabe von frischer *Cv*-(*S*)TA stieg die Konzentration des Zielprodukts (1*R*,2*S*)-NE ($de > 98\%$, $ee > 99\%$) auf 12.9 mM. Dies entspricht etwa 65% der möglichen Produktkonzentration (bezogen auf insgesamt 20 mM eingesetztem Benzaldehyd; Abbildung 3A).

Im Falle der Kombination AHAS-I/*At*-(*R*)TA ist der sequenzielle Kaskadenmodus noch deutlich effizienter. (1*R*,2*R*)-NPE ist über die sequenzielle Eintopf-Zweistufen-Reaktionsführung mit einem Umsatz von >96% in hoher optischer Reinheit ($de > 98\%$, $ee > 99\%$) zugänglich. Nach Zugabe von weiteren 10 mM Benzaldehyd und frischer AHAS-I war die *At*-(*R*)TA noch aktiv, sodass ohne Zusatz weiterer Transaminase in 5 h bereits 16.6 mM (1*R*,2*R*)-NPE (83% Umsatz) durch den zusätzlichen Rezyklierungsschritt generiert wurden. Eine weitere Zugabe der *At*-(*R*)TA erhöhte die Endproduktkonzentration nicht nennenswert.

Zusammenfassend haben wir eine neue Strategie zur Synthese von (1*R*,2*S*)-NE und (1*R*,2*R*)-NPE entwickelt. Beide Verbindungen sind über biokatalytische Eintopf-Zweistufen-Reaktionen in hohen optischen Reinheiten ($de > 98\%$, $ee > 99\%$) aus preiswerten Ausgangsstoffen ohne Isolierung des Zwischenprodukts zugänglich. Darüber hinaus können diese Kaskadenreaktionen im neuartigen „Rezyklierungsmodus“ durchgeführt werden, wobei ein Coprodukt der zweiten Reaktion ohne Zugabe weiterer Katalysatoren oder Cosubstrate entfernt und als Substrat des ersten Reaktionsschritts rezykliert werden kann.

Die Kombination aus Reaktions- und Prozessoptimierung führte im sequenziellen Kaskadenmodus mit den Enzymen AHAS-I und *Cv*-(*S*)TA zu einem auf 80% (8.0 mM) gesteigerten Umsatz des Zielprodukts (1*R*,2*S*)-NE. Zur Herstellung von (1*R*,2*R*)-NPE konnten wir (*R*)-selektive ω-TAs identifizieren, die die Zweistufen-Reaktion in einem Gefäß auch im simultanen Modus mit Umsätzen von bis zu 85% (8.5 mM) ausführen. Durch Einsatz des sequenziellen Modus konnte die Nebenproduktbildung (Benzylamin) signifikant reduziert werden. Hierbei lag der Umsatz von (1*R*,2*R*)-NPE nach 13 h über beide Reaktionsschritte bei mehr als 96% (9.6 mM). Im optionalen Rezyklierungsschritt konnte allein durch erneute Zugabe von 10 mM Benzaldehyd die Gesamtkonzentration des Zielprodukts auf 16.6 mM (83% Umsatz) gesteigert werden.

Der Rezyklierungsmodus kann für jede Kaskadenreaktion angewendet werden, bei der die Nebenprodukte einer Reaktion als Substrate für einen anderen Reaktionsschritt wiederverwendet werden können. Dies optimiert nicht nur die Atombilanz der Reaktion, sondern reduziert auch die Menge gebildeter Nebenprodukte.

Experimentelles

L-Alanin (Merck), D-Alanin (Sigma Aldrich) und Pyruvat (Sigma–Aldrich) hatten eine Reinheit >99%. Benzaldehyd (Sigma–Aldrich) wurde vor der Verwendung frisch destilliert. Die Herstellung der Katalysatoren *Cv*-(*S*)TA und AHAS-I ist in den Hintergrundinformationen beschrieben. Die (*R*)-selektiven ω-Transaminasen sind von der Enzymicals AG (Deutschland) als lyophilisierte Rohzellextrakte erhältlich. Reaktionsdetails, Reaktionsanalytik, Kaskadenoptimierungen und die Bestimmung der Gleichgewichtskonstante sind ebenfalls in den Hintergrundinformationen zu finden.

Eingegangen am 27. Januar 2013
Online veröffentlicht am 9. Mai 2013

Stichwörter: Asymmetrische Synthesen · Biokatalyse · Enzymkaskaden · Phenylpropanolamin · ω-Transaminasen

[1] a) F. Cavani, *J. Chem. Technol. Biotechnol.* **2010**, *85*, 1175–1183; b) E. Ricca, B. Brucher, J. H. Schrittwieser, *Adv. Synth. Catal.* **2011**, *353*, 2239–2262.

[2] a) S. Shanmuganathan, D. Natalia, L. Greiner, P. Dominguez de Maria, *Green Chem.* **2012**, *14*, 94–97; b) M. J. Climent, A. Corma, S. Iborra, M. Mifsud, A. Velty, *Green Chem.* **2010**, *12*, 99–107.

[3] a) M. Sherman, *Spatial Statistics and Spatio-Temporal Data: Covariance Functions and Directional Properties*, Wiley, Hoboken **2010**; b) G. Blay, I. Fernández, B. Monje, J. R. Pedro, *Tetrahedron Lett.* **2004**, *45*, 8039–8042; c) F. K. Cheung, A. M. Hayes, J. Hannedouche, A. S. Y. Yim, M. Wills, *J. Org. Chem.* **2005**, *70*, 3188–3197; d) D. A. Evans, M. D. Ennis, T. Le, N. Mandel, G. Mandel, *J. Am. Chem. Soc.* **1984**, *106*, 1154–1156; e) J. L. García Ruano, C. Alemparte, M. T. Aranda, M. M. Zarzuelo, *Org. Lett.* **2003**, *5*, 75–78; f) R. Guo, A. J. Lough, R. H. Morris, D. Song, *Organometallics* **2004**, *23*, 5524–5529; g) S. R. Hitchcock, D. M. Casper, J. F. Vaughn, J. M. Finefield, G. M. Ferrence, J. M. Esken, *J. Org. Chem.* **2004**, *69*, 714–718; h) C. Unaleroglu, A. E. Aydin, A. S. Demir, *Tetrahedron: Asymmetry* **2006**, *17*, 742–749.

[4] a) N. A. Flavahan, *J. Pharmacol. Exp. Ther.* **2005**, *313*, 432–439; b) R. B. Rothman, N. Vu, J. S. Partilla, B. L. Roth, S. J. Hufeisen, B. A. Compton-Toth, J. Birkes, R. Young, R. A. Glennon, *J. Pharmacol. Exp. Ther.* **2003**, *307*, 138–145; c) R. Krizevski, N. Dudai, E. Bar, E. Lewinsohn, *J. Ethnopharmacol.* **2007**, *114*, 432–438.

[5] J. A. Groeper, S. R. Hitchcock, G. M. Ferrence, *Tetrahedron: Asymmetry* **2006**, *17*, 2884–2889.

[6] H. K. Lee, S. Kang, E. B. Choi, *J Org Chem.* **2012**, *77*, 5454–5460.

[7] F. Lopez-Gallego, C. Schmidt-Dannert, *Curr. Opin. Chem. Biol.* **2010**, *14*, 174 – 183.
[8] a) A. Bruggink, R. Schoevaart, T. Kieboom, *Org. Process Res. Dev.* **2003**, *7*, 622 – 640; b) S. F. Mayer, W. Kroutil, K. Faber, *Chem. Soc. Rev.* **2001**, *30*, 332 – 339; c) J. H. Schrittwieser, J. Sattler, V. Resch, F. G. Mutti, W. Kroutil, *Curr. Opin. Chem. Biol.* **2011**, *15*, 249 – 256; d) R. A. Sheldon, *Green Chem.* **2007**, *9*, 1273 – 1283; e) R. A. Sheldon, *Chem. Commun.* **2008**, 3352 – 3365.
[9] C. V. Voss, C. C. Gruber, W. Kroutil, *Angew. Chem.* **2008**, *120*, 753 – 757; *Angew. Chem. Int. Ed.* **2008**, *47*, 741 – 745.
[10] S. Engel, M. Vyazmensky, S. Geresh, Z. Barak, D. M. Chipman, *Biotechnol. Bioeng.* **2003**, *83*, 833 – 840.
[11] T. Sehl, R. C. Simon, H. C. Hailes, J. M. Ward, U. Schell, M. Pohl, D. Rother, *J. Biotechnol.* **2012**, *159*, 188 – 194.

3.3 Efficient 2-step biocatalytic strategies for the synthesis of all nor(pseudo)ephedrine isomers

Journal Name RSCPublishing

ARTICLE

Efficient 2-step biocatalytic strategies for the synthesis of all nor(pseudo)ephedrine isomers

Cite this: DOI: 10.1039/x0xx00000x

Torsten Sehl,*[a] Helen C. Hailes,[b] John M. Ward,[c] Ulf Menyes,[d] Martina Pohl,[a] and Dörte Rother[a]

Received 00th January 2012,
Accepted 00th January 2012

DOI: 10.1039/x0xx00000x

www.rsc.org/

Chiral 1,2-amino alcohols are important building blocks for chemistry and pharmacy. Here, we developed two different biocatalytic 2-step cascades for the synthesis of all four nor(pseudo)ephedrine (N(P)E) stereoisomers. In the first one, the combination of an (*R*)-selective thiamine diphosphate (ThDP)-dependent carboligase with an (*S*)- or (*R*)-selective ω-transaminase resulted in the formation of (1*R*,2*S*)-NE or (1*R*,2*R*)-NPE in excellent optical purities (*ee* >99 % and *de* >98 %). For the synthesis of (1*R*,2*R*)-NPE space-time yields up to ~26 g l^{-1} d^{-1} have been achieved. Since a highly (*S*)-selective carboligase is currently not available for this reaction, another strategy was followed to complement the nor(pseudo)ephedrine platform. Here, the combination of an (*S*)-selective transaminase with an (*S*)-selective alcohol dehydrogenase yielded (1*S*,2*S*)-NPE with an *ee* >98 % and a *de* >99 %. Although lyophilized whole cells are cheap to prepare and were shown to be appropriate as biocatalysts, higher optical purities were observed with purified enzymes. These synthetic enzyme cascade reactions make the N(P)E-products accessible from inexpensive, achiral starting materials in only two reaction steps and without isolation of the reaction intermediates.

1. Introduction

Norpseudoephedrine (NPE) and norephedrine (NE) belong to the amphetamine family of ephedra alkaloids and can be found in plants like Khat (*Catha edulis*)[1, 2] and in some *Ephedra* species[3]. In the human body they are known to have sympathomimetic function[4] and act as non-selective adrenergic receptor agonists and norepinephrine re-uptake inhibitors[5]. As pharmaceuticals, they have been used to induce mydriasis (dilation of pupils), to stabilize blood pressure, as nasal decongestants, appetite suppressants, and in cold/flu medication.[6-9] In most countries N(P)Es are available only on prescription.[10] On the German market cathine ((1*S*,2*S*)-NPE) is currently sold for its appetite suppressant function as an active ingredient in ALVALIN®[11, 12]. In addition to the pharmacological interest, the four N(P)Es stereoisomers are valuable synthons, ligands, and chiral auxiliaries in organic syntheses.[13, 14] Indeed, a SciFinder® search revealed that N(P)Es have been used as reactants in >5000 different reactions.[15]

Currently >350 different synthetic strategies towards N(P)E stereoisomers have been described in SciFinder®.[15] Still, ethods for the asymmetric synthesis of nor(pseudo)ephedrines from inexpensive starting materials are rare and require either multi-step preparative routes, are based on relatively expensive reagents or lack high enantio- and diastereomeric selectivities.[16] Single enzymatic steps[17-20] and enzyme cascades[21-25] have significant potential in chiral asymmetric synthesis. If a suitable multi-step cascade is performed in one pot, it can be a highly selective, step- and atom efficient strategy, which circumvents time consuming and expensive isolation of intermediates.[26, 27] For the synthesis of (1*R*,2*R*)-norpseudoephedrine and (1*S*,2*R*)-norephedrine we recently described a 1-pot 2-step enzyme cascade with overall conversions of up to >95 %. The combination of a highly (*R*)-selective carboligase with either an (*S*)- or (*R*)-selective ω-transaminase (TA) gave access to these products in high optical purities of *ee* >99 % and *de* >98 %.[28] However, synthesis of the two remaining stereoisomers (1*S*,2*S*)-NPE and (1*S*,2*R*)-NE requires a highly (*S*)-selective thiamine diphosphate (ThDP)-dependent carboligase in the first reaction step (Scheme 1-A), which is currently not available among known wild-type enzymes. Due to our knowledge of the reaction mechanism and factors influencing chemo- and stereoselectivities of ThDP-dependent enzymes, a variant has been designed of the pyruvate decarboxylase from *Acetobacter pasteurianus,* producing phenylacetylcarbinol (PAC) (*S*)-selectively for the first time.[29]

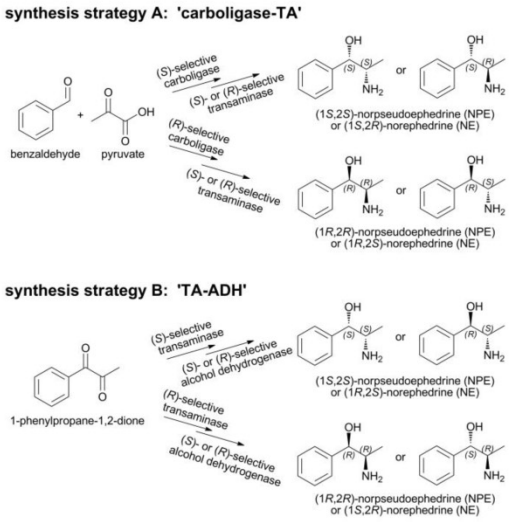

Scheme 1 Two 1-pot 2-step strategies for the synthesis of nor(pseudo)ephedrines combining (**A**) carboligases and transaminases (TAs) and (**B**) TAs and alcohol dehydrogenases (ADHs)

Here, we describe the evaluation of this enzyme for the analogous 1-pot 2-step synthesis of (1*S*,2*R*)-NE and (1*S*,2*S*)-NPE. To avoid a chiral purification step of the resulting nor(pseudo)ephedrine diastereomers, an alternative synthetic strategy ('TA-ADH', scheme 1-B) was investigated. Starting from 1-phenylpropane-1,2-dione (1,2-PPDO), in principle all four N(P)E isomers should be accessible in two steps by combining respective stereoselective ω-TAs in the first with alcohol dehydrogenases (ADHs) in the second cascade step. We here discuss advantages and bottlenecks of both strategies.

Synthesis strategy A: carboligase-TA

A-1: (1*R*,2*R*)-NPE - high space-time-yields using benzaldehyde emulsions

To date, the biocatalytic 2-step synthesis of (1*R*,2*R*)NPE (Scheme 2) was only performed in aqueous buffer with low substrate concentrations (maximum of 20 mM benzaldehyde) with space-time-yields (STY) of ~2 g l^{-1} d^{-1}.[28] To increase the productivity of this cascade, the enzyme concentration was optimized and its performance in the presence of higher benzaldehyde concentrations was investigated (up to 100 mM benzaldehyde).

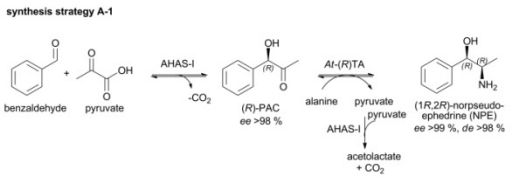

Scheme 2 Strategy A-1: Combination of the (*R*)-selective AHAS-I from *E. coli* and (*R*)-selective transaminase from *A. terreus* (*At*-(*R*)TA) for the synthesis of (1*R*,2*R*)-NPE.

The 2-step cascade, a combination of the AHAS-I from *E. coli* and the (*R*)-selective TA from *Aspergillus terreus* (*At*-(*R*)TA) for the synthesis of (1*R*,2*R*)-NPE, could be performed in one pot.[28] Starting from equimolar concentrations of pyruvate and benzaldehyde (10 mM each) in the carboligation step, the reductive amination could be performed in an optimized manner with a 5-fold excess of D-alanine as co-substrate. This one pot approach is feasible without addition of further compounds or enzymes, despite the low equilibrium constant of the reductive amination (K_{eq} = 2.31·10^{-3}), because AHAS-I removes the co-product pyruvate by converting it to acetolactate and thus shifts the equilibrium to the product side.[28] Although the cascade could be performed in a simultaneous mode (both enzymes added simultaneously), the sequential mode (TA added after the AHAS-I reaction was completed) proved to be advantageous due to a lower by-product formation (benzylamine, formed by reductive amination of benzaldehyde).[28] In order to further optimize the biocatalytic approach, the minimum amount of enzymes required for a reaction containing 20 mM benzaldehyde, 20 mM pyruvate, and 100 mM D-alanine (see Fig. 1) was determined.

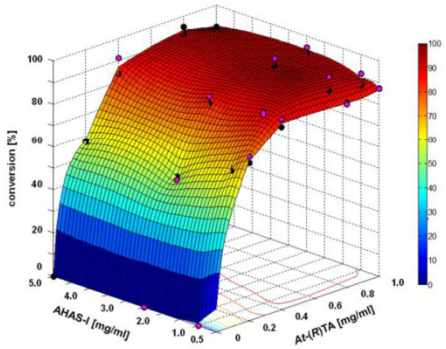

Figure 1 Reaction optimization for the 1-pot 2-step sequential cascade of (1*R*,2*R*)-NPE with different concentrations of AHAS-I and *At*-(*R*)TA.
Reaction parameters: 20 mM benzaldehyde, 20 mM pyruvate and 100 mM D-alanine in 100 mM HEPES (pH 7.5 with 200 µM PLP, 50 µM FAD, 100 µM ThDP, 5 mM $MgCl_2$). Without isolation of the reaction intermediate (*R*)-PAC, lyophilized *At*-(*R*)TA was added 90 min after addition of AHAS-I (in the given concentrations (pink dots)). The complete reaction was analyzed after another 12 h.

It was found that 0.5 mg mL^{-1} AHAS-I and 0.4 mg mL^{-1} *At*-(*R*)TA were sufficient to achieve 95 % conversion of 20 mM benzaldehyde within 13.5 h (Fig. 1). This corresponds to a space-time yield of ~5 g l^{-1} d^{-1} over both reaction steps.

To enhance the reaction efficiency further, the initial benzaldehyde (BA) and pyruvate concentration was increased to 25, 50, 75 and 100 mM but using a constant 5-fold excess of alanine. In line with the optimized reaction parameters, per mmol benzaldehyde 0.025 mg mL^{-1} AHAS-I (90 min reaction time) and 0.02 mg mL^{-1} *At*-(*R*)TA (12 h reaction time) were added.

Although benzaldehyde is not soluble in aqueous buffer >50 mM, in all cases conversions of up to 90 % were observed with less than 5 % benzylamine by-product formation (Fig. 2). Interestingly, this emulsion system did not significantly influence the reaction performance. In line with this data, finally space-time-yields up to26 g l^{-1} d^{-1} (1*R*,2*R*)-NPE were achieved starting from 100 mM benzaldehyde and 90 % conversion could be observed within 13.5 h.

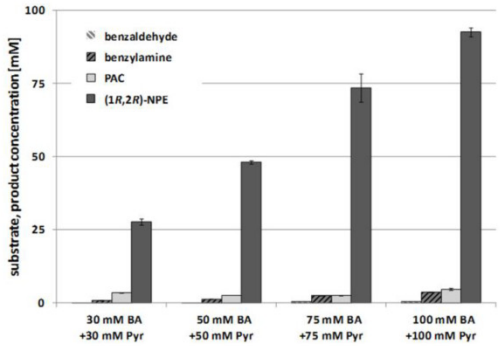

Figure 2 1-pot 2-step sequential cascade for the synthesis of (1*R*,2*R*)-NPE with 25, 50, 75 or 100 mM benzaldehyde (BA) and equimolar concentrations of pyruvate (Pyr). 0.025 mg mL^{-1} AHAS-I were used per mM benzaldehyde. After 90 min reaction time 0.02 mg mL^{-1} *At*-(*R*)TA and 2.5 mM D-alanine was added per mM initial benzaldehyde concentration. The solution was extracted after further 12 h reaction time. Reaction parameter: 100 mM HEPES pH 7.5, 200 µM PLP, 50 µM FAD, 100 µM ThDP, 5 mM $MgCl_2$, 25 °C.

A-2: (1*R*,2*S*)-NE – application of lyophilized whole cells

The use of whole cells can reduce catalyst costs by a factor of 10 and is particularly advantageous if side reactions do not occur.[30] For an economically feasible large scale application, access to (1*R*,2*S*)-NE has been demonstrated by a combination of AHAS-I and *Cv*-(*S*)TA (Scheme 3).[28] Here, the use of enzymes as lyophilized whole cells without enzyme purification was investigated, which features the benefit of easy handling compared to wet cells (e.g. in terms of weighing out small quantities).

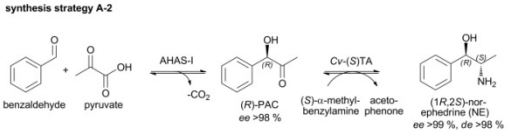

Scheme 3 Synthetic strategy A-2: combination of the (*R*)-selective AHAS-I and the (*S*)-selective transaminase *Cv*-(*S*)TA gives access to (1*R*,2*S*)-NE.

Concerning the first step, purified AHAS-I shows a high initial rate activity of ~1.8 U mg$^{-1}_{protein}$ for the catalyzed carboligation of benzaldehyde and (decarboxylated) pyruvate, which is within the range of industrially suitable catalysts[17] (Fig. 3-A). The use of 5 mg mL^{-1} of lyophilized recombinant *E. coli* whole cells (LWC) yielded a similar reaction velocity under equivalent reaction conditions (Fig. 3-B), which is a consequence of the lower protein amount per mg$_{catalyst}$.(see SDS-PAGE ESI-Figure 1) In both cases a complete conversion of 10 mM benzaldehyde was achieved within ~0.5 h. This corresponds to a STY of ~72 g l^{-1} d^{-1} and a specific STY (STY $g_{catalyst}^{-1}$) for LWC of ~14 g l^{-1} d^{-1} g_{LWC}^{-1} and for purified enzyme of ~144 g l^{-1} d^{-1} g_{enzyme}^{-1}.

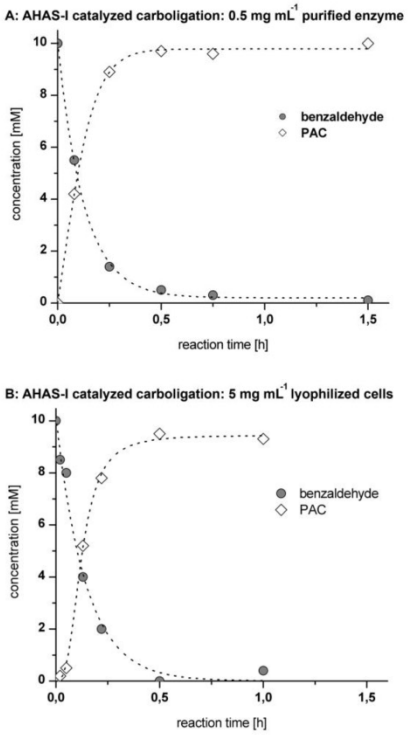

Figure 3 Carboligation of 10 mM benzaldehyde and 10 mM pyruvate catalyzed either by 0.5 mg mL^{-1} purified AHAS-I (**A**) or 5 mg mL^{-1} lyophilized whole cells (**B**). Each reaction was performed in 100 mM HEPES (pH 7.5, 50 µM FAD, 100 µM ThDP, 5 mM $MgCl_2$) at 25 °C.

Additionally, a comparison of LWC and purified enzymes for the second reductive amination step of (*R*)-PAC using the *Cv*-(*S*)TA was investigated. In a first trial with L-alanine as amine donor no NPE product formation was observed (data not shown). However, exchange of L-alanine by (*S*)-α-methylbenzylamine ((*S*)-α-MBA) in a reaction containing 10 mM (*R*)-PAC and 5 mg mL^{-1} LWC, resulted in a conversion of 85 % (see Fig. 4). Notably, we observed a lag phase of 60 min before product formation started when the reductive amination step was catalyzed with lyophilized whole cells (Figure 4). We assumed that this lag phase is caused by required rehydration time of the *E. coli* cells when dry, lyophilized whole cells were added to the aqueous buffer. Further investigations demonstrated that pre-incubated LWC in reaction buffer reduced the lag phase. ((see Supp. Information chapter 3.1.4). Still, the reaction rate with 5 mg mL^{-1} LWC was almost as fast as with 1 mg mL^{-1} purified enzyme. In both cases a conversion of ~85 % was reached within 3 h, which corresponds to a STY of ~10 g l^{-1} d^{-1}. According to this, the calculated specific STY for LWC is ~2 g l^{-1} d^{-1} g_{LWC}^{-1} and for purified enzyme ~10 g l^{-1} d^{-1} g_{enzyme}^{-1}.

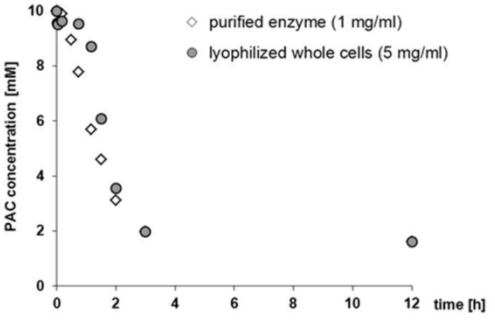

Figure 4 *Cv*-(*S*)TA catalyzed reductive amination of 10 mM (*R*)-PAC in the presence of 10 mM (*S*)-α-MBA catalyzed by either purified enzyme (1 mg mL^{-1}) or lyophilized cells (5 mg mL^{-1}).

The application of lyophilized whole cells in general was found to be suitable for the "carboligase-TA" cascade. This is of special interest for a reaction process, since overall process costs are reduced when enzyme purification can be avoided. Compared to a similar reaction with lyophilized enzymes, the catalysts cost can be significantly lowered by a factor of 10, as was suggested by a general estimation for catalyst cost by Tufvesson and co-workers.[30]

A-3, A-4: Access to (1*S*,2*R*)-NE and (1*S*,2*S*)-NPE

The most promising enzyme for (*S*)-selective carboligation of benzaldehyde and acetaldehyde is *Ap*PDC-E469G.[29, 31] Although the stereoselectivity for (*S*)-PAC of 89 % *ee* is not optimal, the 2-step cascade in combination either with an (*S*)- or (*R*)-selective ω-TA would result in the formation of (1*S*,2*S*)-NPE (Scheme 4; A-3) or (1*S*,2*R*)-NE (Scheme 4; A-4).

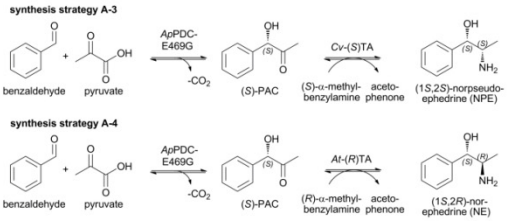

Scheme 4 Synthesis strategy A-3, A-4: combination of the (*S*)-selective carboligase *Ap*PDC-E469G with either the (*S*)-selective TA *Cv*-(*S*)TA (A-3) or the (*R*)-selective TA *At*-(*R*)TA (A-4) gives access to (1*S*,2*S*)-NPE (A-3) or (1*S*,2*R*)-NE (A-4), respectively.

The carboligation step catalyzed by *Ap*PDC-E469G resulted in a final conversion of 95 % within 48 h (40 mM benzaldehyde, 400 mM pyruvate, 2.5 mM $MgSO_4$, 100 µM ThDP, 50 mM potassium phosphate pH 7).[32] Under these reaction conditions, the obtained (*S*)-PAC had an *ee* of only ~70 %. Its following reductive amination using 10 mM isolated (*S*)-PAC with 15 mM (*R*)- or (*S*)-α-MBA, respectively, and (*R*)-selective *At*-(*R*)TA resulted in the formation of predominantly (1*S*,2*R*)-NE with >95 % conversion. With the (*S*)-selective *Cv*-(*S*)TA, (1*S*,2*S*)-NPE was produced with similar conversions >95 %. As expected, both products had a high enantiomeric purity of >99 %, but only a low diastereomeric excess of ~70 %. These results highlight that both PAC enantiomers are accepted by both ω-TAs and are further reduced with high stereoselectivity. The missing influence of the chiral vicinal hydroxyl group on the TA reactivity is in line with data for a similar substrate (1,3-dihydroxy-1-phenylpropane-2-one) published earlier.[33] To further increase the optical purities of the N(P)E in our synthetic cascade approach, a catalyst with higher stereoselectivity for the (*S*)-PAC synthesis would be required. Since so far further rational design attempts were not successful, the combination of ω-TA with oxidoreductases (synthesis strategy B) was subsequently investigated to access these two products with higher optical purities.

Synthesis strategy B: TA-ADH

A novel reaction cascade consisting of a TA in the first step and an ADH in the second step could circumvent the low optical purity in the "carboligase-TA" cascade for the synthesis of (1*S*,2*R*)-NE and (1*S*,2*S*)-NPE. Using 1-phenylpropane-1,2-dione (1,2-PPDO) as substrate, the combination of an (*S*)-selective TA (here *Cv*-(*S*)TA) either with the (*R*)-selective ADH from *Ralstonia spec.* (*R*ADH) or the (*S*)-selective ADH from *Lactobacillus brevis* (*Lb*ADH) could give access to (1*R*,2*S*)-NE and (1*S*,2*S*)-NPE (strategy B-1; Scheme 5). Since the enzymes for both steps are highly selective for aryl-aliphatic substrates, as was earlier demonstrated for

oxidoreductases[34] and ω-TAs[28], the products should be accessible in high optical purity. To complete the strategies towards all possible stereoisomers of N(P)E with high stereoselectivities, the access to (1*S*,2*R*)-NE and (1*R*,2*R*)-NPE was investigated by a combination of the (*R*)-selective *At*-(*R*)TA with *LB*ADH and *R*ADH, respectively (strategy B-2; scheme 5). Finally, the application of different enzyme preparations (lyophilized whole cells, purified enzymes or crude cell extract) was compared.

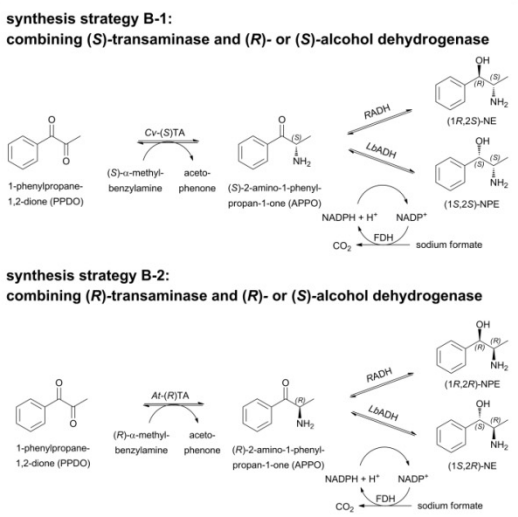

Scheme 5 Strategy B: enzymatic 1-pot 2-step reaction for the synthesis of all nor(pseudo)ephedrines combining either an (*S*)-selective (*Cv*-(*S*)TA, strategy B-1) or an (*R*)-selective transaminase (*At*-(*R*)TA, strategy B-2) in the first step and an (*R*)- (*R*ADH) or (*S*)-selective (*Lb*ADH) alcohol dehydrogenase (ADH) in the second step.

In order to determine optimal reaction conditions for the reductive amination of 1,2-PPDO, reactions with lyophilized whole cells (LWC) containing *Cv*-(*S*)TA and different concentrations of the amine donor (*S*)-α-MBA were investigated and applied to the reductive amination with *At*-(*R*)TA (see Supp. Information). A concentration of 15 mM (*S*)-α-MBA was sufficient to achieve full conversion of 10 mM 1,2-PPDO with *Cv*-(*S*)TA in 48 h. With higher concentrations of the amine donor (*S*)-α-MBA the acetophenone concentration (co-product formed upon deamination of (*S*)-α-MBA) did not increase to more than 10 mM indicating that the theoretically possible di-amination of the diketone 1,2-PPDO did not occur. This is in accordance to previous results in which the reductive amination of aryl-aliphatic ketones can only be achieved if the aliphatic group is not larger than an ethyl group.[35] The initial rate activity for the reductive amination of 1,2-PPDO towards (*S*)-APPO was ~0.005 U mg^{-1}_{LWC} with LWC containing over-expressed *Cv*-(*S*)TA or ~0.008 U $mg^{-1}_{protein}$ with purified *Cv*-(*S*)TA (see Supp. Information; 1 U corresponds to the amount of enzyme that catalyzes the conversion of 1 µmol min^{-1} 1,2-PPDO under standard conditions). In contrast to this, in a reaction with *E. coli* crude cell extract containing *At*-(*R*)TA (scheme 5 B-1) a significantly higher activity of ~0.1 U $mg^{-1}_{protein}$ was measured for the synthesis of (*R*)-APPO. Here, in all cases a complete conversion of the diketone substrate was observed in only 3 h (see Supp. Information).

The subsequent reduction reaction of the intermediate product APPO can in principle be performed in the same pot without intermediate isolation. The required cofactor NADPH (0.5 mM) was regenerated by the addition of formate dehydrogenase (FDH) from *Pseudomonas spec.* and sodium formate, based upon a method described previously.[36] When the cascade was performed in the sequential mode without quenching the TA reaction, 1-phenylpropane-1,2-diol was detected as by-product. This was most likely due to the reversibility of the TA reaction and an equilibrium that favoured the di-reduction of PPDO by ADH. To suppress the diol formation, inactivation of the TA after the first reaction step was investigated. Either a pH-shift (pH 7.5 to pH 2 with 20 % (v/v) HCl – and re-titration to pH 7.5 with 1 M NaOH) or an ultrafiltration step to remove the TA was tested. Using inactivation by pH-shift, the combination *Cv*-(*S*)TA/*Lb*ADH as purified enzymes gave an overall conversion of 80 % after 52 h. With this biocatalytic cascade the product (1*S*,2*S*)-NPE was accessible for the first time with high optical purity: *de* >99 % and *ee* >98 % (Tab. 1; entry #4). When ultrafiltration was used to remove the TA for the combination of *Cv*-(*S*)TA/*Lb*ADH with purified enzymes, the 2-step conversion was significantly lower (57 % after 60 h), but *ee* and *de* remained equally high (Tab. 1; entry #2 compared to #4). The same trend was found for the combination of *Cv*-(*S*)TA/*R*ADH with purified enzymes, were the product (1*R*,2*S*)-NE was accessible with *ee* >98 % and *de* >95 % (Tab. 1; entry #3). Here, the 2-step cascade with an ultrafiltration step after the TA reaction resulted in an overall conversion of 55 %, whereas 82 % conversion to (1*R*,2*S*)-NE was achieved using the pH-shift for TA inactivation (Tab. 1; entry #3 compared to #5). Possible explanations for the reduced yields upon ultrafiltration might be that centrifugation was carried out in plastic ware (all other steps were performed in closed glass vials) and evaporation and adsorption of the intermediate might lower the final yield significantly. However, this was not investigated in detail because the cheaper pH-shift method solved the problem.

Compared to the excellent optical purity of (1*S*,2*S*)-NPE obtained in the 2-step reaction with purified enzymes (see above), the biotransformations using lyophilized whole cells yielded products with decreased optical purities (Tab. 1; entry #8, 9): *Cv*-(*S*)TA/*Lb*ADH ((1*S*,2*S*)-NPE: *ee* >92 %, *de* 90 %) and *Cv*-(*S*)TA/*R*ADH ((1*R*,2*S*)-NE: *ee* >99 %, *dr* ~8:2). Here, a decrease in optical purity might be caused by the isomerization of (*S*)-APPO, induced by other *E. coli* enzymes. Although, it was not possible to measure the *ee* for the intermediate product APPO, this isomerization could lead to a decrease of the *de* for

Table 1 Reaction overview for the synthesis strategy B: "transaminase-ADH"

	TA reaction[a]			ADH reaction[c]		overall conversion & total reaction time[d]		specific STY[e]	product ratio [%] and optical purity of major isomer (**bold**)					
entry	catalyst	type	termi-nation[b]	catalyst	type			[g l^{-1} d^{-1} g_{cat}^{-1}]	(1*S*,2*S*)-NPE	(1*R*,2*R*)-NPE	(1*S*,2*R*)-NE	(1*R*,2*S*)-NE	optical purity *ee*	optical purity *de* or *dr*
#1	*Cv*-(*S*)TA	purif.	-	*Lb*ADH	purif.	0 %	48 h	-	-	-	-	-	-	-
#2	*Cv*-(*S*)TA	purif.	filtration	*Lb*ADH	purif.	57 %	60 h	0.17	**99.3**	0.7	-	-	>98 %	*de* >99 %
#3			filtration	*R*ADH	purif.	55 %	60 h	0.17	-	2.4	-	**97.6**	>99 %	*de* ~95 %
#4	*Cv*-(*S*)TA	purif.	pH-shift	*Lb*ADH	purif.	80 %	52 h	0.28	**99.4**	0.6	-	-	>98 %	*de* >99 %
#5			pH-shift	*R*ADH	purif.	82 %	40 h	0.37	-	1.5	-	**98.5**	>99 %	*de* 97 %
#6	*At*-(*R*)TA	CCE	pH-shift	*Lb*ADH	purif.	40 %	36 h	0.20	**79.9**	-	20.1	-	>99 %	*de* ~60 %
#7			pH-shift	*R*ADH	purif.	>95 %	8 h	2.15	-	**77.4**	-	22.6	>99 %	*de* ~55 %
#8	*Cv*-(*S*)TA	LWC	pH-shift	*Lb*ADH	LWC	62 %	36 h	0.03	**92.0**	3.0	5.0	-	~92 %	*de* ~90 %
#9			pH-shift	*R*ADH	LWC	67 %	27 h	0.05	2.1	17.6	-	**80.3**	>99 %	*dr* ~8:2
#10	*At*-(*R*)TA	CCE	pH-shift	*Lb*ADH	LWC	77 %	30 h	0.08	**77.3**	2.0	20.7	-	~95 %	*de* ~80 %
#11			pH-shift	*R*ADH	LWC	93 %	11 h	0.28	-	**75.2**	0.9	23.9	>99 %	*dr* ~7.5:2.5

TA: transaminase, ADH: alcohol dehydrogenase, purif.: purified, CCE: crude cell extract, LWC: lyophilized whole cells, NE: norephedrine, NPE: norpseudoephedrine - time dependent reaction curves and reaction analytics can be found in the Supplementary Information.

[a] reaction conditions for reductive amination was carried out as indicated with purified enzyme (1 $mg_{protein}$ mL^{-1}), CCE (1 $mg_{protein}$ mL^{-1}) or LWC (10 mg_{LWC} mL^{-1}) of the respective transaminases (*At*-(*R*)TA or *Cv*-(*S*)TA) in 100 mM HEPES (pH 7.5), 200 µM PLP_2 with ~10 mM 1,2-PPDO (see Supp. Information) and 15 mM (*R*)- or respective (*S*)-α-MBA at a reaction temperature of 21 °C. As indicated (by joined columns: #2,3 - #4,5 – #6,7 – #8,9 and #10,11), the reaction solutions were split for the subsequent oxidoreduction step.

[b] reactions were terminated either by ultrafiltration (membrane cut-off: 10 kDa), pH-shift (titrated with 20 % (v/v) HCl to pH 2 then re-titrated with 10 M NaOH to pH 7.5) or not terminated.

[c] reaction conditions for reductive hydrogenation: 0.5 mM $NADP^+$, 150 mM sodium formate, 10 µL mL^{-1} FDH. Either purified enzyme (1 $mg_{protein}$ mL^{-1}), or lyophilized whole cells (10 mg_{LWC} mL^{-1}) of the respective alcohol dehydrogenases (*Lb*ADH or *R*ADH) were added to this reaction solution and incubated at 21 °C.

[d] overall conversion (sum of N(P)E related to the initial substrate concentration) and the total reaction time is given for the complete 2-step reaction.

[e] specific space-time-yields (STY) are calculated from the overall conversion values[d], the reaction times[d] and the amount of used catalyst[a].

the N(P)E products even if both cascade enzymes (ADH and TA) are highly selective.

Similar results were obtained when crude cell extract containing *At*-(*S*)TA was used for the reductive amination step. In combination with *R*ADH (purified enzyme) high conversions (>90 %) but rather low optical purities ((1*R*,2*R*)-NPE: *ee* >99 %, *de* >55 %) were detected (Tab. 1; entry #7). Moreover, the combination *At*-(*R*)TA/*Lb*ADH did not result in (1*S*,2*R*)-NE as the major product, but gave (1*S*,2*S*)-NPE (Tab. 1; entry #6,10). As mentioned for the cascades with *Cv*-(*S*)TA lyophilized whole cells, an isomerization of APPO could lead to a decrease in *de* values even if the enzymes applied are highly selective.

As a consequence, purified enzymes rather than whole cells or crude cell extracts are the method of choice for the TA/ADH reaction cascade. As shown for the combination *Cv*-(*S*)TA/*Lb*ADH, (1*S*,2*S*)-NPE is accessible in high optical purities (>99 % *de*, >98 % *ee*) when purified enzymes are used in both reaction steps (Tab. 1; entry #4).

Conclusions

In summary, two biocatalytic cascade strategies have been developed for the synthesis of all four phenylpropanolamine stereoisomers and the use of inexpensive whole cells for the reaction steps has been investigated. In the "carboligase-TA" strategy, a combination of the (*R*)-selective AHAS-I from *E. coli* either with an (*S*)- or a (*R*)-selective ω-TA gave access to (1*R*,2*S*)-NE and (1*R*,2*R*)-NPE in high optical purities (*ee* >99 % and *de* >98 %). As a proof-of-principle we demonstrated that the synthesis of (1*R*,2*R*)-NPE could be performed with substrate concentrations of up to 100 mM by the combination AHAS-I/*At*-(*R*)TA. Space-time yields up to ~26 g l^{-1} d^{-1} were achievable. Moreover, the application of LWC is possible, but lead to a reduction in specific STY by a factor of 10 for the carboligation and by a factor of 5 for the transaminases. Since a highly (*S*)-selective enzyme for the synthesis of the intermediate (*S*)-PAC is currently not available, the products (1*S*,2*R*)-NE and (1*S*,2*S*)-NPE were only accessible in moderate optical purities using this strategy.

An alternative 2-step synthesis strategy combining ω-TA with ADHs was evaluated to give access to all N(P)E isomers in higher optical purities. Indeed, the isomer (1*S*,2*S*)-NPE, also known as cathine, was synthesized enzymatically in high optical purities. Here, the combination of the (*S*)-selective TA *Cv*-(*S*)TA with the (*S*)-selective alcohol dehydrogenase *Lb*ADH gave (1*S*,2*S*)-NPE with an *ee* >98 % and a *de* >99 % when purified enzymes were used. This novel biocatalyic reaction cascade can be performed in one pot without isolation of intermediates. However, a deactivation of the ω-TA prior to the reductive hydrogenation was required. Although it was demonstrated that this reaction could be carried out with cheaply produced lyophilized whole cells, there are two major drawbacks. On the one hand, the specific STYs are significantly lower with lyophilized whole cells, which partially negate the 10-fold lower catalyst production costs of cells. On the other hand, the optical purity of the product was higher with purified enzymes. Since chiral product purification methods

might dramatically increase production costs, the use of purified enzymes can be beneficial if the additional enzyme purification costs are below downstream processing costs. For industrial applications immobilization of enzymes might be a method to decrease production costs (e.g. in terms of downstream processing, recyclability) and in some cases immobilization results in an increased catalyst stability and/or activity.[37-42]

In general, it has been demonstrated that enzymes from different toolboxes can be efficiently combined yielding all stereoisomers of desired N(P)E. Here, the "TA-ADH" reaction cascade was developed as an alternative to the "carboligase-TA" cascade giving access to optically pure (1*S*,2*S*)-NPE in only two biocatalytic steps.

Acknowledgements

This work was supported by the CLIB Graduate Cluster Industrial Biotechnology of the Heinrich-Heine-University Düsseldorf.

Notes and references

[a] *IBG-1: Biotechnology, Forschungszentrum Jülich GmbH, Leo-Brandt-Str. 1, 52425 Jülich, Germany*
[b] *Department of Chemistry, University College London, 20 Gordon Street, London WC1H OAJ, UK*
[c] *The Advanced Centre for Biochemical Engineering, Department of Biochemical Engineering, University College London, Torrington Place, London, WC1E 7JE, UK*
[d] *Enzymicals AG, Walther-Rathenau-Str 49a,17489 Greifswald, Germany*

† Electronic Supplementary Information (ESI) available: Catalyst preparation, reaction details, reaction analytics and configuration determination can be found in the ESI. See DOI: 10.1039/b000000x/

1. J. M. Hagel, R. Krizevski, K. Kilpatrick, Y. Sitrit, F. Marsolais, E. Lewinsohn and P. J. Facchini, *Genet. Mol. Biol.*, 2011, **34**, 640-646.
2. O. Wolfes, *Arch. Pharm.*, 1930, **268**, 81-83.
3. R. Krizevski, E. Bar, O. Shalit, A. Levy, J. M. Hagel, K. Kilpatrick, F. Marsolais, P. J. Facchini, S. Ben-Shabat and Y. Sitrit, *Phytochemistry*, 2012, **81**, 71-79.
4. *Micromedex 2.0®, Micromedex® Healthcare Series [Internet database]. Greenwood Village, Colo: Thomson Reuters (Healthcare) Inc., Updated periodically.*
5. B. B. Hoffman and R. J. Lefkowitz, in *The pharmacological basis of therapeutics*, The McGraw-Hill Companies Inc., 1996, pp. 222-224.
6. L. Lasagna, *Phenylpropanolamine: A review*, John Wiley & Sons Inc., 1988.
7. J. P. Morgan, *Phenylpropanolamine: A critical analysis of reported adverse drug reactions and overdosage.*, Jack K Burgess, 1986.
8. M. Weintraub, in *Phenylpropanolamine: Risks, Benefits and Controversies, 5th ed.*, Greenwood Pub Group, Inc., 1985, pp. 53-79.
9. W. N. Kernan, C. M. Viscoli, L. M. Brass, J. P. Broderick, T. Brott, E. Feldmann, L. B. Morgenstern, J. L. Wilterdink and R. I. Horwitz, *New Engl. J. Med.*, 2000, **343**, 1826-1832.
10. M. Yakoot, *J. Pharmacol. Pharmacother.*, 2012, **3**, 4-6.
11. Aponet Arzneimitteldatenbank - Arzneimitteldetails zu "ALVALIN", http://www.aponet.de/wissen/arzneimitteldatenbank/suchergebnis/arzneimitteldetails/alvalin-40mg-g_3345428700/dosierung.html.
12. G. Laux and O. Dietmaier, in *Psychopharmaka*, Springer, 2013, pp. 189-195.
13. L. Yan, Z. Diansong, S. S. Ferguson, P. Dorff, T. R. Simpson and S. W. Grimm, *Xenobiotica*, 2010, **40**, 721-729.
14. D. G. Allen, N. M. Aston, N. Trivedi and C. D. Edlin, Patent No.: WO2004024728 A3, 2007.
15. American Chemical Society - SciFinder®, https://scifinder.cas.org/scifinder/view/scifinder/scifinderExplore.jsf.
16. H. K. Lee, S. Kang and E. B. Choi, *J. Org. Chem.*, 2012, **77**, 5454-5460.
17. H. Gröger, Y. Asano and O. May, in *Enzyme Catalysis in Organic Synthesis*, Wiley-VCH Verlag GmbH & Co. KGaA, 2012, pp. 1-42.
18. J. Wang and W. Lu, in *Chiral Drugs*, John Wiley & Sons, Inc., 2011, pp. 77-136.
19. K. Faber, in *Biotransformations in Organic Chemistry*, Springer Berlin Heidelberg, 2010, ch. 1, pp. 1-30.
20. A. Schmid, J. S. Dordick, B. Hauer, A. Kiener, M. Wubbolts and B. Witholt, *Nature*, 2001, **409**, 258-268.
21. A. Bruggink, R. Schoevaart and T. Kieboom, *Org. Process Res. Dev.*, 2003, **7**, 622-640.
22. S. F. Mayer, W. Kroutil and K. Faber, *Chem. Soc. Rev.*, 2001, **30**, 332-339.
23. J. H. Schrittwieser, J. Sattler, V. Resch, F. G. Mutti and W. Kroutil, *Curr. Org. Chem. Biol.*, 2011, **15**, 249-256.
24. R. A. Sheldon, *Green Chem.*, 2007, **9**, 1273-1283.
25. R. A. Sheldon, *Chem. Commun.*, 2008, 3352-3365.
26. F. Lopez-Gallego and C. Schmidt-Dannert, *Curr. Org. Chem. Biol.*, 2010, **14**, 174-183.
27. E. Ricca, B. Brucher and J. H. Schrittwieser, *Adv. Synth. Catal.*, 2011, **353**, 2239-2262.
28. T. Sehl, H. C. Hailes, J. M. Ward, R. Wardenga, E. von Lieres, H. Offermann, R. Westphal, M. Pohl and D. Rother, *Angew. Chem. Int. Ed.*, 2013, 6772–6775.
29. D. Rother, G. Kolter, T. Gerhards, C. L. Berthold, E. Gauchenova, M. Knoll, J. Pleiss, M. Müller, G. Schneider and M. Pohl, *ChemCatChem*, 2011, **3**, 1587-1596.
30. P. r. Tufvesson, J. Lima-Ramos, M. Nordblad and J. M. Woodley, *Org. Process Res. Dev.*, 2010, **15**, 266-274.
31. T. Gerhards, U. Mackfeld, M. Bocola, E. von Lieres, W. Wiechert, M. Pohl and D. Rother, *Adv. Synth. Catal.*, 2012, **354**, 2805-2820.
32. Á. Baraibar, E. Lieres, W. Wiechert, M. Pohl and D. Rother, *Top Catal*, 2013, 1-11(DOI: 10.1007/s11244-11013-10194-z).
33. K. Smithies, M. E. B. Smith, U. Kaulmann, J. L. Galman, J. M. Ward and H. C. Hailes, *Tetrahedron: Asymmetry*, 2009, **20**, 570-574.

34. J. Kulig, R. C. Simon, C. A. Rose, S. M. Husain, M. Hackh, S. Ludeke, K. Zeitler, W. Kroutil, M. Pohl and D. Rother, *Catal. Sci. Tech.*, 2012, **2**, 1580-1589.
35. T. Sehl, R. C. Simon, H. C. Hailes, J. M. Ward, U. Schell, M. Pohl and D. Rother, *J. Biotechnol.*, 2012, **159**, 188-194.
36. D. Kihumbu, T. Stillger, W. Hummel and A. Liese, *Tetrahedron: Asymmetry*, 2002, **13**, 1069-1072.
37. R. C. Rodrigues, C. Ortiz, Á. Berenguer-Murcia, R. Torres and R. Fernández-Lafuente, *Chem. Soc. Rev.*, 2013, **42**, 6290-6307.
38. C. Garcia-Galan, Á. Berenguer-Murcia, R. Fernandez-Lafuente and R. C. Rodrigues, *Adv. Syn. Catal.*, 2011, **353**, 2885-2904.
39. R. Fernandez-Lafuente, *Enzyme Microb. Technol.*, 2009, **45**, 405-418.
40. D. Brady and J. Jordaan, *Biotechnol. Let.*, 2009, **31**, 1639-1650.
41. P. V. Iyer and L. Ananthanarayan, *Process Biochem.*, 2008, **43**, 1019-1032.
42. C. Mateo, J. M. Palomo, G. Fernandez-Lorente, J. M. Guisan and R. Fernandez-Lafuente, *Enzyme Microb. Technol.* , 2007, **40**, 1451-1463.

Efficient 2-step biocatalytic strategies for the synthesis of all nor(pseudo)ephedrine isomers

--- Supplementary Information ---

Table of contents:

3.2) Synthesis strategy A-2

3.2.1) 2-Step cascade for the synthesis of (1*S*,2*S*)-NPE or (1*S*,2*R*)-NE

3.3) Synthesis strategy B-1 and B-2:

3.3.1) Optimization of the amine donor ratio for the reductive amination of 1,2-PPDO with *Cv*-(*S*)TA containing lyophilized whole cells

3.3.2) Synthesis strategy B - first cascade step: reductive amination of 1,2-PPDO with *At*-(*R*)TA or *Cv*-(*S*)TA

3.3.3) Termination of the transaminase reaction

3.3.4) Synthesis strategy B - second cascade step: reductive hydrogenation catalyzed by *R*ADH or *Lb*ADH

3.3.5) Time-dependent reaction curves for the synthesis strategy B: "transaminase-ADH"

4.) References

1.) Catalyst preparation - crude cell extract, purified enzyme and lyophilized whole cells

All catalysts were cloned and heterologously expressed in *Escherichia coli* as described below. If not otherwise indicated, the same cell stocks were either lyophilized directly (catalyst batch: lyophilized whole cells) or disrupted and the target protein purified chromatographically before the lyophilization step.

1.1) AHAS-I - purified enzyme and lyophilized whole cells

AHAS-I was cloned[1] and expressed[2] as described in literature. The purification was performed as described previously. The purity of AHAS-I lyophilized powder was >90 % with a protein content of 15 % (w/w).

1.2) *Ap*PDC-E469G - lyophilized whole cells

*Ap*PDC variant E469G (pyruvate decarboxylase from *Acetobacter pasteurianus*) was cloned and expressed as described before.[3]

1.3) *Cv*-(*S*)TA - purified enzyme and lyophilized whole cells

For the preparation of purified lyophilized *Cv*-(*S*)TA the cloning[4], expression[5], preparation of the cell-free extract[6] and the purification were performed as previously described.[7] The enzyme was obtained in purity >90 % and the lyophilized powder had a protein content of 70 % (w/w). Lyophilized whole cells were prepared by an optimized protocol for expression. *E. coli* BL21(DE3) was transformed with the HIS-tagged *Cv*-(*S*)TA coding plasmids.[4] A pre-culture was grown overnight in lysogeny broth (LB) medium containing 50 mg L^{-1} kanamycin at 37 °C. The main culture was inoculated in Terrific Broth medium (containing 4 % (v/v) glycerin and 50 mg L^{-1} kanamycin) to an OD_{600nm} of 0.1 in a 10 L bioreactor (Labfors, Infors AG, Switzerland). The pH (7.0) and temperature (30 °C) of the cultivation were constant while the gas exposure rate (0-600 L h^{-1}, 21 % oxygen) and the stirring rate (400-1.200 rpm) was varied to keep the oxygen partial pressure in a range of 20-30 %. Enzyme expression was induced by addition of 50 µM isopropyl-β-D-thiogalactopyranoside at an OD_{600nm} of 3. Cells were harvested after 20 h and stored at -20 °C. These cells were either lyophilized directly or used for protein purification according to the protocol described before. The purity of purified *Cv*-(*S*)TA was >90 % and the lyophilized powder hat a protein content of ~70 % (w/w).

1.4) *At*-(*R*)TA – lyophilized crude cell extract

The (*R*)-selective transaminase *At*-(*R*)TA is commercially available by Enzymicals AG as lyophilized crude cell extract.[8]

1.5) *R*ADH and *Lb*ADH – purified enzyme and lyophilized whole cells

The preparation of *R*ADH cells and optional protein purification steps were performed as indicated elsewhere.[9] *Lb*ADH was expressed and purified as mentioned in the work of Kulishova *et al.*.[10]

1.6) Expression level of enzymes in lyophilized whole cells, crude cell extracts and purity of purified enzymes

The expression level of the target protein *Ap*PDC-E469G, AHAS-I, *Cv*-(*S*)TA, *R*ADH, *Lb*ADH in lyophilized whole cells (LWC) of *E. coli* (see ESI chapter 1.1-1.3 and 1.5) and of *At*-(*R*)TA in *E. coli* crude cell extract (ESI chapter 1.4), and the purity of purified lyophilized enzymes was analyzed with SDS-PAGE. For the sample preparation of LWC, a suspension of 1.66 mg_{LWC} $mL_{SDS\text{-}buffer}^{-1}$ (w/v, SDS-buffer: 1-fold NuPAGE® LDS Sample Buffer) was heated for 25 min at 95 °C in Eppendorf Thermomixer. For samples of crude cell extract and purified proteins, a solution of 1.5 $mg_{protein}$ $mL_{SDS\text{-}buffer}^{-1}$ was heated for 2 min at 95 °C in Eppendorf Thermomixer. 10 µL of these solutions were added to a NuPAGE® Novex® 4-12% Bis-Tris Protein Gels (1.0 mm, 12 well; Thermo Fisher Scientific Inc.). SDS-PAGE and staining of the gel was performed in accordance with the NuPAGE® user manual.

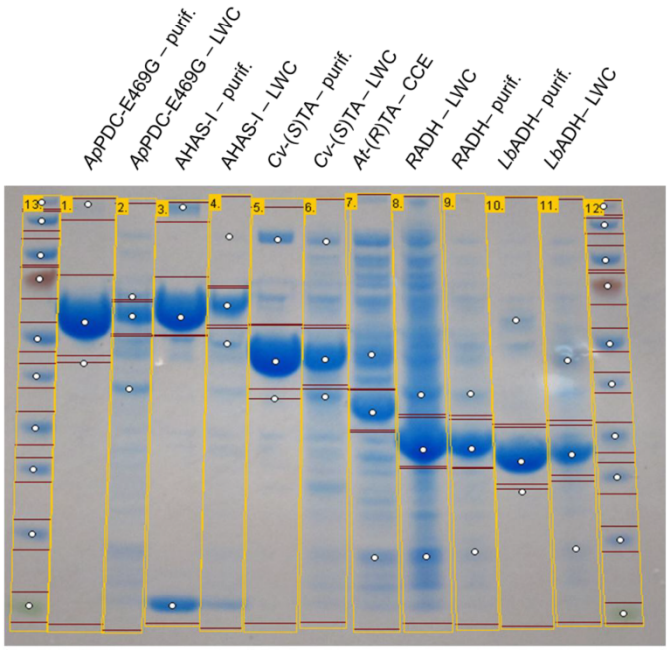

Figure 1 Expression level of enzymes in lyophilized whole cells (LWC) or crude cell extracts (CCE) and purity of purified enzymes (purif.) determined by SDS-PAGE.

The bands' intensities of the target protein relative to other proteins in the lane were quantified by using the freeware tool "GelAnalyzer 2010a" to give a more precise estimation of the protein expression level and protein purities:

*Ap*PDC-E469G purif.: >95 %, *Ap*PDC-E469G LWC.: ~40 %, AHAS-I purif.: >90 %, AHAS-I LWC: ~52 %, *Cv*-(*S*)TA purif.: >90 %, *Cv*-(*S*)TA LWC: ~52 %, *At*-(*R*)TA CCE: ~28 %, *R*ADH LWC: ~45 %, *R*ADH purif.: ~54 %, *Lb*ADH purif.: ~80 %, *Lb*ADH LWV: ~60 %.

2.) Reaction analytics

2.1) Quantification of benzaldehyde, phenylacetylcarbinol (PAC), acetophenone and 1-phenylpropane-1,2-dione

PAC (R_t = 8.7 min) and benzaldehyde (R_t = 17.1 min) were quantified by achiral HPLC-analysis as described before.[6, 7] For the quantification of acetophenone and 1-phenylpropane-1,2 dione, 20 µL reaction solution were added to 180 µL acetonitrile and analysed using a LiChrospher RP-8 reverse phase column, 250x4 mm, 5 µm pore-size column with a linear gradient of 45 % (v/v) acetonitrile in H_2O (containing 0.3 % (v/v) H_3PO_4). Typical retention times (200 nm) for acetophenone were 7.2 min and for 1-phenylpropane-1,2 dione 4.4 min.

2.2) Quantification of benzylamine, nor(pseudo)ephedrine isomers and 1-amino-1-phenyl-propan-2-one (APPO)

For the quantification of benzylamine, nor(pseudo)ephedrine and 1-amino-1-phenyl-propan-2-one (APPO) the reaction was extracted by the addition of 50 µL NaOH (1 M) to a 100 µL reaction solution. The solution was centrifuged (1000 rpm, Eppendorf centrifuge 5424, 3 min) and the supernatant (125 µL) extracted with 125 µL ethyl acetate containing 0.1 µL mL^{-1} decane as internal standard. The organic phase was analyzed by chiral gas chromatography with a Chirasil-DEX CB column (25 m x 320 µm x 25 µm) at a constant column temperature of 150 °C. Typical retention times were: decane = 1.8 min, benzylamine = 2.1-2.4 min, APPO = 4.4 min and nor(pseudo)ephedrines = 6.3-6.9 min.

2.3) Absolute configuration of all nor(pseudo)ephedrine isomers

The absolute configuration of all nor(pseudo)ephedrine isomers were determined as described previously.[7] Typical retention times of the four possible isomers on the Chirasil-DEX CB column (25 m x 0.25 mm x 0.25 µm) with a constant column temperature of 130 °C were: (1*S*,2*S*)-norpseudoephedrine = 24.4 min, (1*R*,2*R*)-norpseudoephedrine = 25.7 min, (1*S*,2*R*)-norephedrine = 28.0 min, (1*R*,2*S*)-norpseudoephedrine = 29.5 min.

2.4) Determination of the enantiomeric excess of (*R*)- and (*S*)-PAC

The configuration of (*R*)- and (*S*)-PAC was determined according to literature.[3] Typical retention times for the enantiomers were: (*R*)-PAC = 11.40 min and (*S*)-PAC = 11.95 min.

3.) Reaction procedure

3.1) Synthetic strategy A-1

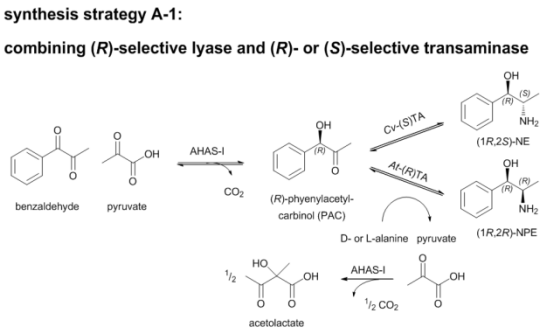

3.1.1) Reaction optimization for the 1-pot 2-step sequential cascade combining AHAS-I and *At*-(*R*)TA

In order to determine the minimum amount of AHAS-I (purified lyophilized enzyme - see 1.1) and *At*-(*R*)TA (lyophilized crude cell extract – sell 1.3) required for the 1-pot 2-step sequential cascade, these enzymes were applied in different concentrations. In the first step, in the carboligation reaction 20 mM benzaldehyde and 20 mM pyruvate (in 100 mM HEPES pH 7.5 with 200 µM PLP, 50 µM FAD, 100 µM ThDP, 5 mM $MgCl_2$) were used, and the concentration of AHAS-I was varied between 0.5 mg mL^{-1} and 5 mg mL^{-1}. Each reaction was performed in a volume of 1.5 mL in 2 mL closed glass vials (CS-Chromatographie Service GmbH, Germany) at 25 °C and 300 rpm shaking in a Eppendorf Thermomixer with a glass vial adapter (Eppendorf AG, Germany). After 90 min reaction time, 100 mM D-alanine and *At*-(*R*)TA were added in different concentrations (0-1 mg mL^{-1}) without isolation or quantification of the reaction intermediate (*R*)-PAC. The complete reaction was analyzed concerning the (1*R*,2*R*)-NPE product concentration after another 12 h. For the statistical data analysis and the data interpolation (see main article - Figure 1), the Kriging method was used as previously described.[7]

3.1.2) 1-Pot 2-step sequential cascade combining AHAS-I and *At*-(*R*)TA with higher substrate concentrations

The 1-pot 2-step sequential synthesis of (1*R*,2*R*)-NPE with benzaldehyde and pyruvate substrate concentrations of up to 100 mM was performed with optimized enzyme concentrations for AHAS-I (purified lyophilizate) and *At*-(*R*)TA (lyophilized crude cell extract). For the carboligation step, 0.025 $mg_{protein}\,mL^{-1}\,mM^{-1}{}_{BA}$ of AHAS-I was added to 25, 50, 75 or 100 mM benzaldehyde with equimolar concentrations of pyruvate (Pyr). The reactions were performed in a volume of 1.5 mL in 2 mL closed glass vials (CS-Chromatographie Service GmbH, Germany) at 25 °C and 300 rpm in a Eppendorf Thermomixer with a glass vial adapter (Eppendorf AG, Germany). The reaction buffer 100 mM HEPES (pH 7.5) contained 200 µM PLP, 50 µM FAD, 100 µM ThDP, and 5 mM $MgCl_2$. After 90 min reaction time 0.02 $mg_{protein}\,mL^{-1}\,mM^{-1}{}_{BA}$ of *At*-(*R*)TA and 2.5 mM $mM_{BA}{}^{-1}$ D-alanine were added. The solution was analyzed after another 12 h reaction time and concentrations of benzaldehyde, benzylamine, PAC and (1*R*,2*R*)-NPE were quantified as described (see ESI chapter 2.1 and 2.2).

3.1.4) Synthesis of (1*R*,2*S*)-NE combining AHAS-I and *Cv*-(*S*)TA in lyophilized whole cells and purified enzymes

The AHAS-I catalyzed carboligation of 10 mM benzaldehyde with 10 mM pyruvate was performed in 100 mM HEPES (pH 7.5) containing 50 µM FAD, 100 µM ThDP, and 5 mM $MgCl_2$ with either 0.5 $mg_{protein}$ mL^{-1} purified enzyme or 5 mg_{cells}/mL lyophilized whole cells. The reactions were carried out in 1.5 mL reaction volume in 2 mL glass vials at 25 °C (see ESI chapter 3.1.1). Reactions with LWC were performed at an increased shaking rate of 800 rpm. The decrease of benzaldehyde and the formation of PAC were analyzed after different time points between 5 min and 1 h (see ESI chapter 2.1). Separately, the reductive amination of 10 mM (*R*)-PAC (provided by BASF with an *ee* = 84 %)[6] with 10 mM (*S*)-α-methylbenzylamine (MBA) catalyzed by the *Cv*-(*S*)TA was investigated with either 1 $mg_{protein}$ mL^{-1} purified enzyme or 5 mg_{cells} mL^{-1} lyophilized whole cells. The reactions were performed in 100 mM HEPES (pH 7.5) containing 200 µM PLP in a reaction volume of 1.5 mL (2 mL glass vials, 25 °C, and 300 rpm or 800 rpm in the case of LWC, respectively (see ESI chapter 3.1.1). At different time points (between 10 min and 12 h) the reaction was analyzed regarding the conversion of PAC (see ESI chapter 2.1).

3.1.4) Synthesis of (1*R*,2*S*)-NE: Reduction of the lag-phase by per-incubation of lyophilised whole cells in buffer

In order to investigate if an observed lag phase in the synthesis of (1*R*,2*S*)-NE from (*R*)-PAC by *Cv*-(*S*)TA containing lyophilised whole cells (see main text, Figure 4) can be reduced, 10 mg_{cells} mL^{-1} lyophilised whole cells were pre-incubated for 2 h in 100 mM HEPES (pH 7.5) containing 200 µM PLP at 25 °C and 800 rmp shaking rate of 800 rpm in 2 mL glass vials. After 2 h the cell suspension was diluted with the same volume of 20 mM (*S*)-α-MBA and 20 mM (*R*)-PAC to a final concentration of 5 mg_{cells} mL^{-1} lyophilised whole cells, 10 mM (*S*)-α-MBA and 10 mM (*R*)-PAC. Analogously to the reactions described before (see Supp. Inf. chapter 3.1.1, and main article Figure 4) lyophilised whole cells were given directly to a solution of 10 mM (*S*)-α-MBA and 10 mM (*R*)-PAC without pre-incubation. Both reactions were performed in a reaction volume of 1.5 mL in 2 mL glass vials at 25 °C with a shaking speed of 800 rpm. The conversion of PAC was analysed at different time points (Supp. Inf. chapter 2.1).

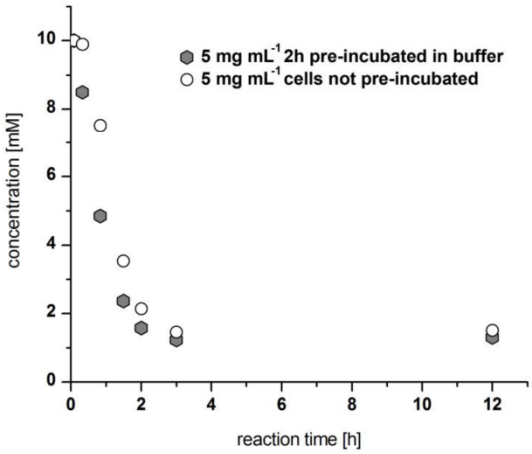

Figure 2 *Cv*-(*S*)TA catalyzed reductive amination of 10 mM (*R*)-PAC in the presence of 10 mM (*S*)-α-MBA catalyzed with lyophilized cells (5 mg mL^{-1}) wich were either per-incubated for 2 h in reaction buffer (dark combs) or added directly to a solution of the reactants (white dots).

3.2) Synthetic strategy A-2

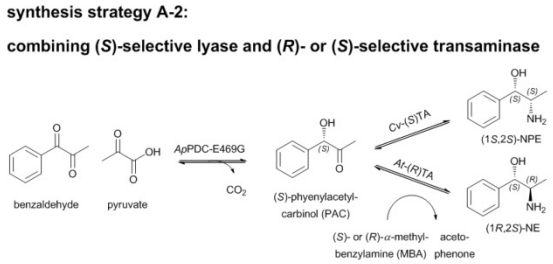

3.2.1) 2-Step cascade for the synthesis of (1*S*,2*S*)-NPE or (1*S*,2*R*)-NE

For the synthesis of (1S,2S)-NPE or (1S,2R)-NE the first reaction step, the carboligation of 40 mM benzaldehyde with 400 mM pyruvate, was catalyzed by the *Ap*PDC variant E469G. The reaction was performed in 100 mM potassium phosphate buffer (pH 7) containing 2.5 mM $MgSO_4$, 100 µM ThDP and 0.5 mg mL^{-1} purified enzyme. The reactions were carried out in glass vials at 25 °C. The reaction mixture was extracted with ethyl acetate after 48 h and dried over magnesium sulfate. After evaporation of the solvents, flash chromatography (eluent: petrol ether : ethyl acetate = 85 : 15) was performed. The compound (*S*)-PAC was obtained in a yield of 95 % with an *ee* of 70 %.[3, 11] The subsequent reductive amination of 10 mM (*S*)-PAC with 15 mM (*S*)-α-MBA or (*R*)-α-MBA, respectively, was carried out with *At*-(*R*)TA (0.5 $mg_{protein}$ mL^{-1} – lyophilized crude cell extract) or *Cv*-(*S*)TA (1 $mg_{protein}$ mL^{-1} – purified protein) in 100 mM HEPES (pH 7.5) containing 200 µM PLP. The reactions (reaction volume: 1.5 mL, 2 mL glass vials, 25 °C, 300 rpm) were analyzed regarding conversion (see ESI chapter 2.2) and optical purity (see ESI chapter 2.2) of the product N(P)E after 16 h reaction time.

3.3) Synthetic strategy B-1 and B-2:

The two strategies of the 1-pot 2-step reaction combining either the *Cv*-(*S*)TA (synthesis strategy B-1) or the *At*-(*R*)TA (synthesis strategy B-2) in the first cascade step and the *R*ADH or *Lb*ADH in the second cascade step were performed using the same methods. For both cascade steps the application of purified enzymes and lyophilized whole cells (LWC) were investigated (exception: reaction with *At*-(*R*)TA, which was only available as lyophilized crude cell extract; see ESI chapter 1.4). As an example, the reductive amination of 10 mM 1,2-PPDO (1-phenylpropane-1,2-dione) with *Cv*-(*S*)TA containing LWC was optimized with respect to different concentrations of the amine donor (*S*)-α-MBA (see ESI chapter 3.3.1). The reduction reaction was performed using a previously published protocol.[12]

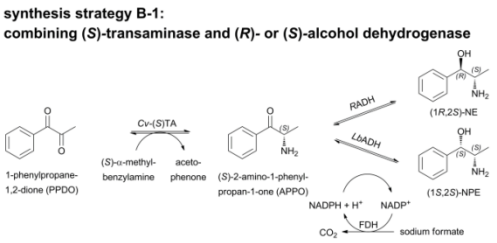

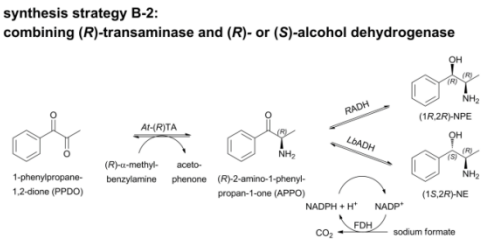

3.3.1) Optimization of the amine donor ratio for the reductive amination of 1,2-PPDO with *Cv*-(*S*)TA containing lyophilized whole cells

The reductive amination of 10 mM 1,2-PPDO with LWC containing the *Cv*-(*S*)TA (10 mg_{LWC} mL^{-1}) was carried out with different concentrations of the amine donor (*S*)-α-MBA (10-20 mM, see Fig. 1). The reaction was performed in 100 mM HEPES (pH 7.5) containing 200 µM PLP at 25 °C in 1.5 mL reaction volume in 2 mL closed glass vials (CS-Chromatographie Service GmbH, Germany) and 800 rpm shaking speed in a Eppendorf Thermomixer comfort with a glass vial adapter (Eppendorf AG, Germany). The reaction was analyzed after 16 h regarding the concentration of acetophenone and the substrate 1,2-PPDO (see ESI chapter 2.1).

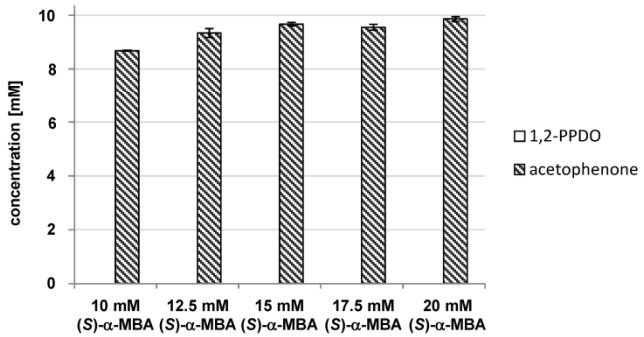

Figure 2 *Cv*-(*S*)TA catalyzed reductive amination of 10 mM 1,2-PPDO with different concentrations of (*S*)-α-MBA and 10 mg_{LWC} mL^{-1} in 100 mM HEPES (pH 7.5) containing 200 µM PLP at 25 °C and 800 rpm.

3.3.2) Synthetic strategy B - first cascade step: reductive amination of 1,2-PPDO with *At*-(*R*)TA or *Cv*-(*S*)TA

The reductive amination of 1,2-PPDO was carried out in case of the *Cv*-(*S*)TA with 15 mM (*S*)-α-MBA and either 1 $mg_{protein}$ mL^{-1} purified enzyme or 10 mg_{LWC} mL^{-1} LWC. Reactions with *At*-(*R*)TA were performed with 1 $mg_{protein}$ mL^{-1} lyophilized crude cell extract and 15 mM (*R*)-α-MBA. As a reaction buffer 100 mM HEPES (pH 7.5) containing 200 µM PLP was used. The reaction volumes were added up to ~10 mL (in 15 mL closed glass vials) and were shaken at room temperature (21 °C) and 500 rpm in a Barloworld Scientific Ltd. (UK) vortex shaker. At different time points (see Figure 2-A, 3-A, 4-A and 5-A) the reactions were analyzed regarding the concentration of the co-product acetophenone and the substrate 1,2-PPDO (see ESI chapter 2.1)

3.3.3) Termination of the transaminase reaction

As indicated (see Tab. 1 – main article), two general strategies for the termination of the transaminase reaction (chapter 3.3.2) were applied: ultrafiltration and pH-shift. In the ultrafiltration method, the TA was removed from the reaction solution (volume ~10 mL, see ESI chapter 3.3.2) by centrifugation (4 °C, 30 min, 4.000 rpm, universal centrifuge 32-R – Hettrich GmbH & Co.KG (Germany)) in a VivaSpin-20 (Vivascience AG, Germany) with a membrane cut-off of 10 kDa. For the pH-shift method, the solution was titrated with 20 % (v/v) HCl to pH 2 and then re-titrated with 10 M NaOH to pH 7.5. This solution was then used in the reduction reaction (see ESI chapter 3.3.4). Here, the transaminase was deactivated by titration to pH 2 with 20 % (v/v) HCl. The reaction was incubated for 1 min at room temperature (21 °C) before re-titration with 10 M NaOH to pH 7.5. The denatured enzymes (visible as precipitate) were removed by centrifugation in closed glass vials (4 °C, 5 min, 4.000 rpm, universal centrifuge 32-R-Hettrich GmbH (Germany)). The supernatant was used for the reduction reaction (see ESI chapter 3.3.4).

3.3.4) Synthetic strategy B - second cascade step: reductive reaction catalyzed by *R*ADH or *Lb*ADH

The reductive reaction was performed as specified (see Tab. 1 – main article) either directly with the reaction solutions from the TA reaction (see ESI chapter 3.3.2), or with the permeate/supernatant from the termination step (see ESI chapter 3.3.3). Reaction solutions performed in the first cascade step with *Cv*-(*S*)$TA_{purified\ enzyme}$, *Cv*-(*S*)TA_{LWC} or *At*-(*R*)TA_{CCE} were split as indicated for the corresponding reductive step (see main article, Tab. 1). In general 0.5 mM $NADP^+$, 150 mM sodium formate, 10 µL mL^{-1} FDH (Jülich Fine Chemicals, Jülich, now Codexis, no. 25.10) and either purified enzyme (1 $mg_{protein}$ mL^{-1}) or lyophilized whole cells (10 mg_{LWC} mL^{-1}) of the respective alcohol dehydrogenases (*Lb*ADH *or R*ADH) were added to the corresponding solution. Without changing any further reaction conditions (like buffer, shaking rate and reaction temperature) the 1-pot 2-step cascades were continued in ~4 mL reaction volume (in 5 mL closed glass vials) as in the first reaction step (see ESI chapter 3.3.2). At different time points, the concentration of the intermediate 1-amino-1-phenyl-propan-2-one and the N(P)Es were quantified (see chapter 2.2). Moreover, at the endpoint of the reactions the absolute configuration (*de*, *ee*) of the products N(P)E were determined (see ESI chapter 2.3).

3.3.5) Time-dependent reaction curves for the synthesis strategy B: "transaminase-ADH"

The time-dependent reaction curves for all 1-pot 2-step cascade reactions are shown in Fig. 2-4 and summarized in Tab. 1 of the main article.

A:1st step: 1,2-PPDO converted with *Cv*-(*S*)TA purified enzyme

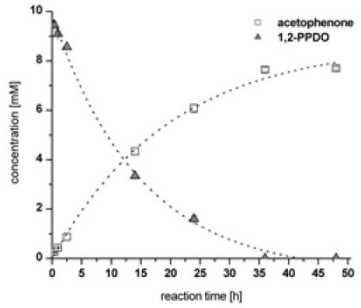

A:1st step: 1,2-PPDO converted with *At*-(*R*)TA as CCE

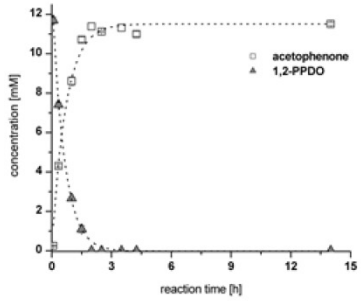

B:2nd step: APPO converted with *R*ADH purified enzyme

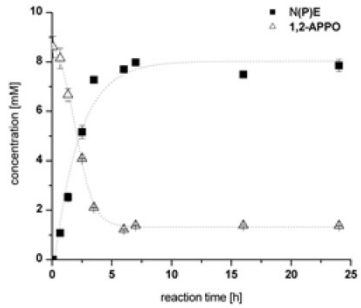

B:2nd step: APPO converted with *R*ADH purified enzyme

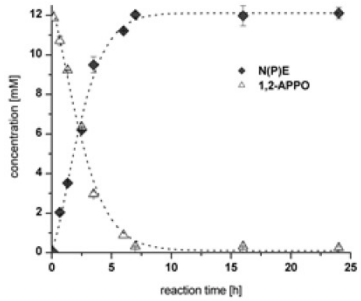

C:2nd step: APPO converted with *Lb*ADH purified enzyme

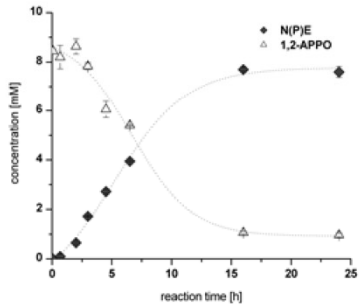

C:2nd step: APPO converted with *Lb*ADH purified enzyme

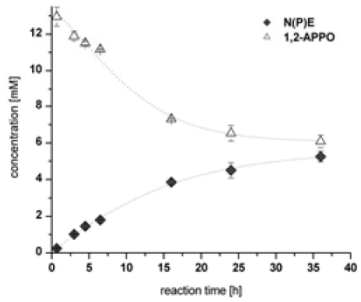

Figure 3 1-Pot 2-step sequential cascade combining the *Cv*-(*S*)TA$_{\text{purified enzeme}}$ (left) or the *At*-(*R*)TA$_{\text{CCE}}$ (right) in the first reaction step (A: reductive amination of 1,2-PPKO) with either the *R*ADH$_{\text{purified enzyme}}$ (B) *or* *Lb*ADH$_{\text{purified enzyme}}$ (C) in the second step (reductive hydrogenation)

A: The reductive amination was carried out with 1 $mg_{protein}\,mL^{-1}$ *Cv*-(*S*)TA (purified enzyme) or 1 $mg_{protein}\,mL^{-1}$ *At*-(*R*)TA (crude cell extract - CCE) in 100 mM HEPES (pH 7.5), 200 µM PLP, with ~10 mM 1,2-PPDO (*At*-(*R*)TA: 12 mM) and 15 mM (*R*)- or (*S*)-α-MBA, respectively, at room temperature (21 °C). The reactions were terminated in this case by a pH-shift (titrated with 20 % (v/v) HCl to pH 2 then re-titrated with 10 M NaOH to pH 7.5).

B, C: For the reductive hydrogenation the corresponding solutions (A) were split and 0.5 mM $NADP^+$, 150 mM sodium formate, 10 µL mL^{-1} FDH and either 1 $mg_{protein}\,mL^{-1}$ purified enzyme of the *R*ADH (B) or *Lb*ADH (C) were added and subsequently further incubated at room temperature (21 °C). The concentration of N(P)E is given as a sum of all N(P)E isomers.

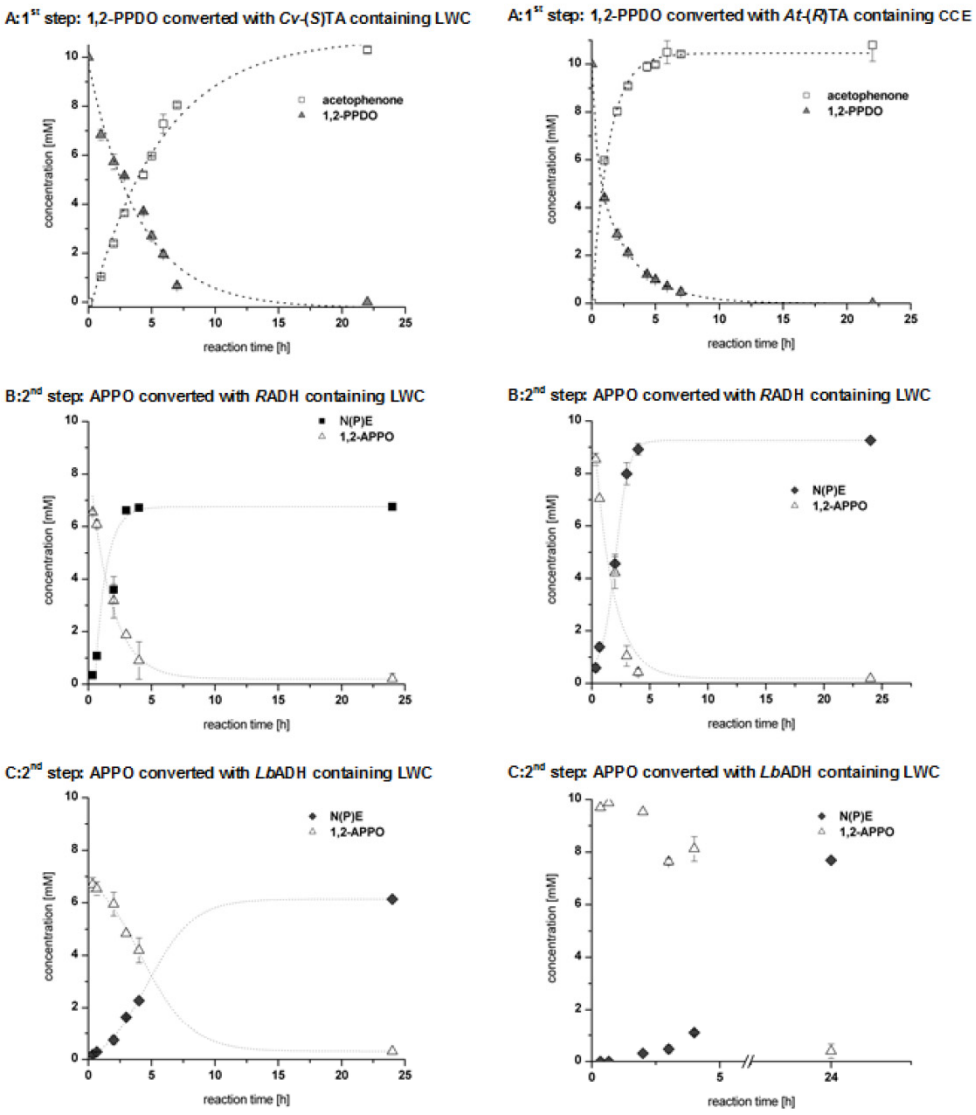

Figure 4 1-Pot 2-step sequential cascade combining the *Cv*-(*S*)TA_{LWC} (left) or the *At*-(*R*)TA_{CCE} (right) in the first reaction step (A: reductive amination of 1,2-PPKO) with either the *R*ADH_{LWC} (B) *or* *Lb*ADH_{LWC} (C) in the second step (reductive hydrogenation)

A: The reductive amination was carried out with 10 mg_{cells} mL^{-1} *Cv*-(*S*)TA (lyophilized whole cells - LWC) or 1 $mg_{protein}$ mL^{-1} *At*-(*R*)TA (crude cell extract - CCE) in 100 mM HEPES (pH 7.5), 200 µM PLP, with ~10 mM 1,2-PPDO and 15 mM (*R*)- or (*S*)-α-MBA, respectively, at room temperature (21 °C). The reactions were terminated in this case by a pH-shift (titrated with 20 % (v/v) HCl to pH 2 then re-titrated with 10 M NaOH to pH 7.5)

B, C: For the reductive hydrogenation the corresponding solutions (A) were split and 0.5 mM $NADP^+$, 150 mM sodium formate, 10 µL mL^{-1} FDH and either 10 mg_{yells} mL^{-1} lyophilized whole cells of the *R*ADH (B) or *Lb*ADH (C) were added and subsequently further incubated at room temperature (21 °C). The concentration of N(P)E is given as a sum of all N(P)E isomers.

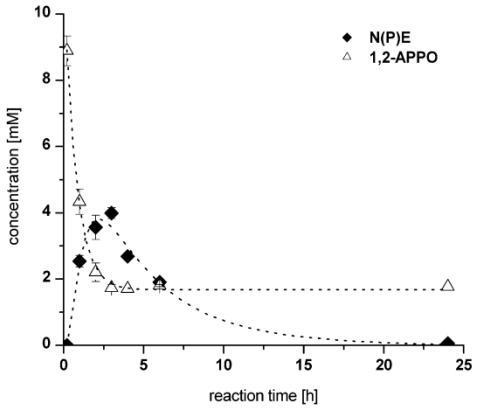

Figure 5 Second reaction step (reductive hydrogenation) of the 1-pot 2-step sequential cascade combining the *Cv*-(*S*)TA/*Lb*ADH (each as purified enzyme) without inactivation of the TA after the first reaction step.

The reductive amination (data not shown) had been carried out with 1 $mg_{protein}$ mL^{-1} *Cv*-(*S*)TA (purified enzyme) in 100 mM HEPES (pH 7.5), 200 µM PLP, with ~10 mM 1,2-PPDO and 15 mM (*S*)-α-MBA at room temperature (21 °C). The reactions were not terminated in this case.

For the reductive hydrogenation 0.5 mM $NADP^+$, 150 mM sodium formate, 10 µL mL^{-1} FDH and 1 $mg_{protein}$ mL^{-1} purified enzyme of the *Lb*ADH was added and subsequently further incubated at room temperature (21 °C). The concentration of N(P)E is given as a sum of all N(P)E isomers.

4.) References

1. G. Cox and H. Rampes, *Adv. Psychiatr. Treat.*, 2003, **9** (6), 456-463.
2. D. F. Larder, *J. Chem. Educ.*, 1967, **44** (11), 661.
3. Baraibar A. G., Lieres von E., Wiechert W, Pohl M and R. D, *Top. Catal.*, 2013 1-11 (DOI: 10.1007/s11244- 11013- 10194- z).
4. U. Schell, R. Wohlgemuth and J. M. Ward, *J. Mol. Cat. B: Enzym.*, 2009, **59** (4), 279-285.
5. U. Kaulmann, K. Smithies, M. E. B. Smith, H. C. Hailes and J. M. Ward, *Enzyme Microb. Tech.*, 2007, **41** (5), 628-637.
6. T. Sehl, R. C. Simon, H. C. Hailes, J. M. Ward, U. Schell, M. Pohl and D. Rother, *J. Biotechnol.*, 2012, **159** (3), 188-194.
7. T. Sehl, H. C. Hailes, J. M. Ward, R. Wardenga, E. von Lieres, H. Offermann, R. Westphal, M. Pohl and D. Rother, *Angew. Chem. Int. Ed.*, 2013, **52** (26), 6772–6775.
8. Enzymicals AG, http://www.enzymicals.com/Enzymicals_Enzymes_v011.pdf.
9. J. Kulig, A. Frese, W. Kroutil, M. Pohl and D. Rother, *Biotechnol. Bioeng.*, 2013, **110** (7), 1838-1848.
10. L. Kulishova, K. Dimoula, M. Jordan, A. Wirtz, D. Hofmann, B. Santiago-Schübel, J. Fitter, M. Pohl and A. C. Spiess, *J. Mol. Cat. B: Enzym.*, 2010, **67** (3–4), 271-283.
11. Á. G. Baraibar, Heinrich-Heine University Düsseldorf, dissertation in publishing process.
12. D. Kihumbu, T. Stillger, W. Hummel and A. Liese, *Tetrahedron: Asymmetry*, 2002, **13** (10), 1069-1072.

4 Discussion

Context of publications and invention disclosures

The combination of ThDP-dependent enzymes, alcohol dehydrogenases and ω-transaminases can constitute two different routes towards chiral vicinal amino alcohols (chapter 1.5.4). A main focus of this thesis was set on the identification and characterisation of ω-transaminases for the 2-step syntheses of vicinal amino alcohols. For a fast and reliable screening of ω-transaminases (chapter 1.5.5), a novel screening assay was developed. Enzymes with most promising properties were investigated in combination with ThDP-dependent enzymes or alcohol dehydrogenases in different 2-step cascade modes for the synthesis of optically pure nor(pseudo)ephedrines.

Publication I describes the functionality and reliability of the established screening assay for ω-transaminases. Results for the reductive amination of nine 2-hydroxy ketones in combination with three amine donors were shown for four selected enzymes. The complete screening set and the possibility to expand the assay's application are discussed in the following.

Publication II reports the results for the synthesis of (1*R*,2*R*)-norpseudoephedrine and (1*R*,2*S*)-norephedrine in two reaction steps by combining highly (*R*)-selective ThDP-dependent enzymes with ω-transaminases. The reaction equilibrium constant for the reductive amination step was determined. A solution for a required reaction equilibrium shift without addition of further reactants or catalysts is presented. For the 2-step cascade a parameter optimisation (pH, temperature, enzyme concentrations and amine donor/PAC ratio) was performed.

Publication III describes and compares the synthesis routes to all nor(pseudo)-ephedrine stereoisomers either by a combination of ThDP-dependent enzymes with ω-transaminases in the one strategy or ω-transaminases and dehydrogenases in the other. In both strategies the application of (*S*)- and (*R*)-selective enzymes is investigated. Moreover, reactions with lyophilised whole cells, crude cell extracts and purified enzymes were compared.

Invention disclosures I and II [214, 215] demonstrates the specifically the access to (1*S*,2*S*)-norpseudoephedrine (trivial name: Cathine) in the two different synthesis routs presented in publication III. This compound is sold e.g. on the German market as the main drug as an appetite suppressant for short-term use.[149-151] Invention disclosure I reports access to (1*S*,2*S*)-norpseudoephedrine by combination of the pyruvate decarboxylase variant *Ap*PDC-E469G from *Acetobacter pasteurianus* with the ω-transaminase CV2025 from *Chromobacterium violaceum*.[214] Moreover, the concept of chiral enrichment (also referred to as "chiral polishing") of the intermediate (*S*)-phenylacetylcarbinol to gain high optical purities (*ee* >97 %) is shown. In invention disclosure II the access to (1*S*,2*S*)-norpseudoephedrine in high optical purities is shown by using the ω-transaminase CV2025 in the first step and the alcohol dehydrogenase *Lb*ADH from *Lactobacillus brevis* in the second step.[215]

4.1 A novel screening assay for ω-transaminases

In the beginning of this work a toolbox of 18 putatively (*S*)-selective ω-transaminases (chapter 1.5.5.3) and later on eight (*R*)-selective enzymes were accessible. Without detailed knowledge about their amine acceptor range and amine donor preference at hand, the combination of these catalysts with 10 synthesised or available 2-hydroxy ketones and 12 selected amine donors would have resulted in an enormous number of single reactions to analyse. In order to achieve a quick and reliable analysis of these reactions, an ω-transaminase screening assay had to be established first.

The few existing screening assays were limited to a specific set of amine donors or amine acceptors (chapter 1.4.3.3). Since one intention of this work was the identification of enzymes for reductive amination of 2-hydroxy ketones, we would have been restricted to a screening with either alanine or α-methylbenzylamine as amine donors. On the basis of work from Breuer *et al.*,[216] an assay which had been developed for the detection of 2-hydroxy ketones in carboligation reaction, was used. In this assay, the colourless reagent 2,3,4-triphenyltetrazolium chloride (TTC) is reduced at basic conditions to a red-coloured 1,3,5-triphenylformazan, whereby the 2-hydroxy ketone is oxidised to the corresponding diketone. In this thesis, this concept was used to analyse the ω-transaminase catalysed reductive amination of

2-hydroxy ketones, by analysing the concentration of remaining 2-hydroxy ketones (scheme 4-1). The conversion can be quantified relative to a calibration curve with known 2-hydroxy ketone concentration (publication I, chapter 3.1).

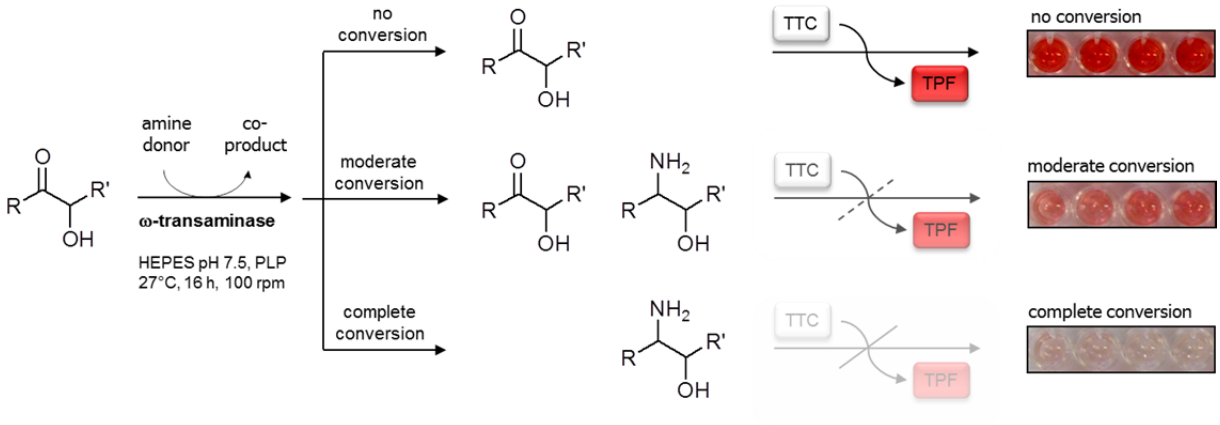

Scheme 4-1: TTC-based screening assay for ω-transaminases activity.

The TTC-reagent oxidises very specifically 2-hydroxy ketones to the corresponding diketones and is thereby reduced to red-coloured formazan. Therewith conversion of 2-hydroxy ketones by ω-transaminases can be quantified photometrically at 510 nm and is related to the amount of remaining substrate after a certain reaction time. Further details are described in publication I (chapter 3.1).

4.1.1 Characterisation of the TTC-based screening assay

For a precise quantification of 2-hydroxy ketones with this TTC-assay, the linear measuring range for each substrate needed to be determined (publication I and chapter 3.1). An important factor is the compound specific factors colouration rate, which is given by the reactivity of the 2-hydroxy ketones with the TTC-reagent.

The colouration rate for acetoin is for instance one order of magnitude higher than for propioin. Similar trends were observed for the substrate pairs 2-hydroxyaceto-phenone (2-HAP) and 2-hydroxypropiophenone (HPP) or for phenylacetylcarbinol (PAC) and phenylpropionylcarbinol (PPC), which differ only in one methyl/methylene group, respectively, like acetoin and propioin (see table 4-1).

Table 4-1: Amine donors and amine acceptors used in the TTC-assay

Given is the compound specific colouration rate after TTC-addition and the recommended steps for the TTC-colouration reaction (A). All tested amine donors did not cause any background reaction (B)

A: amine acceptors

structure	name	colouration rate [mAU/(mM*min)]	recommended steps	
			dilution of the reaction solution before TTC addition	incubation after TTC addition
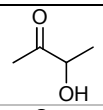	acetoin	0.034	-	2 min
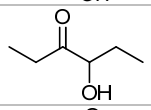	propioin	0.004	-	10 min
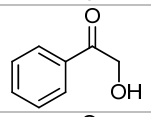	2-HAP	1.096	1:10	1 min
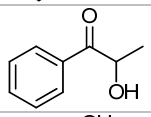	HPP	0.022	-	4 min
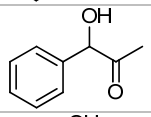	PAC	0.329	1:10	2 min
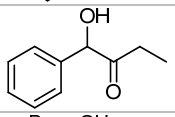	PPC	0.090	-	1 min
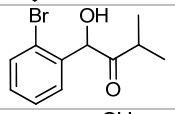	oBr-HMBP	0.012	-	10 min
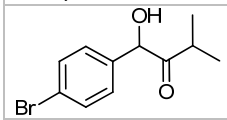	pBr-HMBP	0.013	-	10 min
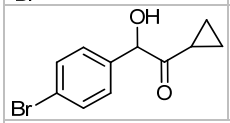	pBr-HCPPP	0.005	-	30 min

B: amine donors

 isopropylamine	 (*S*)-sec-butylamine	 (*R*)-sec-butylamine	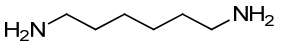 hexane-1,6-diamine
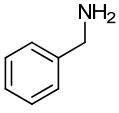 benzylamine	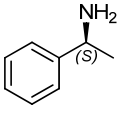 (*S*)-α-MBA	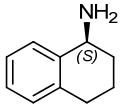 (*S*)-tetrahydronaphthalen-1-amine (THNA)	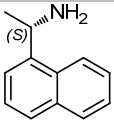 (*S*)-1-(naphthalen-1-yl)-ethanamine (NEA)
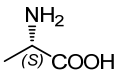 L-alanine	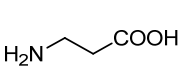 β-alanine	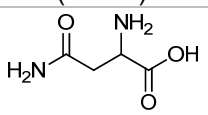 D- and L-asparagine	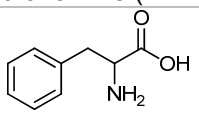 D- and L-phenylalanine

As the assay is specifically sensitive for PAC (0.33 mAU mM^{-1} min^{-1}) and 2-HAP (1.10 mAU mM^{-1} min^{-1}), a pre-dilution of the reaction solution is recommended before the TTC-reagent is added to initiate the colour reaction. Bulky-bulky 2-hydroxy ketones like *ortho*- and *para*-bromo-2-hydroxy-3-methyl-butylpropiophenone (o/p-Br-HMBP) or *para*-bromo-2-hydroxy-3-cyclopropyl-propiophenone (p-Br-HCPPP) can also be quantified but require a longer incubation time after TTC addition. Only benzoin could not be used since precise quantification within the low solubility range of benzoin (~1 mM) was not possible. Moreover, 2-hydroxy ketones with a tertiary alcohol group cannot be oxidised to the corresponding diketone and thus cannot be used in this assay.

Compared to the high sensitivity for 2-hydroxy ketones, none of the 12 different amine donors used in the screenings showed significant background colouration (chapter 3.1). The same holds for the buffer (100 mM HEPES), the cofactor (200 µM PLP), the crude cell lysates and the corresponding amino alcohols (publication I, chapter 3.1).

4.1.2 Reliability of the TTC-based screening assay

The general reliability of the TTC-assay was evaluated by a comparison of positive TTC-screening results with instrumental analyses data for selected reactions (publication I, chapter 3.1). Gas chromatography (GC) and high performance liquid-chromatography (HPLC) analyses data for TTC-reactions with acetoin, 2-HAP, PAC with (*S*)-α-methylbenzylamine (MBA) and four different ω-transaminases showed in almost all cases only 5 % to maximal 10 % deviation in conversion values compared to the TTC-screening assay results.

As a single exception, positive TTC-screening results with HPP as amine acceptor did not fit to data determined by instrumental analysis. More detailed investigation of this divergence, which would have contradicted the general reliability of TTC-based screening results, indicated that a chemical instability of the substrate under the applied reaction conditions was responsible for these false positive screening hits. When 10 mM HPP is incubated for 16 h at 27 °C in 100 mM HEPES (pH 7.5, containing 200 µM PLP and 10 mM (*S*)-α-MBA) in the presence of 1 mg mL^{-1} crude cell extract of BL21(DE3), HPLC analyses indicated that ~5 % of initially pure HPP was isomerised to the regioisomer PAC. As mentioned above, PAC shows a ~15-fold

higher colouration rate in the TTC-assay than HPP (table 4-1). Therefore, already 5 % PAC in a HPP solution account for ~50 % of the colour intensity, resulting in a false positive signal. Theoretically, such problems can occur with all instable 2-hydroxy ketones for which the respective regioisomer has a higher colouration rate. However, in case of HPP a significant lower PAC concentration was observed when purified enzymes were used instead of crude cell extracts (<1 % PAC detected by HPLC). This indicates that the isomerisation of HPP was caused by the *E. coli* crude cell extract and thus can be overcome by the use of purified enzyme.

4.1.3 Results of the TTC-based screening assay for (*S*)-selective ω-transaminases

After the general reliability was validated, the TTC-based screening assay was used to identify and moreover quantify conversion of nine different 2-hydroxy ketones (see table 4-1). First all substrates were tested in combination with the 18 ω-transaminases of the (*S*)-selective toolbox and with at least three different amine donors: (*S*)-α-methylbenzylamine, benzylamine and L-alanine.

Only for three of the nine tested substrates conversion was detected: acetoin, 2-hydroxyacetophenone (2-HAP) and phenylacetylcarbinol (PAC). These substrates are all small-bulky substrates with respect to the carbonyl group, carrying either a methyl group (acetoin, PAC) or a hydroxymethyl group (2-HAP) as the small substituent. All substrates with larger substituents were not accepted, indicating that none of the enzymes has a “small pocket” in the active site (see chapter 1.4.3.2) where residues larger than hydroxymethyl groups fit in. Due to the random error of the TTC-assay (standard deviation of the negative control: $\pm$10 %), values for a substrate depletion lower than 10 % are not significantly detectable. However, low activities and conversion values might be an interesting starting point for further enzyme engineering. In order to overcome these limitations, we developed a refined protocol for these purposes (see chapter 4.1.4).

As mentioned above, significant conversions of acetoin, 2-HAP and PAC with some of these enzymes were detected using this assay. One advantage of this assay is that it is independent of the selected amine donors, which was not possible with any of the already published screening assays (chapter 1.4.3.3). This allowed to test

another 12 amine donors (table 4-1-B) as co-substrates for the (*S*)-selective transaminases toolbox. Outstanding conversion values for the reductive amination of acetoin and PAC (see table 4-2-A and table 4-2-C) were detected for the enzymes CV2025 (from *Chromobacterium violaceum*), PP5182, PP2799 and PP0596 (all from *Pseudomonas putida*) and PA0221 (from *Pseudomonas aeruginosa*). Here, a general trend could be deduced from different amine donors combination (highest conversion values listed first): (*S*)-α-methylbenzylamine ~ isopropylamine ~ (*S*)-/(*R*)-sec-butylamine > (*S*)-NEA > (*S*)-THNA ~ benzylamine ~ L-alanine (table 4-2). Only with few enzymes very low conversions were found also with hexane-1,6-diamine and β-alanine. However, these low conversion values should be validated with instrumental analysis in case its application would become of interest in the future. No significant conversations were detected for D- and L-asparagine or D- and L-phenylalanine as amine donors. Although exceptions are known, ω-transaminases generally don't accept α-amino acids as amine donors (see chapter 1.4.3.4). In contrast to the high conversions found for acetoin and PAC, reductive amination of 2-HAP was detected only with CV2025 and different amine donors and with PP5182 in the presence of (*S*)-α-methylbenzylamine (table 4-2-B). Although higher chemical reactivity can be expected for 2-HAP compared to PAC, the terminal hydroxymethyl group in 2-HAP might already cause steric hindrance, which might explain the lower conversions observed with 2-HAP.

For the reductive amination of PAC, which is the intermediate in the desired 2-step synthesis of nor(pseudo)ephedrine (chapter 1.5), highest conversions in the TTC-assay were detected with CV2025, which catalysed the conversion of >95 % PAC using (*S*)-α-methylbenzylamine as amine donor. Further suitable amine donors for this enzyme under the tested conditions were isopropylamine (~90 % conv.), (*S*)-sec-butylamine (~90 % conv.) and (*R*)-sec-butylamine (~80 % conv.); even (*S*)-NEA (~70 % conv.) might be suitable alternative amine donor. Besides, (*S*)-THNA, benzylamine and L-alanine (each ~20 % conv.) are also accepted, but their application would require further reaction optimisation to improve the overall conversions.

Table 4-2: Screening results for the conversion of acetoin, 2-hydroxyacetophenone (2-HAP) and phenylacetylcarbinol (PAC) with 18 (*S*)-selective ω-transaminase measured using the TTC-assay

reaction conditions: 10 mM acetoin and 10 mM amine donor (isopropylamine and (*S*)-/(*R*)-sec-butylamine: 200 mM) in HEPES buffer (100 mM, pH 7.5), containing 200 µM PLP, 1 mg mL^{-1} crude cell extract, incubated in 96-well plate at 27 °C, 100 rpm, 16 h. Conversions (given in % of 2-hydroxy ketone consumption) were determined relative to an internal calibration curve at 510 nm after colouration with TTC (see publication I and chapter 3.1)

"-": no significant conversion (cut-off: 10 %) detectable

negative control: 1 mg mL^{-1} clarified crude cell extract of *E. coli* BL21(DE3) cells transformed with an empty plasmid (pET-29a)

A) reductive amination of acetoin

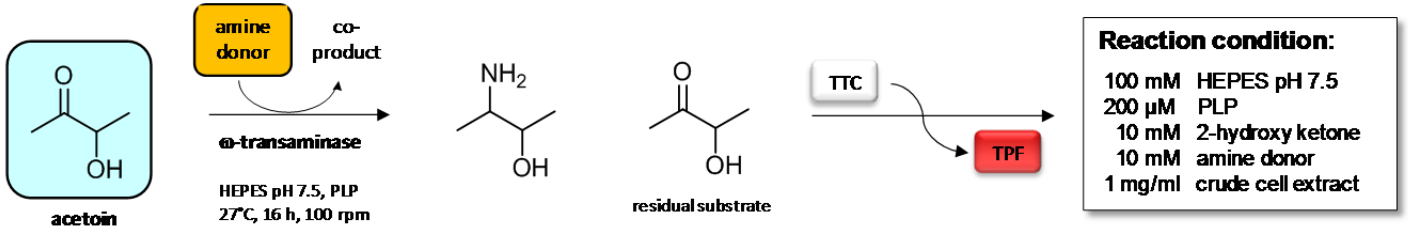

	small aliphatic				bulky aromatic				amino acids			
neg. control	-	-	-	-	-	-	-	-	-	-	-	-
CV2025	65.8	82.2	66.0	-	88.2	18.8	23.3	63.7	26.4	-	-	-
Sery1824	-	-	-	-	-	-	-	-	-	-	-	-
Sace4673	-	-	-	-	-	-	-	-	-	-	-	-
Sery1902	-	-	-	-	-	-	-	-	-	-	-	-
Sav4551	-	-	-	-	12.6	-	-	-	-	-	-	-
Sav2612	-	-	-	-	12.6	-	-	-	-	-	-	-
Sco5655	-	-	-	-	10.9	-	-	-	-	-	-	-
PP5182	48.5	49.4	42.4	-	60.7	16.4	20.9	18.8	15.7	-	-	-
PP2799	43.8	45.9	26.6	-	49.1	-	-	-	26.8	-	-	-
PP2588	-	13.9	11.1	-	13.0	-	-	-	26.3	-	-	-
PA0221	21.1	30.7	23.2	-	10.9	-	-	-	23.4	-	-	-
PA4805	-	-	-	-	19.7	-	-	-	-	-	-	-
PA5313	-	-	-	-	-	-	-	-	-	-	-	-
POAB80	-	-	-	-	-	-	-	-	-	-	-	-
KPN04441	-	-	-	-	-	-	-	-	-	-	-	-
POAB80	-	-	-	-	-	-	-	10.0	-	-	-	-
POAB80	-	-	-	-	-	-	-	-	-	-	-	-
PP0596	22.6	25.0	18.1	-	12.6	-	-	10.1	-	14.2	-	-

Table 4-2 – continued from page 96.

B) reductive amination of 2-hydroxyacetophenone (2-HAP)

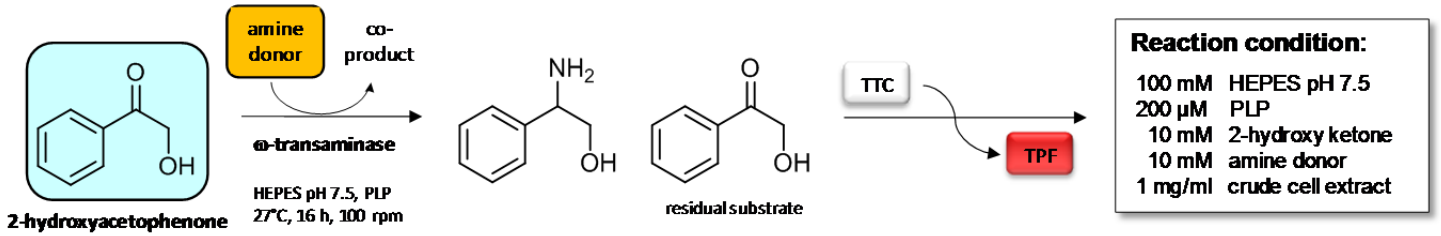

	small aliphatic				bulky aromatic				amino acids			
neg. control	-	-	-	-	-	-	-	-	-	-	-	-
CV2025	29.4	50.2	36.9	-	37.5	-	-	26.5	11.6	-	-	-
Sery1824	-	-	-	-	-	-	-	-	-	-	-	-
Sace4673	-	-	-	-	-	-	-	-	-	-	-	-
Sery1902	-	-	-	-	-	-	-	-	-	-	-	-
Sav4551	-	-	-	-	-	-	-	-	-	-	-	-
Sav2612	-	-	-	-	-	-	-	-	-	-	-	-
Sco5655	-	-	-	-	-	-	-	-	-	-	-	-
PP5182	-	-	-	-	12.1	-	-	-	-	-	-	-
PP2799	-	-	-	-	-	-	-	-	-	-	-	-
PP2588	-	-	-	-	-	-	-	-	-	-	-	-
PA0221	-	-	-	-	-	-	-	-	-	-	-	-
PA4805	-	-	-	-	-	-	-	-	-	-	-	-
PA5313	-	-	-	-	-	-	-	-	-	-	-	-
POAB80	-	-	-	-	-	-	-	-	-	-	-	-
KPN04441	-	-	-	-	-	-	-	-	-	-	-	-
POAB80	-	-	-	-	-	-	-	-	-	-	-	-
POAB80	-	-	-	-	-	-	-	-	-	-	-	-
PP0596	-	-	-	-	-	-	-	-	-	-	-	-

Table 4-2 – continued from page 96.

C) reductive amination of phenylacetylcarbinol (PAC)

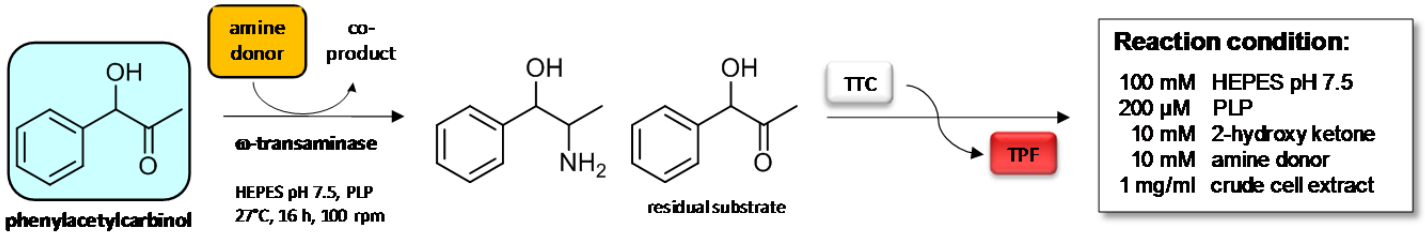

	small aliphatic				bulky aromatic				amino acids			
neg. control	-	-	-	-	-	-	-	-	-	-	-	-
CV2025	90.8	89.3	82.8	-	96.3	18.8	17.6	68.5	19.1	-	-	-
Sery1824	20.9	-	-	-	-	-	-	-	-	-	-	-
Sace4673	-	-	-	-	-	-	-	-	-	-	-	-
Sery1902	-	-	-	-	-	-	-	-	-	-	-	-
Sav4551	-	-	-	-	-	-	-	-	-	-	-	-
Sav2612	-	-	-	-	-	-	-	-	-	-	-	-
Sco5655	-	-	-	-	-	-	-	-	-	-	-	-
PP5182	85.8	69.6	51.4	-	94.4	16.4	31.2	22.2	22.1	-	-	-
PP2799	54.1	66.4	24.0	-	89.4	-	-	-	19.4	-	-	-
PP2588	-	-	-	-	17.5	-	-	-	-	-	-	-
PA0221	61.1	53.1	33.3	-	36.5	-	-	-	-	-	-	-
PA4805	-	-	-	-	-	-	-	-	-	-	-	-
PA5313	-	-	-	-	-	-	-	-	-	-	-	-
POAB80	-	-	-	11.9	-	-	-	-	-	-	-	-
KPN04441	-	-	-	-	-	-	-	-	-	-	-	-
POAB80	-	-	-	15.0	-	-	-	-	-	-	-	-
POAB80	-	-	-	-	-	-	-	-	-	-	-	-
PP0596	-	11.1	11.9	24.8	-	-	-	10.3	-	-	-	-

4.1.4 "Reverse" TTC-based screening assay

With a slight modification of the setup for the TTC-based screening assay compared to the published procedure (see publication I, chapter 3.1) the application of the assay could be expanded. Using chiral 2-hydroxy ketones as substrates this assay allows also a screening for stereoselectivity on the one hand and on the other hand a reliable screening with instable substrates (like HPP, see chapter 4.1.2) was feasible. The reductive amination catalysed by transaminases is in general a reversible reaction. As a consequence, it is possible to screen not only for the forward but also for the reverse reaction. In contrast to the typical setup where an 2-amino alcohol is produced from a 2-hydroxy ketone, the amino alcohols are used as substrates in the "reverse TTC-assay" (scheme 4-2). Therewith the conversion refers to deamination of the 2-amino alcohol. The corresponding 2-hydroxy ketones can be detected analogously (chapter 3.1). As a consequence an amine acceptor is required for the reaction. For ω-transaminase reaction with alanine as an amine donor (yielding pyruvate) the thermodynamic equilibrium is known to be on the substrate (alanine) side (chapter 1.4.3.5). By using pyruvate as an amine acceptor in the reverse reaction, this disadvantage was turned into an advantage. Therefore, pyruvate is recommended as a suitable amine acceptor in the "reverse" TTC-assay setup.

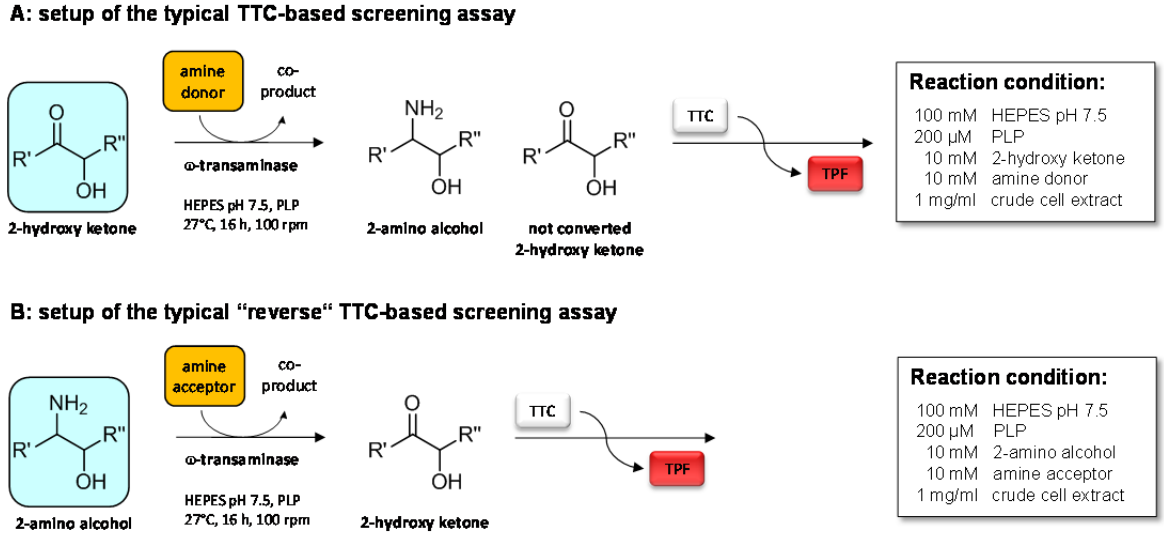

Scheme 4-2: Classical and "reverse" TTC-based screening assay for ω-transaminases.

In contrast to the typical TTC-assay (A), in the "reverse" setup (B) amino alcohols are used as substrates for the reaction. With an amine acceptor (e.g. pyruvate) the corresponding 2-hydroxy ketone is produced in the reductive amination reaction. Using the same colouration parameters as for the typical setup (publication I, chapter 3.1), the 2-hydroxy ketone can be quantified.

4.1.4.1 Application of the "reverse" TTC-assay to screen for enzyme stereoselectivity

Later in the project, we got access to seven (*R*)-selective ω-transaminases provided by the company Enzymicals AG (Greifswald, Germany) and to the putatively (*R*)-selective double variant CV2025-F88A/A231F (see chapter 1.5.5.3) by Prof. Per Berglund (KTH Stockholm, Sweden). The "reverse" setup of the TTC-assay was applied to determine enzyme stereoselectivity for the nor(pseudo)ephedrine synthesis. Here, (1*R*,2*R*)-norpseudoephedrine and (1*R*,2*S*)-norephedrine were used in independent reaction setups as substrates for the oxidative deamination in combination with the amine acceptor pyruvate. Conversion of the deamination of nor(pseudo)ephedrine was detected by following the formation of PAC using the TTC-assay. The idea behind was that a highly (*R*)-selective enzyme would only accept (1*R*,2*R*)-norpseudoephedrine. In contrast, conversion with a highly (*S*)-selective transaminase would only be detectable with (1*R*,2*S*)-norephedrine as a substrate. Thus, a comparison of the conversion values for one or the other substrate stereoisomer allowed estimation of the enzyme stereoselectivity (scheme 4-3).

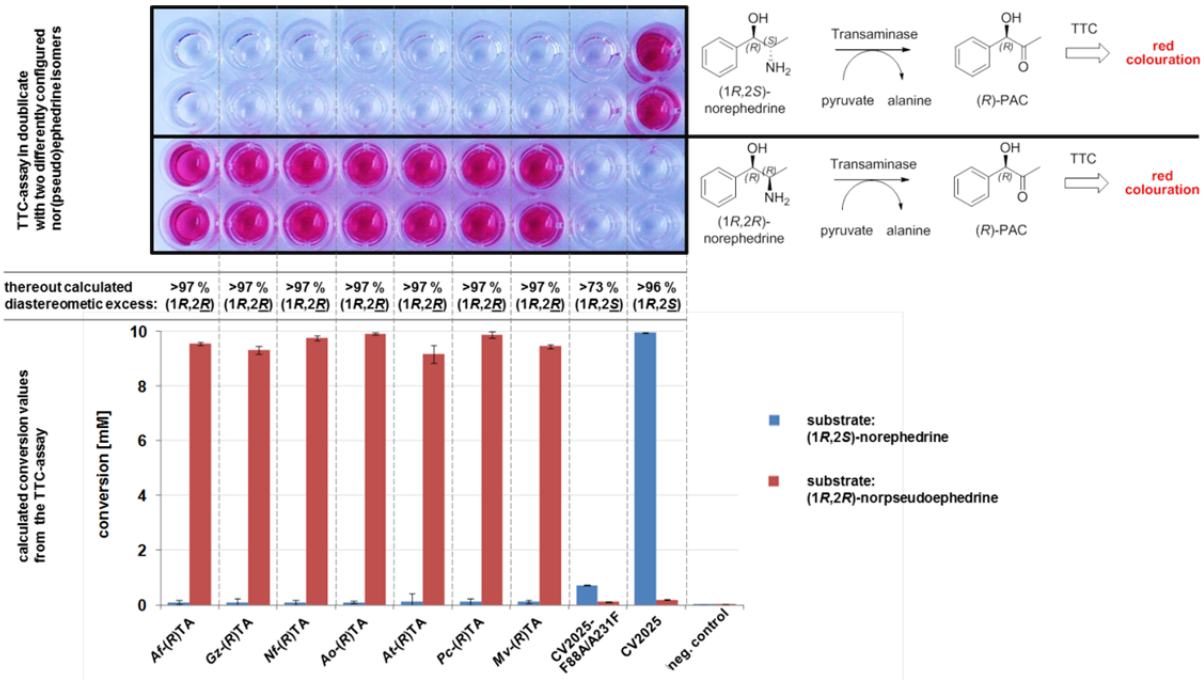

Scheme 4-3: "Reverse" TTC-assay for screening of ω-transaminase stereoselectivities with (*R*)- and (*S*)-configured amine groups of nor(pseudo)ephedrine.

reaction condition: 10 mM (1*R*,2*R*)-norpseudoephedrine or (1*R*,2*S*)-norephedrine were incubated with 10 mM pyruvate in 100 mM HEPES buffer (pH 7.5, containing 200 µM PLP) and 1 mg mL^{-1} crude cell extract in closed 96-well plate at 27 °C and 100 rpm for 16 h. Conversion values (given as % of 2-hydroxy ketone formation) were determined relative to an internal calibration curve at 510 nm after colouration with TTC-colouration (publication I, chapter 3.1). Information on enzymes can be found in chapter 1.5.5.3.

negative control: 1 mg mL^{-1} clarified crude cell extract of *E. coli* BL21(DE3) transformed with an empty plasmid (pET-29a)

"theoretical" *de*: calculated from conversion values of both stereoisomers in the reverse synthesis direction.

The results for this “reverse” TTC-assay indicate that all enzymes of the toolbox provided by Enzymicals AG are highly (*R*)-selective for nor(pseudo)ephedrines (scheme 4-3). Here, the concentration of PAC, generated from (1*R*,2*S*)-norephedrine, is in all cases lower than 2 % (which is at the detection limit of this assay setup). In contrast to this, conversion values higher than 90 % were obtained with (1*R*,2*R*)-norpseudoephedrine. This can be taken as a hint for a high stereoselectivity of these enzymes, which was additionally confirmed by instrumental analysis. Calculated “theoretical” *de* values for the reverse (synthesis) direction were >97 %. The respective results for the CV2025 variant F88A/A231F indicated that the enzyme is more (*S*)- than (*R*)-selective for the tested substrates. As a control for this reverse TTC-assay, the ω-transaminase CV2025 was used, since the enzyme is known to be highly (*S*)-selective. The results point out that a very high selectivity for the synthesis of (1*R*,2*S*)-norephedrine can be expected with CV2025 (“theoretical” *de* >96 %). This fits well to respective GC data, demonstrating a selectivity >99 % for the (*S*)-selective reductive amination of PAC catalysed by CV2025 (see chapter 3.2).
In general these data underline that the “reverse” TTC-assay mode is a useful tool for the screening of ω-transaminase libraries not only towards activities, but as well towards stereoselectivities.

4.1.4.2 Application of the “reverse” TTC-assay for instable 2-hydroxy ketones

As mentioned above (see chapter 4.1.2), substrate instability can disturb the general reliability of the screening assay. An isomerisation of HPP to its regioisomer PAC caused false-positive signals due to a higher colouration rate of PAC compared to HPP. Also this problem could be overcome by “reverse” TTC-assay. The respective product from the reductive amination of HPP is 1-amino-1-phenylpropane-2-ol (APP). This 2-amino alcohol was stable under the tested conditions and was therefore used as substrate in the “reverse” TTC-assay setup (scheme 4-4).

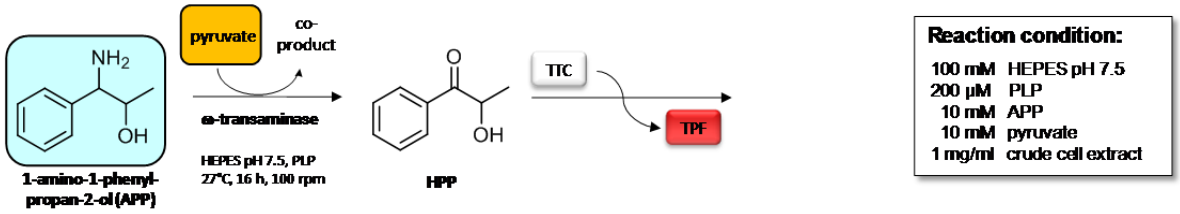

Scheme 4-4: "Reverse" TTC screening assay for instable 2-hydroxy ketones (here HPP).

reaction condition: 10 mM (1*R*,2*R*)-1-amino-1-phenylpropane-2-ol (*ee* ~80 %) were incubated with 10 mM pyruvate in 100 mM HEPES buffer (pH 7.5, containing 200 µM PLP) and 1 mg mL^{-1} crude cell extract (here CV2025) in closed 96-well plate at 27 °C and 100 rpm for 16 h. Conversion values (given as % of 2-hydroxy ketone synthesis) were determined relative to an internal calibration curve at 510 nm after TTC-colouration would be possible (here only uses as a yes-no answer). Colouration procedure see publication I (chapter 3.1)

negative control: 1 mg mL^{-1} clarified crude cell extract of *E. coli* BL21(DE3) transformed with an empty plasmid (pET-29a)

Since APP was not commercially available, (1*R*,2*R*)-APP was chemically synthesised with an *ee* ~80 % (detail information for the synthesis procedure see appendix). As a consequence of the low optical purity, this APP-batch could be used to screen for both, (*S*)- and (*R*)-selective ω-transaminases. The product of this oxidative amination reaction is HPP, which can be detected by the TTC-assay. Due to the chemical isomerisation of HPP to the regioisomer PAC, a precise determination of conversion values is not recommended, but the application as a yes-no answer is compared to the normal assay mode reliable in this setup.

So far, this assay setup was tested as a first proof of principle only with the (*S*)-selective ω-transaminase CV2025. Here, the colouration after TTC-addition was below the significant conversion detection limit of <2 %. These results were validated by GC for the synthesis of APP from HPP (see chapter 4.1.3), indicating that neither HPP nor APP are accepted by CV2025 substrates. However, this reaction setup provides a highly reliable, rapid and easy to handle screening assay, which is now available for the screening of large variant libraries for future applications.

4.1.5 Summary TTC-based screening assay for ω-transaminases

The TTC-based screening assay is a novel tool to expand the ω-transaminase toolbox. It can be applied for all 2-hydroxy ketones which react with the TTC-reagent to give a quantifiable colour response. The assay is fast, highly reliable and can be used to measure conversion curves. Moreover, it was demonstrated in this thesis, that the whole assay procedure could be fully automated (reaction setup, incubation, TTC-colouration and photometrical readout) can be performed with a Tecan Infinite

M1000 robotic system. By a modification of the assay setup (“reverse” TTC-assay), it was possible to use the assay to screen for stereoselectivity. With the same setup, the limitation caused by instable 2-hydroxy ketone substrates was overcome. One of the major advantages compared to all other published screening assay (see chapter 1.4.3.3) is that the amine donor may be varied. So far, none of the amine donors tested influenced the assay properties significantly.

Table 4-3: Advantages and limitations of the TTC-based screening assay for the detection of reductive amination by ω-transaminases

advantages	Limitation
+ absolute conversion values (not only initial rate activities) + inexpensive and rapid method + suitable for 96-well plates + reproducible within an error range of 5-10 % + time-depended conversion curves + different donor-acceptor/hydroxy ketone ratios ++ crude cell extracts & pure enzyme ++ fully automatable +++ independent of the amine donor +++ screening for stereoselectivity possible +++ reverse mode for instable 2-hydroxy ketones	- “TTC-active” compound required - error range makes cut-off for significant conversion values necessary in the “normal” mode - substrate instability might cause false positive screening hits => validation of screening results => “reverse” mode can overcome these limitations

Using this assay, we were able to identify enzymes catalysing the reductive amination of 2-hydroxy ketones like PAC, 2-HAP and acetoin. Moreover, the substrate range of amine donors was investigated.

It should be noted that the assay has also been considered as useful by other groups as could be deduced from recent presentations of the ACIB GmbH (Graz, Austria; talk on 1st ω-transaminases conference 2013, Stockholm, Sweden) and Prof. Per Berglund and co-workers (talk on the conference BioTrans 2013, Manchester, GB). With the help of this assay, the ACIB GmbH could e.g. identify a novel ω-transaminases which accepts bulky-bulky residues. This application highlights the high potential of this assay to enlarge the toolbox of ω-transaminase as versatile industrial biocatalysts in the future.

4.2 Combining lyases and ω-transaminases for the synthesis of nor(pseudo)ephedrines in two steps (strategy 1)

Another major tasks of this thesis was the investigation of the 2-step reaction for nor(pseudo)ephedrines combining ThDP-dependent lyases and ω-transaminases (see chapter 1.5.4). Theoretically all stereoisomers are accessible in four different combination of (*S*)- and (*R*)-selective enzymes in both reaction steps (scheme 4-5, strategy 1 A-D).

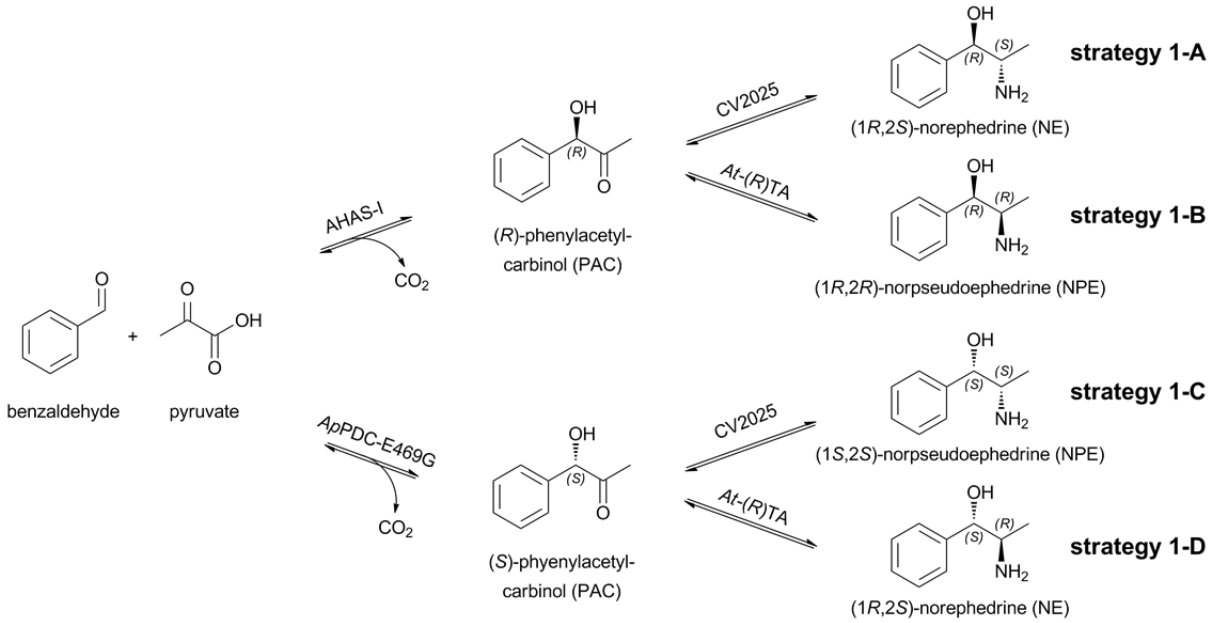

Scheme 4-5: 2-Step cascades for the synthesis of nor(pseudo)ephedrines combining ThDP-dependent enzymes and ω-transaminases. In the first reaction step (carboligation) either an (*R*)- (AHAS-I) or (*S*)-selective (*Ap*PDC-E469G) results in the formation of (*R*)- or (*S*)-PAC, respectively. In the second (reductive amination) step, nor(pseudo)-ephedrines are accessible in different configuration by either an (*R*)- (*At*-(*R*)TA) or (*S*)-selective (CV2925) ω-transaminases. Theoretically all isomers are accessible via four different routes (strategy 1 A-D).

As mentioned above, PAC is an intermediate of the first reaction step from which a reductive amination will lead to the desired products. As was deduced from results obtained with the TTC-assay, the enzyme CV2025 showed most promising properties for the synthesis of nor(pseudo)ephedrine among the toolbox of available (*S*)-selective ω-transaminases (chapter 1.5.5.3). Using this enzyme, conversions of PAC >95 % were detected using (*S*)-α-methylbenzylamine as an amine donor. In contrast to this, all enzymes of the (*R*)-selective toolbox from the Enzymicals AG showed similarly high conversion values and excellent stereoselectivities (publication II, chapter 3.2). As a consequence, all of these enzymes were further investigated concerning their properties in the 2-step synthesis.

4.2.1 2-Step synthesis of (1*R*,2*S*)-norephedrine with α-methylbenzylamine as amine donor (strategy 1-A)

The synthesis of (1*R*,2*S*)-norephedrine can be performed in two biocatalytic steps by combining the (*R*)-selective acetohydroxyacid synthase I (AHAS-I, chapter 1.5.5.1) for the carboligation step and the (*S*)-selective ω-transaminase CV2025 (also referred to as *Cv*-(*S*)TA, chapter 1.5.5.3) for the reductive amination reaction (scheme 4-5, strategy 1-A).

Finding a compromise for reaction parameters in 1-pot cascade reactions:

If two reactions are performed in one reaction pot, a compromise in terms of reaction parameter needs to be found for an optimal reaction process. The carboligation reaction was known to be highly enantioselective ($ee_{(R)\text{-PAC}}$ >98 %) and relatively fast (>3 U $mg^{1}_{purified\ enzyme}$) if benzaldehyde and pyruvate are used as substrates.[179] The initial rate activity for the reductive amination of (*R*)-PAC with (*S*)-α-methylbenzylamine catalysed by CV2025 was determined as ~0.06 U mg^{-1} (100 mM HEPES pH 7.5, 200 µM PLP, 30 °C - publication II, chapter 3.2). The differences in reaction velocities suggested that the transaminase rather than the AHAS-I-catalysed reaction would be rate limiting in a 2-step reaction cascade. Therefore, the cascade was performed under optimal reaction parameters for the reductive amination reaction as known from literature for the enzyme CV2025 (see chapter 1.5.5.3). Under analogous reaction conditions (100 mM HEPES pH 7.5, 200 µM PLP, 100 µM ThDP, 50 µM FAD, 5 mM $MgSO_4$, 30 °C), the carboligase activity of AHAS-I was still >1.5 U $mg^{-1}_{purified\ enzyme}$, using 10 mM benzaldehyde and 10 mM pyruvate as substrates (publication II, chapter 3.2).

2-step cascade combining of AHAS-I and CV2025 as purified enzyme:

As mentioned in chapter 1.6.1, there are different options to perform 2-step reaction cascades. In a 2-pot 2-step reaction (scheme 4-6-A), the intermediate (*R*)-PAC was isolated and purified after the first reaction step by flash chromatography. Although high conversion was observed in the carboligation step (>95 %) as well as in the reductive amination step (~97 %), the isolation of the intermediate reduced the overall conversion to ~85 %.

In a 1-pot 2-step simultaneous cascade (scheme 4-6-B), both enzymes were added at the same time. Here, an isolation of the reaction intermediate was not necessary. However, the overall conversion towards (1*R*,2*S*)-norephedrine was with 7 % significantly lower. In this setup, not the targeted norephedrine but benzylamine was detected as the main product (>90 %). These results suggested that benzylamine is produced in a competitive side reaction (reductive amination of benzaldehyde) by the ω-transaminase CV2025. Further investigation pointed out (publication II, chapter 3.2) that the adverse product/by-product ratio is caused by a difference in reaction velocities for PAC (~0.06 U mg^{-1}) and benzaldehyde (~1 U mg^{-1}) of the ω-transaminase CV2025.

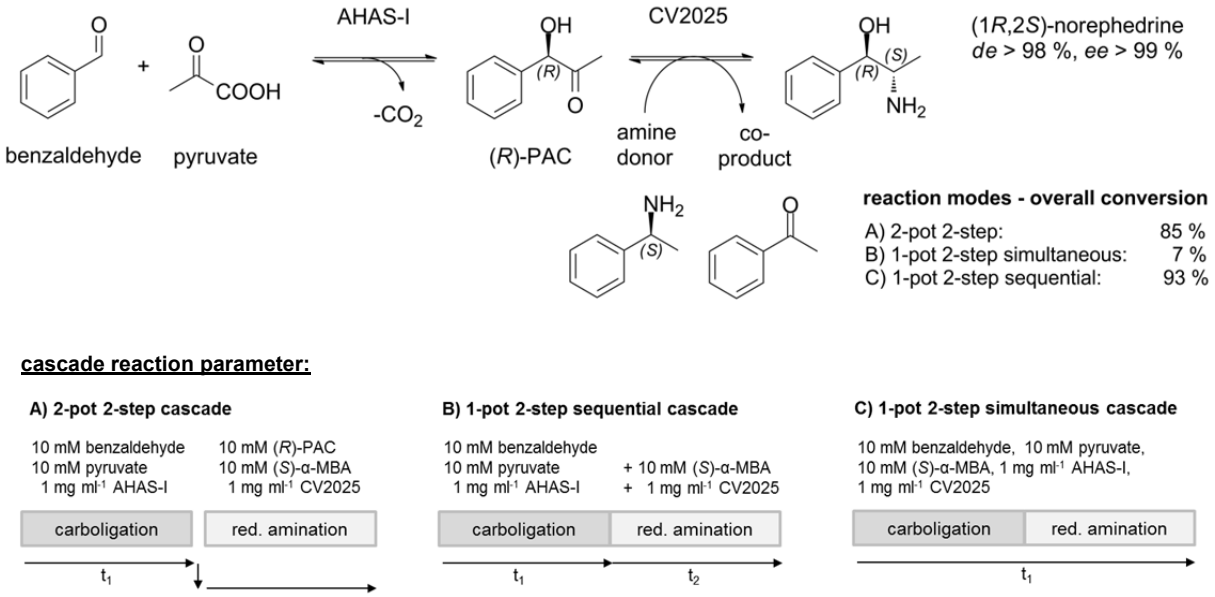

Scheme 4-6: Different reaction modes (A-C) for the 2-step cascades towards (1*R*,2*S*)-norephedrine combining the acetohydroxyacid synthase I and the ω-transaminases CV2025 with (*S*)-α-methylbenzylamine (MBA) as amine donor.

2-pot 2-step cascade (A): Carboligation was performed in 100 mM HEPES (pH 7.5) with 100 µM ThDP, 50 µM FAD and 5 mM $MgSO_4$ at 30 °C in 10 mL reaction volume with stirrer mixing (100 rpm) for 12 h (t_1). (*R*)-PAC (*ee*>98 %) was isolated (extracted three times with ethyl acetate; dried over $MgSO_4$; solvent evaporated under reduced pressure) and purified (flash chromatography with ethylacetate:petrol ether = 85:15). The yield of this step was 85 %. Reductive amination was performed in 100 mM HEPES (pH 7.5) and 200 µM PLP in a volume of 2 mL at 27 °C and 200 rpm shaking in 2.5 mL glass vials for 16 h (t_2).

1-pot 2-step cascades (B, C): were performed in 100 mM HEPES (pH 7.5) with 200 µM PLP, 100 µM ThDP, 50 µM FAD and 5 mM $MgSO_4$ at 30 °C in 2 mL reaction volume in 2.5 mL closed glass vials. Reaction times for the sequential mode (B) was: t_1 = 2 h, t_2 = 12 h and for the simultaneous mode: t_1 = 16 h.

By performing the 1-pot 2-step reaction as a sequential cascade (scheme 4-6-C), the by-product formation was overcome by adding the ω-transaminase after the carboligation step (conversion: >95 %), when benzaldehyde was already almost completely converted to PAC. As a result the benzylamine formation was reduced to <5 % and ~93 % of the benzaldehyde were finally converted to (1*R*,2*S*)-norephedrine. In all cascade modes the product (1*R*,2*S*)-norephedrine was obtained in high optical purity of >99 % *ee* and >98 % *de* (scheme 4-6).

2-step cascade combining AHAS-I and CV2025 lyophilised whole cells:

Since the cascade was demonstrated successfully with purified lyophilised enzymes, the application of lyophilised whole cells (LWC) for both reaction steps was subsequently investigated (publication II, chapter 3.3). Whole cells offer the potential to reduce catalyst production costs by a factor of 10 compared to purified enzymes.[217] The specific activity of AHAS-I for the formation of (*R*)-PAC from benzaldehyde and pyruvate is ~1.5 U $mg^{-1}_{purified\ enzyme}$. 1 mg purified AHAS-I equals to 5 mg mL^{-1} lyophilised recombinant *E. coli* cells. In both cases a complete conversion of 10 mM benzaldehyde was reached within 1 h reaction time (publication III, chapter 3.3). A similar trend was observed for the reductive amination of (*R*)-PAC. Reactions with 1 mg mL^{-1} purified CV2025 showed an analogous conversion curve as reactions with 5 mg mL^{-1} lyophilised whole cells (publication III, chapter 3.3). Within 3 h a conversion of ~85 % (1*R*,2*S*)-norephedrine was reached with whole cells, corresponding to a space-time yield of ~10 g L^{-1} d^{-1}. In general, this clearly demonstrates that whole cells can be a valuable alternative for a cost and time efficient production of (1*R*,2*S*)-norephedrine.

4.2.2 2-Step synthesis of nor(pseudo)ephedrines with alanine as amine donor

In the previous chapter the enzymatic synthesis of (1*R*,2*S*)-norephedrine in two reaction steps from inexpensive achiral starting was demonstrated. Although the product was obtained with good conversion and high stereoselectivity (>99 % *ee* and >98 % *de*), the major drawback of this cascade setup was the necessity to separate the co-product and especially the residual amine donor from the desired product. Due to the structural similarity of (*S*)-α-methylbenzylamine and (1*R*,2*S*)-norephedrine, a chromatographic separation with MeOH/$CHCl_3$ = 1:1 was necessary.

4.2.2.1 The challenge of alanine as an amine donor

As was identified by the TTC-assay, other amine donors can be used for the reductive amination of PAC which might in general provide an easier downstream processing (chapter 4.1.2, table 4-2). In contrast to α-methylbenzylamine, which is known to be an amine donor with product favouring thermodynamics, other amine donors often show lower reaction equilibrium constants.[66, 68, 105] One example of a frequently used amine donor with benefits in terms of low product/substrate inhibition, but poor reaction thermodynamics is alanine. In order to make alanine as amine donor in ω-transaminase reactions applicable, several methods have been developed to shift the reaction equilibrium towards the product (pyruvate) side.[66, 67]
The TTC-assay results showed that L-alanine is accepted by the enzyme CV2025 for the reductive amination of PAC (table 4-2; publication I). Conversions of ~20 % were observed with equimolar concentrations of both substrates (table 4-2; publication I). In contrast to this, only 5 % conversion was detected with purified CV2025 instead of crude cell extract (publication II, chapter 3.2). As known from literature, *E. coli* housekeeping proteins (e.g. alcohol dehydrogenase, lactate dehydrogenases, pyruvate dehydrogenases) can shift the reaction equilibrium in whole cells.[66]

Thermodynamic equilibrium constant for the reductive amination of PAC with alanine:
To investigate whether the reaction is limited by thermodynamics, the equilibrium constant for the reductive amination of (*R*)-PAC with L-alanine as an amine donor was determined according to the method of Tufvesson *et al.*[105] (scheme 4-7-A). A value of $K_{eq} = 2.31 \cdot 10^{-3}$ (scheme 4-7-A, publication II) clearly shows that the reaction

thermodynamic is on the substrate side of the reaction. As a consequence of the low equilibrium constant, a theoretical conversion of maximal ~5 % is possible with equimolar concentrations of PAC and alanine (scheme 4-7-B). A 5.000-fold excess of alanine would be required to achieve >90 % conversion (scheme 4-7-B). As summarised in chapter 1.4.3.5, chemical engineering, enzyme engineering and reaction engineering approaches are known to shift the reaction equilibrium towards the product side. Among these, enzyme-catalysed pyruvate removal is a frequently used method.[66, 82] Here, lactate dehydrogenases (LDH), pyruvate decarboxylases (PDC), acetolactate synthase (ALS), acetohydroxyacid synthase (AHAS) or amino acid dehydrogenases (AADH) can be added to remove the co-product pyruvate (chapter 1.4.3.5) and thus shift the reaction equilibrium to the product side. Although high conversions can be reached, the major drawback of this cascade setup is that at least one additional enzyme is needed (two in case of an additional cofactor regeneration step). Compared to reactions without an equilibrium shift, this increases the system complexity and moreover the process costs.

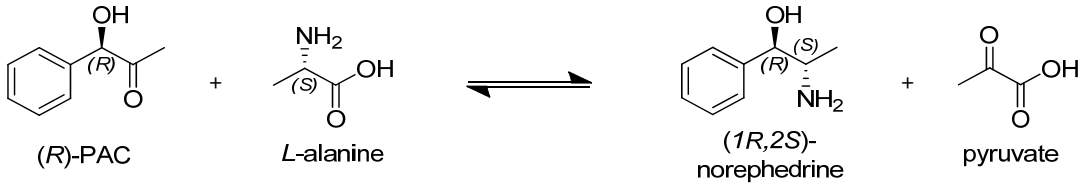

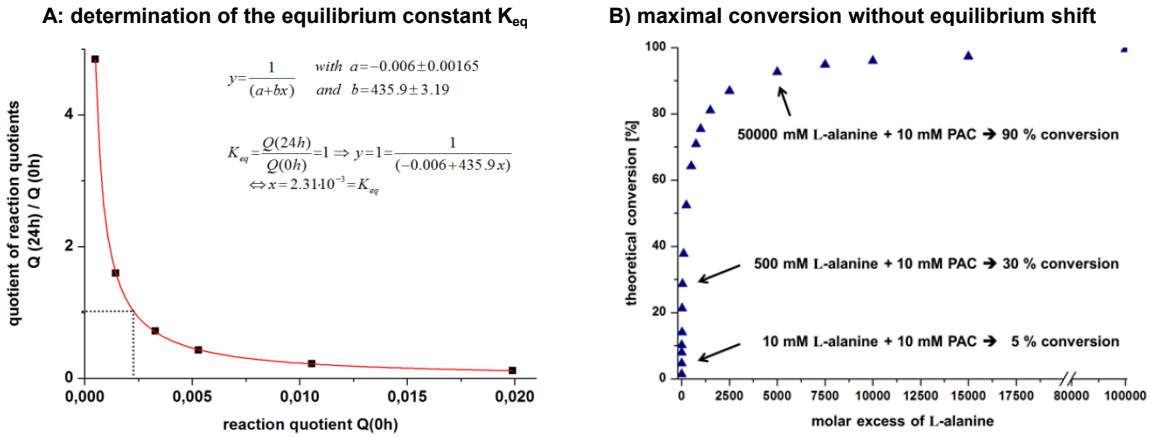

Scheme 4-7: Determination of the thermodynamic equilibrium for the reaction of (*R*)-PAC to (1*R*,2*S*)-norephedrine with alanine as an amine donor (A, left) and theoretical maximal conversion for this reaction without equilibrium shift (B, right). Reaction details and calculations can be found in the supporting information of publication II (chapter 3.2)

As described above, the 1-pot 2-step synthesis of (1*R*,2*S*)-norephedrine could be performed by the combination of an acetohydroxyacid synthase and an ω-transaminase. As known from literature, the AHAS-I from *E. coli* is not only able to catalyse the carboligation of (decarboxylated) pyruvate and benzaldehyde to PAC, but also the carboligation of two pyruvate molecules to acetolactate.[178, 179] If alanine is used as an amine donor in the reductive amination step, AHAS-I can catalyse the required reaction equilibrium shift for the transaminase step intrinsically as soon as pyruvate is produced. In the 1-pot 2-step cascade, the AHAS-I is already present in the reaction solution from the first reaction step. Thus, the equilibrium shift needed for the transaminase reaction in the second step of the cascade should be possible without addition of further enzymes, co-substrates or reagents.

To test this hypothesis, the system complexity was reduced in a first approach and the AHAS-I coupled equilibrium shift was studied only for the reductive amination step. As a first proof of principle, the reductive amination of 10 mM (*R*)-PAC was performed with CV2025 and 30 mM L-alanine in presence of AHAS-I (both enzymes: 0.5 mg mL^{-1} purified protein). Compared to a reaction without AHAS-I where only 5 % conversion could be achieved, the combination with AHAS-I increased the conversion to ~48 % (scheme 4-8), which clearly indicates a successful equilibrium shift (publication II, chapter 3.2).

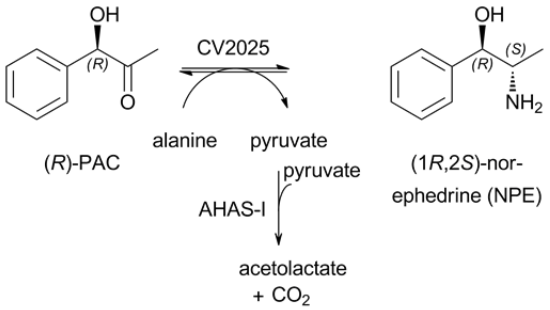

reductive amination with/without equilibrium shift

A) conversion without AHAS-I: ~5 %
B) conversion with AHAS-I: ~48 %

Scheme 4-8: AHAS-I coupled equilibrium shift for the CV2025-catalysed reductive amination of (*R*)-PAC with alanine as amine donor.

Reaction conditions: The reductive amination was performed with 10 mM (*R*)-PAC (*ee* 84 %) and 30 mM L-alanine 100 mM HEPES (pH 7.5) with 100 µM ThDP, 50 µM FAD and 5 mM $MgSO_4$ in a volume of 2 mL in 2.5 mL closed glass vials. 0.5 mg mL^{-1} CV2025 was added as purified enzyme without (A) or with 0.5 mg mL^{-1} AHAS-I (B). The reactions were incubated at 27 °C for 24 h.

4.2.2.2 Reaction parameter optimisation for AHAS-I coupled equilibrium shift of ω-transaminase reactions

To further improve the conversion of the reductive amination step via AHAS-I coupled equilibrium shift (see chapter 4.2.2.1, scheme 4-8), the reaction parameters like enzyme concentrations and amine donor/PAC ratio (scheme 4-9) or pH and temperature (scheme 4-10) were optimised.

Highest conversions for the reductive amination of (*R*)-PAC with alanine as amine donor and AHAS-I coupled equilibrium shift were achieved at pH 7.5, 25 °C with 1 mg mL^{-1} CV2025, 0.5 mg mL^{-1} AHAS-I and a 5-fold excess of L-alanine relative to the hydroxy ketone. Under these optimised cascade conditions 80 % of (*R*)-PAC was converted to (1*R*,2*S*)-norephedrine (publication II, chapter 3.2).

varied reaction parameter: AHAS-I concentration and PAC/alanine ratio

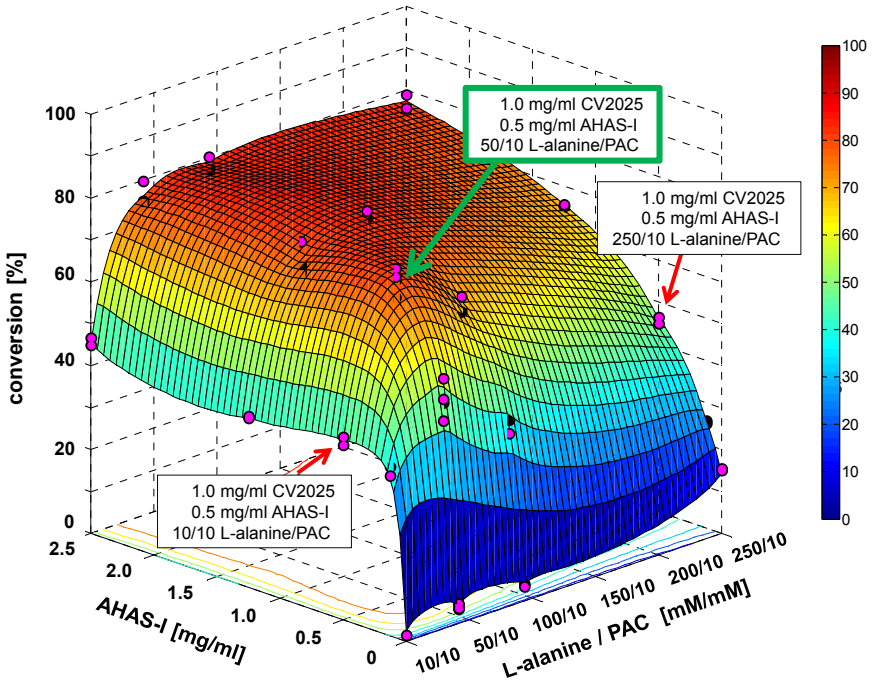

Scheme 4-9: Examples of the reaction parameter optimisation for the CV2025-catalysed reductive amination of (*R*)-PAC with AHAS-I coupled equilibrium shift (part 1).

Reaction conditions: constant parameters: 1 mg mL^{-1} CV2025, pH 7.5, 25 °C – varied parameter: AHAS-I concentration and PAC/alanine ratio. All reactions were performed in 100 mM HEPES containing 200 µM PLP, 50 µM FAD, 100 µM ThDP and 5 mM $MgCl_2$ and incubated for 20 h at different temperatures in 2.5 mL glass vials. For statistical data analysis and interpolation (pink dots) the 'kriging algorithm' (see publication II, chapter 3.2) was used.

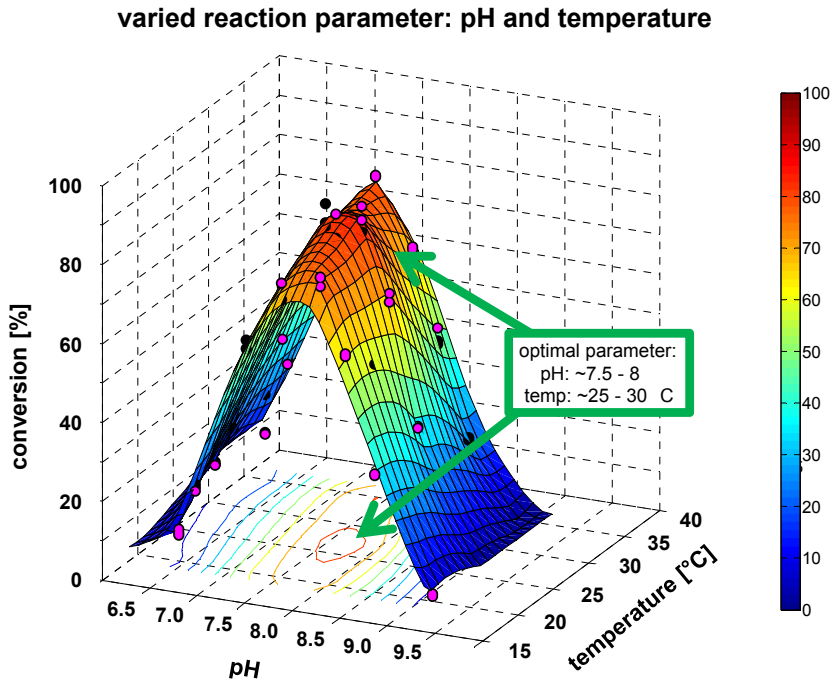

Scheme 4-10: Examples of the reaction parameter optimisation for the CV2025-catalysed reductive amination of (*R*)-PAC with AHAS-I coupled equilibrium shift (part 2).

Reaction conditions: constant parameters: 1 mg mL^{-1} CV2025, 0.5 mg mL^{-1} AHAS-I, 10 mM PAC, 50 mM L-alanine – varied parameters: pH and reaction temperature. All reactions were performed in 100 mM HEPES containing 200 µM PLP, 50 µM FAD, 100 µM ThDP and 5 mM $MgCl_2$ and incubated for 20 h at different temperatures in 2.5 mL glass vials. For statistical data analysis and interpolation (pink dots) the 'kriging algorithm' (see publication II, chapter 3.2) was used.

4.2.2.3 1-Pot 2-step cascade for the synthesis of (1*R*,2*S*)-norephedrine under optimised reaction conditions with alanine as amine donor (strategy 1-A)

With optimised reaction parameters for the reductive amination step (chapter 4.2.2.2), the 1-pot 2-step cascade for the synthesis of (1*R*,2*S*)-norephedrine was performed in the sequential and the simultaneous cascade mode (publication II, chapter 3.2). In the simultaneous reaction mode, where AHAS-I and CV2025 were added at once, only 2 % of the initial benzaldehyde was converted to the 2-amino alcohol (scheme 4-11-A). Similar to the cascade with (*S*)-α-methylbenzylamine (chapter 4.2.1) the major product was benzylamine, which was caused by fast reductive amination of benzaldehyde in a competitive side reaction. As pointed out earlier (chapter 2.2), this problem could be overcome by performing the cascade in a 1-pot 2-step sequential reaction mode (scheme 4-11-B), yielding an overall conversion of 78 % to the desired product (1*R*,2*S*)-norephedrine with a *de* >98 % and an *ee* >99 % (publication II, chapter 3.2).

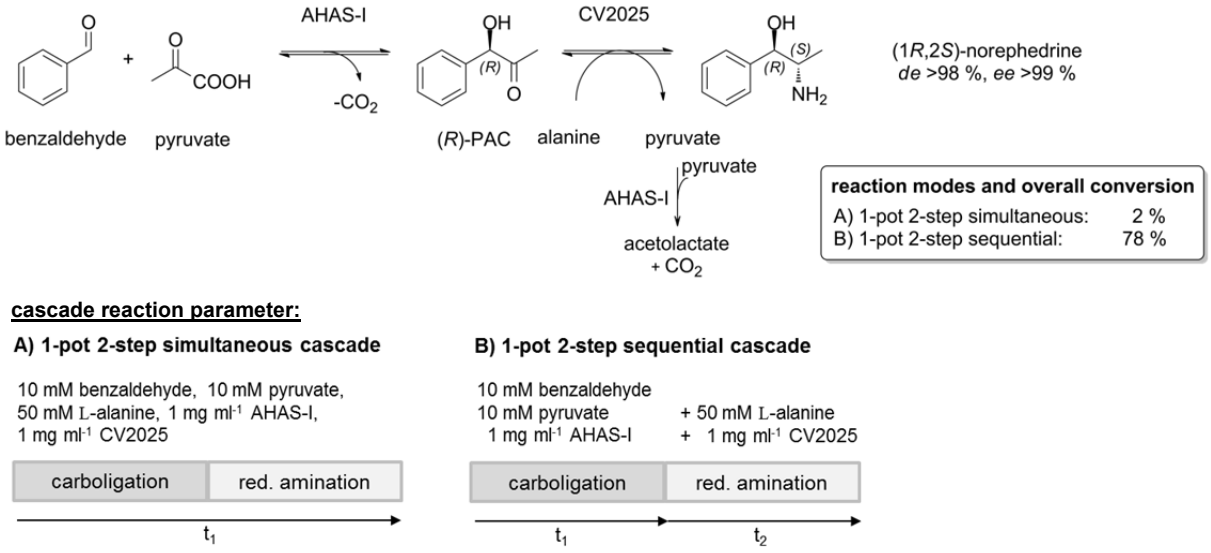

Scheme 4-11: 1-Pot 2-step cascade for the synthesis of (1*R*,2*S*)-norephedrine with alanine as amine donor. The 1-pot 2-step cascade combining the AHAS-I with the (*S*)-selective ω-transaminases CV2025 can be run in different cascade modes (see chapter 1.6.1): simultaneously (A) or sequentially (B). Further reaction details can be found in publication II (chapter 3.2).

4.2.2.4 1-Pot 2-step cascade for the synthesis of (1*R*,2*R*)-norpseudoephedrine under optimised reaction conditions with alanine as amine donor (strategy 1-B)

In contrast to the 2-step synthesis of (1*R*,2*S*)-norephedrine, the 1-pot 2-step cascade for the production of (1*R*,2*R*)-norpseudoephedrine requires a highly (*R*)-selective ω-transaminase (scheme 4-5, strategy 1-B). Since all enzymes of the (*R*)-selective toolbox (supplied by Enzymicals AG as lyophilised crude cell extracts, see chapter 1.5.5.3) showed very high conversions for the reductive amination of PAC in the TTC-assay (chapter 4.1.4.1), all ω-transaminase were investigated for the application in the 2-step cascade.

As a conclusion from the cascade results for the combination AHAS-I/CV2025 (chapter 4.2.1 and 4.2.2.3), the most challenging but still in general most efficient cascade mode (see chapter 1.6.1) is the 1-pot 2-step simultaneous cascade. Therefore, the application of all (*R*)-selective ω-transaminases was investigated in this simultaneous cascade mode (scheme 4-12) using the reaction parameters previously optimised for the combination of AHAS-I and CV2025 (chapter 4.2.2.2). Under these conditions, all (*R*)-selective ω-transaminases showed a significant

higher conversion in the simultaneous cascade mode than CV2025. Such high conversions resulted from a significantly lower benzylamine by-product formation (scheme 4-12). Surprisingly, without further reaction optimisation, conversions ≥85 % were detected for the combinations of AHAS-I with the transaminases *Pc*-(*R*)TA or *At*-(*R*)TA. Although the cascade was performed in a simultaneous mode, less than 10 % benzylamine was produced. To investigate this further, the initial rate activity for the reductive amination of PAC and benzaldehyde was measured independently for *At*-(*R*)TA. Compared to the initial reaction rates of CV2025, which was significantly higher for benzaldehyde compared to PAC), *At*-(*R*)TA showed an almost similar initial rate activity (~0.08-0.09 U mg^{-1}) for both amine acceptors (see publication II, chapter 3.2). These activity differences in combination with the high carboligase activity of AHAS-I (>1.5 U mg^{-1}) enables an efficient simultaneous 1-pot 2-step cascade with minimised by-product formation.

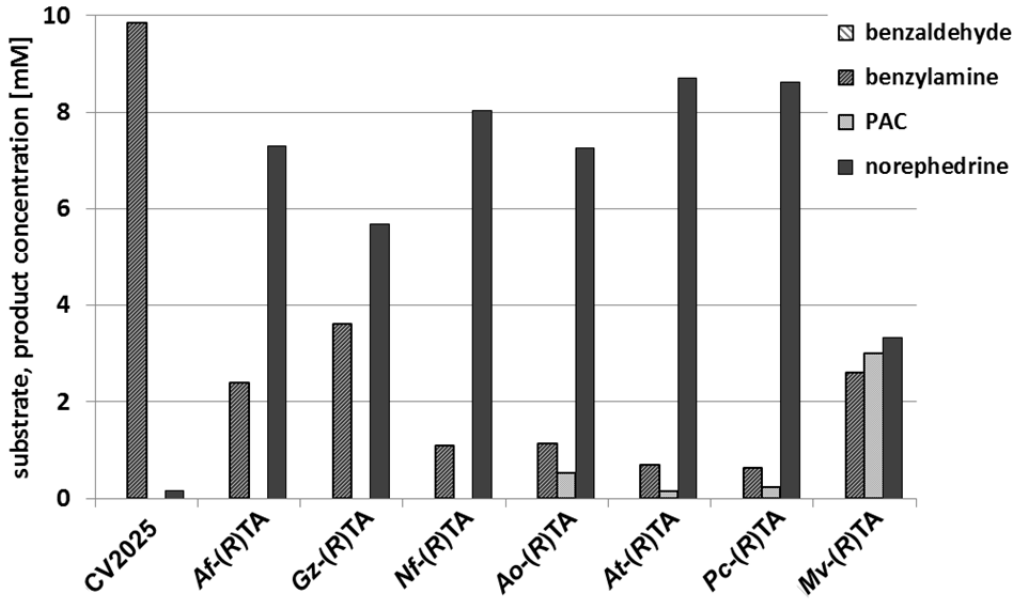

Scheme 4-12: 1-Pot 2-step simultaneous cascade for the synthesis of (1*R*,2*R*)-norpseudoephedrine combining AHAS-I and seven (*R*)-selective ω-transaminases.

Reaction conditions: For the 1-pot 2-step reaction 10 mM benzaldehyde, 10 mM pyruvate and 50 mM D- or L-alanine in 100 mM HEPES (pH 7.5 with 200 µM PLP, 50 µM FAD, 100 µM ThDP, 5 mM $MgCl_2$) were added simultaneously to both enzymes (AHAS-I: 0.5 mg mL^{-1} and ω-TA 1 mg mL^{-1}). Further reaction details can be found in publication II (chapter 3.2). The (*S*)-selective transaminase CV2025 was used as a control.

Based on these promising results, *At*-(*R*)TA was tested in combination with AHAS-I in the 1-pot 2-step sequential cascade mode. As a result 96 % of the initially added benzaldehyde were converted to (1*R*,2*R*)-norpseudoephedrine. The product was obtained with an excellent stereoselectivity (>98 % *de* and >99 % *ee*, scheme 4-13).

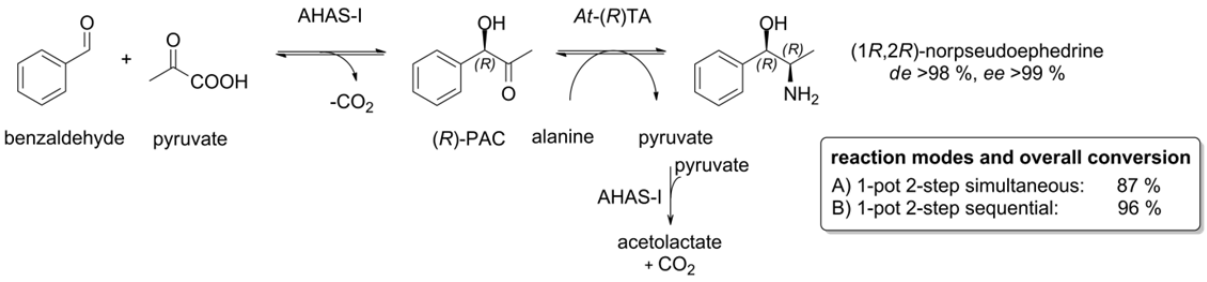

Scheme 4-13: 1-Pot 2-step cascade for the synthesis of (1*R*,2*R*)-norpseudoephedrine with alanine as amine donor. The 1-pot 2-step cascade combining the AHAS-I with the (*R*)-selective *At*-(*R*)TA can be run in different cascade modes (see chapter 1.6.1): simultaneously (A) or sequentially (B). Further reaction details can be found in publication II (chapter 3.2).

To increase the cascade efficiency further, the minimal amount of required enzyme for this 1-pot 2-step sequential cascade was determined. 0.5 mg mL^{-1} AHAS-I and 0.4 mg mL^{-1} *At*-(*R*)TA were sufficient to reach 95 % conversion of 20 mM benzaldehyde, 20 mM pyruvate with 100 mM D-alanine within 13.5 h (scheme 4-12). Compared to the non-optimised data, this corresponds to a reduction in catalyst load of 50 % for AHAS-I and of 80 % for the *At*-(*R*)TA.

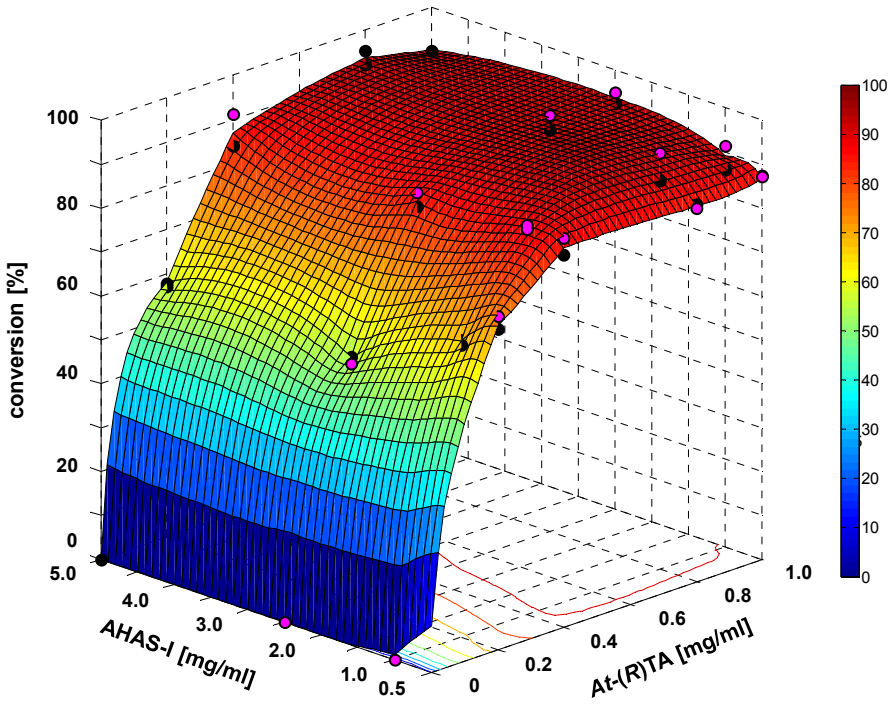

Scheme 4-14: Determination of minimal catalyst load for the 1-pot 2-step sequential cascade for the synthesis of (1*R*,2*R*)-norpseudoephedrine with of AHAS-I and *At*-(*R*)TA.

Reaction parameter: 20 mM benzaldehyde, 20 mM pyruvate and 100 mM D-alanine in 100 mM HEPES (pH 7.5 with 200 µM PLP, 50 µM FAD, 100 µM ThDP, 5 mM $MgCl_2$). In accordance to the initial reaction rates of AHAS-I (~1.5 U mg^{-1}, see chapter 4.2.1), *At*-(*R*)TA was added in 90 min after AHAS-I without isolation of the reaction intermediate (*R*)-PAC. The complete reaction was analysed after another 12 h as an endpoint determination (pink dots). Further reaction details can be found in publication III (chapter 3.3).

However, due to the low substrate concentrations the space-time-yields were with 5 g L^{-1} d^{-1} relatively low. To further increase the space-time-yield, the equimolar substrate concentration (benzaldehyde and pyruvate) wre increased to 25, 50, 75 and 100 mM. Under the optimised catalyst/substrate ratios (per mM benzaldehyde: 0.025 mg mL^{-1} AHAS-I, 0.02 mg mL^{-1} *At*-(*R*)TA, 2.5 mM D-alanine - scheme 4-15), more than 90 % conversion was detected even for substrate concentrations of up to 100 mM. Interestingly, even emulsion systems (>50 mM benzaldehyde) did not significantly reduce the reaction performance. Thereby ~90 mM of the product (1*R*,2*R*)-norpseudoephedrine were obtained within 13.5 h, corresponding to a 5-fold increased space-time-yield of ~26 g L^{-1} d^{-1} (publication III, chapter 3.3).

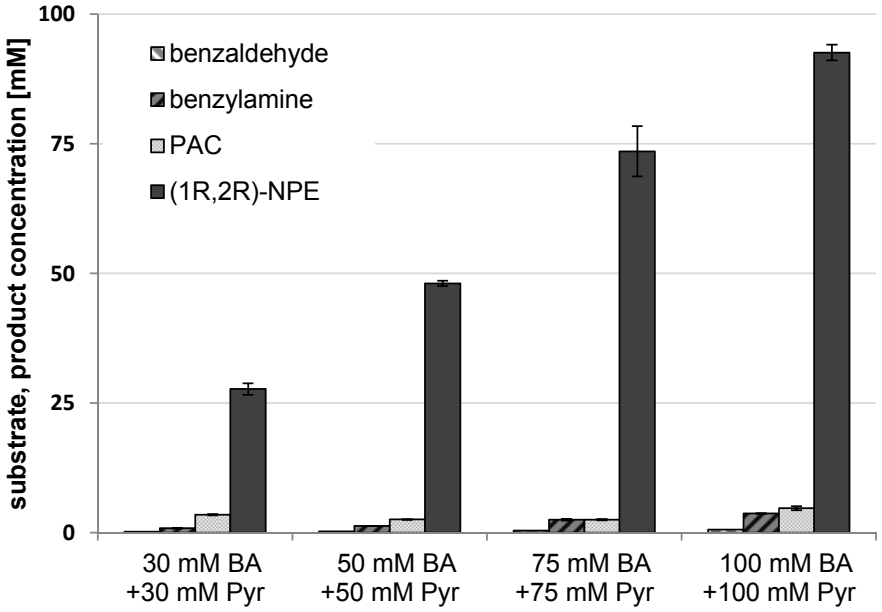

Scheme 4-15: 1-Pot 2-step sequential cascade for the synthesis of (1*R*,2*R*)-norpseudo-ephedrine with high substrate concentrations.

Reaction parameter: 1-Pot 2-step sequential cascade for the synthesis of (1*R*,2*R*)-NPE with 25, 50, 75 or 100 mM benzaldehyde (BA) and equimolar concentrations of pyruvate. In accordance to the optimisation date (scheme 4-14), per mM benzaldehyde 0.025 mg mL^{-1} AHAS-I were used and after 90 min reaction time 0.02 mg mL^{-1} *At*-(*R*)TA and 2.5 mM D-alanine was added per mM initial benzaldehyde concentration. The solution was analysed after another 12 h reaction time. Reaction parameter: 100 mM HEPES pH 7.5, 200 µM PLP, 50 µM FAD, 100 µM ThDP, 5 mM $MgCl_2$, 25 °C.

4.2.2.5 1-Pot 2-step recycling cascade for the synthesis of (1*R*,2*R*)-norpseudoephedrine and (1*R*,2*S*)-norephedrine with alanine as amine donor

In the 1-pot 2-step cascade with alanine as amine donor we demonstrated that a co-product removal (here: pyruvate) was possible without the addition of any further catalysts or reactants (chapter 4.2.2.3 and 4.2.2.4). However, acetolactate is accumulated as waste in the reaction mixture, which reduced the atom efficiency of the process.

To further increase the atom efficiency, a co-product recycling rather than a simple removal was investigated. Pyruvate, which accumulates in the second reaction step, is a substrate of the carboligation reaction in the first carboligation step. In general, there are two possible ways of pyruvate recycling for this cascade. One is a direct consumption of pyruvate by the AHAS-I, the other is a recycling via AHAS-I catalysed acetolactate cleavage. More precisely, in the acetolactate cleavage reaction one pyruvate molecule is released from the active site while the second one remains bound to the ThDP-cofactor as hydroxy-ethyl group and is thus directly available for the carboligation with benzaldehyde to PAC (see scheme 4-16).

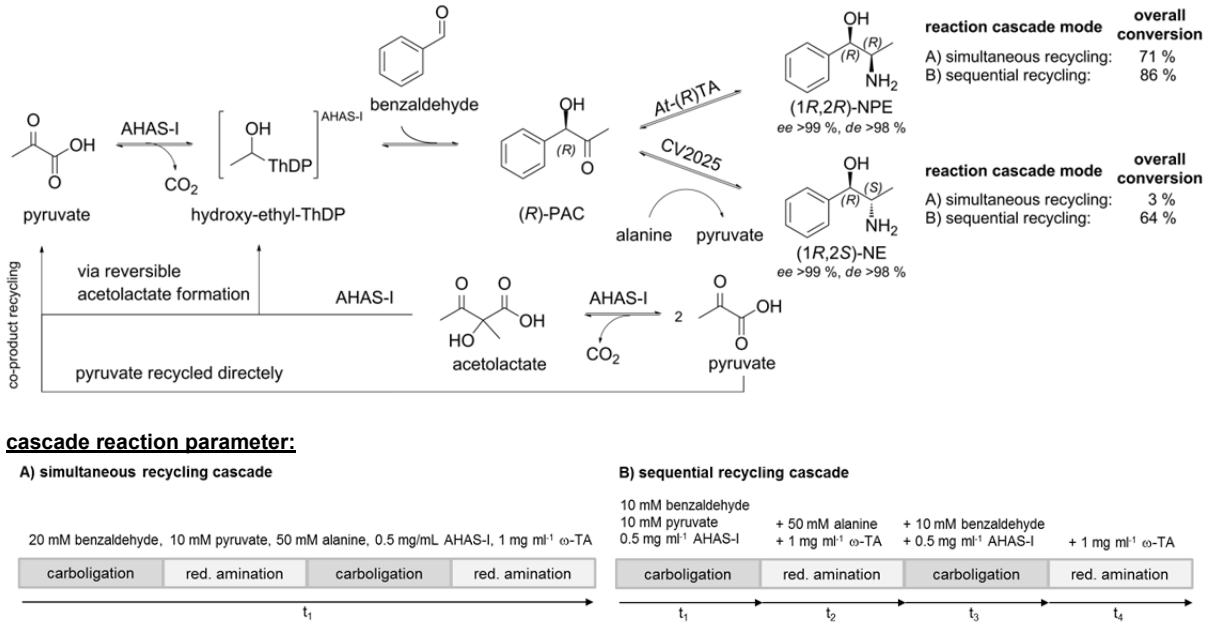

Scheme 4-16: 1-Pot 2-step recycling cascade for the synthesis of (1*R*,2*S*)-norephedrine and (1*R*,2*R*)-norpseudoephedrine with alanine as amine donor.

The cascade combines AHAS-I in the first step and either an (*S*)-selective (CV2025) or (*R*)-selective (*At*-(*R*)TA) ω-transaminases in the second step. Pyruvate, generated in the reductive amination step as a co-product, is used as substrate in the first reaction step and is recycled directly or via reversible acetolactate formation. The 1-pot 2-step cascade can be run in different cascade modes (see chapter 1.6.1): simultaneously (A) or sequentially (B). Further details can be found in publication II (chapter 3.2).

Also this novel recycling cascade could be performed in two different cascade modes. In the simultaneous mode (scheme 4-16-A) all catalysts and reactants were added at once, while in the sequential cascade mode (scheme 4-16-B) the transaminase was added after the carboligation step. Addition of additional benzaldehyde (but no further pyruvate) started the carboligation again. It was expected that with an excess of benzaldehyde (20 mM) relative to the initial pyruvate concentration (10 mM) conversions >10 mM could only be achieved in both cascade modes, if the pyruvate (generated as the co-product in the reductive amination step) is successfully recycled.

In line with the experimental data from the 1-pot 2-step cascade described in chapter 4.2.2.3, the combination AHAS-I/CV2025 in the simultaneous recycling cascade mode resulted in a low overall conversion of 3 % (scheme 4-16). As expected, most of the benzaldehyde (>95 %) was converted to benzylamine. In the sequential recycling cascade mode the by-product formation could significantly be reduced and 64 % (=12.8 mM) of the benzaldehyde was converted to (1*R*,2*S*)-norephedrine with high optical purity of >99 % *ee* and >98 % *de*.

By contrast, the combination AHAS-I/*At*-(*R*)TA resulted in both cascade modes in significantly higher conversions compared to the cascade with CV2025. As discussed previously (chapter 4.2.2.4) this is a consequence of the different reaction rates for reductive amination of benzaldehyde and pyruvate, which is equally fast for both substrates with *At*-(*R*)TA but much faster for benzaldehyde in case of CV2025. As a result, in the 1-pot 2-step simultaneous recycling cascade an overall conversion of 71 % (=14.2 mM) was obtained. However, the highest concentration was achieved in the sequential mode. Here 86 % (=17.2 mM) of the benzaldehyde was converted to (1*R*,2*R*)-norpseudoephedrine. The product was obtained as well in high optical purity of >99 % *ee* and >98 % *de*.

Compared to the already efficient method of co-product removal in the 1-pot 2-step sequential cascade, the ‘recycling cascade’ might help to increase the reaction efficiency in terms of atom economy and sustainability further. In the presented setup, the amount of pyruvate required for the 2-step synthesis could be reduced by 50 % compared to the simple 2-step sequential cascade (chapter 4.2.2.3 and 4.2.2.4). From the process point of view, the most valuable approach would be the simultaneous recycling cascade mode. However, highly selective catalysts with a low

by-product formation rate in all cascade steps are required. If such an enzyme is not available, the sequential (recycling) cascade mode offers a valuable alternative to reduce the amount of by-products. In general, this recycling approach is not limited to applications with ω-transaminases. The removal of co-products with a catalyst of another reaction step can be applied for any multi-reaction cascade where a smart combination of enzymes (or even chemical catalysts) is possible.

4.2.3 2-Step synthesis of (1*S*,2*S*)-norpseudoephedrine and (1*S*,2*R*)-norephedrine (strategy 1-C and 1-D)

For the synthesis of the two missing N(P)E stereoisomers, (1*S*,2*S*)-norpseudoephedrine and (1*S*,2*R*)-norephedrine, a highly (*S*)-selective lyase is required for the first reaction step (see scheme 4-5; strategy 1-C and 1-D). However, such a lyase is currently not available. The *Ap*PDC-E469G from *Acetobacter pasteurianus* is the enzyme with the highest selectivity for the synthesis of (*S*)-PAC.[175] Here, a whole cell biotransformation (40 mM benzaldehyde, 400 mM pyruvate, 2.5 mM $MgSO_4$, 100 mM potassium phosphate, 100 µM ThDP) resulted in formation of (*S*)-PAC with a good isolated yield of 95 % but an optical purity of only ~70 % *ee*.[184] Still, since it is the best variant, this enzyme was studied for the synthesis of (1*S*,2*S*)-norpseudoephedrine and (1*S*,2*R*)-norephedrine by combining it with either the (*R*)-selective *At*-(*R*)TA or the (*S*)-selective CV2025.

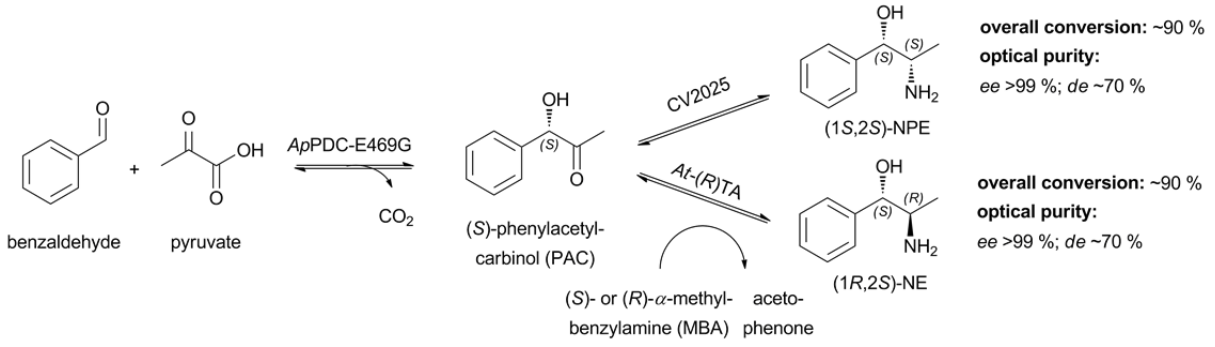

Scheme 4-17: 2-Pot 2-step synthesis of (1*S*,2*S*)-norpseudoephedrine and (1*S*,2*R*)-norephedrine combining an (*S*)-selective lyase (*Ap*PDC-E469G) in the first step with either an (*S*)-selective (CV2025) or (*R*)-selective (*At*-(*R*)TA) ω-transaminase in the second step. Further reaction details can be found in publication III (chapter 3.3).

Carboligation: 40 mM benzaldehyde, 400 mM pyruvate, 2.5 mM $MgSO_4$, 100 mM potassium phosphate, 100 µM ThDP. Incubated for 48 h in glass vials with 100 rpm magnetic stirring. The product was isolated by extraction (3x with ethyl acetate), dried over $MgSO_4$ and purified via flash chromatography (petrol ether : ethyl acetate = 90 : 10).[184]

Reductive amination: 10 mM (*S*)-PAC (*ee* 70 %) were incubated with 10 mM (*R*)- or (*S*)-α-methylbenzylamine in 100 mM HEPES (pH 7.5) with 200 µM PLP and 1 mg mL^{-1} CV2025 purified enzyme or 1 mg mL^{-1} *At*-(*R*)TA in closed glass vials for 24 h.

Since in this reaction a high pyruvate concentration (400 mM) was used for the carboligation step, the cascade was not performed in a 1-pot mode. Here, a by-product, caused in the reaction of pyruvate to alanine, was avoided by a 2-pot 2-step mode (see chapter 1.6.1). As a consequence, the advantage of an internal co-product removal is not possible. Thus, methylbenzylamine and was used as an amine donor instead of alanine. The reductive amination of isolated (*S*)-PAC with (*R*)- or (*S*)-α-methylbenzylamine, respectively, resulted in both cascades in the desired products (1*S*,2*R*)-norephedrine (with *At*-(*R*)TA) and (1*S*,2*S*)-norpseudoephedrine (with CV2025) with conversions >95 %. Due to the high stereoselectivity of both transaminases both products were obtained with high *ee* (>99 %). However, due to the initially low optical purity of the (*S*)-PAC the resulting diastereomeric excess was only ~70 %. It can be concluded that (*S*)-PAC is accepted by the transaminases, but higher purity of this intermediate is needed in order to obtain the amino alcohols in high optical purities.

As a consequence, a protocol for the synthesis of (*S*)-PAC in high enantiomeric excess will be target of future investigations. Here, further enzyme engineering of the *Acetobacter pasteurianus* PDC may improve stereoselectivity. If this is not suitable, chiral enrichment technologies like chiral chromatographic methods or kinetic resolution can be used. As a proof of principle, the so called “chiral polishing” of (*S*)-PAC (scheme 4-18) with the (*R*)-selective benzaldehyde lyase (BAL) from *Pseudomonas fluorescens* was described in the thesis of A.G. Baraibar[184] and in the invention disclosure I [214]. Here, (*S*)-PAC could be enriched to an *ee* >97 %. However, this “chiral polishing” reaction was only performed on analytical scale.

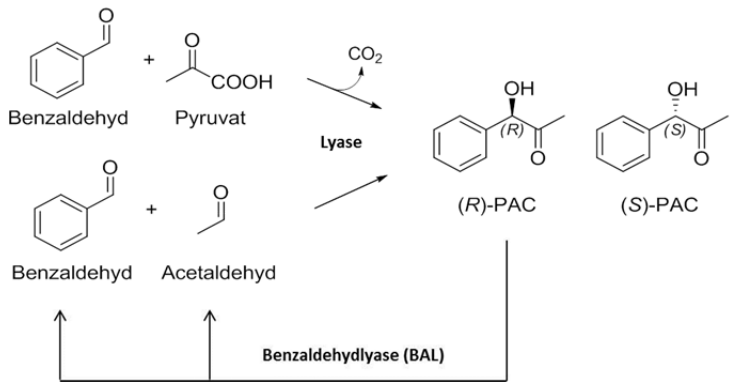

Scheme 4-18: The concept for “chiral polishing” of (*S*)-PAC to gain high optical purities.
(*S*)-PAC with a low optical purity generated by catalysis of a lyase (e.g. by *Ap*PDC-E469G) can be converted to highly pure (*S*)-PAC with an *ee* >97 % by the highly (*R*)-selective *Pf*BAL.[184, 214]

4.3 Combining ω-transaminases and alcohol dehydrogenases for the synthesis of nor(pseudo)ephedrines in two steps (strategy 2)

To overcome the required chiral purification effort in the syntheses of (1*S*,2*S*)-norpseudoephedrine (NPE) and (1*S*,2*R*)-norephedrine (NE), an alternative synthetic strategy was investigated (see chapter 1.5.4). Starting from 1-phenylpropane-1,2-dione (PPDO), the combination of a highly selective biotransformation with an ω-transaminases (TA, chapter 1.5.5.3) in the first reaction step and alcohol dehydrogenases (ADH, chapter 1.5.5.2) in the second step was expected to give access to all nor(pseudo)ephedrine isomers. Combination of the (*S*)-selective ω-transaminase CV2025 with the (*S*)-selective *Lb*ADH (from *Lactobacillus brevis*) should result in (1*S*,2*S*)-NPE (scheme 4-19; strategy 2-A), while the combination with the (*R*)-selective *R*ADH (from *Ralstonia* sp.) would give access to (1*R*,2*S*)-NE (scheme 4-19; strategy 2-B). Further, the (*R*)-selective *At*-(*R*)TA in combination with the same set of alcohol dehydrogenases would lead to (1*S*,2*R*)-NE and (1*R*,2*R*)-NPE (scheme 4-19; strategy 2-C and 2-D).

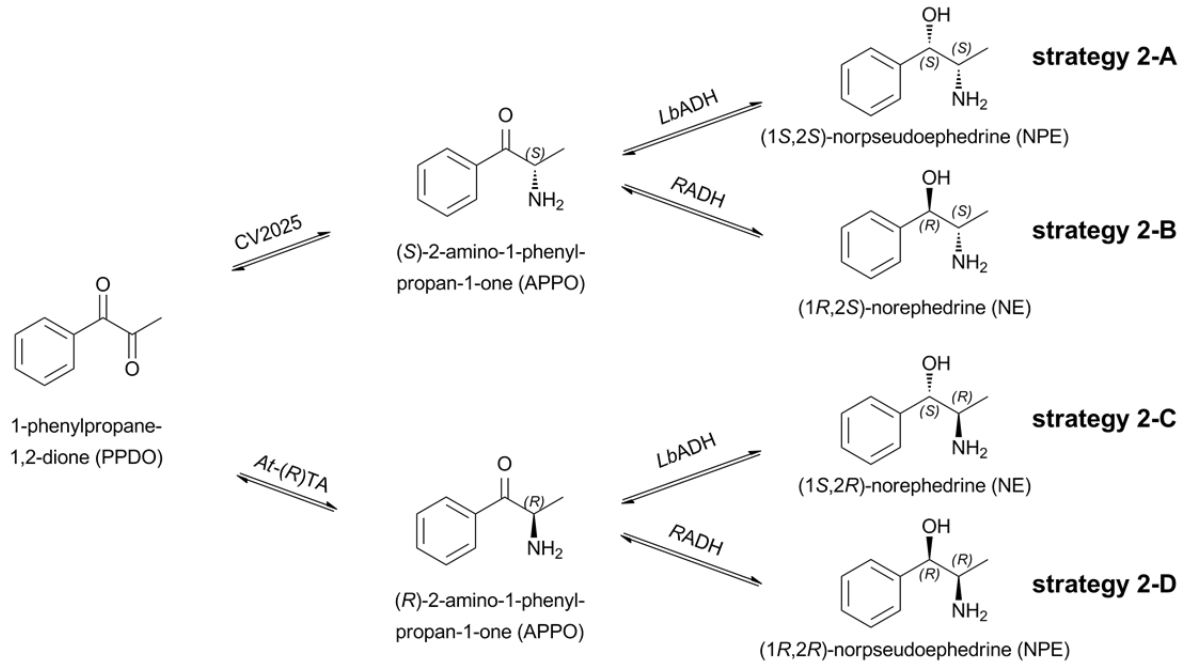

Scheme 4-19: Overview of the 1-pot 2-step reaction for the synthesis all nor(pseudo)-ephedrines combining an (*S*)-selective (CV2025) or an (*R*)-selective (*At*-(*R*)TA) ω-transaminase in the first step with either an (*R*)-selective (*R*ADH) or (*S*)-selective (*Lb*ADH) alcohol dehydrogenase (ADH) in the second step. Theoretically all isomers are accessible via four different routes (strategy 2 A-D).

Diol by-product formation in the 1-pot 2-step sequential cascade (strategy 2-A):

Based on the optimised reaction parameters for the transaminase step for the enzyme CV2025 (1.5 fold excess of (*S*)-α-methylbenzylamine relative to PPDO), it was tested whether the subsequent ADH reaction could be performed in the same reaction vessel without isolation of the reaction intermediate 1-amino-1-phenyl-propane-2-one (APPO). For both ADH reactions, the cofactor NADPH was regenerated by using the formate dehydrogenase (FDH) from *Pseudomonas* sp. and sodium formate as co-substrate.[185]

The combination of the (*S*)-selective CV2025 with *Lb*ADH was expected to give (1*S*,2*S*)-norpseudoephedrine (scheme 4-19; strategy 2-A). The reaction was performed with isolated enzymes in both steps as a 1-pot 2-step sequential cascade. For the first reaction step (reductive amination of 10 mM PPDO) an initial reaction rate of ~0.008 U mg^{-1} was measured (detail information see publication III in chapter 3.3). Compared to the reductive amination of PAC in the nor(pseudo)ephedrine synthesis strategy 1-A (~0.06 U mg^{-1}; see chapter 4.2), the reaction rate is about one order of magnitude lower. However, still a complete conversion of 10 mM PPDO was reached within 48 h. In the second reaction step, the amino alcohol product accumulated in the beginning of the ADH reaction (over ~4 h reaction time to ~40 % product), but within the next 2 h product formation stopped completely. Further HPLC investigations indicated that 1-phenylpropane-1,2-diol was formed as a by-product. However, the diol can only be formed, in case of a reversible ω-transaminase PPDO<=>APPO reductive amination reaction (publication III, chapter 3.3).

Suppression of the diol by-product formation:

In order to suppress this undesired by-product formation, an inactivation of the ω-transaminase by a pH shift or by a removal of the biocatalyst (ultrafiltration) was investigated after the reductive amination step (publication III, chapter 3.3). For these cascade reactions purified enzymes were used in order to avoid further side reactions by further enzymes in *E. coli* crude cell extracts.

Using the pH shift inactivation of the enzyme CV2025 before the *Lb*ADH was added, an overall conversion of 80 % was reached in 52 h reaction time. The product, (1*S*,2*S*)-NPE, was obtained in excellent optical purity of >99 % *de* and >98 % *ee* (table 4-4, entry #4) and did not degrade in the course of the reaction. Compared to

the pH shift method, a removal of the CV2025 by ultrafiltration before *Lb*ADH addition resulted in a slightly lower conversion of 57 % in 60 h (table 4-4, entry #2).

The same trend was found for the combination of CV2025 with *R*ADH (scheme 4-19; strategy 2-B). Using the pH shift method (table 4-4, entry #5), 82 % of the substrate PPDO was converted in the 1-pot 2-step sequential cascade to (1*R*,2*S*)-NE, again with high optical purity (>99 % *de*, >97 % *ee*). Compared to this, in the ultrafiltration method a slightly lower optical purity (>99 % *de*, >97 % *ee*) and a significantly lower conversion (57 % compared to 80 %) was measured. This difference in conversion and *ee* was not further investigated, since the easier and less expensive pH shift method resulted in higher values than the ultrafiltration.

Table 4-4: Reaction overview for the synthesis strategy: "transaminase-ADH"

	TA reaction[a]			ADH reaction[c]		overall conversion & total reaction time[d]	product ratio [in %] and optical purity of major isomer (bold)					
Entry	catalyst	type	termination[b]	catalyst	type		(1*S*,2*S*)-NPE	(1*R*,2*R*)-NPE	(1*S*,2*R*)-NE	(1*R*,2*S*)-NE	optical purity *ee*	optical purity *de* or *dr*
#1	CV2025	purif.	-	*Lb*ADH	purif.	0 % 48 h	-	-	-	-	-	-
#2	CV2025	purif.	filtration	*Lb*ADH	purif.	57 % 60 h	**99.3**	0.7	-	-	>98 %	*de* >99 %
#3			filtration	*R*ADH	purif.	55 % 60 h	-	2.4	-	**97.6**	>99 %	*de* ~95 %
#4	CV2025	purif.	pH shift	*Lb*ADH	purif.	80 % 52 h	**99.4**	0.6	-	-	>98 %	*de* >99 %
#5			pH shift	*R*ADH	purif.	82 % 40 h	-	1.5	-	**98.5**	>99 %	*de* 97 %
#6	*At*-(*R*)TA	CCE	pH shift	*Lb*ADH	purif.	40 % 36 h	**79.9**	-	20.1	-	>99 %	*de* ~60 %
#7			pH shift	*R*ADH	purif.	>95 % 8 h	-	**77.4**	-	22.6	>99 %	*de* ~55 %
#8	CV2025	LWC	pH shift	*Lb*ADH	LWC	62 % 36 h	**92.0**	3.0	5.0	-	~92 %	*de* ~90 %
#9			pH shift	*R*ADH	LWC	67 % 27 h	2.1	17.6	-	**80.3**	>99 %	*dr* ~8:2
#10	*At*-(*R*)TA	CCE	pH shift	*Lb*ADH	LWC	77 % 30 h	**77.3**	2.0	20.7	-	~95 %	*de* ~80 %
#11			pH shift	*R*ADH	LWC	93 % 11 h	-	**75.2**	0.9	23.9	>99 %	*dr* ~7.5:2.5

TA: transaminase, ADH: alcohol dehydrogenase, purif.: purified, CCE: crude cell extract, LWC: lyophilised whole cells, NE: norephedrine, NPE: norpseudoephedrine - time dependent reaction curves and reaction analytics can be found in the Supp. Information of publication III (chapter 3.3).

[a] reaction conditions for reductive amination was carried out as indicated with purified enzyme (1 $mg_{protein}$ mL^{-1}), CCE (1 $mg_{protein}$ mL^{-1}) or LWC (10 mg_{LWC} mL^{-1}) of the respective transaminases (*At*-(*R*)TA or CV2025) in 100 mM HEPES (pH 7.5), 200 µM PLP, with ~10 mM 1,2-PPDO (see Supp. Information) and 15 mM (*R*)- or respectively (*S*)-α-MBA at 27 °C. As indicated (by joined columns in the TA step), the reaction solutions were spit for the subsequent reductive hydrogenation step.

[b] reactions were terminated either by ultrafiltration (membrane cut-off: 10 kDa), pH shift (titrated with 20 % (v/v) HCl to pH 2, then re-titrated with 10 M NaOH to pH 7.5) or not terminated.

[c] reaction conditions for reductive hydrogenation: 0.5 mM $NADP^+$, 150 mM sodium formate, 10 µL mL^{-1} FDH. Either purified enzyme (1 $mg_{protein}$ mL^{-1}), or lyophilised whole cells (10 mg_{LWC}/mL) of the respective alcohol dehydrogenases (*Lb*ADH or *R*ADH) were added to the corresponding solution and incubated at 27 °C.

[d] overall conversion (sum of N(P)E related to the initial substrate concentration) and the total reaction time is given for the complete 2-step reaction.

Comparison of purified enzymes, crude cell extracts and lyophilised whole cells:

The results of the 1-pot 2-step cascade for the synthesis of N(P)E with the combination of lyases and ω-transaminases (chapter 4.2) suggested that lyophilised whole cells might be used in this cascade setup as well. Therefore, we compared the application of purified enzymes with lyophilised whole cells (LWC) in both cascade steps. As an exception, the *At*-(*R*)TA was only available as crude cell extract, which has to be considered for reactions with this enzyme. All cascades were performed as 1-pot 2-step sequential reactions with pH shift inactivation of the transaminase before the ADH was added.

With lyophilised whole cells, the combination CV2025/*Lb*ADH (scheme 4-19; strategy 2-A) gave (1*S*,2*S*)-NPE (*ee* >89 %, *de* 87 %) (table 4-4, entry #8). Under analogous reaction conditions, reactions with purified enzymes led to significant higher optical purities than reactions with lyophilised whole cells. According to these data the 2-step cascade with lyophilised whole cells of CV2025 and *R*ADH (strategy 2-B) resulted in the formation of (1*S*,2*R*)-NE with an optical purity of >99 % *ee* but a diastereomeric ratio (*dr*) of ~8:2 (table 4-4, entry #5). A possible reason might be a background reactions mediated by *E. coli* cellular enzymes or the instability of the APPO intermediate (e.g. amine-imine tautomerisation). Both could decrease the optical purity of the N(P)E products although the cascade enzymes (ADH and ω-transaminase) are highly selective.

In contrast to the CV2025, the *At*-(*R*)TA was only available as crude cell extract (see chapter 1.5.5.3). In combination with the *R*ADH (strategy 2-D) as purified enzyme or as LWC conversions >90 % were detected (table 4-4, entry #7 and #11). Compared to the reactions with CV2025, the diastereomeric excess of the product (1*R*,2*R*)-NPE was with ~55 % *de* rather low even when purified ADH was used for the second reaction step (table 4-4, entry #7). Moreover, the cascade with *At*-(*R*)TA and *Lb*ADH (strategy 2-C) did not produce (1*S*,2*R*)-NE, but (1*S*,2*S*)-NPE as the major isomer. If *Lb*ADH was used as lyophilised whole cells, the undesired product (1*S*,2*R*)-NE had an optical purity of >95 % *ee*, >80 % *de* (table 4-4, entry #10), while application of *Lb*ADH as purified enzyme resulted in >92 % *ee* and >90 % *de* for (1*S*,2*S*)-NPE (table 4-4, entry #6). As mentioned above, an isomerisation of APPO could result in a decrease of the diastereomeric excess although the *At*-(*R*)TA is highly selective for

this compound. However, we were not able to measure the *ee* of the intermediate APPO to investigate the reason for the reduced optical purity obtained with crude cell extracts or whole cells. In case the synthesis of (1*R*,2*R*)-NPE and/or (1*S*,2*R*)-NE in this 2-step strategy is of interest in the future, the application of purified enzymes in both reaction steps is currently the method of choice to achieve high optical purities as demonstrated for the combination CV2025/*Lb*ADH or CV2025/*R*ADH.

Alternative 2-step cascade combining ω-transaminases and alcohol dehydrogenases for the synthesis of (1*S*,2*S*)-norpseudoephedrine:

(1*S*,2*S*)-norpseudoephedrine is a compound with challenging synthetic strategy and is e.g. sold as a natural isolate from the plant *khat*. Since resources are limited, effort to develop respective synthesis strategies of this pharmaceutical is worthwhile. As mentioned above, a highly (*S*)-selective lyase for the synthesis of (*S*)-PAC as an intermediate is currently not available (see chapter 4.2.3). Therefore, an alternative novel synthesis strategy combing a ω-transaminases with an alcohol dehydrogenase was developed. A 2-step strategy combining the (*S*)-selective CV2025 with the (*S*)-selective *Lb*ADH results in the formation of (1*S*,2*S*)-NPE with excellent optical purity (*ee* >98 %, *de* >99 %) when purified enzymes were used. Although the space-time-yields are still relatively low (~0.5 g L^{-1} d^{-1}), this cascade can be performed in one reaction pot without isolation of the intermediate product, if the transaminase is inactivated via a pH shift prior to addition of the *Lb*ADH. According to our results, lyophilised whole cells should not be used in this process since the optical purities were significantly higher with purified proteins in both reaction steps. Beside (1*S*,2*S*)-norpseudoephedrine, (1*R*,2*S*)-norephedrine could also be synthesised using this strategy in high optical purity of *ee* >97 % and a *de* >99 %.

5 Conclusion and future perspectives

Chiral primary vicinal amino alcohols are valuable compounds for the pharmaceutical industry and find as well various applications e.g. as synthons or chiral ligands in organic chemistry. These chiral compounds are hardly accessible with classical chemical synthesis strategies. In this thesis, the general access to such compounds in only two reaction steps and with high stereoselectivities was demonstrated. The biocatalytic cascade reaction, combining ThDP-dependent enzymes in the first reaction step followed by subsequent reductive amination catalysed by ω-transaminases in the second step, offers great potential for the production of vicinal amino alcohols.

The synthesis of nor(pseudo)ephedrines was investigated in more detail. It was possible to perform the reaction in one reaction vessel without isolation of the respective reaction intermediate. One pot reactions in general lower process costs by reducing downstream processing effort. For the 1-pot 2-step cascade towards (1*R*,2*S*)-norephedrine and (1*R*,2*R*)-norpseudoephedrine in the sequential mode, high conversion values and excellent stereoselectivities were obtained. The simultaneous cascade, where both enzymes are active at the same time, would be the most process-efficient approach for cascades reactions, which is especially true in terms of reaction times and simplicity. However, the simultaneous strategy is as well the most challenging one since highly selective catalysts in all cascade steps are required to avoid the formation of undesired by-products. In our 2-step cascade we observed an undesired benzylamine formation, resulting from a reductive amination of benzaldehyde by the ω-transaminases. The by-product/product ratio could successfully be reduced by application of ω-transaminases with decreased affinity towards benzaldehyde relative to the 2-hydroxy ketone.

A further increase of transaminase affinity for mixed aromatic-aliphatic 2-hydroxy ketones relative to aromatic aldehydes by structure- and mechanism-guided enzyme engineering would be a promising project for the future. However, the sequential recycling cascade mode offers a valuable alternative to the simultaneous cascade mode. Here as well, high efficiency and sustainability by novel process designs are feasible. Reactions in preparative scales as well as efficient downstream processing

protocols must be developed to demonstrate the benefit of the 2-step cascade in larger scales. Here, analyses of process costs and sustainability would be useful to evaluate the different strategies and process designs, which were studied in this thesis for larger scale applications. To decrease overall process costs, it could already be demonstrated that whole cell biocatalysis can be used in some cascades as an alternative to purified enzymes or crude cell extracts. Furthermore, the 'recycling cascade' offers the potential to increase the atom economy by reducing waste production. To perform this cascade type even more efficiently, highly selective biocatalysts are required to avoid by-product formation as far as possible.

As an alternative to these approaches, the 2-step synthesis of amino alcohols combing ω-transaminases and alcohol dehydrogenases was developed to complement the amino alcohol platform. By using purified enzymes in both reaction steps, (1*S*,2*S*)-norpseudoephedrine was produced for the first time in high optical purity (>98 % and *ee* >99 %) by a 2-step cascade. In addition, (1*R*,2*S*)-norephedrine can be obtained with similar high purities (table 5-1).

Table 5-1: Optical purity of nor(pseudo)ephedrines obtained via the two different 2-step synthesis strategies developed in this thesis

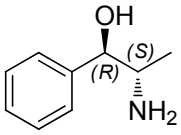

(1*R*,2*S*)-nor ephedrine

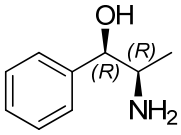

(1*R*,2*R*)-nor pseudoephedrine

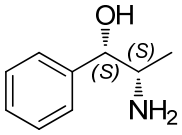

(1*S*,2*S*)-nor pseudoephedrine

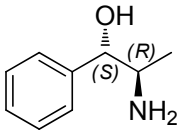

(1*S*,2*R*)-nor ephedrine

Strategy 1: combining ThDP-dependent enzymes and ω-transaminases				
strategy	**1-A**	**1-B**	**1-C**	**1-D**
enzyme combination	AHAS-I with CV2025	AHAS-I with *At*-(*R*)TA	*Ap*PDC-E469G with CV2025	*Ap*PDC-E469G with *At*-(*R*)TA
optical purity	*de* >98 %, *ee* >99 %	*de* >98 %, *ee* >99 %	*de* >98 %, *ee* >70 %	*de* >98 %, *ee* >70 %
space-time-yield	2.1 g L^{-1} d^{-1}	26 g L^{-1} d^{-1}	2-pot reaction	2-pot reaction

Strategy 2: combining ω-transaminases and dehydrogenases				
strategy	**2-B**	**2-D**	**2-A**	**2-C**
enzyme combination	CV2025 with *R*ADH	*At*-(*R*)-TA with *R*ADH	CV2025 with *Lb*ADH	CV2025 with *Lb*ADH
optical purity	*de* >97 %, *ee* >99 %	*de* >55 %, *ee* >99 %	*de* >99 %, *ee* >98 %	only as minor isomer
space-time-yield	0.75 g L^{-1} d^{-1}	4.3 g L^{-1} d^{-1}	~0.5 g L^{-1} d^{-1}	-

For future perspectives, the application of these cascade concepts to other valuable amino alcohols will be of interest. As long-term goal, a platform of various substituted amino alcohols to otherwise hardly accessible chiral compounds can be generated. Two independent factors limit the access to a broad product platform using ThDP-dependent enzymes and ω-transaminases strategy.

On the one hand, the substrate scope of ω-transaminases is still restricted by residues fitting into the “small pocket” of the active site. The number of examples in literature of accepted substrates with residues larger than ethyl groups is still rare. Variants generated by directed evolution or rational design can be screened with the developed TTC-based screening assay. On the one hand, highly (*S*)-selective ThDP-dependent enzymes will be required for the synthesis of (*S*)-PAC and derivatives thereof. Here, on-going enzyme engineering might help to complement the already existing enzyme toolbox. Another method would be the chiral enrichment of (*S*)-PAC (“chiral polishing”), which has already been demonstrated as a proof-of-concept. Using an (*R*)-selective lyase, which cleaves (*R*)-PAC into benzaldehyde and acetaldehyde, the optical purity of (*S*)-PAC could be increased to an *ee* ~97 %. The implementation of this approach at preparative scale will be a target for future research.

In general, the amino alcohol platform itself offers a great potential as synthons for subsequent chemical or enzymatic steps, such as imine-formation, ether- or esterification and addition or elimination reactions.

6 References

1. **R. R. J. Dubos and T. D. Brock**, Pasteur and Modern Science, book published by: American Society for Microbiology Press, 1998.
2. **L. Pasteur and J.-L. Pasteur Vallery-Radot**, Pages illustres : De Pasteur, rassemblées et présentées par Dr. Joseph Louis Pasteur Vallery-Radot,... avec des documents inédits, book published by: Hachette Livre, 1968.
3. **J. Gal and P. Cintas**, Early History of the Recognition of Molecular Biochirality, Top. Curr. Chem., 2013, 333, 1-40.
4. **J. P. Kelly**, Cathinone derivatives: A review of their chemistry, pharmacology and toxicology. *Drug Test Anal.*, 2011, 3, 439-453.
5. **G. Cox and H. Rampes**, Adverse effects of khat: a review. *Adv. Psychiatr. Treat*, 2003, 9, 456-463.
6. **S. W. Smith**, Chiral toxicology: it's the same thing...only different. *Toxicol. Sci.*, 2009, 110, 4-30.
7. **S. F. Mason**, Molecular Handedness and the Origins of Chiral Discrimination. *Int. Rev. Phys. Chem.*, 1983, 3, 217-241.
8. **K. L. Manchester**, Louis Pasteur (1822–1895) — chance and the prepared mind. *Trends Biotechnol.*, 1995, 13, 511-515.
9. **S. T. U. Borman**, FDA issues flexible policy on chiral drugs. *Chem. Eng. News*, 1992, 70, 5.
10. **A. Richards and R. McCague**, Impact of chiral technology on the pharmaceutical industry. *Chem. Ind. (london)*, 1997, 422-425.
11. **S. C. Stinson**, Chiral Drugs. *Chem. Eng. News*, 1992, 70, 46-79.
12. **A. G. Burm, A. D. van der Meer, J. W. van Kleef, P. W. Zeijlmans and K. Groen**, Pharmacokinetics of the enantiomers of bupivacaine following intravenous administration of the racemate. *Br. J. Clin. Pharmacol.*, 1994, 38, 125-129.
13. **R. Kikura-Hanajiri, M. Kawamura, A. Miyajima, M. Sunouchi and Y. Goda**, Chiral analyses of dextromethorphan/levomethorphan and their metabolites in rat and human samples using LC-MS/MS. *Anal. Bioanal. Chem.*, 2011, 400, 165-174.
14. **J. N. Hathcock and A. Shao**, Risk assessment for carnitine. *Regul Toxicol. Pharmacol.*, 2006, 46, 23-28.
15. **John M. Keith, Jay F. Larrow and Eric N. Jacobsen**, Practical Considerations in Kinetic Resolution Reactions. *Adv. Synth. Catal.*, 2001, 343, 5-26.
16. **E. L. Eliel, S. H. Wilen and L. N. Mander**, Stereochemistry of organic compounds, book published by: John Wiley & Sons Inc., 1994.
17. **R. E. Gawley and J. Aubé**, Principles of Asymmetric Synthesis, book published by: Reed Elsevier Group, 2012.
18. **A. Collet**, Separation and purification of enantiomers by crystallisation methods. *Enantiomer*, 1999, 4, 157-172.
19. **D. Wistuba and V. Schurig**, Enantiomer separation of chiral pharmaceuticals by capillary electrochromatography. *J. Chromatogr. A*, 2000, 875, 255-276.
20. **J. Jacques, A. Collet and S. H. Wilen**, Enantiomers, racemates, and resolutions, book published by: John Wiley & Sons Inc., 1981.
21. **B. M. Trost**, Atom Economy—A Challenge for Organic Synthesis: Homogeneous Catalysis Leads the Way. *Angew. Chem. Int. Ed.*, 1995, 34, 259-281.
22. **C. M. Clouthier and J. N. Pelletier**, Expanding the organic toolbox: a guide to integrating biocatalysis in synthesis. *Chem. Soc. Rev.*, 2012, 41, 1585-1605.
23. **H.-P. Meyer, E. Eichhorn, S. Hanlon, S. Lütz, M. Schurmann, R. Wohlgemuth and R. Coppolecchia**, The use of enzymes in organic synthesis and the life sciences: perspectives from the Swiss Industrial Biocatalysis Consortium (SIBC). *Catal. Sci. Technol.*, 2013, 3, 29-40.
24. **D. Munoz Solano, P. Hoyos, M. J. Hernaiz, A. R. Alcantara and J. M. Sanchez-Montero**, Industrial biotransformations in the synthesis of building blocks leading to enantiopure drugs. *Biores. Technol.*, 2012, 115, 196-207.

25. **R. Singh**, Facts, Growth, and Opportunities in Industrial Biotechnology. *Org. Process Res. Dev.*, 2010, 15, 175-179.
26. **R. Ulber and D. Sell**, White Biotechnology, book published by: Springer Publishing, 2010.
27. **J. C. Philp, R. J. Ritchie and J. E. M. Allan**, Biobased chemicals: the convergence of green chemistry with industrial biotechnology. *Trends Biotechnol.*, 2013, 31, 219-222.
28. **A. Liese, K. Seelbach and C. Wandrey**, Industrial Biotransformations, book published by: John Wiley & Sons Inc., 2006.
29. **H. Gröger, Y. Asano and O. May**, Introduction – Principles and Historical Landmarks of Enzyme Catalysis in Organic Synthesis, book section in: Enzyme Catalysis in Organic Synthesis, published by: John Wiley & Sons Inc., 2012, pp. 1-42.
30. **E. C. Webb**, Enzyme nomenclature 1992: recommendations of the Nomenclature Committee of the International Union of Biochemistry and Molecular Biology on the nomenclature and classification of enzymes, book published by: Academic Press, 1992.
31. **J. Wang and W. Lu**, Chiral Drugs via Biocatalytical Approaches, book section in: Chiral Drugs, published by: John Wiley & Sons Inc., 2011, pp. 77-136.
32. **K. Faber**, Introduction and Background Information, book section in: Biotransformations in Organic Chemistry, published by: Springer Publishing, 2011, pp. 1-30.
33. **A. Schmid, J. S. Dordick, B. Hauer, A. Kiener, M. Wubbolts and B. Witholt**, Industrial biocatalysis today and tomorrow. *Nature*, 2001, 409, 258-268.
34. **R. Wolfenden**, Benchmark reaction rates, the stability of biological molecules in water, and the evolution of catalytic power in enzymes. *Annu. Rev. Biochem.*, 2011, 80, 645-667.
35. **D. J. C. Constable, P. J. Dunn, J. D. Hayler, G. R. Humphrey, J. J. L. Leazer, R. J. Linderman, K. Lorenz, J. Manley, B. A. Pearlman, A. Wells, A. Zaks and T. Y. Zhang**, Key green chemistry research areas-a perspective from pharmaceutical manufacturers. *Green Chem.*, 2007, 9, 411-420.
36. **T. C. Nugent**, Chiral Amine Synthesis, book published by: John Wiley & Sons Inc., 2010.
37. **M. Höhne and U. T. Bornscheuer**, Biocatalytic Routes to Optically Active Amines. *ChemCatChem*, 2009, 1, 42-51.
38. **G. K. Friestad**, Chiral *N*-acylhydrazones: Versatile imino acceptors for asymmetric amine synthesis. *Eur. J. Org. Chem.*, 2005, 3157-3172.
39. **T. C. Nugent, A. K. Ghosh, V. N. Wakchaure and R. R. Mohanty**, Asymmetric reductive amination: Convenient access to enantioenriched alkyl-alkyl or aryl-alkyl substituted alpha-chiral primary amines. *Adv. Synth. Catal.*, 2006, 348, 1289-1299.
40. **J. A. Ellman**, Applications of *tert*-butanesulfinamide in the asymmetric synthesis of amines. *Pure Appl. Chem.*, 2003, 75, 39-46.
41. **W. C. Zhang, Y. X. Chi and X. M. Zhang**, Developing chiral ligands for asymmetric hydrogenation. *Acc. Chem. Res.*, 2007, 40, 1278-1290.
42. **H. U. Blaser, W. Brieden, B. Pugin, F. Spindler, M. Studer and A. Togni**, Solvias Josiphos ligands: from discovery to technical applications. *Top. Catal.*, 2002, 19, 3-16.
43. **V. Gotor-Fernandez and V. Gotor**, Biocatalytic routes to chiral amines and amino acids. *Curr. Opin. Drug. Discov. Devel.*, 2009, 12, 784-797.
44. **K. E. Jaeger, K. Liebeton, A. Zonta, K. Schimossek and M. T. Reetz**, Biotechnological application of *Pseudomonas aeruginosa* lipase: efficient kinetic resolution of amines and alcohols. *Appl. Microbiol. Biotechnol.*, 1996, 46, 99-105.
45. **M. T. Reetz and C. Dreisbach**, Highly Efficient Lipase-Catalyzed Kinetic Resolution of Chiral Amines. *CHIMIA International Journal for Chemistry*, 1994, 48, 570-570.
46. **F. Balkenhohl, K. Ditrich, B. Hauer and W. Ladner**, Optisch aktive Amine durch Lipase-katalysierte Methoxyacetylierung. *J. Prakt. Chem. / Chem-Ztg.*, 1997, 339, 381-384.
47. **U. T. Bornscheuer and R. J. Kazlauskas**, Hydrolases in Organic Synthesis, book published by: John Wiley & Sons Inc., 2006.
48. **H. Ismail, R. M. Lau, F. van Rantwijk and R. A. Sheldon**, Fully Enzymatic Resolution of Chiral Amines: Acylation and Deacylation in the Presence of *Candida antarctica* Lipase B. *Adv. Synth. Catal.*, 2008, 350, 1511-1516.
49. **N. J. Turner**, Deracemisation methods. *Curr. Opin. Chem. Biol.*, 2010, 14, 115-121.

50. **T. Nicholas, F. Ian and S. Robert**, Novel Biocatalyst Technology for the Preparation of Chiral Amines. *ChemInform.*, 2005, 36.
51. **R. Carr, M. Alexeeva, A. Enright, T. S. Eve, M. J. Dawson and N. J. Turner**, Directed evolution of an amine oxidase possessing both broad substrate specificity and high enantioselectivity. *Angew. Chem. Int. Ed.*, 2003, 42, 4807-4810.
52. **R. Carr, M. Alexeeva, M. J. Dawson, V. Gotor-Fernandez, C. E. Humphrey and N. J. Turner**, Directed evolution of an amine oxidase for the preparative deracemisation of cyclic secondary amines. *ChemBioChem*, 2005, 6, 637-639.
53. **N. J. Turner and M. D. Truppo**, Biocatalytic Routes to Nonracemic Chiral Amines, book section in: Chiral Amine Synthesis, published by: John Wiley & Sons Inc., 2010, pp. 431-459.
54. **M. J. Abrahamson, E. Vázquez-Figueroa, N. B. Woodall, J. C. Moore and A. S. Bommarius**, Development of an Amine Dehydrogenase for Synthesis of Chiral Amines. *Angew. Chem. Int. Ed.*, 2012, 51, 3969-3972.
55. **N. Itoh, C. Yachi and T. Kudome**, Determining a novel NAD+-dependent amine dehydrogenase with a broad substrate range from *Streptomyces virginiae* IFO 12827: purification and characterization. *J. Mol. Catal. B: Enzym.*, 2000, 10, 281-290.
56. **M. Iwaki, T. Yagi, K. Horiike, Y. Saeki, T. Ushijima and M. Nozaki**, Crystallization and properties of aromatic amine dehydrogenase from *Pseudomonas* sp. *Arch. Biochem. Biophys.*, 1983, 220, 253-262.
57. **K. Mitsukura, T. Kuramoto, T. Yoshida, N. Kimoto, H. Yamamoto and T. Nagasawa**, A NADPH-dependent (*S*)-imine reductase (SIR) from *Streptomyces* sp. GF3546 for asymmetric synthesis of optically active amines: purification, characterization, gene cloning, and expression. *Appl. Microbiol. Biotechnol.*, 2012, 1-8.
58. **O. Dipeolu, J. Gardiner and G. Stephens**, Biocatalytic amide reduction using *Clostridium sporogenes*. *Biotechnology letters*, 2005, 27, 1803-1807.
59. **H. Li, P. Williams, J. Micklefield, J. M. Gardiner, G. Stephens, E. Biotechnology and Biodiversity**, A dynamic combinatorial screen for novel imine reductase activity. *Tetrahedron*, 2004, 60.
60. **T. Vaijayanthi and A. Chadha**, Asymmetric reduction of aryl imines using *Candida parapsilosis* ATCC 7330. *Tetrahedron: Asym.*, 2008, 19, 93-96.
61. **M. M. Heberling, B. Wu, S. Bartsch and D. B. Janssen**, Priming ammonia lyases and aminomutases for industrial and therapeutic applications. *Curr. Opin. Chem. Biol.*, 2013, 17, 250-260.
62. **N. J. Turner**, Ammonia lyases and aminomutases as biocatalysts for the synthesis of alpha-amino and beta-amino acids. *Curr. Opin. Chem. Biol.*, 2011, 15, 234-240.
63. **A. Casablancas, M. Cárdenas-Fernández, G. Álvaro, M. D. Benaiges, G. Carminal, C. d. Mas, G. González, C. López and J. López-Santín**, New ammonia lyases and amine transaminases: Standardization of production process and preparation of immobilized biocatalysts. *Electron. J. Biotechnol.*, 2013, 16, 1-13.
64. **J. S. Shin and B. G. Kim**, Asymmetric synthesis of chiral amines with omega-transaminase. *Biotechnology and bioengineering*, 1999, 65, 206-211.
65. **R. A. Sheldon**, Chirotechnology: Designing economic chiral syntheses. *J. Chem. Technol. Biotechnol.*, 1996, 67, 1-14.
66. **M. Höhne and U. T. Bornscheuer**, Application of Transaminases, book section in: Enzyme Catalysis in Organic Synthesis, published by: John Wiley & Sons Inc., 2012, pp. 779-820.
67. **D. Koszelewski, K. Tauber, K. Faber and W. Kroutil**, omega-Transaminases for the synthesis of non-racemic alpha-chiral primary amines. *Trends Biotechnol.*, 2010, 28, 324-332.
68. **M. S. Malik, E. S. Park and J. S. Shin**, Features and technical applications of omega-transaminases. *Appl. Microbiol. Biotechnol.*, 2012, 94, 1163-1171.
69. **B.-Y. Hwang, B.-K. Cho, H. Yun, K. Koteshwar and B.-G. Kim**, Revisit of aminotransferase in the genomic era and its application to biocatalysis. *J. Mol. Catal. B: Enzym*, 2005, 37, 47-55.
70. **Expasy.org**, "http://enzyme.expasy.org/EC/2.6.1.-".
71. **J. Ward and R. Wohlgemuth**, High-yield biocatalytic amination reactions in organic synthesis. *Curr. Org. Chem.*, 2010, 14, 1914-1927.

72. **P. Berglund, M. S. Humble and C. Branneby**, C–X Bond Formation: Transaminases as Chiral Catalysts: Mechanism, Engineering, and Applications, book section in: Comprehensive Chirality, eds. M. C. Editors-in-Chief: Erick and Y. Hisashi, published by: Reed Elsevier Group, 2012, pp. 390-401.
73. **P. K. Mehta, T. I. Hale and P. Christen**, Aminotransferases: demonstration of homology and division into evolutionary subgroups. *Eur. J. Biochem.*, 1993, 214, 549-561.
74. **J. N. Jansonius**, Structure, evolution and action of vitamin B6-dependent enzymes. *Curr. Opin. Struct. Biol.*, 1998, 8, 759-769.
75. **A. I. Denesyuk, K. A. Denessiouk, T. Korpela and M. S. Johnson**, Functional attributes of the phosphate group binding cup of pyridoxal phosphate-dependent enzymes. *J. Mol. Biol.*, 2002, 316, 155-172.
76. **A. Iwasaki, K. Matsumoto, J. Hasegawa and Y. Yasohara**, A novel transaminase, (*R*)-amine:pyruvate aminotransferase, from *Arthrobacter sp.* KNK168 (FERM BP-5228): purification, characterization, and gene cloning. *Appl. Microbiol. Biotechnol.*, 2012, 93, 1563-1573.
77. **F. W. Alexander, E. Sandmeier, P. K. Mehta and P. Christen**, Evolutionary relationships among pyridoxal-5′-phosphate-dependent enzymes. *Eur. J. Biochem.*, 1994, 219, 953-960.
78. **H. Hayashi, H. Mizuguchi, I. Miyahara, M. M. Islam, H. Ikushiro, Y. Nakajima, K. Hirotsu and H. Kagamiyama**, Strain and catalysis in aspartate aminotransferase. *Biochim. Biophys. Acta*, 2003, 1647, 103-109.
79. **J. M. Goldberg and J. F. Kirsch**, The Reaction Catalyzed by *Escherichia coli* Aspartate Aminotransferase Has Multiple Partially Rate-Determining Steps, While That Catalyzed by the Y225F Mutant Is Dominated by Ketimine Hydrolysis. *Biochem.*, 1996, 35, 5280-5291.
80. **P. A. Frey and A. D. Hegemann**, Enzymatic Reaction Mechanisms, book published by: Oxford University Press, 2006.
81. **M. Höhne, S. Schätzle, H. Jochens, K. Robins and U. T. Bornscheuer**, Rational assignment of key motifs for function guides in silico enzyme identification. *Nat. Chem. Biol.*, 2010, 6, 807-813.
82. **S. Mathew, G. Shin, M. Shon and H. Yun**, High throughput screening methods for ω-transaminases. *Biotechnol. Bioproc.*, 2013, 18, 1-7.
83. **P. Schadewaldt and F. Adelmeyer**, Coupled Enzymatic Assay for Estimation of Branched-Chainl-Amino Acid Aminotransferase Activity with 2-Oxo Acid Substrates. *Anal. Biochem.*, 1996, 238, 65-71.
84. **B.-Y. Hwang and B.-G. Kim**, High-throughput screening method for the identification of active and enantioselective omega-transaminases. *Enzyme Microb. Tech.*, 2004, 34, 429-436.
85. **S. Schätzle, M. Höhne, K. Robins and U. T. Bornscheuer**, Conductometric Method for the Rapid Characterization of the Substrate Specificity of Amine-Transaminases. *Anal. Chem.*, 2010, 82, 2082-2086.
86. **J. Hopwood, M. D. Truppo, N. J. Turner and R. C. Lloyd**, A fast and sensitive assay for measuring the activity and enantioselectivity of transaminases. *Chem. Commun.*, 2011, 47, 773-775.
87. **H. Yun, B. Y. Hwang, J. H. Lee and B. G. Kim**, Use of enrichment culture for directed evolution of the *Vibrio fluvialis* JS17 omega-transaminase, which is resistant to product inhibition by aliphatic ketones. *Appl. Environ. Microbiol.*, 2005, 71, 4220-4224.
88. **M. D. Truppo, J. D. Rozzell, J. C. Moore and N. J. Turner**, Rapid screening and scale-up of transaminase catalysed reactions. *Org. Biomol. Chem.*, 2009, 7, 395-398.
89. **S. Schätzle, M. Höhne, E. Redestad, K. Robins and U. T. Bornscheuer**, Rapid and Sensitive Kinetic Assay for Characterization of ω-Transaminases. *Anal. Chem.*, 2009, 81, 8244-8248.
90. **A. R. Martin, R. DiSanto, I. Plotnikov, S. Kamat, D. Shonnard and S. Pannuri**, Improved activity and thermostability of (*S*)-aminotransferase by error-prone polymerase chain reaction for the production of a chiral amine. *Biochem. Eng. J.*, 2007, 37, 246-255.
91. **D. I. Stirling, A. L. Zeitlin and G. W. Matcham**, Patent US4950606, Enantiomeric enrichment and stereoselective synthesis of chiral amines using co-amino acid transaminase, 1990
92. **J.-S. Shin and B.-G. Kim**, Optical Resolution of Racemic 1-Phenylethylamine Catalyzed by Aminotransferase and Dehydrogenase. *Ann. N.Y. Acad. Sci.*, 1996, 799, 717-724.

93. **J.-S. Shin and B.-G. Kim**, Kinetic resolution of α-methylbenzylamine with omega-transaminase screened from soil microorganisms: Application of a biphasic system to overcome product inhibition. *Biotechnol. Bioeng.*, 1997, 55, 348-358.

94. **J.-S. Shin and B.-G. Kim**, Kinetic modeling of ω-transamination for enzymatic kinetic resolution of α-methylbenzylamine. *Biotechnol. Bioeng.*, 1998, 60, 534-540.

95. **T. H. Jang, B. Kim, O. K. Park, J. Y. Bae, B. G. Kim, H. Yun and H. H. Park**, Crystallization and preliminary X-ray crystallographic studies of omega-transaminase from *Vibrio fluvialis* JS17. Acta crystallographica. Section F*, Struct. Biol. Crystal. Commun.*, 2010, 66, 923-925.

96. **J. S. Shin, H. Yun, J. W. Jang, I. Park and B. G. Kim**, Purification, characterization, and molecular cloning of a novel amine:pyruvate transaminase from *Vibrio fluvialis* JS17. *Appl. Microbiol. Biotechnol.*, 2003, 61, 463-471.

97. **W. Kroutil, E. M. Fischereder, C. S. Fuchs, H. Lechner, F. G. Mutti, D. Pressnitz, A. Rajagopalan, J. H. Sattler, R. C. Simon and E. Siirola**, Asymmetric Preparation of *prim*-, *sec*-, and *tert*-Amines Employing Selected Biocatalysts. *Org. Process Res. Dev.*, 2013, 17, 751-759.

98. **J. Rudat, B. R. Brucher and C. Syldatk**, Transaminases for the synthesis of enantiopure beta-amino acids. *AMB Express*, 2012, 2, 11.

99. **J. H. Seo, D. Kyung, K. Joo, J. Lee and B. G. Kim**, Necessary and sufficient conditions for the asymmetric synthesis of chiral amines using omega-aminotransferases. *Biotechnol. Bioeng.*, 2011, 108, 253-263.

100. **H. Yun and B.-G. Kim**, Asymmetric Synthesis of (*S*)-α-Methylbenzylamine by Recombinant *Escherichia coli* Co-Expressing Omega-Transaminase and Acetolactate Synthase. *Biosci. Biotechnol. Biochem.*, 2008, 72, 3030-3033.

101. **J.-S. Shin, B.-G. Kim and D.-H. Shin**, Kinetic resolution of chiral amines using packed-bed reactor. *Enzyme Microb. Technol.*, 2001, 29, 232-239.

102. **J.-S. Shin, B.-G. Kim, A. Liese and C. Wandrey**, Kinetic resolution of chiral amines with ω-transaminase using an enzyme-membrane reactor. *Biotechnol. Bioeng.*, 2001, 73, 179-187.

103. **U. Kaulmann, K. Smithies, M. E. B. Smith, H. C. Hailes and J. M. Ward**, Substrate spectrum of ω-transaminase from *Chromobacterium violaceum* DSM30191 and its potential for biocatalysis. *Enzyme Microb. Technol.*, 2007, 41, 628-637.

104. **C. K. Savile, J. M. Janey, E. C. Mundorff, J. C. Moore, S. Tam, W. R. Jarvis, J. C. Colbeck, A. Krebber, F. J. Fleitz, J. Brands, P. N. Devine, G. W. Huisman and G. J. Hughes**, Biocatalytic Asymmetric Synthesis of Chiral Amines from Ketones Applied to Sitagliptin Manufacture. *Science*, 2010, 329, 305-309.

105. **P. Tufvesson, J. S. Jensen, W. Kroutil and J. M. Woodley**, Experimental determination of thermodynamic equilibrium in biocatalytic transamination. *Biotechnol. Bioeng.*, 2012, 109, 2159-2162.

106. **P. Tufvesson, J. Lima-Ramos, J. S. Jensen, N. Al-Haque, W. Neto and J. M. Woodley**, Process considerations for the asymmetric synthesis of chiral amines using transaminases. *Biotechnology and bioengineering*, 2011, 108, 1479-1493.

107. **M. D. Truppo, J. D. Rozzell and N. J. Turner**, Efficient Production of Enantiomerically Pure Chiral Amines at Concentrations of 50 g/L Using Transaminases. *Org. Process Res. Dev.*, 2009, 14, 234-237.

108. **R. C. Simon, F. Zepeck and W. Kroutil**, Chemoenzymatic Synthesis of All Four Diastereomers of 2,6-Disubstituted Piperidines through Stereoselective Monoamination of 1,5-Diketones. *Chem. Eur. J.*, 2013, 19, 2859-2865.

109. **G. Matcham, M. Bhatia, W. Lang, C. Lewis, R. Nelson, A. Wang and W. Wu**, Enzyme and Reaction Engineering in Biocatalysis: Synthesis of (*S*)-Methoxyisopropylamine (= (*S*)-1-Methoxypropan-2-amine). *CHIMIA Int. J. Chem.*, 1999, 53, 584-589.

110. **H. Yun, B.-K. Cho and B.-G. Kim**, Kinetic resolution of (*R*,*S*)-*sec*-butylamine using omega-transaminase from *Vibrio fluvialis* JS17 under reduced pressure. *Biotechnol. Bioeng.*, 2004, 87, 772-778.

111. **B. K. Cho, H. J. Cho, S. H. Park, H. Yun and B. G. Kim**, Simultaneous synthesis of enantiomerically pure (*S*)-amino acids and (*R*)-amines using coupled transaminase reactions. *Biotechnol. Bioeng.*, 2003, 81, 783-789.

112. **T. J. Donohoe, C. K. A. Callens, A. Flores, A. R. Lacy and A. H. Rathi**, Recent Developments in Methodology for the Direct Oxyamination of Olefins. *Chem. Eur. J.*, 2011, 17, 58-76.

113. **S. C. Bergmeier**, The Synthesis of Vicinal Amino Alcohols. *Tetrahedron*, 2000, 56, 2561-2576.

114. **O. K. Karjalainen and A. M. P. Koskinen**, Diastereoselective synthesis of vicinal amino alcohols. *Org. Biomol. Chem.*, 2012, 10, 4311-4326.

115. **D. J. Ager, I. Prakash and D. R. Schaad**, 1,2-Amino Alcohols and Their Heterocyclic Derivatives as Chiral Auxiliaries in Asymmetric Synthesis. *Chem. Rev.*, 1996, 96, 835-876.

116. **J. L. Charlton and G.-L. Chee**, Asymmetric synthesis of lignans using oxazolidinones as chiral auxiliaries. *Can. J. Chem.*, 1997, 75, 1076-1083.

117. **C. Neri and J. M. J. Williams**, New Routes to Chiral Evans Auxiliaries by Enzymatic Desymmetrisation and Resolution Strategies. *Adv. Synth. Catal.*, 2003, 345, 835-848.

118. **K. A. Parker and M. W. Ledeboer**, Asymmetric Reduction. A Convenient Method for the Reduction of Alkynyl Ketones. *J. Org. Chem.*, 1996, 61, 3214-3217.

119. **A. G. Myers, B. H. Yang, H. Chen, L. McKinstry, D. J. Kopecky and J. L. Gleason**, Pseudoephedrine as a Practical Chiral Auxiliary for the Synthesis of Highly Enantiomerically Enriched Carboxylic Acids, Alcohols, Aldehydes, and Ketones. *J. Am. Chem. Soc.*, 1997, 119, 6496-6511.

120. **K. Rück**, Asymmetric Alkylation of Amide Enolates with Pseudoephedrine and Ephedrine as Chiral Auxiliaries—Unexpected Influence of Additives? *Angew. Chem. Int. Ed.*, 1995, 34, 433-435.

121. **J. Clayden and L. W. Lai**, (−)-Ephedrine as an auxiliary for the asymmetric synthesis of atropisomeric amides by dynamic resolution under thermodynamic control. *Tetrahedron Lett.*, 2001, 42, 3163-3166.

122. **S. C. Benson and J. K. Snyder**, Optically pure chiral sulfoxides using ephedrine as a chiral auxiliary. *Tetrahedron Lett.*, 1991, 32, 5885-5888.

123. **T. Sehl, J. Kulig, R. Westphal and D. Rother**, Synthetic Enzyme Cascades for Valuable Diols and Amino Alcohols – Smart Composition and Optimization Strategies, book section in: Industrial Biocatalysis (working title), ed. P. Grunwald,published, in publishing process.

124. **Micromedex® Healthcare Series**, Internet database (Greenwood; Village, Colo), Thomson Healthcare. Updated periodically.

125. **C. Knox, V. Law, T. Jewison, P. Liu, S. Ly, A. Frolkis, A. Pon, K. Banco, C. Mak, V. Neveu, Y. Djoumbou, R. Eisner, A. C. Guo and D. S. Wishart**, DrugBank 3.0: a comprehensive resource for 'omics' research on drugs. *Nucleic Acids Res.*, 2011, 39, 1035-1041.

126. **L. Yan, Z. Diansong, S. S. Ferguson, P. Dorff, T. R. Simpson and S. W. Grimm**, In vitro assessment of metabolic drug-drug interaction potential of AZD2624, neurokinin-3 receptor antagonist, through cytochrome P450 enzyme identification, inhibition, and induction studies. *Xenobiotica*, 2010, 40, 721-729.

127. **D. G. Allen, N. M. Aston, N. Trivedi and C. D. Edlin**, Pyrazolo[3,4-b]pyridine compounds, and their use as phosphodiesterase inhibitors, Patent: WO2004024728 A3, 2007

128. **L. Keinicke, P. Fristrup, P.-O. Norrby and R. Madsen**, Nonradical Zinc−Barbier Reaction for Diastereoselective Synthesis of Vicinal Amino Alcohols. *J. Am. Chem. Soc.*, 2005, 127, 15756-15761.

129. **G. Hildebrandt and W. Klavehn**, Verfahren zur Herstellung von 1-L-Phenyl-2-methylaminopropan-1-ol. Knoll A.-G. Chemische Fabriken in Ludwigshafen 1930. Ger. Patent: DE 548459.

130. **K. Faber**, Biocatalytic Applications, book section in: Biotransformations in Organic Chemistry, published by: Springer Publishing, 2011, pp. 31-313.

131. **H. Yun, J. Kim, K. Kinnera and B. G. Kim**, Synthesis of enantiomerically pure trans-(1*R*,2*R*)- and cis-(1*S*,2*R*)-1-amino-2-indanol by lipase and omega-transaminase. *Biotech. Bioeng.*, 2006, 93, 391-395.

132. **H. C. Hailes, P. A. Dalby, G. J. Lye and J. M. Ward**, Biocatalytic approaches to ketodiols and aminodiols. *ChemInform*, 2009, 27, 28-31.

133. **J. L. Galman, D. Steadman, S. Bacon, P. Morris, M. E. Smith, J. M. Ward, P. A. Dalby and H. C. Hailes**, α, α′-Dihydroxyketone formation using aromatic and heteroaromatic aldehydes with evolved transketolase enzymes. *Chem. Commun.*, 2010, 46, 7608-7610.

134. **M. E. Smith, B. H. Chen, E. G. Hibbert, U. Kaulmann, K. Smithies, J. L. Galman, F. Baganz, P. A. Dalby, H. C. Hailes and G. J. Lye**, A Multidisciplinary Approach Toward the Rapid and Preparative-Scale Biocatalytic Synthesis of Chiral Amino Alcohols: A Concise Transketolase-/ω-Transaminase-Mediated Synthesis of (2S,3*S*)-2-Aminopentane-1,3-diol. *Org. Process Res. Dev.*, 2009, 14, 99-107.

135. **C. Ingram, M. Bommer, M. Smith, P. Dalby, J. Ward, H. Hailes and G. Lye**, One-pot synthesis of amino-alcohols using a de-novo transketolase and β-alanine: Pyruvate transaminase pathway in *Escherichia coli*. *Biotech. Bioeng.*, 2007, 96, 559-569.

136. **J. M. Hagel, R. Krizevski, K. Kilpatrick, Y. Sitrit, F. Marsolais, E. Lewinsohn and P. J. Facchini**, Expressed sequence tag analysis of khat (*Catha edulis*) provides a putative molecular biochemical basis for the biosynthesis of phenylpropylamino alkaloids. *Genet. Mol. Biol.*, 2011, 34, 640-646.

137. **O. Wolfes**, Über das Vorkommen von *d*-nor-iso-Ephedrin in *Catha edulis*. *Arch. Pharm.*, 1930, 268, 81-83.

138. **R. Krizevski, E. Bar, O. Shalit, A. Levy, J. M. Hagel, K. Kilpatrick, F. Marsolais, P. J. Facchini, S. Ben-Shabat and Y. Sitrit**, Benzaldehyde is a precursor of phenylpropylamino alkaloids as revealed by targeted metabolic profiling and comparative biochemical analyses in *Ephedra* spp. *Phytochemistry*, 2012, 81, 71-79.

139. **B. B. Hoffman and R. J. Lefkowitz,** Catecholamines, sympathomimetic drugs, and adrenergic receptor antagonists. book section in: The pharmacological basis of therapeutics, 12th ed., published by: McGraw-Hill Companies Inc., 1996.

140. **L. Lasagna**, Phenylpropanolamine: A review, book published by: John Wiley & Sons Inc., 1988.

141. **J. Morgan**, book: Phenylpropanolamine: A Critical Analysis of Reported Adverse Reactions and Overdosage, 1st ed., published by: Jack K. Burgess Inc., 1986.

142. **M. Weintraub**, Phenylpropanolamine as an anorexiant agent in weight control: a review of published and unpublished studies, book section in: Phenylpropanolamine: Risks, Benefits and Controversies, published by: Praeger Publishers Inc., 1985, pp. 53-79.

143. **W. N. Kernan, C. M. Viscoli, L. M. Brass, J. P. Broderick, T. Brott, E. Feldmann, L. B. Morgenstern, J. L. Wilterdink and R. I. Horwitz**, Phenylpropanolamine and the Risk of Hemorrhagic Stroke. *N. Engl. J Med.*, 2000, 343, 1826-1832.

144. Food and Drug Administration, Phenylpropanolamine-Containing Drug Products for Over-the-Counter Human Use, http://www.gpo.gov/fdsys/pkg/FR-2005-12-22/pdf/E5-7646.pdf.

145. **R. SoRelle**, FDA warns of stroke risk associated with phenylpropanolamine; cold remedies and drugs removed from store shelves. *Circulation*, 2000, 102, E9041.

146. **B. Yoon, H. Bae, K. Hong, S. Lee, B. Park, K. Yu, M. Han, Y. Lee, D. Chung and J. Park**, Phenylpropanolamine contained in cold remedies and risk of hemorrhagic stroke. *Neurology*, 2007, 68, 146-149.

147. **R. SoRelle**, FDA warns of stroke risk associated with phenylpropanolamine; cold remedies and drugs removed from store shelves. *Circulation*, 2000, 102, E9041-9043.

148. **M. Yakoot**, Phenylpropanolamine and the hemorrhagic stroke: A new search for the culprit. *J Pharmacol. Pharmacother.*, 2012, 3, 4.

149. Gesundheitsportal Onmeda http://medikamente.onmeda.de/Wirkstoffe/Cathin.html. 2013.

150. Aponet Arzneimitteldatenbank, Arzneimitteldetails zu "ALVALIN 40mg/g". 2013.

151. **G. Laux and O. Dietmaier**,Psychostimulanzien, book section in: Psychopharmaka, 7th ed., published by: Springer Publishing, 2013., pp. 189-195

152. American Chemical Society - SciFinder https://scifinder.cas.org/scifinder/view/scifinder/scifinderExplore.jsf. 2013.

153. **http://www.sigmaaldrich.com/etc/medialib/docs/Sigma/Datasheet/c222dat.Par.0001.File.tmp/c222dat.pdf**, 2012.

154. **H. K. Lee, S. Kang and E. B. Choi**, Stereoselective synthesis of norephedrine and norpseudoephedrine by using asymmetric transfer hydrogenation accompanied by dynamic kinetic resolution. *J. Org. Chem.*, 2012, 77, 5454-5460.

155. **A. Boerner and H. Krause**, A convenient synthesis of optically pure (*S*,*S*)-norpseudoephedrine. *Tetrahedron Lett.*, 1989, 30, 929-930.

156. **G.-I. Hwang, J.-H. Chung and W. K. Lee**, Efficient Synthesis of Ephedra Alkaloid Analogues Using an Enantiomerically Pure N-[(*R*)-(+)-α-Methylbenzyl]aziridine-2-carboxaldehyde. *J. Org. Chem.*, 1996, 61, 6183-6188.

157. **D. A. Claremon, P. K. Lumma and B. T. Phillips**, Organolithium addition to aldehyde dimethylhydrazones: a highly diastereocontrolled synthesis of threo 2-amino alcohols, and (1*R*,2*R*)-(-)-norpseudoephedrine. *J. Am. Chem. Soc.*, 1986, 108, 8265-8266.

158. **N. S. Barta, D. R. Sidler, K. B. Somerville, S. A. Weissman, R. D. Larsen and P. J. Reider**, Practical Modifications and Applications of the Sharpless Asymmetric Aminohydroxylation in the One-Pot Preparation of Chiral Oxazolidin-2-ones. *Org. Lett.*, 2000, 2, 2821-2824.

159. **S. J. Katz and S. C. Bergmeier**, Convenient methods for the hydrolysis of oxazolidinones to vicinal aminoalcohols. *Tetrahedron Lett.*, 2002, 43, 557-559.

160. **M. Nishimura, S. Minakata, T. Takahashi, Y. Oderaotoshi and M. Komatsu**, Asymmetric N1 Unit Transfer to Olefins with a Chiral Nitridomanganese Complex: Novel Stereoselective Pathways to Aziridines or Oxazolines. *J. Org. Chem.*, 2002, 67, 2101-2110.

161. **T. Purkarthofer, K. Gruber, M. Gruber-Khadjawi, K. Waich, W. Skranc, D. Mink and H. Griengl**, A Biocatalytic Henry Reaction—The Hydroxynitrile Lyase from *Hevea brasiliensis* Also Catalyzes Nitroaldol Reactions. *Angew. Chem. Int. Ed.*, 2006, 45, 3454-3456.

162. **O. C. Kreutz, P. J. S. Moran and J. A. R. Rodrigues**, Baker's yeast reduction of (E)-1-phenyl-1,2-propanedione 2-(O-methyloxime). A key step for a (−)-norephedrine synthesis. *Tetrahedron: Asym.*, 1997, 8, 2649-2653.

163. **T. Hibino, K. Makino, T. Sugiyama and Y. Hamada**, Homogeneous Chiral Nickel-Catalyzed Asymmetric Hydrogenation of Substituted Aromatic α-Aminoketone Hydrochlorides through Dynamic Kinetic Resolution. *ChemCatChem*, 2009, 1, 237-240.

164. **Sigma-Aldrich Corporation**, Best catalogue price for 1-phenylpropane-1,2-dione. 2013.

165. **Sigma-Aldrich Corporation**, Best catalogue price for benzaldehyde. 2013.

166. **R. A. W. Frank, F. J. Leeper and B. F. Luisi**, Structure, mechanism and catalytic duality of thiamine-dependent enzymes. *Cell. Mol. Life S.*, 2007, 64, 829-905.

167. **M. Müller, D. Gocke and M. Pohl**, Exploitation of ThDP-dependent enzymes for asymmetric chemoenzymatic synthesis. *FEBS J.*, 2009, 276, 2894-2940.

168. **M. Müller, G. A. Sprenger and M. Pohl**, C-C bond formation using ThDP-dependent lyases. *Curr. Opin. Chem. Biol.*, 2013, 17, 261-270.

169. **M. Pohl, D. Gocke and M. Müller**, Thiamine-based Enzymes for Biotransformations, book published by: Wiley-VCH Verlag GmbH & Co. KGaA, Weinheim, 2010.

170. **P. Dünkelmann and M. Müller**, Enzymatic C-C coupling in the synthesis of fine chemicals. *Speciality Chemicals Magazine*, 2011, 16-17.

171. **M. Pohl, C. Dresen, M. Beigi and M. Müller**, book section: Acyloin and Benzoin Condensations, in: Enzyme Catalysis in Organic Synthesis, published by: John Wiley & Sons Inc., 2012, pp. 919-945.

172. **M. Müller**, Recent Developments in Enzymatic Asymmetric C-C Bond Formation. *Adv. Synth. Catal.*, 2012, 354, 3161-3174.

173. **K. Chandra Raj, L. O. Ingram and J. A. Maupin-Furlow**, Pyruvate decarboxylase: a key enzyme for the oxidative metabolism of lactic acid by *Acetobacter pasteurianus*. *Archives of microbiology*, 2001, 176, 443-451.

174. **D. Rother, G. Kolter, T. Gerhards, C. L. Berthold, E. Gauchenova, M. Knoll, J. Pleiss, M. Müller, G. Schneider and M. Pohl**, *S*-Selective Mixed Carboligation by Structure-Based Design of the Pyruvate Decarboxylase from *Acetobacter pasteurianus*. *ChemCatChem*, 2011, 3, 1587-1596.

175. **T. Gerhards, U. Mackfeld, M. Bocola, E. von Lieres, W. Wiechert, M. Pohl and D. Rother**, Influence of Organic Solvents on Enzymatic Asymmetric Carboligations. *Adv. Synth. Catal.*, 2012, 354, 2805-2820.

176. **D. M. Chipman, R. G. Duggleby and K. Tittmann**, Mechanisms of acetohydroxyacid synthases. *Current opinion in chemical biology*, 2005, 9, 475-481.

177. **J. McCourt and R. Duggleby**, Acetohydroxyacid synthase and its role in the biosynthetic pathway for branched-chain amino acids. *Amino Acids*, 2006, 31, 173-210.

178. **S. Engel, M. Vyazmensky, D. Berkovich, Z. Barak and D. M. Chipman**, Substrate range of acetohydroxy acid synthase I from *Escherichia coli* in the stereoselective synthesis of α-hydroxy ketones. *Biotechnology and bioengineering*, 2004, 88, 825-831.

179. **S. Engel, M. Vyazmensky, S. Geresh, Z. e. Barak and D. M. Chipman**, Acetohydroxyacid synthase: A new enzyme for chiral synthesis of *R*-phenylacetylcarbinol. *Biotechnology and bioengineering*, 2003, 83, 833-840.

180. **P. N. Chien, J.-Y. Moon, J.-H. Cho, S.-J. Lee, J.-S. Park, D.-E. Kim, Y. Park and M.-Y. Yoon**, Characterization of acetohydroxyacid synthase I from *Escherichia coli* K-12 and identification of its inhibitors. *Biosci., Biotechnol., Biochem.*, 2010, 74, 2281-2286.

181. **P. Hinrichsen, I. Gomez and R. Vicuña**, Cloning and sequencing of the gene encoding benzaldehyde lyase from *Pseudomonas fluorescens* biovar I. *Gene*, 1994, 144, 137-138.

182. **E. Janzen, M. Müller, D. Kolter-Jung, M. M. Kneen, M. J. McLeish and M. Pohl**, Characterization of benzaldehyde lyase from *Pseudomonas fluorescens*: A versatile enzyme for asymmetric C–C bond formation. *Bioorg. Chem.*, 2006, 34, 345-361.

183. **A. S. Demir, M. Pohl, E. Janzen and M. Müller**, Enantioselective synthesis of hydroxy ketones through cleavage and formation of acyloin linkage. Enzymatic kinetic resolution via C–C bond cleavage. *J. Chem. Soc., Perkin Trans. 1*, 2001, 633-635.

184. **Á. G. Baraibar**, Thesis, Development of a Biocatalytic Production Process for (*S*)-α-Hydroxy Ketones, Heinrich-Heine University Düsseldorf, 2013

185. **D. Kihumbu, T. Stillger, W. Hummel and A. Liese**, Enzymatic synthesis of all stereoisomers of 1-phenylpropane-1,2-diol. *Tetrahedron: Asym.*, 2002, 13, 1069-1072.

186. **J. Kulig, A. Frese, W. Kroutil, M. Pohl and D. Rother**, Biochemical characterization of an alcohol dehydrogenase from *Ralstonia* sp. *Biotechnol. Bioeng.*, 2013.

187. **J. Kulig, R. C. Simon, C. A. Rose, S. M. Husain, M. Häckh, S. Lüdeke, K. Zeitler, W. Kroutil, M. Pohl and D. Rother**, Stereoselective synthesis of bulky 1, 2-diols with alcohol dehydrogenases. *Catal. Sci. Technol.*, 2012, 2, 1580-1589.

188. **S. Leuchs and L. Greiner**, Continuous Biocatalytic Synthesis of Enantiopure Alcohols with Integrated Product Separation. *Chem. Biochem. Eng. Q.*, 2011, 25, 267-281.

189. **L. Kulishova, K. Dimoula, M. Jordan, A. Wirtz, D. Hofmann, B. Santiago-Schübel, J. Fitter, M. Pohl and A. C. Spiess**, Factors influencing the operational stability of NADPH-dependent alcohol dehydrogenase and an NADH-dependent variant thereof in gas/solid reactors. *J. Mol. Catal. B: Enzym.*, 2010, 67, 271-283.

190. **T. Daußmann, T. C. Rosen and P. Dünkelmann**, Oxidoreductases and hydroxynitrilase lyases: complementary enzymatic technologies for chiral alcohols. *Eng. Life Sci.*, 2006, 6, 125-129.

191. **I. Lavandera, G. Oberdorfer, J. Gross, S. de Wildeman and W. Kroutil**, Stereocomplementary asymmetric reduction of bulky–bulky ketones by biocatalytic hydrogen transfer. *Eur. J. Org. Chem.*, 2008, 2008, 2539-2543.

192. **M. S. Humble, K. E. Cassimjee, M. Hakansson, Y. R. Kimbung, B. Walse, V. Abedi, H. J. Federsel, P. Berglund and D. T. Logan**, Crystal structures of the *Chromobacterium violaceum* omega-transaminase reveal major structural rearrangements upon binding of coenzyme PLP. *FEBS J.*, 2012, 279, 779-792.

193. **C. Sayer, M. N. Isupov, A. Westlake and J. A. Littlechild**, Structural studies of Pseudomonas and Chromobacterium-aminotransferases provide insights into their differing substrate specificity. *Acta Crystallogr., Sect D: Biol. Crystallogr.*, 2013, 69, 564-576.

194. **M. S. Humble, K. E. Cassimjee, V. Abedi, H.-J. Federsel and P. Berglund**, Key Amino Acid Residues for Reversed or Improved Enantiospecificity of an ω-Transaminase. *ChemCatChem*, 2012, 4, 1167-1172.

195. **S. Schätzle, F. Steffen-Munsberg, A. Thontowi, M. Höhne, K. Robins and U. T. Bornscheuer**, Enzymatic Asymmetric Synthesis of Enantiomerically Pure Aliphatic, Aromatic and Arylaliphatic Amines with (*R*)-Selective Amine Transaminases. *Adv. Synth. Catal.*, 2011, 353, 2439-2445.

196. **http://www.enzymicals.com/Enzymicals_Enzymes_v011.pdf**.

197. **E. Ricca, B. Brucher and J. H. Schrittwieser**, Multi-Enzymatic Cascade Reactions: Overview and Perspectives. *Adv. Synth. Catal.*, 2011, 353, 2239-2262.

198. **F. Lopez-Gallego and C. Schmidt-Dannert**, Multi-enzymatic synthesis. *Curr. Opin. Chem. Biol.*, 2010, 14, 174-183.

199. **S. F. Mayer, W. Kroutil and K. Faber**, Enzyme-initiated domino (cascade) reactions. *Chem. Soc. Rev.*, 2001, 30, 332-339.

200. **P. A. Santacoloma, G. r. Sin, K. V. Gernaey and J. M. Woodley**, Multienzyme-catalyzed processes: next-generation biocatalysis. *Org. Process Res. Dev.*, 2010, 15, 203-212.

201. **I. Oroz-Guinea and E. García-Junceda**, Enzyme catalysed tandem reactions. *Curr. Opin. Chem. Biol.*, 2013.

202. **B.-G. Kim, J.-H. Ahn, G. Sello, P. Di Gennaro, T. van Herk, A. F. Hartog, R. Wever, I. Oroz-Guinea, I. Sánchez-Moreno and E. García-Junceda**, Tandem and Sequential Multi-Enzymatic Syntheses, book section in: Practical Methods for Biocatalysis and Biotransformations 2, published by: John Wiley & Sons Inc., 2012, pp. 313-345.

203. **E. Garcia-Junceda**, Multi-step enzyme catalysis, book published by: John Wiley & Sons Inc., 2008.

204. **L. F. Tietze, G. Brasche and K. Gericke**, Domino reactions in organic synthesis, book published by: John Wiley & Sons Inc., 2006.

205. **S. F. Mayer, W. Kroutil and K. Faber**, Enzyme-initiated domino (cascade) reactions. *Chem. Soc. Rev.*, 2001, 30, 332-339.

206. **J. H. Schrittwieser, J. Sattler, V. Resch, F. G. Mutti and W. Kroutil**, Recent biocatalytic oxidation-reduction cascades. *Curr. Opin. Chem. Biol.*, 2011, 15, 249-256.

207. **A. Bruggink, R. Schoevaart and T. Kieboom**, Concepts of nature in organic synthesis: cascade catalysis and multistep conversions in concert. *Org. Process Res. Dev.*, 2003, 7, 622-640.

208. **M. J. Climent, A. Corma, S. Iborra, M. Mifsud and A. Velty**, New one-pot multistep process with multifunctional catalysts: decreasing the E factor in the synthesis of fine chemicals. *Green Chem.*, 2010, 12, 99-107.

209. **M. Cavazzuti**, Design of Experiments, book section in: Optimization Methods, published by: Springer Publishing, 2013, pp. 13-42.

210. **R. Baragona, F. Battaglia and I. Poli**, Design of Experiments, book section in: Evolutionary Statistical Procedures, published by: Springer Publishing, 2011, pp. 125-157.

211. **D. Silverstein, P. Samuel and N. Decarlo**, Design of Experiments, book published by: John Wiley & Sons Inc., 2009.

212. **N. A. G. Cressie**, Statistics for Spatial Data, Revised Edition, book published by: John Wiley & Sons Inc., 1993.

213. **M. Sherman**, Spatial Statistics and Spatio-Temporal Data: Covariance Functions and Directional Properties, book published by: John Wiley & Sons Inc., 2010.

214. **D. Rother, M. Pohl, T. Sehl and Á. G. Baraibar**, 2-Schritt Synthese zur Herstellung von (1*S*,2*S*)-Norpseudoephedrin (Cathine) durch Kopplung einer (*S*)-selektiven Lyase und einer (*S*)-selektiven Transaminase, german patent: 10 2013 009 631.6, 2013

215. **D. Rother, M. Pohl and T. Sehl**, 2-Schritt Synthese zur Herstellung von (1*S*,2*S*)-Norpseudoephedrin (Cathine) durch Kopplung einer (*S*)-selektiven Transaminase und einer (*S*)-selektiven Alkoholdehydrogenase., german patent: 10 2013 009 145.4, 2013

216. **M. Breuer, M. Pohl, B. Hauer and B. Lingen**, High-throughput assay of (*R*)-phenylacetylcarbinol synthesized by pyruvate decarboxylase. *Anal. Bioanal. Chem.*, 2002, 374, 1069-1073.

217. **P. Tufvesson, J. Lima-Ramos, M. Nordblad and J. M. Woodley**, Guidelines and Cost Analysis for Catalyst Production in Biocatalytic Processes. *Org. Process Res. Dev.*, 2010, 15, 266-274.

Acknowledgements

A wonderful period of my life comes to an end with this thesis. Thus, I would like to thank those, who contributed to the success of the work.

My special thanks go to my both supervisors, Prof. Dr. Martina Pohl and Dr. Dörte Rother for giving me the chance to work on this interesting and novel topic within their working group. Moreover, I want to thank both for their excellent assistance, various constructive discussions and for their instructive input to the scientific publications. Beside this, I am really grateful that I was introduced to their scientific network and that I had the opportunity to attend a lot of conferences, where I met so many interesting people in the scientific area.

I am also greatly indebted to Prof. Dr. Jörg Pietruszka, who not only consented to take over the position as co-referee, but also for all the helpful and informative discussion at any time and especially at the events of the CLIB Graduate Cluster.

During my stay abroad in London at our cooperation partner Prof. Helen C. Hailes and Prof. John M. Ward, I had one of the best and coincidentally intense times of my scientific career. I want to thank both for the great cooperation and in particular my friend and roommate Armando Cázares-Körner, who either worked with me till the security kicked us out in the night and/or introduced me to the pubs and nightlife in London together with all the other wonderful colleagues.

I thank as well the leader of the institute IBG-1: Biotechnology, Prof. Dr. Wolfgang Wiechert. With the help of Dr. Eric von Lieres I was able to perform a lot of experimental design and supported by the mathematical Kriging algorithm.

For the funding of my scholarship within the CLIB-Graduate Cluster Industrial Biotechnology, I thank the Ministry of Innovation, Science and Research of North Rhine-Westphalia and Heinrich-Heine-University Düsseldorf. I had a great time with all the fellows and am very grateful for the events and courses offered by the graduate cluster. I would also like to thank for the opportunity to assist in the organisation of the first CLIB-GC symposium as a student representative.

Embedded in my scholarship, I was able to do a three month industrial internship at the company DSM (Heerlen, Netherlands). I am obliged to the DSM for their financial support during this time and to Dr. Lavinia Panella and Dr. Martin Schürmann for their wonderful support in all matters. I should especially thank Dr. Martin Schürmann for

sharing his impression and thoughts on industrial biotechnology during our daily car rides from and to Jülich.

My current colleagues of the research group “Biocatalysis and Biosensors” always created a pleasant working atmosphere for fun, serious discussions and valuable ideas. Special thanks go to Heike Offermann, who supported me by carrying out a vast number of experiments and to Felix Maiwald for his performance in his bachelor project. I thank my former flat mate Justyna Kulig for the nightly, often controversial, sometime funny biotechnological and biochemical discussions. Moreover, I thank my dear colleague Tina Gerhards, who taught me in a hard school the usage of style and colours in presentations and elsewhere. Beside this, I thank my former colleagues and friends: Carmen Kocot, Daniel Okrob, Kerstin Spornhauer and Daniel Minör.

"A healthy mind lives in a healthy body”; that was known already by the ancient Romans, who shaped the emergence of Iuliacum (Jülich). The *Betriebssport-gemeinschaft Jülich* and their kind members provided diverse sports for body and mind in an enjoyable atmosphere. Here especially, I would like to thank the football team IBOC/IBG-1 who welcomed me as a young student and allowed to share the philosophy of a fair, healthy sportsman(woman)ship as team leader later on. I also consider myself to Jochen Wachtmeister, who introduced me to the 4^{th} dimension on the squash field.

Finally, and most importantly, I would like to thank my friends and family for their excellent support, their patience and undeterred kindheartedness. I thank my brothers Florian, Dominik and Benjamin for their tolerance to prolonged academic lectures e.g. during the annual Christmas dinners, my father for his trustworthy support and my mother for her internal goodness. A special thanks goes as well to my grandma Christine Sehl, my aunt and uncle, my three cousins and the nine children of the “next” generation, who give me a support to believe in the crazy things we do in our labs. An exceptionally big thank goes to my dear grandparents, Marga Drese for her honesty, her down-to-earthness and for the many cakes she baked and to Otto Drese for his unique consistency, his love and good nature, that I will always take as an example to me in my life.

Appendix

I.) Syntheses of reference substances

The syntheses of (1*R*,2*R*)-1-amino-1-phenylpropane-2-ol (APP) was performed in two reaction steps according to the literature. In the first reaction step, Sharpless asymmetric aminohydroxylation[1], (4*R*,5*R*)-5-methyl-4-phenyloxazolidin-2-one is synthesised. The subsequent oxazolidinone hydrolysis[2] results in the formation of (1*R*,2*R*)-APP with an *ee* of ~80 %.

I.a) Sharpless asymmetric aminohydroxylation[1]

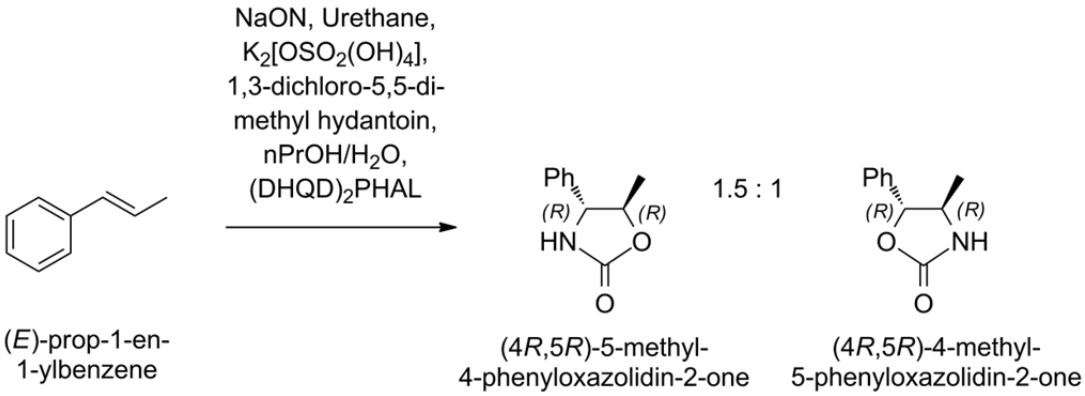

NaOH (26 mmol, 1045 mg) were dissolved in 47 mL distilled water in a 250 mL round-bottom flask. Potassium-osmate-(VI)-oxide-hydrate (0.2 mmol 72.0 mg) was solved in 2 mL of the 0.5 M NaOH solution. 1-propanol (23.4 mL), urethane (26 mmol, 2.40 g) and 1,3-dichloro-5,5-dimethylhydantoin (13 mmol, 2.61 g) were added to the remaining NaOH solution. (*E*)-prop-1-en-1-ylbenzene (8.45 mmol, 998.6 mg) and $DHQD_2$(PHAL) (0.2 mmol, 152 mg) was taken up in 1-propanol (7 mL). The solution was added to the 0.5 M NaOH solution and then potassium osmate solution added. The solution was stirred for 4 hours at room temperature and then NaOH (26 mmol, 1045 mg) was added. After 30 min of stirring, 25 mL H_2O was added. The solution was extracted three times with ethyl acetate (50 mL). The organic layers were combined and dried over magnesium sulphate. The crude product was purified via chromatography (silica, 70 : 30, cyclohexane : ethyl acetate) to separate the regioisomers. (4*R*,5*R*)-5-methyl-4-phenyloxazolidin-2-one was obtained in a yield of 53.4 % (4.52 mmol, 803 mg).

(4*R*,5*R*)-5-methyl-4-phenyloxazolidin-2-one:
^{1}H-NMR (600 MHz, $CDCl_3$): 1.50 (d, $^3J_{1,2}$ = 5.7 Hz, 3 H, 1-H), 4.44 (m, 2 H, 2-H, 3-H), 5.54 (s, 1 H, N-H), 7.24-7.45 (m, 5 H, arom.-H). The NMR data are in accordance to the literature data.[1]

I.b) Oxazolidinone hydrolysis[2]

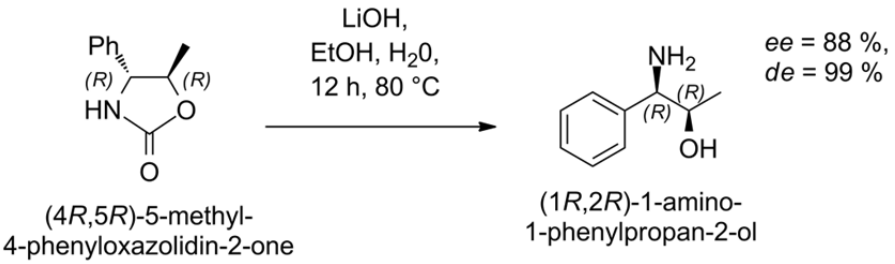

(4*R*,5*R*)-5-methyl-4-phenyloxazolidin-2-one (2.1 mmol, 365 mg) of the Sharpless asymmetric aminohydroxylation product was dissolved in 36 mL ethanol and 15 mL distilled water. Lithium hydroxide (61.8 mmol, 1.48 g) was added. The reaction was heated up to 90 °C and heated under reflux for 12 h. The organic solvent was evaporated under reduced pressure and then three times extracted with 30 mL ethyl acetate. The organic layers were combined, dried over magnesium sulphate and then concentrated under reduced pressure. The product was purified via chromatography (silica, 50 : 50 = methanol : chloroform). (1*R*,2*R*)-1-amino-1-phenylpropane-2-ol was obtained in a yield of 93 % (1.95 mmol, 295 mg).

(1*R*,2*R*)-1-amino-1-phenylpropane-2-ol:
^{1}H-NMR (600 MHz, $CDCl_3$): 1.04 (d, $^{3}J_{1,2}$ = 6.0 Hz, 3 H, 1-H), 2.22 (brs, 3 H, NH_2, OH), 3.55 (d, $^{3}J_{3,2}$ = 7.9 Hz, 3-H), 3.75 (dq, $^{3}J_{2,1}$ = 6.0 Hz, $^{3}J_{2,3}$ = 7.9 Hz, 2-H), 7.25-7.36 (m, 5 H, arom.-H). Spectroscopic data are in agreement with those published previously.[2] The optical purity was determined by chiral HPLC: *ee* = 79.3 % (Daicel CROWNPAK® CR(+) Analytical Column, eluent: H_2O/H_3PO_4 pH 2, 0.4 mL min^{-1}. (1*R*,2*R*)-APP: 20.8 min, (1*S*,2S)-APP: 19.5 min)

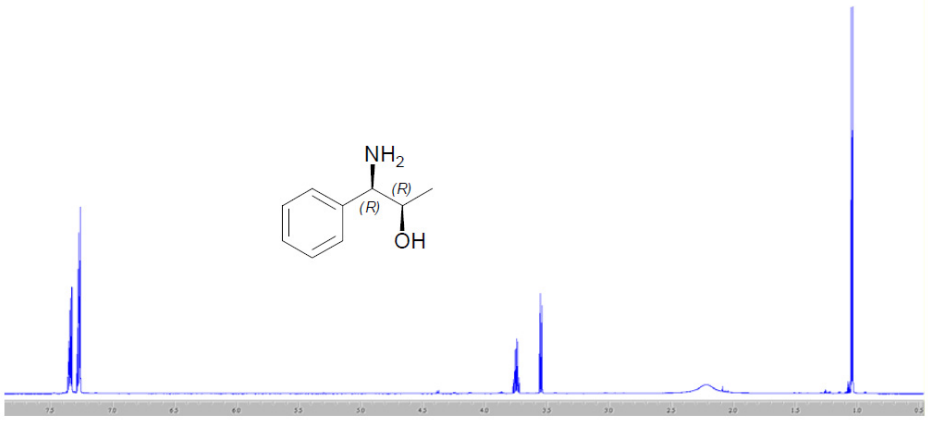

References:

1. **N. S. Barta, D. R. Sidler, K. B. Somerville, S. A. Weissman, R. D. Larsen and P. J. Reider**, Practical modifications and applications of the sharpless asymmetric aminohydroxylation in the one-pot preparation of chiral oxazolidin-2-ones. *Org. Lett.*, 2000, 2, 2821-2824.
2. **S. J. Katz and S. C. Bergmeier**, Convenient methods for the hydrolysis of oxazolidinones to vicinal aminoalcohols. *Tetrahedron Lett.*, 2002, 43, 557-559.

II.) Cloning strategy, gene- and protein sequences of unpublished enzymes

II.a) ω-transaminase Sery1824

Cloning strategy

The coding region of the transaminases Sery1824 was cloned by our cooperation partner into the vector pET-29a vector (Novagen) using the *Nde*I restriction sites at the N-terminus and *Xho*I sites at the C-terminus. The manual was performed like described for the construction of the expression vector for the enzyme CV2025 from *Chromobacterium violaceum* previously.[103]

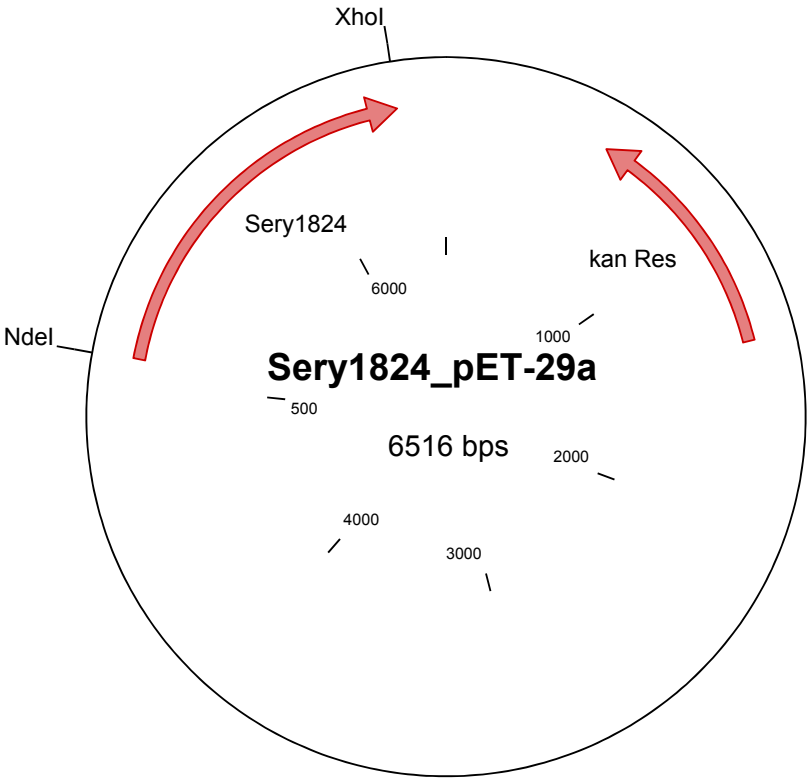

Gene sequence:

```
ATGTCGGCATCGGCCAGTCCGGACACGACCAGCACCCGGCTGTGGCACCCGTTCGCGAACATGGCGGACGTGAAGAACCAGGCCTTCCTGGTGG
ACCGCGCCGAGGGGGTGTGGGTCTACGACCAGGACGGGCGGCAGTACCTGGACGCCACCGCGAGCCTCTGGTACGTCAACATCGGACACGGCAG
GCGCGAGATCGCCGACGCCGTCGCCGCCCAGATGAGCAGGCTCGACGCGTTCAACGTCTTCAACGACTACACCAACCGGCCCGCCGAGGAGCTG
GCCGCCCGCCTGGCCGCGCTGGCGCCGATGGACGACGCGCGGGTGTTCTTCACCTCCGGCGGCGCCGACTCCATCGAGACCGCCGCGAAGCTGG
CCCGGTTGTACTGGGTCAACCGCGGGCAGCCGCAGCGCACCCACCTGCTCAGCCGCGGGCAGGCCTACCACGGCACCCACGGCGTGGGCACGAG
CATCGCGGGCATCCAGGCCAACCGGGACGGCTTCGGCGAGATGATCGCCGACACCACGCGGGTCTCCAACGAGGACCCCGAGGACCTGCGGGAC
GCGATCGAGCGGCTCGGCGCCGACCGGGTCGCCGCCTTCTTCGCCGAACCGGTGATCGGCGCGGGCGGGCTCATCCCGCCCAAGCCGGGATACC
TGGAGGCGGTCGCCAAGATCTGCCGCGAGTACGACGTGCTGTTCGTGGCCGACGAGGTCATCTGCGGTTTCGGCCGCCTCGGGCACTGGTTCGG
CTCGCAGCGCTTCGACCTGCGCCCGGACCTGATCACCTTCGCCAAGGGCGTCACCAGCGGCTACCTCCCACTCGGCGGGGTCATCGCGGCGGGC
TCGGTCGCCGAGCCGTTCTGGACCGACGGCGGCAGGCCGTTCCGGCACGGCCCCACCTACTCCGGGCACCCGACGGTGGCCGCCGCGGCGCTGG
CGAACCTCGACATCCTGGAACGGGAGGACCTGCTGGGCCGCTCCCGCGAGCTTGAGCAACCGCTGTTCGACGTGCTGCGGTCGCTCACCGACCA
CCCCGCCGTCAGCGAGGCCCGCGGCGGTGTGGGCCTGCTGGGCGCGGTGGAGCTCGACGCCGCACTGCTGGCCGAGGAACCCGGGCTGGTTCTG
CGCGCGCACCAGGCGATCCGCGCCGCCGGTGTCATCACCCGCCCGCTGGGCAGCGCACTGGCGGTCTCCCCGCCGCTGACGATCACGACGGAGC
AGGTCGACCTCATCGGCCAGGGCATCCGCGCCGGGCTGGACGCGACGCTGTCCTGA
```

Protein sequence:

```
MSASASPDTTSTRLWHPFANMADVKNQAFLVDRAEGVWVYDQDGRQYLDATASLWYVNIGHGRREIADAVAAQMSRLDAFNVFNDYTNRPAEEL
AARLAALAPMDDARVFFTSGGADSIETAAKLARLYWVNRGQPQRTHLLSRGQAYHGTHGVGTSIAGIQANRDGFGEMIADTTRVSNEDPEDLRD
AIERLGADRVAAFFAEPVIGAGGLIPPKPGYLEAVAKICREYDVLFVADEVICGFGRLGHWFGSQRFDLRPDLITFAKGVTSGYLPLGGVIAAG
SVAEPFWTDGGRPFRHGPTYSGHPTVAAAALANLDILEREDLLGRSRELEQPLFDVLRSLTDHPAVSEARGGVGLLGAVELDAALLAEEPGLVL
RAHQAIRAAGVITRPLGSALAVSPPLTITTEQVDLIGQGIRAGLDATLS
```

II.b) ω-transaminase Sery4673

Cloning strategy

The coding region of the transaminases Sace4673 was cloned by our cooperation partner into the vector pET-29a vector (Novagen) using the *Nde*I restriction sites at the N-terminus and *Xho*I sites at the C-terminus. The manual was performed like described for the construction of the expression vector for the enzyme CV2025 from *Chromobacterium violaceum* previously.[103]

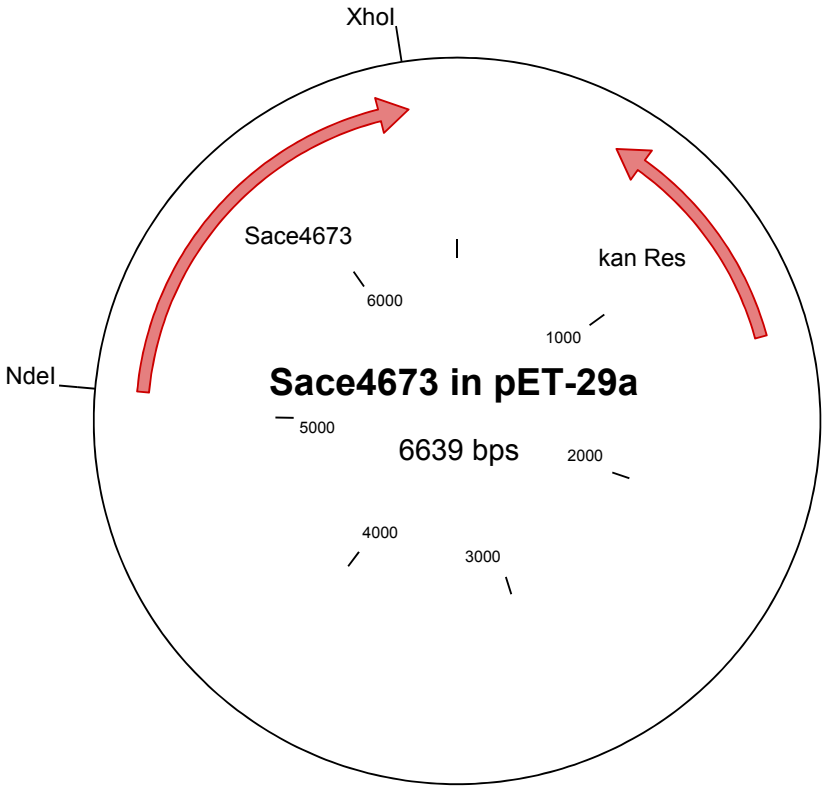

Gene sequence:

```
ATGACCACGCTCGACAACGCCACCGCACCGTCCACATCGCAAACCCCGGCCGCCGAGTCCGCCGCGCGCCACCTCTGGATGCACTTCGCCCGCA
TGGGCGGCCGAGGACCGGAGAACCCCGTCCCGGTCATCACCCGCGGCGAGGGCGTGCACCTCTGGGACGACCGCGGCCGACGCGTCCTCGACGG
CCTGGCCGGGCTGTTCGTGGTGCAGGCCGGCCACGGCCGCCGCGAGCTGGCCGAGGTGGCCGCCCGCCAGGCCTGCGAGCTCGCCTACTTCCCG
GTGTGGGGCTACGCCACTCCGCCGGCGGCCGAGCTCGCCGAGCGCCTGGCCCACCTCGCCCCGGGCGACCTCAACCGCGTCTTCTTCTCACCTCCG
GCGGAGGCGAAGCCGTCGAGTCGGCCTGGAAGGTCGCCAAGCAGTACTTCAAGCTCGTCGGAAAACCGCTGAAGCACAAGGTGATCAGCCGGTC
CGTGGCCTACCACGGCACACCGCACGGCGCGATGGCCATCACCGGGCTGCCGAAGATGAAGCAGGACTTCGAGCCGCTGGCCCCGGGCGGTTTC
CGGGTGCCCAACACCAACATCTACCGGAACCCCGAGTTCGCCGGCGACCCGGAGGCGTTCGGCCGCTGGGCCGCCGACCGCGTCGAGGAGGCCA
TCCTCTTCGAGGGTCCCGACACGGTGGCCGCCGTCGTGCTCGAGCCGGTGCAGAACTCCGGCGGATGCCTGACCGCGCCCCCGAGCTACTTCGC
GCGGGTCCGCGAGATCTGCGACCGCCACGACGTGCTGCTGGTCTCCGACGAGGTCATCTGCGCGTTCGGCAGGCACGGCCACACCTTCGCCTGC
GACAAGTTCGGCTACGTGCCCGACCTGATCACCTGCGCGAAGGGCATGACCTCCGGCTACGGCCCGCTCGGAGCGCTGATCGCCTCCGACCGCG
TGATGGAACCGTTCCTGCGGCCCGGCGTCACCTTCCCCCACGGCTACACCTGGGGCGGCCACCCCGTCTCGGCGGCCGTCGCGCTCGCCAATCT
CGAGCTGATGGCGGAGGAAGGACTGCACCAGCGGGTTCTGGACAACGAGCGGGCGTTCGGCGAGACGCTCGGCAAGCTGCTGGACCTGCCGATC
GTCGGCGACGTCCGCGGCGACGGGTACTTCTGGGCCGTCGAGCTGGTCAAGGACAAGGCCACCCGCGAGACCTTCGACGCCGACGAGCGGGAGC
GTCTGGTCCGCGGCTTCCTGCCCGGGGCCCTGTTCGACAACGGGCTGTACTGCCGCCCCGACGACCGCGGCGACGTCGTCGTCCAGCTCGCCCC
GCCGCTGATCGCCGGGCAGGCCGAGTTCGACGAGATCGAGGGCATCCTCCGGCACACGCTGCTCGAAGCCACGTCCGCCCTCTGA
```

Protein sequence:

```
MTTLDNATAPSTSQTPAAESAARHLWMHFARMGGRGPENPVPVITRGEGVHLWDDRGRRVLDGLAGLFVVQAGHGRRELAEVAARQACELAYFP
VWGYATPPAAELAERLAHLAPGDLNRVFFTSGGGEAVESAWKVAKQYFKLVGKPLKHKVISRSVAYHGTPHGAMAITGLPKMKQDFEPLAPGGF
RVPNTNIYRNPEFAGDPEAFGRWAADRVEEAILFEGPDTVAAVVLEPVQNSGGCLTAPPSYFARVREICDRHDVLLVSDEVICAFGRHGHTFAC
DKFGYVPDLITCAKGMTSGYGPLGALIASDRVMEPFLRPGVTFPHGYTWGGHPVSAAVALANLELMAEEGLHQRVLDNERAFGETLGKLLDLPI
VGDVRGDGYFWAVELVKDKATRETFDADERERLVRGFLPGALFDNGLYCRPDDRGDVVVQLAPPLIAGQAEFDEIEGILRHTLLEATSAL
```

II.c) ω-transaminase Sery1902

Cloning strategy

The coding region of the transaminases Sery1902 was cloned by our cooperation partner into the vector pET-29a vector (Novagen) using the *Nde*I restriction sites at the N-terminus and *Xho*I sites at the C-terminus. The manual was performed like described for the construction of the expression vector for the enzyme CV2025 from *Chromobacterium violaceum* previously.[103]

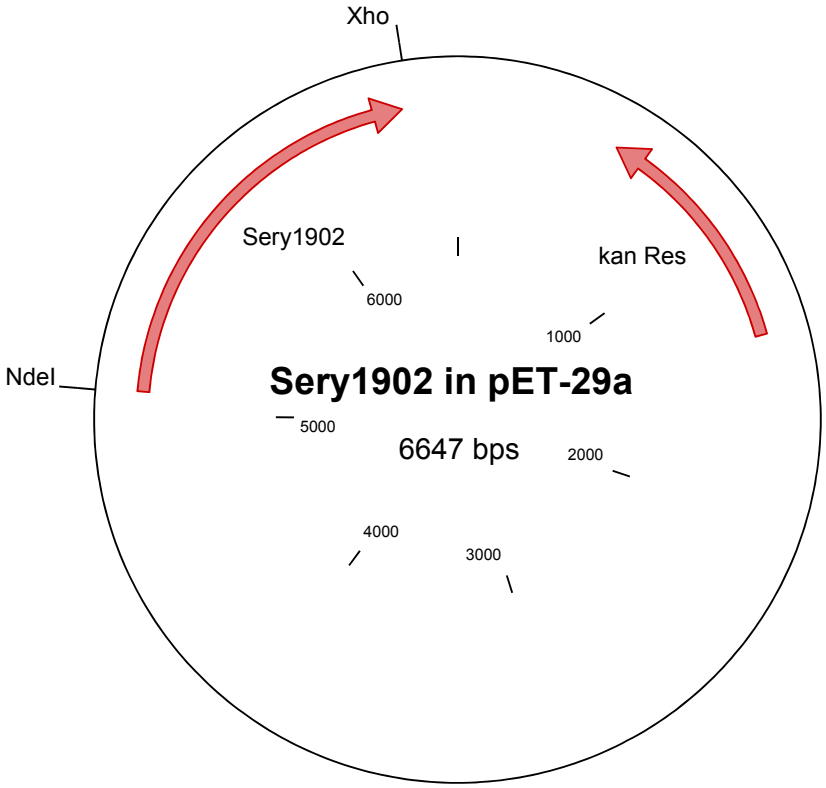

Gene sequence:

```
ATGACCGCGACGGAGAACCCCGCCGCCACCAGGACGCTCGGCGACCGAGCCCGCGACCACCTGTGGTTGCACTTCGCCCAGCACGCCGGCTACG
CCGACCGGGAGATCCCGGTGATCACCCGCGGCGAGGGCGCCTACGTCTACGACGAGCGCGGCAAGCGCTACCTCGACGGCCTGGCCGGGCTGTT
CGCGGTCCAGGTCGGCCACGGCCGCGAGGAGTTGGCGCTGGCCGCGGCCGAGCAGACCCGCAAGCTCGCCTACTTCCCGCTGTGGTCGCACGCG
CACCCCAGCGCCATCGAGCTCGCCGAGCGGATCGCCGCGCAGGCGCCGGGCGAGCTGAACCGGGTCTTCTTCACCGGAGGCGGCGGCGAGGCCG
TCGAAACCGCGTGGAAGCTGGCCAAGCAGTACTTCAAGAAGACCGGCAAGCCGACCAAGCACAAGGTGATCAGCCGCTCGCTGGCCTACCACGG
CACGTCGCAGGGTGCGCTGTCGATCACCGGCATCCCGGGCGCGAAGCAGGACTTCGAACCGCTGGTGCCCAGCGCCATCAAGGTGCCCAACACC
AACTTCTACCGCGCTCCCGAGCACGCCGGCGACTACGAGGCGTTCGGCCGGTGGGCCGCCGACCAGGTCGCGCTGGCCATCGAGATGGAGGGGC
CGGACACCGTGGCGGCGGTGTTCCTCGAACCGCTGCAGAACACCGGCGGCTGCTTCCCGCCGCCGCCCGGCTACTGGCAGCGGGTCCGCGAGAT
CTGCGACGCCTACGACGTCCTGCTGGTCTCCGACGAGGTGATCTGCGCATTCGGCCGCCTGGGGCACGACTTCGGCGCCAACCGCTACGGCTAC
CAGCCCGACATCATCACCACCGCCAAGGGCCTCACCTCCGGCTACGCGCCGCTGGGCGCGATGATCGCCGACGAACGGCTGATGCGGCCGTTCC
TGTCCGGCGGCAGCAGCTTCGCGCACGGCTCGACCTACGGCGGACATCCCGTCTCGTGCGCGGTGGCGATGGCCAACCTCGACGTCATGGAGTC
CGAGGACCTCTACGGCCGGGTGCTGTCCAACGAGGCGAACTTCCGCGCCACGCTGGAGAAGCTGCTCGACCTGCCGATCGTCGGCGACGTGCGC
GGGCAGGGCTACTTCTACGGCATCGAGCTGGTGAAGGACAAAGCGACCAAGGCGACCTTCACCCCGGACGACGCCGAGCGCGTGCTGCGCGGCT
ACGTCTCCGACGCACTGTTCGACGCCGGGCTCTACTGCCGCGCCGACGACCGCGCCGAACCGGTGATCCAGCTCGCGCCGCCGCTGATCTGCAC
CCAGGAGCACTTCGACGAGGTCGAGCAGATCCTGCGCTCGGTGCTGTCGGAGGCGTGGACGCGGCTGTGA
```

Protein sequence:

```
MTATENPAATRTLGDRARDHLWLHFAQHAGYADREIPVITRGEGAYVYDERGKRYLDGLAGLFAVQVGHGREELALAAAEQTRKLAYFPLWSHA
HPSAIELAERIAAQAPGELNRVFFTGGGGEAVETAWKLAKQYFKKTGKPTKHKVISRSLAYHGTSQGALSITGIPGAKQDFEPLVPSAIKVPNT
NFYRAPEHAGDYEAFGRWAADQVALAIEMEGPDTVAAVFLEPLQNTGGCFPPPPGYWQRVREICDAYDVLLVSDEVICAFGRLGHDFGANRYGY
QPDIITTAKGLTSGYAPLGAMIADERLMRPFLSGGSSFAHGSTYGGHPVSCAVAMANLDVMESEDLYGRVLSNEANFRATLEKLLDLPIVGDVR
GQGYFYGIELVKDKATKATFTPDDAERVLRGYVSDALFDAGLYCRADDRAEPVIQLAPPLICTQEHFDEVEQILRSVLSEAWTRL
```

II.d) ω-transaminase Sav4551

Cloning strategy

The coding region of the transaminases Sav4551 was cloned by our cooperation partner into the vector pET-29a vector (Novagen) using the *Nde*I restriction sites at the N-terminus and *Xho*I sites at the C-terminus. The manual was performed like described for the construction of the expression vector for the enzyme CV2025 from *Chromobacterium violaceum* previously.[103]

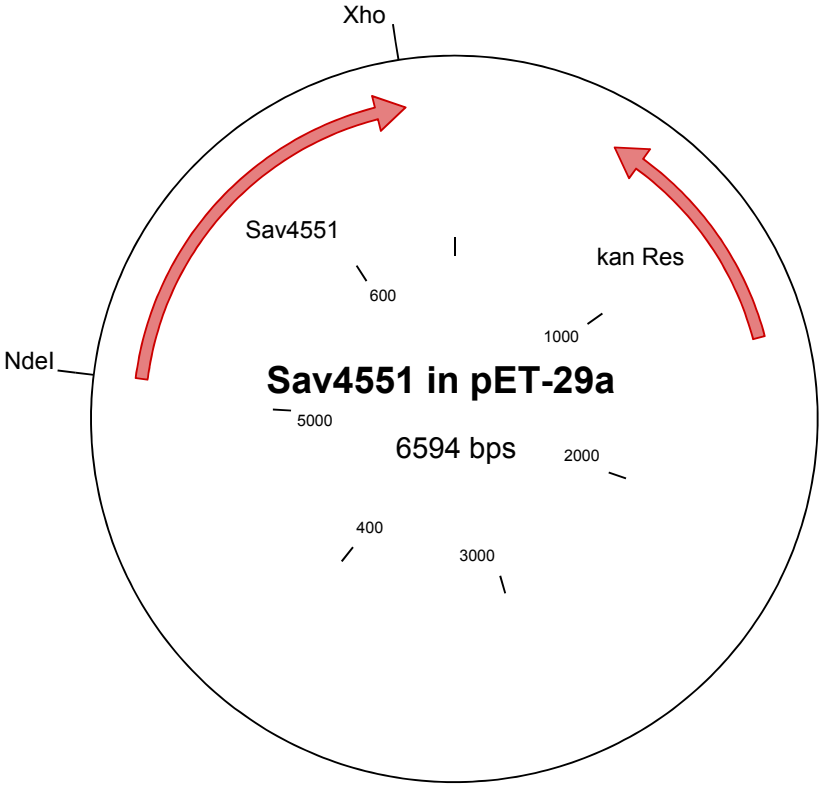

Gene sequence:

```
ATGACCCCTCAGCCGAATCCCCAGGTCGGTGCCGCCGTCAAGGCCGCGGACCGTGCGCATGTCTTCCACTCCTGGTCAGCGCAGGAGCTCATCG
ACCCGCTCGCCGTCGCCGGTGCGGAGGGGTCGTACTTCTGGGACTACGACGGCAGGCGGTACCTGGACTTCACCAGCGGACTCGTCTTCACCAA
CATCGGGTACCAGCACCCCAAGGTCGTCGCCGCCATTCAGGAGCAGGCCGCGAGCCTGACCACCTTCGCGCCCGCCTTCGCCGTCGAGGCGCGG
TCCGAGGCGGCCCGGCTCATCGCCGAGCGGACGCCCGGAGACCTCGACAAGATCTTCTTCACCAACGGCGGGGCCGACGCCATCGAGCACGCCG
TGCGCATGGCGCGGATACACACCGGGCGGCCCAAGGTGCTGTCCGCCTACCGCTCCTACCACGGTGGCACCCAGCAGGCCGTCAACATCACCGG
TGATCCGCGCCGCTGGGCCTCCGACAGCGCCTCGGCGGGCGTCGTGCACTTCTGGGCGCCGTACCTCTACCGGTCGCGCTTCTACGCGGAGACC
GAGCAGCAGGAGTGCGAGCGGGCGCTGGAGCACCTGGAGACGACCATCGCCTTCGAGGGGCCGGGCACGATCGCCGCGATCGTGCTGGAGACCG
TTCCGGGGACCGCGGGGATCATGGTTCCGCCGCCCGGATATCTCGCCGGGGTGCGTGAGCTGTGCGACAAGTACGGCATCGTCTTCGTCCTGGA
CGAGGTGATGGCCGGGTTCGGACGGACCGGTGAGTGGTTCGCCGCGGATCTCTTCGACGTCACACCCGACCTGATGACCTTCGCCAAGGGCGTG
AACTCCGGATATGTGCCGCTGGGCGGTGTCGCGATCTCCGGGAAGATCGCCGAGACCTTCGGGAAGCGGGCCTACCCGGGCGGTCTGACCTACT
CCGGGCATCCGCTCGGCTGCGCCGCCGCCGTCGCCACGATCAACGTCATGGCCGAGGAGGGGGTCGTCGAGAACGCGGCGAACCTCGGCGCCCG
GGTCATCGAGCCGGGGCTGCGCGAGCTGGCCGAGCGGCACCCGTCCGTGGGCGAGGTGCGCGGTGTCGGCATGTTCTGGGCGCTGGAGCTGGTC
AAGGACCGGGAGACGCGGGAGCCGCTGGTGCCGTACAACGCGGCGGGCGAGGCGAACGCGCCGATGGCCGCCTTCGGTGCCGCCGCCAAGGCGA
ACGGCCTGTGGCCGTTCATCAACATGAACCGCACGCACGTCGTGCCCCCGTGCAACGTCACGGAGGCCGAGGCCAAGGAAGGCCTGGCGGCCCT
CGACGCGGCCCTCTCGGTGGCGGACGAGTACACGGTTTAG
```

Protein sequence:

```
MTPQPNPQVGAAVKAADRAHVFHSWSAQELIDPLAVAGAEGSYFWDYDGRRYLDFTSGLVFTNIGYQHPKVVAAIQEQAASLTTFAPAFAVEAR
SEAARLIAERTPGDLDKIFFTNGGADAIEHAVRMARIHTGRPKVLSAYRSYHGGTQQAVNITGDPRRWASDSASAGVVHFWAPYLYRSRFYAET
EQQECERALEHLETTIAFEGPGTIAAIVLETVPGTAGIMVPPPGYLAGVRELCDKYGIVFVLDEVMAGFGRTGEWFAADLFDVTPDLMTFAKGV
NSGYVPLGGVAISGKIAETFGKRAYPGGLTYSGHPLACAAAVATINVMAEEGVVENAANLGARVIEPGLRELAERHPSVGEVRGVGMFWALELV
KDRETREPLVPYNAAGEANAPMAAFGAAAKANGLWPFINMNRTHVVPPCNVTEAEAKEGLAALDAALSVADEYTV
```

II.e) ω-transaminase Sav2612

Cloning strategy

The coding region of the transaminases Sav2612 was cloned by our cooperation partner into the vector pET-29a vector (Novagen) using the *Nde*I restriction sites at the N-terminus and *Xho*I sites at the C-terminus. The manual was performed like described for the construction of the expression vector for the enzyme CV2025 from *Chromobacterium violaceum* previously.[103]

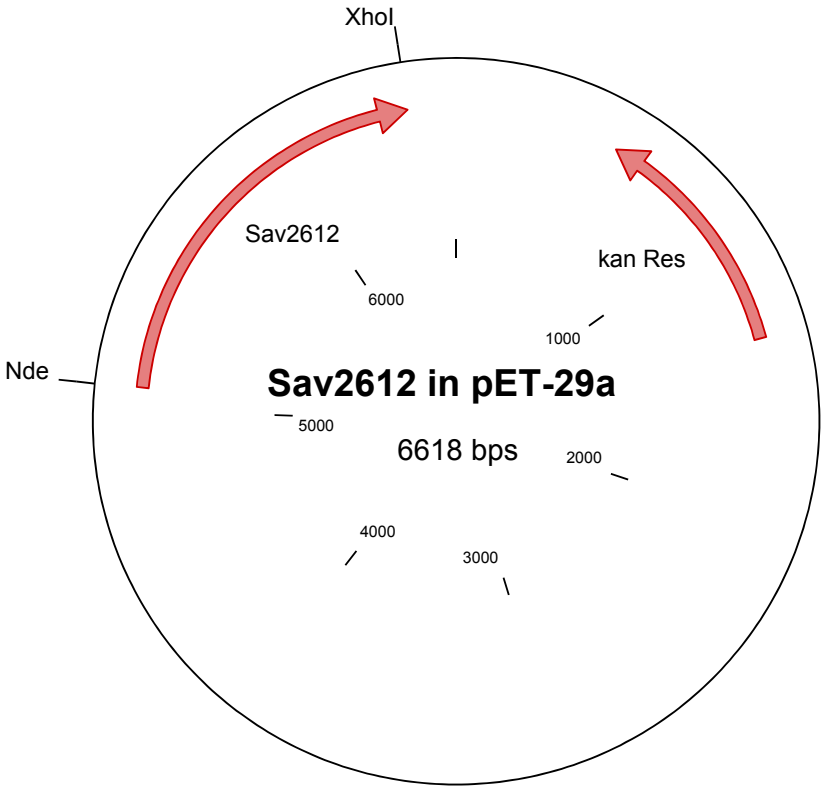

Gene sequence:

```
ATGGGGAACCCGATAGCCGTGAGCAAGGACCTCAGCCGAACCGCGTACGACCACCTGTGGATGCACTTCACCCGCATGTCCTCGTACGAGAACG
CGCCCGTTCCCACCATCGTCCGTGGTGAGGGCACCTACATCTACGACGACAAGGGCAAGCGCTACCTCGACGGTCTCTCGGGTCTGTTCGTGGT
CCAGGCGGGCCACGGCCGCACGGAGCTGGCGGAGACCGCGTTCAAGCAGGCTCAGGAACTGGCCTTCTTCCCGGTGTGGTCCTACGCCCACCCG
AAGGCCGTGGAACTGGCCGAGCGCCTTGCGAACTACGCCCCGGGCGACCTCAACAAGGTCTTCTTCACCACCGGCGGCGGCGAGGCGGTCGAGA
CCGCCTGGAAGCTCGCCAAGCAGTACTTCAAGCTCCAGGGCAAGCCGACCAAGTACAAGGTCATCTCGCGCGCGGTCGCCTACCACGGCACCCC
GCAGGGCGCCCTGTCCATCACCGGCCTGCCGGCCCTGAAGGCCCCCTTCGAGCCGCTGGTCCCGGGCGCCCACAAGGTCCCGAACACCAACATC
TACCGCGCCCCGCTCTTCGGCGACGACCCCGAGGCCTTCGGCCGCTGGGCCGCCGACCAGATCGAGCAGCAGATCCTCTTCGAGGGCCCGGAGA
CGGTCGCGGCCGTCTTCCTGGAGCCGGTGCAGAACGCCGGCGGCTGCTTCCCGCCGCCGCCCGGCTACTTCCAGCGCGTGCGCGAGATCTGCGA
CCAGTACGACGTGCTGCTGGTGTCGGACGAGGTCATCTGTGCCTTCGGCCGCCTCGGCACGATGTTCGCCTGCGACAAGTTCGGCTACGTACCG
GACATGATCACCTGCGCCAAGGGCATGACCTCGGGCTACTCCCCGATCGGCGCGTGCATCGTCTCCGACCGCATCGCCGAGCCGTTCTACAAGG
GCGACAACACCTTCCTGCACGGCTACACGTTCGGCGGCCACCCGGTCTCCGCCGCCGTGGGTGTCGCCAACCTCGACCTGTTCGAGCGCGAGGG
CCTCAACCAGCACGTGCTGGACAACGAGTCCGCGTTCCTCACGACGCTCCAGAAGCTGCACGACCTGCCGATCGTCGGCGACGTCCGCGGCAAC
GGCTTCTTCTACGGCATCGAGCTGGTGAAGGACAAGGCCACCAAGGAGACGTTCACGGACGAGGAGTCGGAGCGCGTGCTCTACGGCTTCGTCT
CCAAGAAGCTCTTCGAGTACGGCCTCTACTGCCGCGCCGACGACCGCGGTGACCCGGTCATCCAGCTGTCGCCGCCGCTGATCTCCAACCAGTC
GACCTTCGACGAGATCGAATCGATCATCCGGCAGGTGCTGACGGAGGCGTGGACGAAGCTCTGA
```

Protein sequence:

```
MGNPIAVSKDLSRTAYDHLWMHFTRMSSYENAPVPTIVRGEGTYIYDDKGKRYLDGLSGLFVVQAGHGRTELAETAFKQAQELAFFPVWSYAHP
KAVELAERLANYAPGDLNKVFFTTGGGEAVETAWKLAKQYFKLQGKPTKYKVISRAVAYHGTPQGALSITGLPALKAPFEPLVPGAHKVPNTNI
YRAPLFGDDPEAFGRWAADQIEQQILFEGPETVAAVFLEPVQNAGGCFPPPPGYFQRVREICDQYDVLLVSDEVICAFGRLGTMFACDKFGYVP
DMITCAKGMTSGYSPIGACIVSDRIAEPFYKGDNTFLHGYTFGGHPVSAAVGVANLDLFEREGLNQHVLDNESAFLTTLQKLHDLPIVGDVRGN
GFFYGIELVKDKATKETFTDEESERVLYGFVSKKLFEYGLYCRADDRGDPVIQLSPPLISNQSTFDEIESIIRQVLTEAWTKL
```

II.f) ω-transaminase Sco5655

Cloning strategy

The coding region of the transaminases Sco5655 was cloned by our cooperation partner into the vector pET-29a vector (Novagen) using the *Xho*I restriction sites at the N-terminus and *Xho*I sites at the C-terminus. The manual was performed like described for the construction of the expression vector for the enzyme CV2025 from *Chromobacterium violaceum* previously.[103]

Gene sequence:

```
ATGAGCACCGACAGCCCCAAGGACCTCAGCCGGACCGCCTACGACCACCTGTGGATGCACTTCACCCGCATGTCGTCGTACGAGAACGCCCCCG
TCCCCACCATCGTCCGCGGTGAGGGCACCCACATCTACGACGACAAGGGCAGGCGCTACCTCGACGGTCTCGCCGGCCTGTTCGTGGTCCAGGC
CGGACACGGCCGCCAGGAGCTCGCGGAGACCGCCTCCAAGCAGGCGCAGGAGCTCGCCTTCTTCCCGGTGTGGTCCTACGCCCACCCCAAGGCC
GTCGAGCTGGCCGAGCGGCTGGCCAACGAGGCCCCCGGCGACCTCAACAAGGTCTTCTTCACCACCGGCGGCGGCGAGGCGGTGGAGACCGCCT
GGAAGCTCGCCAAGCAGTACTTCAAGCTGACCGGCAAGCCCACCAAGTACAAGGTGATCTCCCGCGCGGTGGCCTACCACGGCACCCCGCAGGG
CGCCCTGTCCATCACCGGCCTGCCCGCCCTGAAGGCTCCCTTCGAGCCGCTGGTCCCCGGCGCGCACAAGGTGCCGAACACCAACATCTACCGC
GCCCCGATCCACGGCGACGACCCCGAGGCCTACGGCCGCTGGGCCGCCGACCAGATCGAGCAGCAGATCCTGTTCGAGGGTCCGGAGACCGTCG
CGGCGGTCTTCCTTGAGCCGGTGCAGAACGCGGGCGGCTGCTTCCCGCCCCCGCCCGGCTACTTCCAGCGGGTGCGCGAGATCTGCGACCAGTA
CGACGTACTGCTCGTCTCGGACGAGGTCATCTGCGCCTTCGGCCGCCTGGGCACCACCTTCGCCTGCGACAAGTTCGGCTACGTCCCGGACATG
ATCACCTGCGCCAAGGGCATGACCTCGGGCTACTCCCCGATCGGCGCCTGCGTCATCTCCGACCGCCTGGCCGAGCCCTTCTACAAGGGCGACA
ACACCTTCCTGCACGGCTACACCTTCGGCGGCCACCCGGTCTCCGCCGCGGTCGGCATCGCCAACCTCGACCTCTTCGAGCGCGAGGGCCTCAA
CCAGCACGTGCTGGACAACGAGGGCGCCTTCCGCGCCACCCTGGAGAAGCTGCACGACCTGCCGATCGTCGGCGACGTCCGCGGCAACGGCTTC
TTCTACGGCATCGAGCTGGTGAAGGACAAGGCCACCAAGGAGTCCTTCGACGAGGAGGAGACCGAGCGCGTCCTGTACGGCTTCCTCTCCAAGA
AGCTCTTCGAGAACGGCCTGTACTGCCGTGCCGACGACCGCGGCGACCCGGTCATCCAGCTCGCCCCGCCGCTGATCTCCAACCAGGAGACCTT
CGACGAGATCGAGCAGATCCTGCGCGCCACGCTGACGGAGGCGTGGACGAAGCTCTGA
```

Protein sequence:

```
MSTDSPKDLSRTAYDHLWMHFTRMSSYENAPVPTIVRGEGTHIYDDKGRRYLDGLAGLFVVQAGHGRQELAETASKQAQELAFFPVWSYAHPKA
VELAERLANEAPGDLNKVFFTTGGGEAVETAWKLAKQYFKLTGKPTKYKVISRAVAYHGTPQGALSITGLPALKAPFEPLVPGAHKVPNTNIYR
APIHGDDPEAYGRWAADQIEQQILFEGPETVAAVFLEPVQNAGGCFPPPPGYFQRVREICDQYDVLLVSDEVICAFGRLGTTFACDKFGYVPDM
ITCAKGMTSGYSPIGACVISDRLAEPFYKGDNTFLHGYTFGGHPVSAAVGIANLDLFEREGLNQHVLDNEGAFRATLEKLHDLPIVGDVRGNGF
FYGIELVKDKATKESFDEEETERVLYGFLSKKLFENGLYCRADDRGDPVIQLAPPLISNQETFDEIEQILRATLTEAWTKL
```

II.g) ω-transaminase PP5182

Cloning strategy

The coding region of the transaminases PP5182 was cloned by our cooperation partner into the vector pET-29a vector (Novagen) using the *Nde*I restriction sites at the N-terminus and *Xho*I sites at the C-terminus. The manual was performed like described for the construction of the expression vector for the enzyme CV2025 from *Chromobacterium violaceum* previously.[103]

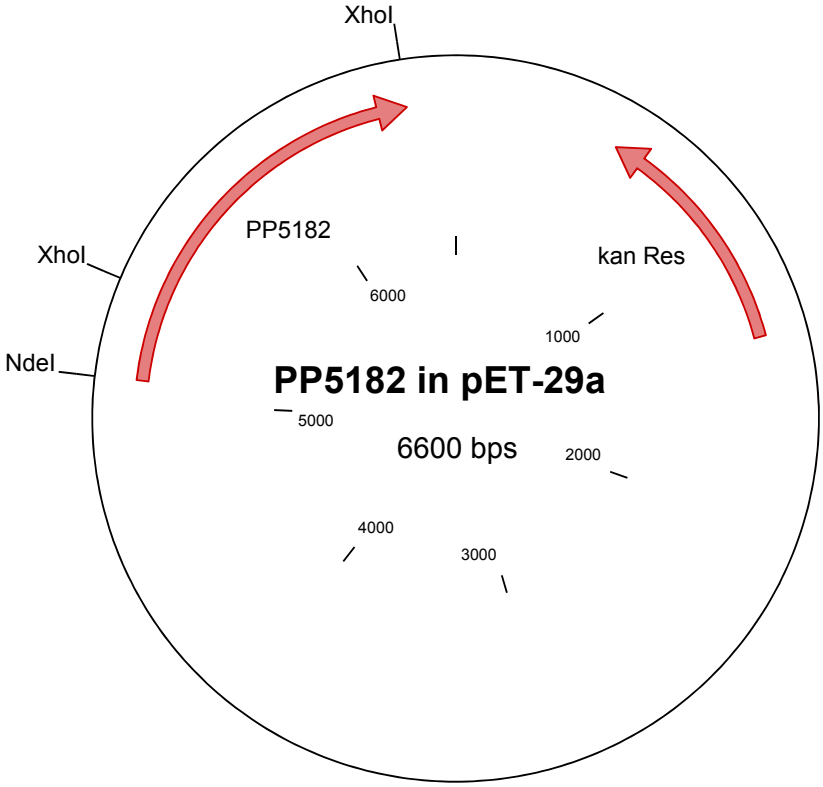

Gene sequence:

```
ATGAGCGTCAACAACCCGCAAACCCGTGAATGGCAAACCCTGAGCGGGGAGCATCACCTCGCACCTTTCAGTGACTACAAGCAGCTGAAGGAGA
AGGGGCCGCGCATCATCACCAAGGCCCAGGGTGTGCATTTGTGGGATAGCGAGGGGCACAAGATCCTCGACGGCATGGCCGGTCTATGGTGCGT
GGCGGTCGGCTACGGACGTGAAGAGCTGGTGCAGGCGGCGGAAAAACAGATGCGCGAGCTGCCGTACTACAACCTGTTCTTCCAGACCGCTCAC
CCGCCTGCGCTCGAGCTGGCCAAGGCGATCACCGACGTGGCGCCGAAAGGTATGACCCATGTGTTCTTCACCGGCTCCGGCTCCGAAGGCAACG
ACACTGTGCTGCGCATGGTGCGTCACTACTGGGCGCTGAAGGGCAAACCGCACAAGCAGACCATCATCGGCCGCATCAACGGTTACCACGGCTC
CACCTTCGCCGGTGCATGCCTGGGCGGTATGAGCGGCATGCACGAGCAGGGTGGCCTGCCGATCCCGGGCATCGTGCACATCCCTCAGCCGTAC
TGGTTCGGCGAGGGAGGCGACATGACCCCTGACGAATTCGGTGTCTGGGCCGCCGAGCAGTTGGAGAAGAAGATCCTCGAAGTCGGCGAAGACA
ACGTCGCGGCCTTCATCGCCGAGCCGATCCAGGGCGCTGGTGGCGTGATCATCCCGCCGGAAACCTACTGGCCGAAGGTGAAGGAGATCCTCGC
CAGGTACGACATCCTGTTCGTCGCCGACGAGGTGATCTGCGGCTTCGGCCGTACCGGCGAGTGGTTCGGCTCGGACTACTACGACCTCAAGCCC
GACCTGATGACCATCGCGAAAGGCCTGACCTCCGGTTACATCCCCATGGGCGGTGTGATCGTGCGTGACACCGTGGCCAAGGTGATCAGCGAAG
GCGGCGACTTCAACCACGGTTTCACCTACTCCGGCCACCCGGTGGCGGCCGCGGTGGGCCTGGAAAACCTGCGCATTCTGCGTGACGAGAAAAT
TGTCGAGAAGGCGCGCACGGAAGCGGCACCGTATTTGCAAAAGCGTTTGCGCGAGCTGCAAGACCATCCACTGGTGGGTGAAGTGCGCGGCCTG
GGCATGCTGGGAGCGATCGAGCTGGTCAAGGACAAGGCAACCCGCAGCCGTTACGAGGGCAAGGGCGTTGGCATGATCTGTCGCACCTTCTGCT
TCGAGAACGGCCTGATCATGCGTGCGGTGGGTGACACCATGATCATCGCGCCGCCGCTGGTAATCAGCCATGCGGAGATCGACGAACTGGTGGA
AAAGGCGCGCAAGTGCCTGGACCTGACCCTTGAGGCGATTCAATAA
```

Protein sequence:

```
MSVNNPQTREWQTLSGEHHLAPFSDYKQLKEKGPRIITKAQGVHLWDSEGHKILDGMAGLWCVAVGYGREELVQAAEKQMRELPYYNLFFQTAH
PPALELAKAITDVAPKGMTHVFFTGSGSEGNDTVLRMVRHYWALKGKPHKQTIIGRINGYHGSTFAGACLGGMSGMHEQGGLPIPGIVHIPQPY
WFGEGGDMTPDEFGVWAAEQLEKKILEVGEDNVAAFIAEPIQGAGGVIIPPETYWPKVKEILARYDILFVADEVICGFGRTGEWFGSDYYDLKP
DLMTIAKGLTSGYIPMGGVIVRDTVAKVISEGGDFNHGFTYSGHPVAAAVGLENLRILRDEKIVEKARTEAAPYLQKRLRELQDHPLVGEVRGL
GMLGAIELVKDKATRSRYEGKGVGMICRTFCFENGLIMRAVGDTMIIAPPLVISHAEIDELVEKARKCLDLTLEAIQ
```

II.h) ω-transaminase PP2799

Cloning strategy

The coding region of the transaminases PP2799 was cloned by our cooperation partner into the vector pET-29a vector (Novagen) using the *Nde*I restriction sites at the N-terminus and *Xho*I sites at the C-terminus. The manual was performed like described for the construction of the expression vector for the enzyme CV2025 from *Chromobacterium violaceum* previously.[103]

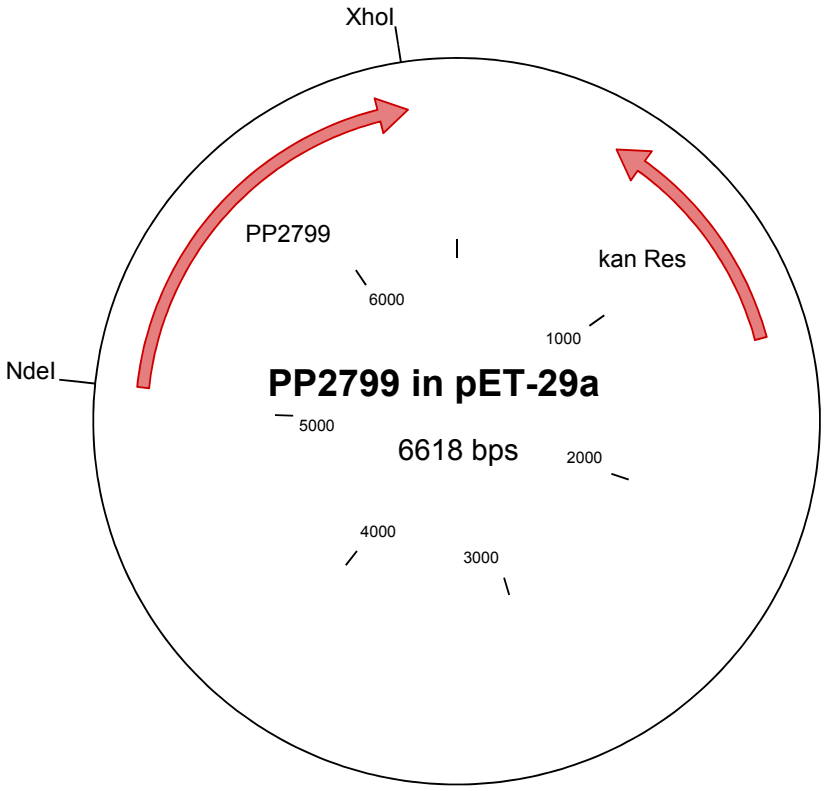

Gene sequence:

```
ATGAGCACCCACTCTTCAACCGTTCAGAACGATCTGGCGGCACTCATTCATCCCAACACCAACCTGGCCCAGCACCGAGAGGTCGGGCCACTCG
TGATCGCCAGAGGTGACGGCGTCCGGGTCTTTGACGAGCAAGGCAATGCCTACATCGAAGCCATGTCGGGCCTGTGGAGCGCGGCATTGGGCTT
CAGTGAACAGCGCCTGGTCGATGCTGCCGTCGAGCAGTTCAAGCAACTGCCCTACTACCACAGCTTCAGCCACAAGACCAATGCGCCTGCCGCA
GCGCTCGCCGCCAAGTTGGCAGCGCTGGCGCCGGGTGATCTGAACCATGTGTTCTTCACCAACTCAGGTTCCGAGGCCAATGATTCGGTGGTGA
AAATGGTGTGGTACGTGAACAACGCACTGGGCCGGCCCGCCAAAAAGAAATTCATCTCTCGACAACAGGCCTATCACGGCGCCACCGTCGCCGC
AGCAAGCCTGACCGGCATCCCATCGATGCACCGTGACTTCGATCTGCCGGCCATCCCGGTTCATCACCTGACCTGCCCGAACTTCTACCGATTT
GCTCGGCCAGGAGAATCGCAAGAGGCCTTTACGGTCCGTCTGGCGAACGAACTGGAACGCTATATCCTTGCCGAAGGGCCGGAAACCATCGCCG
CGTTCATCGGCGAGCCGGTAATCGCGGCAGGTGGCGTGATCCCTCCTCCCACAGGCTACTGGGCGGCGATCCAGGCGGTGTGCAAACGCTACGA
CATCCTCGTGGTGATCGACGAAATCATCACCGGCTTTGGCAGGCTTGGCACAATGTTCGGCTCTCAGTTGTACGGCATCCAGCCCGACATCATG
GTGCTCTCCAAGCAGCTCACCTCCTCATACCAGCCGCTGGCGGCCGTGGTGGTGTCCGATGCCATGAACGATGTACTGGTGAGCCAGAGCCAGC
GCCTGGGGGCATTCGCCCACGGCCTGACCTGCACGGGCCACCCCGTCGCCACGGCGGTTGCGCTGGAAAACATCCGCATCATCGAAGAGCGCGA
TCTGGTCGGCCATGTGCAGCACCTGGCCCCCGTGTTCCAGCGCCACCTGCGCGCGTTCGAAGACCACCCGTTGGTCGGCAACGTCAGAGGCGTC
GGGCTGATGGGCGGGATCGAACTGGTTGCCGACAAGGCCACCCGCCAACCGTTCGCCCAGCCAGGGACGTTGGGCGGCTACGTGTTCAAACAGG
CTCACAAGCATGGGCTGATCATTCGCGCCATCTACGACACGATCGCCTTCTGTCCTCCGTTGATTACCACCCAGGACGATATCGAGGCGATCTT
CAGCGCCTTCGAGCGGACGCTGGCTGACGCGACGGATTGGGCGCGCTCACAGCACCTGCTGTAA
```

Protein sequence:

```
MSTHSSTVQNDLAALIHPNTNLAQHREVGPLVIARGDGVRVFDEQGNAYIEAMSGLWSAALGFSEQRLVDAAVEQFKQLPYYHSFSHKTNAPAA
ALAAKLAALAPGDLNHVFFTNSGSEANDSVVKMVWYVNNALGRPAKKKFISRQQAYHGATVAAASLTGIPSMHRDFDLPAIPVHHLTCPNFYRF
ARPGESQEAFTVRLANELERYILAEGPETIAAFIGEPVIAAGGVIPPPTGYWAAIQAVCKRYDILVVIDEIITGFGRLGTMFGSQLYGIQPDIM
VLSKQLTSSYQPLAAVVVSDAMNDVLVSQSQRLGAFAHGLTCTGHPVATAVALENIRIIEERDLVGHVQHLAPVFQRHLRAFEDHPLVGNVRGV
GLMGGIELVADKATRQPFAQPGTLGGYVFKQAHKHGLIIRAIYDTIAFCPPLITTQDDIEAIFSAFERTLADATDWARSQHLL
```

II.i) ω-transaminase PP2588

Cloning strategy

The coding region of the transaminases PP2588 was cloned by our cooperation partner into the vector pET-29a vector (Novagen) using the *Nde*I restriction sites at the N-terminus and *Xho*I sites at the C-terminus. The manual was performed like described for the construction of the expression vector for the enzyme CV2025 from *Chromobacterium violaceum* previously.[103]

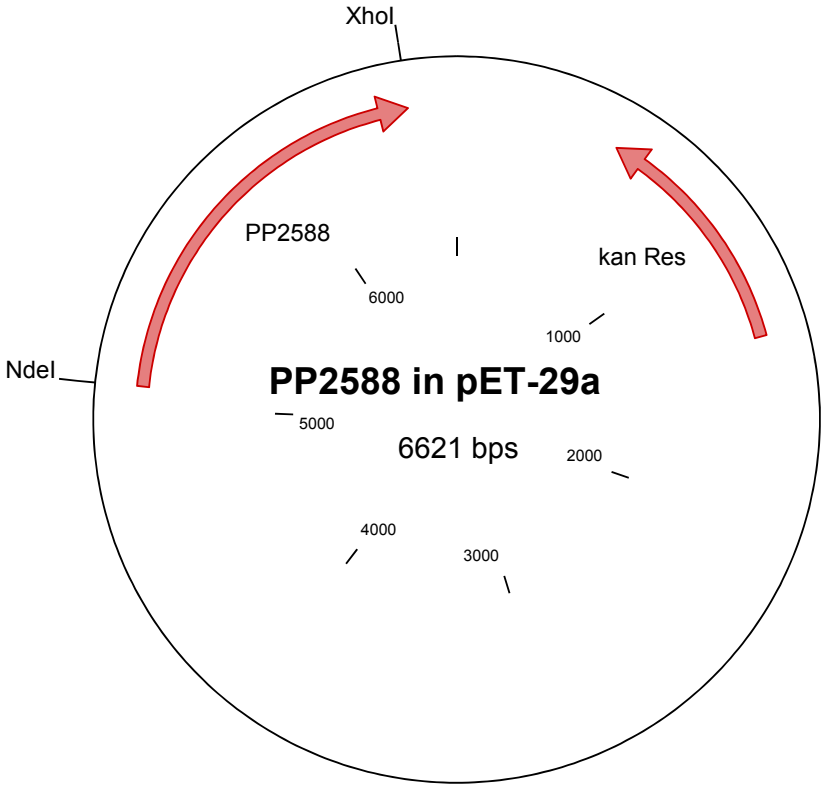

Gene sequence:

```
ATGAACGCGCCTTTCGCCCCGCAACGCCAGACCCGTGACTACCAGGCAGCCGATGCCGCCCACCACATTCATGCCTTCCTCGACCAGAAGGCGC
TGAACGCCGAAGGGCCGCGGGTGATCGTCGGTGGCGAACGCCTGCACCTGTGGGACAGCGAGGGCAAGCGTTACCTGGATGGCATGTCCGGCCT
GTGGTGCACCCAGCTCGGTTATGGCCGTCGTGACCTGACGGCCGCCGCGGCCACGCAGATGGATCAGCTGGCCTACTACAACATGTTTTTCCAC
ACCACCCACCCGGCGGTGATCGAACTGTCCGAGTTGCTGTTCAGCCTGCTGCCGGGGCACTACAGCCACGCGATCTACACCAACTCCGGCTCCG
AGGCCAACGAGGTACTGATCCGCACCGTGCGCCGCTACTGGCAGGTGGTTGGCCAGCCAGGCAAGAAAATCATGATCGGCCGCTGGAACGGCTA
CCACGGCTCGACCCTGGCGGCCACGGCGCTGGGTGGGATGAAGTTCATGCACGACATGGGCGGGTTGATTCCGGATGTGGCACACATCGACGAA
CCCTACTGGTACGCCGAGGGCGGTGAACTGACTCCGGCCGAGTTCGGCCGCCGCTGCGCCCTGCAGCTGGAGGAAAAAATCCTCGAACTGGGTG
CCGAGAACGTTGCCGGCTTCATTGCCGAACCCTTCCAGGGGGCCGGCGGCATGATCTTCCCGCCGGAAAGCTACTGGCCGGAAATCCAGCGTAT
CTGCCGCCAGTACGACGTGCTGCTGTGCGCCGATGAGGTGATCGGTGGCTTTGGCCGCACCGGCGAATGGTTCGCCCATGAATACTTCGGCTTC
GAGCCCGACACCTTGTCGATTGCCAAGGGCCTGACCAGCGGCTATGTGCCCATGGGCGGCCTGGTGCTGAGCAAGCGCATTGCCGAGGCGTTGG
TGGAGCGCGGCGGGGTATTTGCCCACGGCCTGACCTATTCCGGCCACCCGGTGGCGGCGGCAGTGGCCATCGCCAACCTGAAGGCGCTGCGTGA
CGAAGGCATCGTGCGCCAGGTGAAGGACGACACGGGGCCGTACCTGCAGCGCATCCTGCGGGAAGTGTTTGCCGACCACCCATTGATCGGCCAG
GTGCAAGGGGCCGGGCTGGTGGCGGCGCTGCAGTTCGCCGAGCACAAGCCGACGCGCAAGCGCTTTGCCAACGAGAACGACCTGGCCTGGCAGT
GCCGCACCTTTGGTTTCGAGGAAGGGGTGATCATTCGCTCGACCCTGGGCCGGATGATCATGGCCCCGGCCTTGATCGCCAACCACAGCGAGCT
GGATGAGCTGGTGGAGAAGACCCGGATAGCCGTAGACCGCACGGCGCGGCTGGTCGGCAAGCTGTAA
```

Protein sequence:

```
MNAPFAPQRQTRDYQAADAAHHIHAFLDQKALNAEGPRVIVGGERLHLWDSEGKRYLDGM
SGLWCTQLGYGRRDLTAAAATQMDQLAYYNMFFHTTHPAVIELSELLFSLLPGHYSHAIYTNSGSEANEVLIRTVRRYWQVVGQPGKKIMIGRW
NGYHGSTLAATALGGMKFMHDMGGLIPDVAHIDEPYWYAEGGELTPAEFGRRCALQLEEKILELGAENVAGFIAEPFQGAGGMIFPPESYWPEI
QRICRQYDVLLCADEVIGGFGRTGEWFAHEYFGFEPDTLSIAKGLTSGYVPMGGLVLSKRIAEALVERGGVFAHGLTYSGHPVAAAVAIANLKA
LRDEGIVRQVKDDTGPYLQRILREVFADHPLIGQVQGAGLVAALQFAEHKPTRKRFANENDLAWQCRTFGFEEGVIIRSTLGRMIMAPALIANH
SELDELVEKTRIAVDRTARLVGKL
```

II.j) ω-transaminase PP0596

Cloning strategy

The coding region of the transaminases PP0596 was cloned by our cooperation partner into the vector pET-24a vector (Novagen) using the *Nde*I restriction sites at the N-terminus and *Xho*I sites at the C-terminus. The manual was performed like described for the construction of the expression vector for the enzyme CV2025 from *Chromobacterium violaceum* previously.[103]

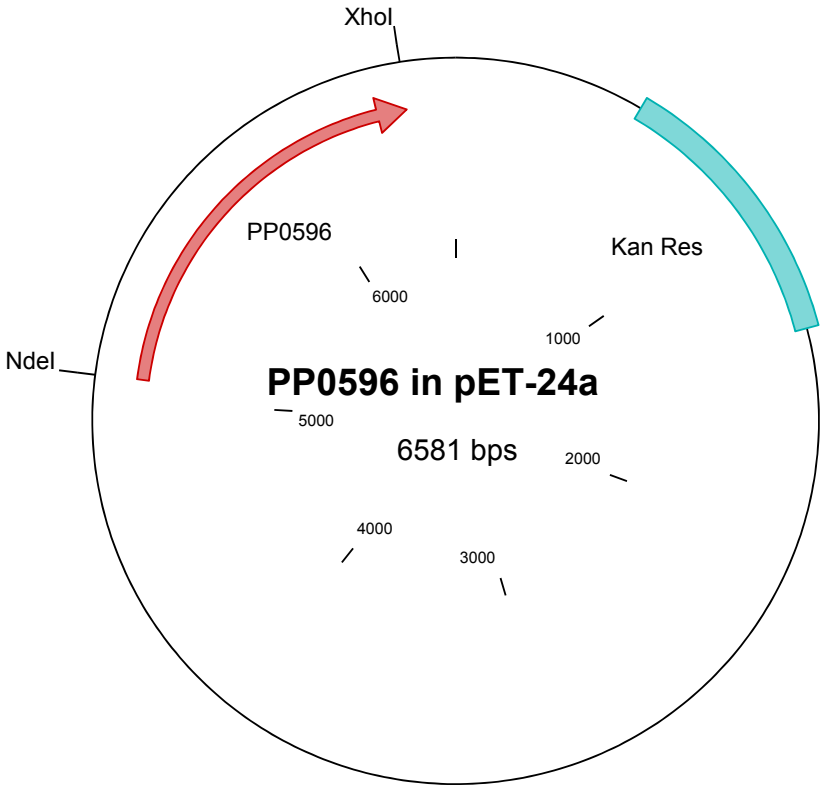

Gene sequence:

```
ATGAACATGCCCGAAACTGGTCCTGCCGGTATCGCCAGCCAGCTCAAGCTGGACGCCCACTGGATGCCCTACACCGCCAACCGCAACTTCCAGC
GCGACCCACGCCTGATCGTGGCGGCCGAAGGCAACTACCTGGTCGATGACCACGGGCGCAAGATCTTCGACGCCCTGTCCGGCCTGTGGACCTG
CGGCGCAGGGCACACTCGCAAGGAAATCGCTGACGCGGTGACCCGTCAACTGAGTACGCTGGACTACTCCCCAGCGTTCCAGTTCGGCCACCCG
CTGTCGTTCCAGCTGGCGGAAAAGATCGCCGAGCTGGTTCCGGGCAATCTGAATCACGTCTTCTATACCAACTCCGGTTCCGAGTGCGCCGATA
CCGCACTGAAGATGGTGCGTGCCTACTGGCGCCTGAAAGGCCAGGCAACCAAGACCAAGATCATCGGCCGTGCCCGTGGTTACCATGGCGTGAA
CATCGCCGGTACCAGCCTGGGTGGCGTCAACGGTAACCGCAAGATGTTTGGCCAGCTGCTGGACGTCGACCACCTGCCTCACACTGTATTGCCG
GTGAACGCCTTCTCGAAAGGCTTGCCGGAAGAGGGCGGTATCGCGCTGGCTGACGAAATGCTCAAGCTGATCGAGCTGCACGATGCCTCCAACA
TCGCAGCAGTCATCGTCGAGCCGCTGGCCGGTTCGGCCGGTGTGCTGCCGCCGCCAAAGGGTTACCTGAAGCGCCTGCGTGAAATCTGCACCCA
GCACAACATTCTGCTGATCTTCGACGAAGTGATCACAGGCTTCGGCCGCATGGGCGCGATGACCGGCTCGGAAGCCTTCGGCGTTACCCCGGAC
CTGATGTGCATCGCCAAGCAGGTGACCAACGGCGCCATCCCGATGGGCGCAGTGATTGCCAGCAGCGAGATCTACCAGACCTTCATGAACCAGC
CGACCCCGGAATACGCCGTGGAATTCCCACACGGCTACACCTATTCGGCGCACCCGGTAGCCTGTGCCGCCGGTCTCGCCGCGCTGGACCTGCT
GCAGAAGGAAAACCTGGTGCAGTCCGCGGCTGAACTGGCGCCGCATTTCGAGAAGCTGCTGCACGGCGTGAAGGGCACCAAGAATATCGTCGAT
ATCCGCAACTACGGCCTGGCCGGCGCCATCCAGATCGCCGCCCGTGACGGTGATGCCATCGTTCGCCCTTACGAAGCGGCCATGAAGCTGTGGA
AAGCGGGCTTCTATGTACGCTTTGGTGGCGACACCCTGCAGTTCGGCCCAACCTTCAATACCAAGCCGCAGGAACTGGACCGCTTGTTCGATGC
TGTTGGCGAAACCCTGAACCTGATCGACTGA
```

Protein sequence:

```
MNMPETGPAGIASQLKLDAHWMPYTANRNFQRDPRLIVAAEGNYLVDDHGRKIFDALSGLWTCGAGHTRKEIADAVTRQLSTLDYSPAFQFGHP
LSFQLAEKIAELVPGNLNHVFYTNSGSECADTALKMVRAYWRLKGQATKTKIIGRARGYHGVNIAGTSLGGVNGNRKMFGQLLDVDHLPHTVLP
VNAFSKGLPEEGGIALADEMLKLIELHDASNIAAVIVEPLAGSAGVLPPPKGYLKRLREICTQHNILLIFDEVITGFGRMGAMTGSEAFGVTPD
LMCIAKQVTNGAIPMGAVIASSEIYQTFMNQPTPEYAVEFPHGYTYSAHPVACAAGLAALDLLQKENLVQSAAELAPHFEKLLHGVKGTKNIVD
IRNYGLAGAIQIAARDGDAIVRPYEAAMKLWKAGFYVRFGGDTLQFGPTFNTKPQELDRLFDAVGETLNLID
```

II.k) ω-transaminase PA0221

Cloning strategy

The coding region of the transaminases PA0221 was cloned by our cooperation partner into the vector pET-29a vector (Novagen) using the *Nde*I restriction sites at the N-terminus and *Xho*I sites at the C-terminus. The manual was performed like described for the construction of the expression vector for the enzyme CV2025 from *Chromobacterium violaceum* previously.[103]

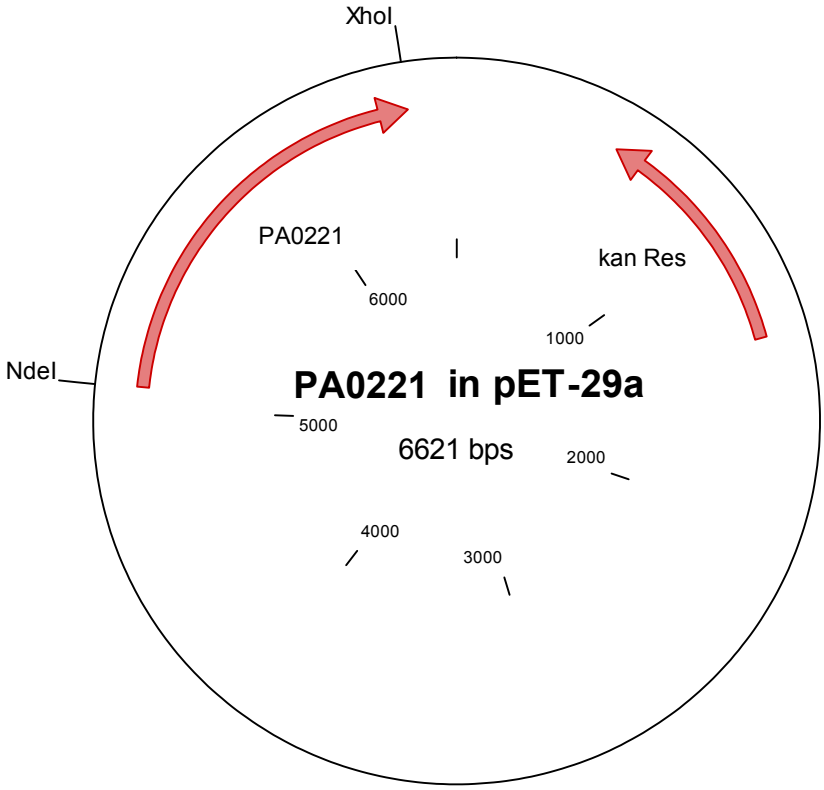

Gene sequence:

ATGACCGCTCAGCTCAACCCGCAGCGCGACACCCGCGACTACCAGCAACTGGACGCCGCGCACCACATCCACGCCTTCCTCGACCAGAAGGCGC
TGAACCGCGAAGGCCCGCGGGTGATGGTCCGCGGCGATGGCCTGCAGCTCTGGGACAACGACGGCAAGCGCTACCTGGACGGCATGTCCGGCCT
CTGGTGCACCAACCTCGGCTACGGCCGCCAGGACCTCGCCGCCGCCGCCAGCCGCCAGCTGGAACAACTGCCGTACTACAACATGTTCTTCCAC
ACCACCCACCCGGCGGTGGTGGAGCTTTCCGAGATGCTCTTCAGCCTGCTGCCGGACCACTACAGCCACGCGATCTACACCAACTCCGGCTCCG
AGGCCAACGAGGTGCTGATCCGTACCGTGCGGCGCTACTGGCAGATCCTCGGCAAGCCGCAGAAGAAGATCATGATCGGCCGCTGGAACGGCTA
CCACGGCTCGACCCTGGGCAGCACCGCGCTCGGCGGGATGAAGTTCATGCACGAGATGGGCGGCATGCTGCCGGACTTCGCCCACATCGACGAA
CCCTACTGGTACGCCAACGGCGGCGAGCTGAGCCCGGCCGAGTTCGGTCGCCGCGCGGCGCTGCAACTGGAGGAGAAGATCCTCGAACTGGGCG
CGGAGAACGTCGCCGCCTTCGTCGCCGAGCCCTTCCAGGGCGCCGGCGGCATGATCTTCCCGCCGCAAAGCTATTGGCCGGAGATCCAGCGCAT
CTGCCGGCAGTACGACGTGCTGCTGTGCGCCGACGAAGTGATCGGCGGCTTCGGCCGCACCGGCGAATGGTTCGCCCACGAACACTTCGGCTTC
CAGCCGGACACCCTGTCCATCGCCAAGGGCCTGACGTCCGGCTACATCCCCATGGGCGGCCTGGTACTCGGCAAGCGCATCGCCGAGGTGCTGG
TGGAGCAGGGCGGGGTGTTCGCCCACGGCCTGACCTATTCCGGCCACCCGGTGGCGGCGGCGGTGGCCATCGCCAACCTCAAGGCGCTGCGCGA
CGAGGGCGTGGTCACGCGGGTCAGGGAGGAGACCGGCCCCTACCTGCAACGCTGCCTGCGCGAGGTCTTCGGCGACCATCCGCTGGTCGGCGAG
GTCCAGGGCGCCGGCTTCGTCGCCGCGCTGCAGTTCGCCGAGGACAAGGTGACCCGCAAGCGCTTCGCCAACGAGAACGATCTGGCCTGGCGCT
GCCGCACCATCGGCTTCGAGGAGGGCGTGATCATCCGCTCCACCCTCGGCCGCATGATCATGGCCCCGGCGCTGGTGGCCGGGCGTGCCGAGAT
CGACGAACTGATCGACAAGACCCGTATCGCGGTGGATCGCACCGCGCGCGAGATCGGCGTGCTCTGA

Protein sequence:

MTAQLNPQRDTRDYQQLDAAHHIHAFLDQKALNREGPRVMVRGDGLQLWDNDGKRYLDGMSGLWCTNLGYGRQDLAAAASRQLEQLPYYNMFFH
TTHPAVVELSEMLFSLLPDHYSHAIYTNSGSEANEVLIRTVRRYWQILGKPQKKIMIGRWNGYHGSTLGSTALGGMKFMHEMGGMLPDFAHIDE
PYWYANGGELSPAEFGRRAALQLEEKILELGAENVAAFVAEPFQGAGGMIFPPQSYWPEIQRICRQYDVLLCADEVIGGFGRTGEWFAHEHFGF
QPDTLSIAKGLTSGYIPMGGLVLGKRIAEVLVEQGGVFAHGLTYSGHPVAAAVAIANLKALRDEGVVTRVREETGPYLQRCLREVFGDHPLVGE
VQGAGFVAALQFAEDKVTRKRFANENDLAWRCRTIGFEEGVIIRSTLGRMIMAPALVAGRAEIDELIDKTRIAVDRTAREIGVL

II.l) ω-transaminase PA4805

Cloning strategy

The coding region of the transaminases PA4805 was cloned by our cooperation partner into the vector pET-29a vector (Novagen) using the *Nde*I restriction sites at the N-terminus and *Xho*I sites at the C-terminus. The manual was performed like described for the construction of the expression vector for the enzyme CV2025 from *Chromobacterium violaceum* previously.[103]

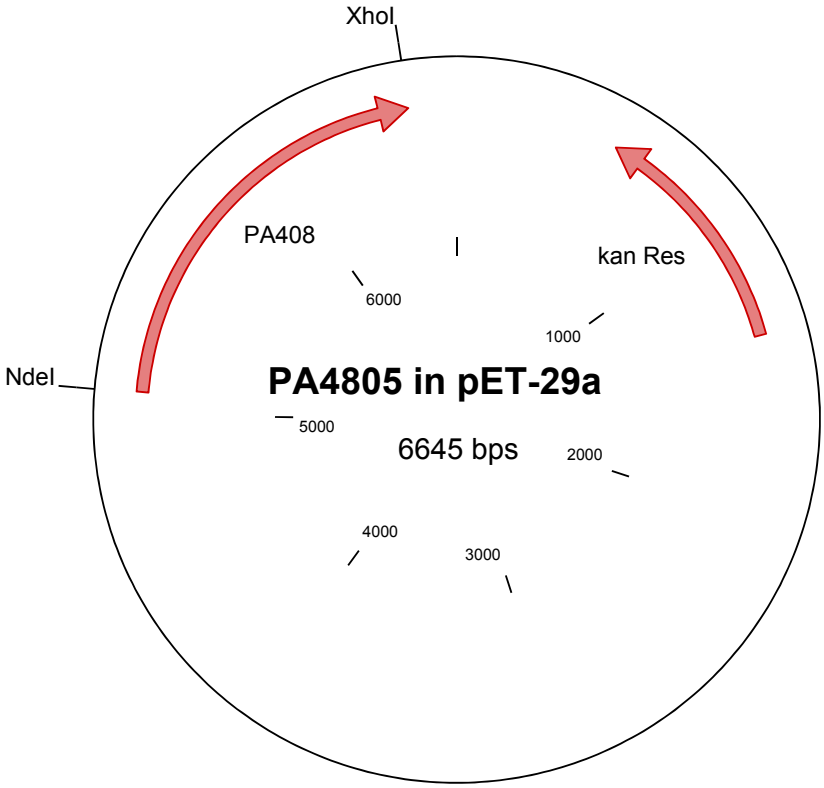

Gene sequence:

```
ATGAACGCAAGACTGCACGCCACGTCCCCCCTCGGCGACGCCGACCTGGTCCGTGCCGACCAGGCCCACTACATGCACGGCTACCACGTGTTCG
ACGACCACCGCGTCAACGGCTCGCTGAACATCGCCGCCGGCGACGGCGCCTATATCTACGACACCGCCGGCAACCGCTACCTCGACGCGGTGGG
CGGCATGTGGTGCACCAACATCGGCCTGGGGCGCGAGGAAATGGCTCGCACCGTGGCCGAGCAGACCCGCCTGCTGGCCTATTCCAATCCCTTC
TGCGACATGGCCAACCCGCGCGCCATCGAACTCTGCCGCAAGCTCGCCGAGCTGGCCCCCGGCGACCTCGACCACGTGTTCCTCACCACCGGCG
GTTCCACCGCCGTGGACACCGCGATCCGCCTCATGCACTACTACCAGAACTGCCGCGGCAAGCGCGCCAAGAAGCACGTCATCACGCGGATCAA
CGCCTACCACGGCTCGACCTTCCTCGGCATGTCGCTGGGCGGCAAGAGCGCCGACCGGCCGGCCGAGTTCGACTTCCTCGACGAGCGCATCCAC
CACCTCGCCTGTCCCTATTACTACCGCGCTCCGGAAGGGCTGGGCGAAGCCGAGTTCCTCGATGGCCTGGTGGACGAGTTCGAACGCAAGATCC
TCGAACTGGGCGCCGACCGGGTGGGGGCGTTCATCTCCGAGCCGGTGTTCGGCTCCGGCGGCGTGATCGTCCCGCCCGCGGGCTACCACAGGCG
GATGTGGGAGCTGTGCCAGCGCTACGACGTGCTGTACATCTCCGACGAAGTGGTGACCTCCTTCGGCCGCCTCGGCCACTTCTTCGCCAGCCAG
GCGGTGTTCGGCGTACAGCCGGACATCATCCTCACCGCCAAGGGCCTCACCTCCGGCTACCAGCCGCTGGGCGCGTGCATCTTCTCCCGGCGCA
TCTGGGAGGTGATCGCCGAGCCGGACAAGGGCCGCTGCTTCAGCCATGGTTTCACCTACTCCGGCCACCCGGTGGCCTGCGCGGCGGCGCTGAA
GAACATCGAGATCATCGAGCGCGAGGGCTTGCTCGCCCACGCCGACGAGGTCGGCCGCTACTTCGAGGAGCGCCTGCAAAGCCTCCGCGACCTG
CCCATCGTCGGCGACGTGCGCGGGATGCGCTTCATGGCCTGTGTCGAGTTCGTCGCCGACAAGGCGAGCAAGGCGCTGTTTCCGGAAAGCCTGA
ACATCGGCGAGTGGGTCCACCTGCGGGCGCAGAAGCGCGGCCTGCTGGTTCGTCCGATCGTCCACCTGAACGTGATGTCGCCGCCGCTGATCCT
CACCCGCGAACAGGTCGATACCGTGGTCCGGGTGCTGCGCGAGAGCATCGAGGAAACCGTGGAGGATCTTGTCCGCGCCGGTCACCGGTAA
```

Protein sequence:

```
MNARLHATSPLGDADLVRADQAHYMHGYHVFDDHRVNGSLNIAAGDGAYIYDTAGNRYLDAVGGMWCTNIGLGREEMARTVAEQTRLLAYSNPF
CDMANPRAIELCRKLAELAPGDLDHVFLTTGGSTAVDTAIRLMHYYQNCRGKRAKKHVITRINAYHGSTFLGMSLGGKSADRPAEFDFLDERIH
HLACPYYYRAPEGLGEAEFLDGLVDEFERKILELGADRVGAFISEPVFGSGGVIVPPAGYHRRMWELCQRYDVLYISDEVVTSFGRLGHFFASQ
AVFGVQPDIILTAKGLTSGYQPLGACIFSRRIWEVIAEPDKGRCFSHGFTYSGHPVACAAALKNIEIIEREGLLAHADEVGRYFEERLQSLRDL
PIVGDVRGMRFMACVEFVADKASKALFPESLNIGEWVHLRAQKRGLLVRPIVHLNVMSPPLILTREQVDTVVRVLRESIEETVEDLVRAGHR
```

II.m) ω-transaminase PA5313

Cloning strategy

The coding region of the transaminases PA5313 was cloned by our cooperation partner into the vector pET-29a vector (Novagen) using the *Nde*I restriction sites at the N-terminus and *Xho*I sites at the C-terminus. The manual was performed like described for the construction of the expression vector for the enzyme CV2025 from *Chromobacterium violaceum* previously.[103]

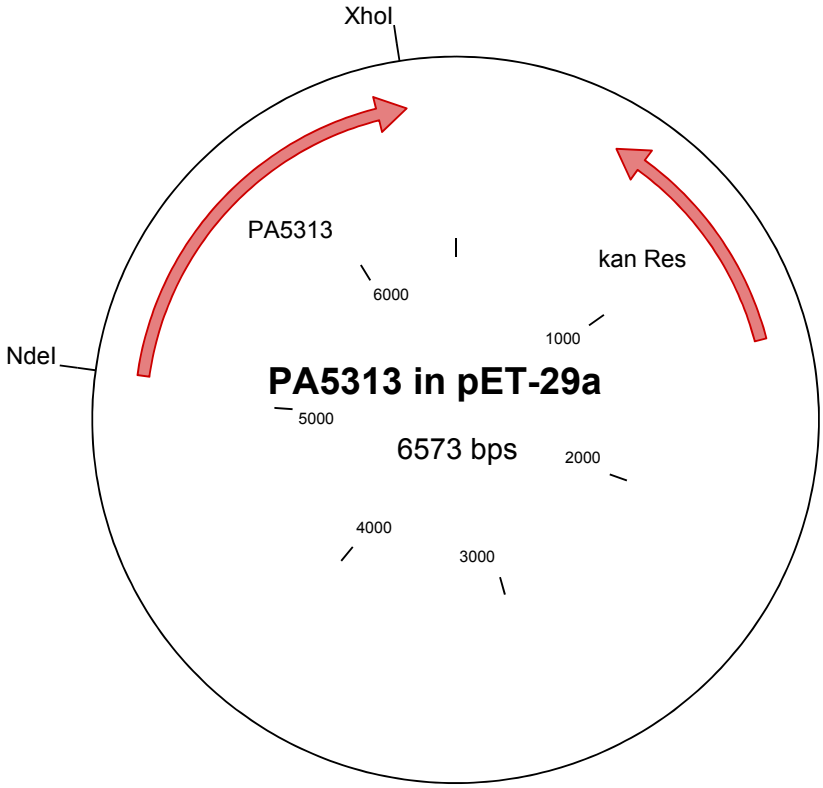

Gene sequence:

```
ATGACAATGAATGACGAGCCGCAGTCGAGCAGCCTCGACAACTTCTGGATGCCCTTCACCGCCAACCGCCAGTTCAAGGCGCGGCCGCGCCTGC
TGGAAAGCGCCGAAGGCATCCACTATATCGCCCAGGGCGGGCGCCGCATCCTCGACGGCACCGCCGGCCTCTGGTGCTGCAATGCCGGCCACGG
CCGGCGCGAGATCAGCGAAGCGGTGGCCCGGCAGATCGCCACCCTCGACTACGCCCCGCCGTTCCAGATGGGTCACCCGCTGCCGTTCGAACTC
GCCGCGCGGCTGACGGAAATCGCCCCGCCGAGCCTGAACAAAGTATTCTTCACCAACTCCGGCTCGGAATCGGCGGACACCGCGCTGAAGATCG
CCCTTGCCTACCAGCGCGCCATCGGCCAGGGCACCCGCACCCGCCTGATCGGCCGCGAACTGGGCTACCACGGGGTCGGCTTCGGCGGCCTGTC
GGTAGGCGGTATGGTCAACAACCGCAAGGCCTTCTCCGCCAACCTGCTGCCGGGGGTCGACCACCTGCCGCACACCCTGGACGTCGCCCGCAAC
GCCTTCACCGTCGGCCTGCCCGAGCATGGCGTGGAAAAGGCCGAGGAGCTGGAACGCCTGGTGACCCTGCACGGCGCCGAGAATATCGCCGCGG
TGATCGTCGAGCCGATGTCCGGCTCGGCCGGCGTGGTGCTGCCGCCCAAGGGCTACCTTCAGCGGCTGCGCGAGATAACCCGCAAGCATGGCAT
CCTGCTGATCTTCGACGAAGTGATCACCGGTTTCGGCCGCGTCGGCGAAGCCTTCGCCGCGCAGCGCTGGGGCGTCGTCCCGGACCTGCTGACC
TGCGCCAAGGGGCTGACCAACGGCAGCATCCCGATGGGCGCCGTATTCGTCGACGAGAAGATCCATGCTGCCTTCATGCAAGGCCCGCAGGGCG
CCATCGAGTTCTTCCACGGCTATACCTATTCCGGCCATCCGGTAGCCTGCGCCGCCGCCCTGGCGACCCTGGACATCTACCGTCGCGACGACCT
GTTCCAGCGGGCCGTCGAACTGGAAGGCTACTGGCAGGACGCGCTGTTCAGCCTGCGCGACCTGCCCAACGTGGTCGACATCCGCGCCGTAGGC
CTGGTCGGCGGCGTGCAACTGGCGCCGCACGCGGACGGCCCCGGCAAGCGCGGCTACGACGTCTTCGAGCGCTGCTTCTGGGAGCACGACCTGA
TGGTCCGGGTGACCGGCGACATCATCGCCATGTCGCCGCCGCTGATCATCGACAAGCCCCACATCGACCAGATCGTCGAGCGCCTGGCCCAGGC
CATCCGCGCCAGCGTCTAA
```

Protein sequence:

```
MTMNDEPQSSSLDNFWMPFTANRQFKARPRLLESAEGIHYIAQGGRRILDGTAGLWCCNAGHGRREISEAVARQIATLDYAPPFQMGHPLPFEL
AARLTEIAPPSLNKVFFTNSGSESADTALKIALAYQRAIGQGTRTRLIGRELGYHGVGFGGLSVGGMVNNRKAFSANLLPGVDHLPHTLDVARN
AFTVGLPEHGVEKAEELERLVTLHGAENIAAVIVEPMSGSAGVVLPPKGYLQRLREITRKHGILLIFDEVITGFGRVGEAFAAQRWGVVPDLLT
CAKGLTNGSIPMGAVFVDEKIHAAFMQGPQGAIEFFHGYTYSGHPVACAAALATLDIYRRDDLFQRAVELEGYWQDALFSLRDLPNVVDIRAVG
LVGGVQLAPHADGPGKRGYDVFERCFWEHDLMVRVTGDIIAMSPPLIIDKPHIDQIVERLAQAIRASV
```

II.n) ω-transaminase CV2025

Cloning strategy

The coding region of the transaminases CV2025 was cloned by our cooperation partner into the vector pET-29a vector (Novagen) using the *Nde*I restriction sites at the N-terminus and *Xho*I sites at the C-terminus. The manual was performed like described previously.[103]

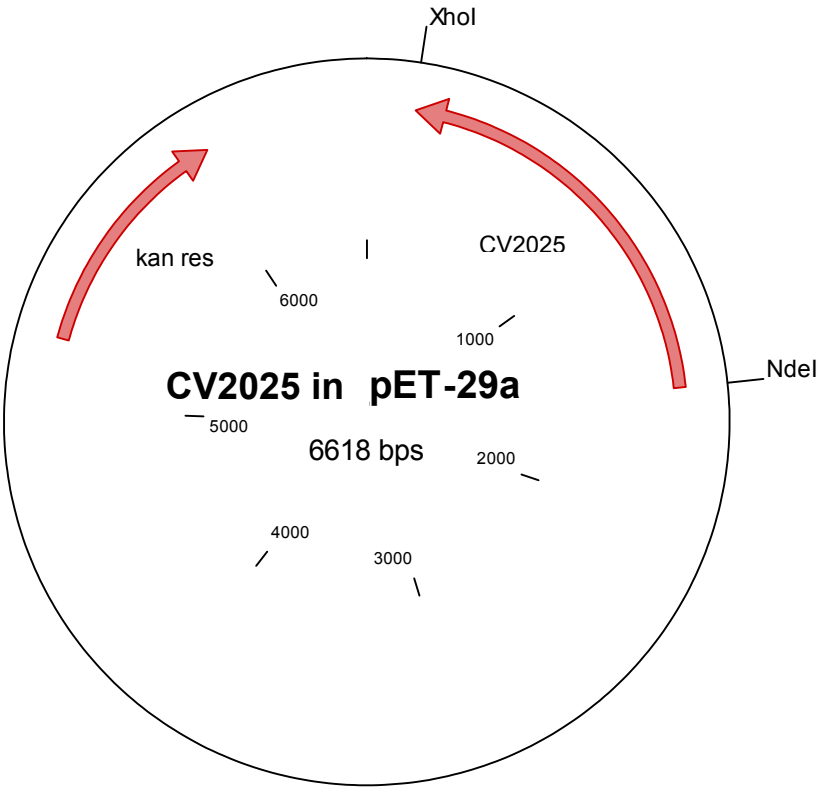

Gene sequence:

```
ATAATTTTGTTTAACTTTAAGAAGGAGATATACATATGCAGAAGCAACGTACGACCAGCCAATGGCGCGAACTGGATGCCGCCCATCACCTGCA
TCCGTTCACCGATACCGCATCGCTGAACCAGGCGGGCGCGCGCGTGATGACGCGCGGAGAGGGCGTCTACCTGTGGGATTCGGAAGGCAACAAG
ATCATCGACGGCATGGCCGGACTGTGGTGCGTGAACGTCGGCTACGGCCGCAAGGACTTTGCCGAAGCGGCGCGCCGGCAGATGGAAGAGCTGC
CGTTCTACAACACCTTCTTCAAGACCACCCATCCGGCGGTGGTCGAGCTGTCCAGCCTGCTGGCTGAAGTGACGCCGGCCGGTTTCGACCGCGT
GTTCTATACCAATTCCGGTTCCGAATCGGTGGACACCATGATCCGCATGGTGCGCCGCTACTGGGACGTGCAGGGCAAGCCGGAGAAGAAGACG
CTGATCGGCCGCTGGAACGGCTATCACGGCTCCACCATCGGCGGCGCCAGCCTGGGCGGCATGAAGTACATGCACGAGCAGGGCGACTTGCCGA
TTCCGGGCATGGCCCACATCGAGCAGCCTTGGTGGTACAAGCACGGCAAGGACATGACGCCGGACGAGTTCGGCGTGGTGGCCGCGCGCTGGCT
GGAAGAGAAGATTCTGGAAATCGGCGCCGACAAGGTGGCCGCCTTCGTCGGCGAACCCATCCAGGGCGCCGGCGGCGTGATCGTCCCGCCGGCC
ACCTACTGGCCGGAAATCGAGCGCATTTGCCGCAAGTACGACGTGCTGCTGGTGGCCGACGAAGTGATCTGCGGCTTCGGGCGTACCGGCGAAT
GGTTCGGCCATCAGCATTTCGGCTTCCAGCCCGACCTGTTCACCGCCGCCAAGGGCCTGTCCTCCGGCTATCTGCCGATAGGCGCGGTCTTTGT
CGGCAAGCGCGTGGCCGAAGGCCTGATCGCCGGCGGCGACTTCAACCACGGCTTCACCTACTCCGGCCACCCGGTCTGCGCCGCCGTCGCCCAC
GCCAACGTGGCGGCGCTGCGCGACGAGGGCATCGTCCAGCGCGTCAAGGACGACATCGGCCCGTACATGCAAAAGCGCTGGCGTGAAACCTTCA
GCCGTTTCGAGCATGTGGACGACGTGCGCGGCGTCGGCATGGTGCAGGCGTTCACCCTGGTGAAGAACAAGGCGAAGCGCGAGCTGTTCCCCGA
TTTCGGCGAGATCGGCACGCTGTGCCGCGACATCTTCTTCCGCAACAACCTGATCATGCGGGCATGCGGCGACCACATCGTGTCGGCGCCGCCG
CTGGTGATGACGCGGGCGGAAGTGGACGAGATGCTGGCGGTGGCGGAACGCTGTCTGGAGGAATTCGAGCAGACGCTGAAGGCGCGCGGGCTGG
CTTAGCTCGAGCACCACCACCACCACCACTGAGATCCGGCTGCTAACAAAGCCCGAA
```

Protein sequence:

```
MQKQRTTSQWRELDAAHHLHPFTDTASLNQAGARVMTRGEGVYLWDSEGNKIIDGMAGLWCVNVGYGRKDFAEAARRQMEELPFYNTFFKTTHP
AVVELSSLLAEVTPAGFDRVFYTNSGSESVDTMIRMVRRYWDVQGKPEKKTLIGRWNGYHGSTIGGASLGGMKYMHEQGDLPIPGMAHIEQPWW
YKHGKDMTPDEFGVVAARWLEEKILEIGADKVAAFVGEPIQGAGGVIVPPATYWPEIERICRKYDVLLVADEVICGFGRTGEWFGHQHFGFQPD
LFTAAKGLSSGYLPIGAVFVGKRVAEGLIAGGDFNHGFTYSGHPVCAAVAHANVAALRDEGIVQRVKDDIGPYMQKRWRETFSRFEHVDDVRGV
GMVQAFTLVKNKAKRELFPDFGEIGTLCRDIFFRNNLIMRACGDHIVSAPPLVMTRAEVDEMLAVAERCLEEFEQTLKARGLA
```

II.o) ω-transaminase CV2025-His

Cloning strategy

The coding region of the transaminases CV2025-His (CV2025 with His-tag) was cloned by our cooperation partner into the vector pET-29a vector (Novagen) using the *Nde*I restriction sites at the N-terminus and *Xho*I sites at the C-terminus. The manual was performed like described for the construction of the expression vector for the enzyme CV2025 from *Chromobacterium violaceum* previously.[103]

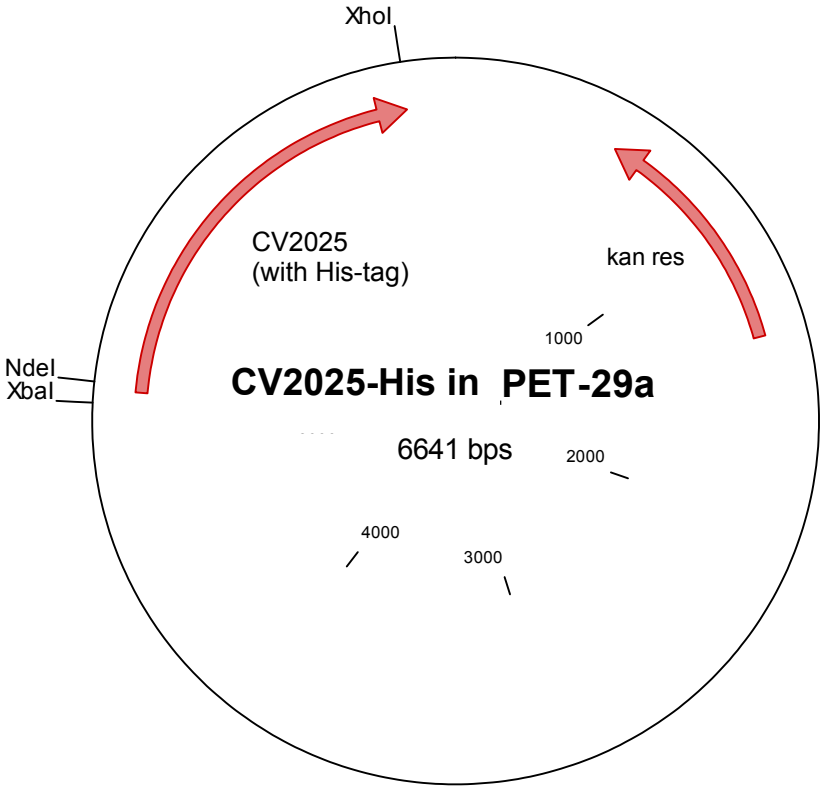

Gene sequence:

```
ATGGGCCATCATCATCATCATCATATGCAGAAGCAACGTACGACCAGCCAATGGCGCGAACTGGATGCCGCCCATCACCTGCATCCGTTCACCG
ATACCGCATCGCTGAACCAGGCGGGCGCGCGCGTGATGACGCGCGGAGAGGGCGTCTACCTGTGGGATTCGGAAGGCAACAAGATCATCGACGG
CATGGCCGGACTGTGGTGCGTGAACGTCGGCTACGGCCGCAAGGACTTTGCCGAAGCGGCGCGCCGGCAGATGGAAGAGCTGCCGTTCTACAAC
ACCTTCTTCAAGACCACCCATCCGGCGGTGGTCGAGCTGTCCAGCCTGCTGGCTGAAGTGACGCCGGCCGGTTTCGACCGCGTGTTCTATACCA
ATTCCGGTTCCGAATCGGTGGACACCATGATCCGCATGGTGCGCCGCTACTGGGACGTGCAGGGCAAGCCGGAGAAGAAGACGCTGATCGGCCG
CTGGAACGGCTATCACGGCTCCACCATCGGCGGCGCCAGCCTGGGCGGCATGAAGTACATGCACGAGCAGGGCGACTTGCCGATTCCGGGCATG
GCCCACATCGAGCAGCCTTGGTGGTACAAGCACGGCAAGGACATGACGCCGGACGAGTTCGGCGTGGTGGCCGCGCGCTGGCTGGAAGAGAAGA
TTCTGGAAATCGGCGCCGACAAGGTGGCCGCCTTCGTCGGCGAACCCATCCAGGGCGCCGGCGGCGTGATCGTCCCGCCGGCCACCTACTGGCC
GGAAATCGAGCGCATTTGCCGCAAGTACGACGTGCTGCTGGTGGCCGACGAAGTGATCTGCGGCTTCGGGCGTACCGGCGAATGGTTCGGCCAT
CAGCATTTCGGCTTCCAGCCCGACCTGTTCACCGCCGCCAAGGGCCTGTCCTCCGGCTATCTGCCGATAGGCGCGGTCTTTGTCGGCAAGCGCG
TGGCCGAAGGCCTGATCGCCGGCGGCGACTTCAACCACGGCTTCACCTACTCCGGCCACCCGGTCTGCGCCGCCGTCGCCCACGCCAACGTGGC
GGCGCTGCGCGACGAGGGCATCGTCCAGCGCGTCAAGGACGACATCGGCCCGTACATGCAAAAGCGCTGGCGTGAAACCTTCAGCCGTTTCGAG
CATGTGGACGACGTGCGCGGCGTCGGCATGGTGCAGGCGTTCACCCTGGTGAAGAACAAGGCGAAGCGCGAGCTGTTCCCCGATTTCGGCGAGA
TCGGCACGCTGTGCCGCGACATCTTCTTCCGCAACAACCTGATCATGCGGGCATGCGGCGACCACATCGTGTCGGCGCCGCCGCTGGTGATGAC
GCGGGCGGAAGTGGACGAGATGCTGGCGGTGGCGGAACGCTGTCTGGAGGAATTCGAGCAGACGCTGAAGGCGCGCGGGCTGGCTTAG
```

Protein sequence:

```
MGHHHHHHMQKQRTTSQWRELDAAHHLHPFTDTASLNQAGARVMTRGEGVYLWDSEGNKIIDGMAGLWCVNVGYGRKDFAEAARRQMEELPFYN
TFFKTTHPAVVELSSLLAEVTPAGFDRVFYTNSGSESVDTMIRMVRRYWDVQGKPEKKTLIGRWNGYHGSTIGGASLGGMKYMHEQGDLPIPGM
AHIEQPWWYKHGKDMTPDEFGVVAARWLEEKILEIGADKVAAFVGEPIQGAGGVIVPPATYWPEIERICRKYDVLLVADEVICGFGRTGEWFGH
QHFGFQPDLFTAAKGLSSGYLPIGAVFVGKRVAEGLIAGGDFNHGFTYSGHPVCAAVAHANVAALRDEGIVQRVKDDIGPYMQKRWRETFSRFE
HVDDVRGVGMVQAFTLVKNKAKRELFPDFGEIGTLCRDIFFRNNLIMRACGDHIVSAPPLVMTRAEVDEMLAVAERCLEEFEQTLKARGLA
```

II.p) ω-transaminase KPN04441

Cloning strategy

The coding region of the transaminases KPN04441 was cloned by our cooperation partner into the vector pET-21a vector (Novagen) using the *Nde*I restriction sites at the N-terminus and *Xho*I sites at the C-terminus. The manual was performed like described for the construction of the expression vector for the enzyme CV2025 from *Chromobacterium violaceum* previously.[103]

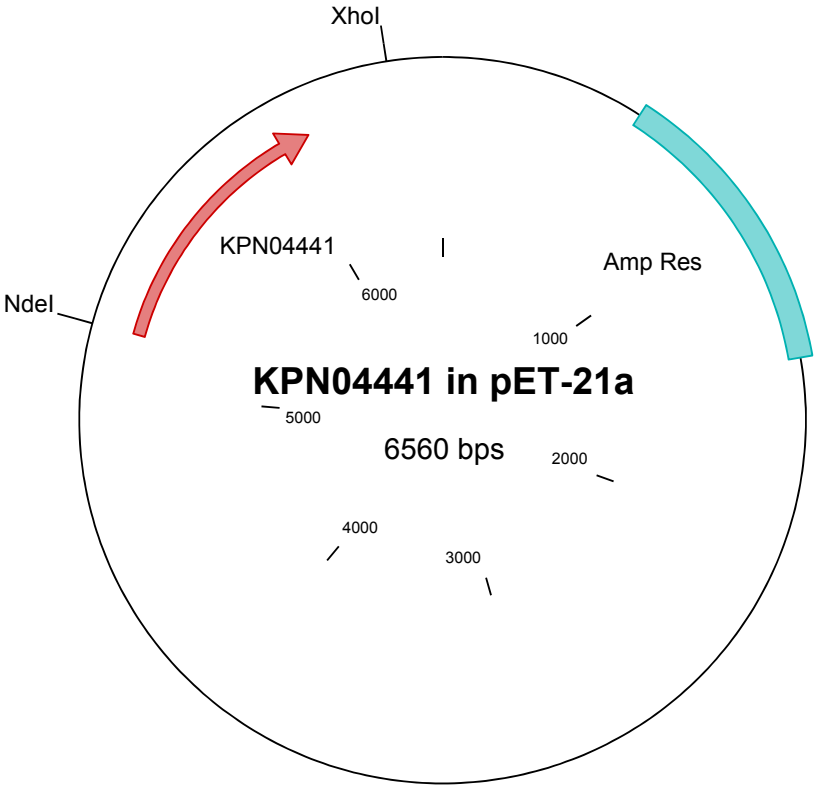

Gene sequence:

```
ATGTTTCAAAAAGTTGACGCCTACGCCGGCGACCCTATTCTTTCTCTGATGGAACGCTTCAAAGAAGACCCGCGAAGCGACAAAGTCAACCTGA
GTATCGGGCTGTACTACAACGATGACGGCATTATCCCGCAGCTGCAGGCGGTGGCGGAAGCGGAAGCACGCCTGAACGCCGAGCCACATGGCGC
CTCGCTGTATCTGCCAATGGAAGGGTTGAGCGGCTACCGTCAGGCGATTGCGCCGCTGCTGTTTGGCGCAGAGCATACCGCGCTTAAGCAAAAT
CGCATTGCCTCTATTCAGACGGTCGGCGGTTCGGGCGCACTGAAGGTCGGGGCCGACTTCCTCAAACGTTACTTTCCTGAGTCTCATGTCTGGG
TCAGCGATCCGACCTGGGAAAACCACATCGCCATTTTTGAAGGGGCTGGCTTCGAAGTAAGTACTTACCCCTGGTTTGATAAAGCCACCAACGG
CGTGCGCTTTGAGGACCTGCTGGCGACGCTGCAAACGCTGCCGGCGCGCGATATTGTGCTGCTGCACCCTTGCTGCCACAACCCGACCGGCGCC
GACCTTACGCCAGCCCAGTGGGACCGCGTGGTTGAGGTATTAAAAGCGCGTCAGCTGATCCCCTTCCTCGACATCGCCTACCAGGGCTTTGGCG
GGGGGCTGGAAGAGGATGCCTACGCTATTCGCGCCATCGCCAGCGCCGGGATGCCGATGCTGGTCAGCAACTCGTTCTCCAAAATTTTCTCGCT
GTACGGGGAGCGCGTCGGCGGTCTGTCCGTGGTCTGTGAAGACAGCGAAACCGCGGGCCGCGTGCTGGGGCAGCTGAAGGCCACCGTGCGCCGC
AACTACTCCAGCCCGCCGAGCTTTGGCGCGCAGTGGTGGCGACGGTGCTGA
```

Protein sequence:

```
MFQKVDAYAGDPILSLMERFKEDPRSDKVNLSIGLYYNDDGIIPQLQAVAEAEARLNAEPHGASLYLPMEGLSGYRQAIAPLLFGAEHTALKQN
RIASIQTVGGSGALKVGADFLKRYFPESHVWVSDPTWENHIAIFEGAGFEVSTYPWFDKATNGVRFEDLLATLQTLPARDIVLLHPCCHNPTGA
DLTPAQWDRVVEVLKARQLIPFLDIAYQGFGGGLEEDAYAIRAIASAGMPMLVSNSFSKIFSLYGERVGGLSVVCEDSETAGRVLGQLKATVRR
NYSSPPSFGAQWWRRC
```

II.q) ω-transaminase POAB80-1

Cloning strategy

The coding region of the transaminases POAB80-1 (pQR902) was cloned by our cooperation partner into the vector pET-21a vector (Novagen) using the *Nde*I restriction sites at the N-terminus and *Xho*I sites at the C-terminus. The manual was performed like described for the construction of the expression vector for the enzyme CV2025 from *Chromobacterium violaceum* previously.[103]

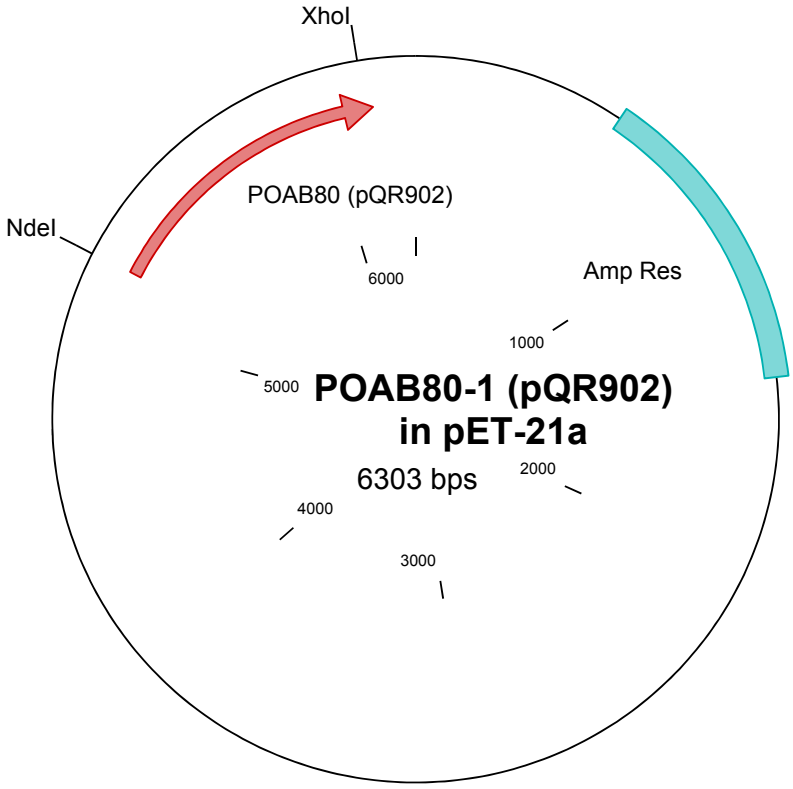

Gene sequence:

```
ATGGCTAGCATGACCACGAAGAAAGCTGATTACATTTGGTTCAATGGGGAGATGGTTCGCTGGGAAGACGCGAAGGTGCATGTGATGTCGCACG
CGCTGCACTATGGCACTTCGGTTTTTGAAGGCATCCGTTGCTACGACTCGCACAAAGGACCGGTTGTATTCCGCCATCGTGAGCATATGCAGCG
TCTGCATGACTCCGCCAAAATCTATCGCTTCCCGGTTTCGCAGAGCATTGATGAGCTGATGGAAGCTTGTCGTGACGTGATCCGCAAAAACAAT
CTCACCAGCGCCTATATCCGTCCGCTGATCTTCGTCGGTGATGTTGGCATGGGAGTAAACCCGCCAGCGGGATACTCAACCGACGTGATTATCG
CTGCTTTCCCGTGGGGAGCGTATCTGGGCGCAGAAGCGCTGGAGCAGGGGATCGATGCGATGGTTTCCTCCTGGAACCGCGCAGCACCAAACAC
CATCCCGACGGCGGCAAAAGCCGGTGGTAACTACCTCTCTTCCCTGCTGGTGGGTAGCGAAGCGCGCCGCCACGGTTATCAGGAAGGTATCGCG
CTGGATGTGAACGGTTATATCTCTGAAGGCGCAGGCGAAAACCTGTTTGAAGTGAAAGATGGTGTGCTGTTCACCCCACCGTTCACCTCCTCCG
CGCTGCCGGGTATTACCCGTGATGCCATCATCAAACTGGCGAAAGAGCTGGGAATTGAAGTACGTGAGCAGGTGCTGTCGCGCGAATCCCTGTA
CCTGGCGGATGAAGTGTTTATGTCCGGTACGGCGGCAGAAATCACGCCAGTGCGCAGCGTAGACGGTATTCAGGTTGGCGAAGGCCGTTGTGGC
CCGGTTACCAAACGCATTCAGCAAGCCTTCTTCGGCCTCTTCACTGGCGAAACCGAAGATAAATGGGGCTGGTTAGATCAAGTTAATCAACTCG
AGCACCACCACCACCACCACTGA
```

Protein sequence:

```
MASMTTKKADYIWFNGEMVRWEDAKVHVMSHALHYGTSVFEGIRCYDSHKGPVVFRHREHMQRLHDSAKIYRFPVSQSIDELMEACRDVIRKNN
LTSAYIRPLIFVGDVGMGVNPPAGYSTDVIIAAFPWGAYLGAEALEQGIDAMVSSWNRAAPNTIPTAAKAGGNYLSSLLVGSEARRHGYQEGIA
LDVNGYISEGAGENLFEVKDGVLFTPPFTSSALPGITRDAIIKLAKELGIEVREQVLSRESLYLADEVFMSGTAAEITPVRSVDGIQVGEGRCG
PVTKRIQQAFFGLFTGETEDKWGWLDQVNQLEHHHHHH
```

II.r) ω-transaminase POAB80-2

Cloning strategy

The coding region of the transaminases POAB80-2 (pQR907) was cloned by our cooperation partner into the vector pET-21a vector (Novagen) using the *Nde*I restriction sites at the N-terminus and *Xho*I sites at the C-terminus. The manual was performed like described for the construction of the expression vector for the enzyme CV2025 from *Chromobacterium violaceum* previously.[103]

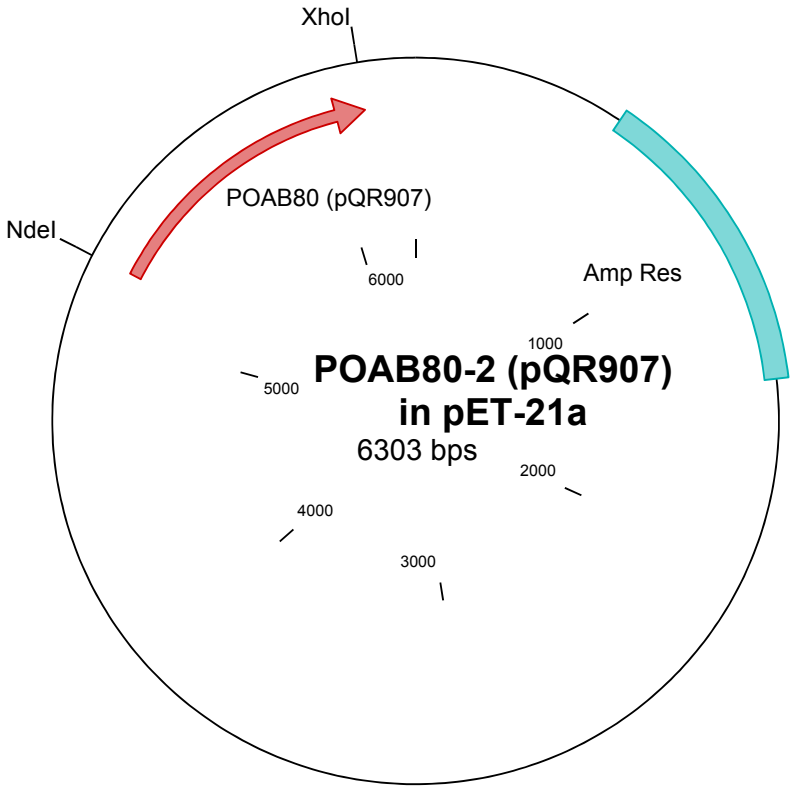

Gene sequence:

```
ATGGCTAGCATGACCACGAAGAAAGCTGATTACATTTGGTTCAATGGGGAGATGGTTCGCTGGGAAGACGCGAAGGTGCATGTGATGTCGCACG
CGCTGCACTATGGCACTTCGGTTTTTGAAGGCATCCGTTGCTACGACTCGCACAAAGGACCGGTTGTATTCCGCCATCGTGAGCATATGCAGCG
TCTGCATGACTCCGCCAAAATCTATCGCTTCCCGGTTTCGCAGAGCATTGATGAGCTGATGGAAGCTTGTCGTGACGTGATCCGCAAAAACAAT
CTCACCAGCGCCTATATCCGTCCGCTGATCTTCGTCGGTGATGTTGGCATGGGAGTAAACCCGCCAGCGGGATACTCAACCGACGTGATTATCG
CTGCTTTCCCGTGGGGAGCGTATCTGGGCGCAGAAGCGCTGGAGCAGGGGATCGATGCGATGGTTTCCTCCTGGAACCGCGCAGCACCAAACAC
CATCCCGACGGCGGCAAAAGCCGGTGGTAACTACCTCTCTTCCCTGCTGGTGGGTAGCGAAGCGCGCCGCCACGGTTATCAGGAAGGTATCGCG
CTGGATGTGAACGGTTATATCTCTGAAGGCGCAGGCGAAAACCTGTTTGAAGTGAAAGATGGTGTGCTGTTCACCCCACCGTTCACCTCCTCCG
CGCTGCCGGGTATTACCCGTGATGCCATCATCAAACTGGCGAAAGAGCTGGGAATTGAAGTACGTGAGCAGGTGCTGTCGCGCGAATCCCTGTA
CCTGGCGGATGAAGTGTTTATGTCCGGTACGGCGGCAGAAATCACGCCAGTGCGCAGCGTAGACGGTATTCAGGTTGGCGAAGGCCGTTGTGGC
CCGGTTACCAAACGCATTCAGCAAGCCTTCTTCGGCCTCTTCACTGGCGAAACCGAAGATAAATGGGGCTGGTTAGATCAAGTTAATCAACTCG
AGCACCACCACCACCACCACTGA
```

Protein sequence:

```
MASMTTKKADYIWFNGEMVRWEDAKVHVMSHALHYGTSVFEGIRCYDSHKGPVVFRHREHMQRLHDSAKIYRFPVSQSIDELMEACRDVIRKNN
LTSAYIRPLIFVGDVGMGVNPPAGYSTDVIIAAFPWGAYLGAEALEQGIDAMVSSWNRAAPNTIPTAAKAGGNYLSSLLVGSEARRHGYQEGIA
LDVNGYISEGAGENLFEVKDGVLFTPPFTSSALPGITRDAIIKLAKELGIEVREQVLSRESLYLADEVFMSGTAAEITPVRSVDGIQVGEGRCG
PVTKRIQQAFFGLFTGETEDKWGWLDQVNQLEHHHHHH
```

II.s) ω-transaminase POAB80-3

Cloning strategy

The coding region of the transaminases POAB80-3 (pQR908) was cloned by our cooperation partner into the vector pET-21a vector (Novagen) using the *Nde*I restriction sites at the N-terminus and *Xho*I sites at the C-terminus. The manual was performed like described for the construction of the expression vector for the enzyme CV2025 from *Chromobacterium violaceum* previously.[103]

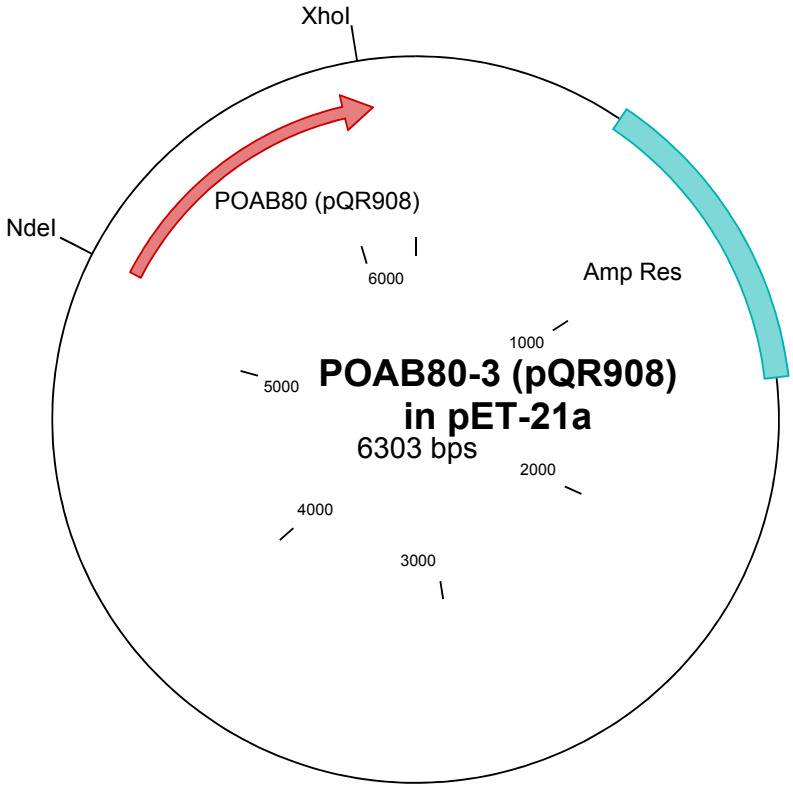

Gene sequence:

```
ATGGCTAGCATGACCACGAAGAAAGCTGATTACATTTGGTTCAATGGGGAGATGGTTCGCTGGGAAGACGCGAAGGTGCATGTGATGTCGCACG
CGCTGCACTATGGCACTTCGGTTTTTGAAGGCATCCGTTGCTACGACTCGCACAAAGGACCGGTTGTATTCCGCCATCGTGAGCATATGCAGCG
TCTGCATGACTCCGCCAAAATCTATCGCTTCCCGGTTTCGCAGAGCATTGATGAGCTGATGGAAGCTTGTCGTGACGTGATCCGCAAAAACAAT
CTCACCAGCGCCTATATCCGTCCGCTGATCTTCGTCGGTGATGTTGGCATGGGAGTAAACCCGCCAGCGGGATACTCAACCGACGTGATTATCG
CTGCTTTCCCGTGGGGAGCGTTACTGGGCGCAGAAGCGCTGGAGCAGGGGATCGATGCGATGGTTTCCTCCTGGAACCGCGCAGCACCAAACAC
CATCCCGACGGCGGCAAAAGCCGGTGGTAACTACCTCTCTTCCCTGCTGGTGGGTAGCGAAGCGCGCCGCCACGGTTATCAGGAAGGTATCGCG
CTGGATGTGAACGGTTATATCTCTGAAGGCGCAGGCGAAAACCTGTTTGAAGTGAAAGATGGTGTGCTGTTCACCCCACCGTTCACCTCCTCCG
CGCTGCCGGGTATTACCCGTGATGCCATCATCAAACTGGCGAAAGAGCTGGGAATTGAAGTACGTGAGCAGGTGCTGTCGCGCGAATCCCTGTA
CCTGGCGGATGAAGTGTTTATGTCCGGTACGGCGGCAGAAATCACGCCAGTGCGCAGCGTAGACGGTATTCAGGTTGGCGAAGGCCGTTGTGGC
CCGGTTACCAAACGCATTCAGCAAGCCTTCTTCGGCCTCTTCACTGGCGAAACTGAAGATAAATGGGGCTGGTTAGATCAAGTTAATCAACTCG
AGCACCACCACCACCACCACTGA
```

Protein sequence:

```
MASMTTKKADYIWFNGEMVRWEDAKVHVMSHALHYGTSVFEGIRCYDSHKGPVVFRHREHMQRLHDSAKIYRFPVSQSIDELMEACRDVIRKNN
LTSAYIRPLIFVGDVGMGVNPPAGYSTDVIIAAFPWGALLGAEALEQGIDAMVSSWNRAAPNTIPTAAKAGGNYLSSLLVGSEARRHGYQEGIA
LDVNGYISEGAGENLFEVKDGVLFTPPFTSSALPGITRDAIIKLAKELGIEVREQVLSRESLYLADEVFMSGTAAEITPVRSVDGIQVGEGRCG
PVTKRIQQAFFGLFTGETEDKWGWLDQVNQLEHHHHHH
```